

CENTRE FOR OPEN AND DISTANCE LEARNING

TEZPUR UNIVERSITY: NAPAAM: SONITPUR

SELF-LEARNING MATERIAL

SOLAR ENERGY

DRE 102

SELF-LEARNING MATERIAL

Course Code: DRE 102

Course Title: SOLAR ENERGY

Course Advisors

Prof D.C.Baruah,Head
Prof S.K.Samdarshi
Prof D.Deka
Dr Rupam Kataki
S.Mahapatra
P.K.Choudhury

Programme Coordinator/s

S.Mahapatra

Course Contributors

Prof S.K.Samdarshi, Dept of Energy, Tezpur University
Dr Rupam Kataki, Associate Professor, Dept of Energy, Tezpur University

Course Editor/s

Dr Santanu Sharma, Associate Professor, Dept of ECE, T.U.

March 2012

@ CODL, Tezpur University

Published by

Director, Centre for Open and Distance Learning (CODL),
on behalf of Tezpur University.

The material provided here can be freely accessed but cannot be reproduced or reprinted for commercial purposes.

COURSE INTRODUCTION

PART -1

COURSE 1: ENERGY AND ENVIRONMENT

- UNIT-1 : ECOLOGICAL PRINCIPLES AND ENERGY FLOW
- UNIT-2 : ENERGY SCENARIO AND DEVELOPMENT
- UNIT-3 : MAJOR ENERGY RESOURCES OF THE WORLD
- UNIT-4 : ENVIRONMENT CONCERNS OF ENERGY EXTRACTION
- UNIT-5 : ENERGY USE & CLIMATE CHANGE
- UNIT-6 : SUSTAINABILITY ISSUES OF ENERGY USE
- UNIT-7 : SOCIO- ECONOMICAL ASPECTS OF ENERGY RESOURCES
- UNIT-8 : INTERNATIONAL TREATIES & CONVENTION ON ENVIRONMENTAL MITIGATION

COURSE 2: SOLAR ENERGY

- UNIT-1 : SOLAR RADIATION
- UNIT-2 : BASICS OF SOLAR THERMAL CONVERSION
- UNIT-3 : SOLAR THERMAL SYSTEMS AND APPLICATIONS
- UNIT-4 : SOLAR THERMAL ENERGY CONVERSION
- UNIT-5 : BASICS OF SOLAR PHOTOVOLTAICS
- UNIT-6 : SOLAR PHOTOVOLTAIC ENERGY CONVERSION AND UTILIZATION SYSTEMS
- UNIT-7 : POWER ELECTRONICS FOR PHOTOVOLTAIC

COURSE 3: BIOMASS ENERGY

- UNIT -1 : INTRODUCTION
- UNIT-2 : BIOMASS AS FUEL
- UNIT-3 : BIOCHEMICAL CONVERSION OF BIOMASS FOR ENERGY PRODUCTION
- UNIT-4 : LIQUID BIOFUEL CR 3
- UNIT-5 : CHEMICAL CONVERSION OF BIOMASS FOR ENERGY PRODUCTION
- UNIT-6 : SYNTHESIS BIOFUEL
- UNIT-7 : THERMO-CHEMICAL CONVERSION OF BIOMASS
- UNIT-8 : ENERGY PLANTATION

COURSE 4: WIND AND HYDRO ENERGY

- UNIT-1 : WIND RESOURCE ASSESSMENT
- UNIT-2 : AERODYNAMICS OF WIND TURBINE
- UNIT-3 : WIND ENERGY CONVERSION SYSTEMS
- UNIT-4 : WIND ENERGY SYSTEMS: ENVIRONMENT AND ECONOMICS
- UNIT-5 : HYDRO-POWER
- UNIT-6 : BASICS OF FLUID MECHANICS
- UNIT-7 : COMPONENTS OF HYDROPOWER PLANTS
- UNIT-8 : HYDROPOWER PLANT DEVELOPMENT

COURSE 5: NEW ENERGY RESOURCES

- UNIT-1 : BACKGROUND
- UNIT-2 : HYDROGEN ENERGY
- UNIT-3 : FUEL CELL
- UNIT-4 : OCEAN ENERGY
- UNIT-5 : GEOTHERMAL ENERGY
- UNIT-6 : MAGNETOHYDRODYNAMIC00.(MHD)
- UNIT-7 : ELECTROCHEMICAL ENERGY STORAGE SYSTEM
- UNIT-8 : MAGNETIC AND ELECTRIC STORAGE SYSTEM

UNIT-1: SOLAR RADIATION

Radiative energy from the sun enters the earth's atmosphere at almost a constant rate before it traverses its atmosphere which is highly fluctuating but having an approximate periodic variability. This along with the vectorial nature of radiation needs utmost care before the quantum of terrestrial availability of solar radiation can be ascertained with high degree of confidence. The governing equations, measurement instrumentation and models for representing the data through simple stochastic relation forms the content of this unit.

1.1 SOLAR RADIATION: EXTRA-TERRESTRIAL AND TERRESTRIAL

Importance of Solar Energy

Energy is the prime-mover of civilization. But human civilization in 21st century is at cross-roads. Why?

- More energy is required for different sectors of human activities for better quality of life than ever before. Energy production from conventional fossil fuel resources are major source of environmental pollutants.
- Environmental concerns are becoming important. Sustainability of development of civilization is being questioned.

Global energy-mix under transition. Why ?

- Rapid decline in non-renewable fossil fuel resources.
- These resources are considered to be major sources of CO₂ emission. Hence other renewable non-polluting resources are being explored and utilized.

With the above background how can we conclude that Solar Energy is important?

The following characteristics of solar energy make it important. Solar energy is

- Renewable
- Environmentally clean
- Available to all
- Equitably distributed

Solar Energy: Is it renewable ? Is it sufficient? Does it conform to the requirements of sustainable development ?

- Solar energy is a product of nuclear fusion process taking place in the core region of solar gaseous mass.
- Life of sun is estimated to be 5×10^9 years – limited. Is it renewable? Energy is obtained from Renewable resources at a rate that is less than or

equal to the rate at which it is replenished. So solar energy is renewable. We shall try to quantify it later to understand its sufficiency and conformity to sustainability as well.

Solar Energy is sufficient

Sufficiency is always related to a requirement which in the present case is quality of life of human life i.e. human development. Human development is quite abstract and can be understood in terms of causality relationship with influencing factors. These factors have been taken into account in to formulate Human Development Index(HDI) to represent the state of human development in time and space. The factors are - Life expectancy, Literacy, and GDP (Gross Domestic Product). The HDI range from 0 to 1 (Lowest level to highest level of development). The HDI for different countries on the basis of one data is shown in Fig. 1. Please note that 2×10^5 MJ per capita is sufficient to achieve high level of HDI(≥ 0.9).

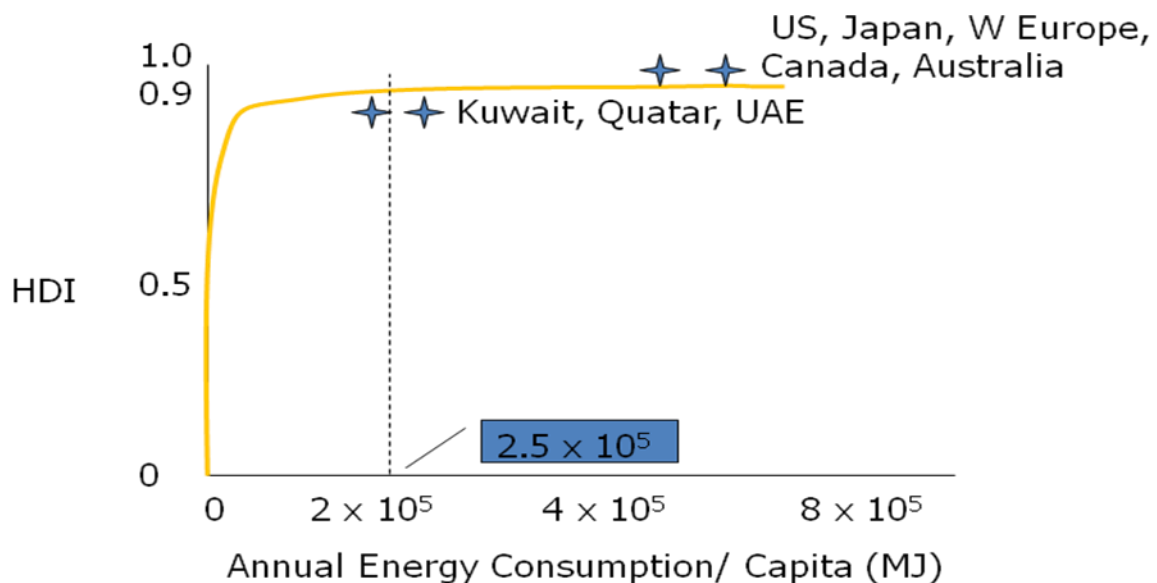


Fig 1. HDI for different countries on the basis of energy consumption/capita

Sufficiency of Solar Energy in Global Context

Assume that the world population stabilizes at 8 billion. In that case energy need $HDI = 1.6 \times 10^{15}$ MJ/year = 1600 Q/year.

- Average insolation received on earth = 1.7×10^{17} J/sec
- Solar Energy per day = 2.4×10^{16} MJ/year

Land area available for this = 10%; Conversion efficiency of solar system = 10%

- Available energy from sun = 2.2×10^{15} MJ/year which is more than required.

Sufficiency of Solar Energy in Indian Context

If Indian population stabilizes at 2 billion. Energy need = 4×10^{14} MJ/year.

- Area of India = 3.28 million sq. km.
- Av. Solar insolation received in India = 5 kWh/m²-day
- Solar Energy per day = 2.4×10^{16} MJ/year

Land area available for solar energy use = 10%

Average conversion efficiency of solar system = 15%

Available energy from sun = 3.6×10^{14} MJ/years which is close to the energy requirement which will be needed as per HDI need.

Solar Energy conforms to sustainability requirements

Sustainability as defined in the Brundtland Commission Report entitled *Our Common Future*¹ as

"Sustainable development is development that meets the needs of the present without compromising the ability of future generations to meet their own needs."

- Intergenerational equity – Equity of resources in time and space
- Sufficient Social capital – Sufficiency in terms of technology, environment including other
- Resource capacity utilization – It is not a terrestrial resource but comes from outside i.e extra terrestrial sources and hence does not put extra burden of wasted capacity if not utilized efficiently.

India recognizes the importance of solar energy : National Action Plan on Climate Change(NAPCC)

- i. Published by the Government in 2008
- ii. 8 key areas chosen for National Missions
- iii. Jawaharlal Nehru National Solar Mission is one of these 8 Missions.
- iv. It was committed by the Prime Minister of India at United Nations Framework Convention on Climate Change(UNFCCC) summit held at Copenhagen in November 2009
- v. Suggests Renewable Purchase Obligations (RPO) at 5% in year 2010, increasing 1% every year for 10 years. RPO includes other renewables also.

Jawaharlal Nehru National Solar Mission(JLNNSM)

¹ World Commission on Environment and Development (WCED). *Our common future*. Oxford: Oxford University Press, 1987 p. 43.

Jawaharlal Nehru National Solar Mission was launched under the National action Plan on Climate Change with the objectives

- To establish India as a global leader in solar energy, by creating the policy conditions for its diffusion across the country.
- Mission anticipates achieving grid parity by 2022 and parity with coal based thermal power by 2030.
- To adopt a 3-phase approach from 2010 to 2022.
- Aim of the mission is to focus on setting up an enabling environment for solar technology both at centralized and decentralized level.

JLNNSM Mission Targets

Application Segment	Phase - I	Phase-II	Phase- III
	2010-13	2013-17	2017-22
Utility grid power	1,000-2,000 MW	4000-10,000 MW	20,000 MW
Off- grid Applications	200 MW	1,000 MW	2,000 MW
Solar Thermal Collectors Area	7 million Sqm	15 million Sqm	20 million Sqm
Manufacturing Base	--	--	4,000-5,000 MW
Solar Lighting Systems	--	--	20 million
Solar RPO	0.25%	--	3%

The 3- phase approach has been formulated as follows

Enabling ProvE

Electricity Act 2003: Enabling provisions adopted by Central Electricity Regulatory Commission(CERC)

- Tariff regulations of the Regulatory Commissions to be guided by promotion of generation of electricity from renewable energy sources
- State Electricity Regulatory Commissions (SERCs) required to specify Renewable Purchase Obligations (RPOs)

- The National Electricity Policy to aim for optimal utilization of resources including renewable sources
- Regulatory Commissions required to promote the development of power markets.

Renewable Purchase Obligations(RPO)

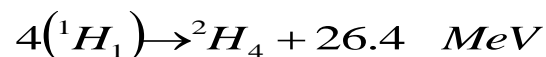
- SERCs in all major States have specified RPOs
- RPOs vary from 1% to 10% in different States
- Presently the share of renewable energy is about 5% in total electricity generation
- Share of solar energy presently is negligible
- Renewable energy Certificate (REC) mechanism is expected to overcome geographical constraints and provide flexibility to achieve RPO compliance.

1 MWhr → 1 REC

Extra-terrestrial Solar Radiation

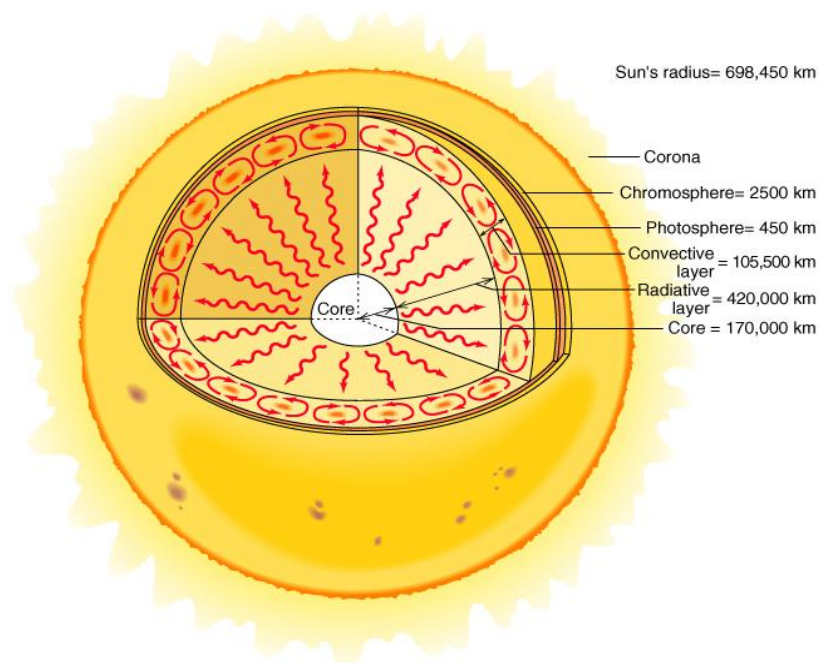
The sun and its interior:

- Temp Range of sun's core is 8×10^6 to 40×10^6 K
- Solar gaseous mass rotates such that the Equatorial region takes 27 days/rotation while polar region takes 30 days/rotation
- Energy production is produced in the innermost part called core which acts as Fusion reactor with its constituents retained by gravitational forces
- The most dominant fusion Reaction is



- Energy is transfer out from its core through a combination of radiative and convective process with emission, absorption, and re-radiation
- Structure of Interior of sun: The sun constitutes gaseous mass of a range of constituents given in the box. The radius R of the sun corresponds to the radius of the photosphere which is the outer opaque region of the sun's gasous mass
 - **Core extends from 0-0.23R** and is source of 90% of total energy generated by the fusion process by 40% of total mass of the sun enclosed 15% of the total volume of the sun. It is at a temperature of $8-40 \times 10^6$ K and has a density of 10^5 kg/m^3 which is about 100 times the density of water.
 - **Transition zone** envelops the core and extends from 0.23-0.7R. This is the region in which the process of convection of solar mass begins.

- **Convective zone extend from 0.7-1.0R. It is at a temperature of 130000 K and the gaseous mass present in this has a low density of 70 kg/m^3**
- **Photosphere is the outermost opaque layer of sun at a temperature of 5000 K and density of 10^{-5} kg/m^3**
- **Reversing Layer is an unique layer only few hundred km in thickness and relatively cool layer at $T < 5000 \text{ K}$. The exact explanation of the uniqueness of this layer is still elusive to the researchers.**
- **Chromosphere is about 10000 km and is at a temperature above 5000 K**
- **Corona is the outermost layer of undefined thickness which is normally visible during total solar eclipse in the background. It is at a temperature as high as 10^6 K**



Copyright 1999 John Wiley and Sons, Inc. All rights reserved.

Solar Spectrum and Energy

Total extra-terrestrial solar irradiance normal to a surface at earth-sun mean distance is **1366 Watts/m²**. This is called **Solar Constant**. The **extra-terrestrial and terrestrial solar irradiance spectrum** is shown in the figure 2.

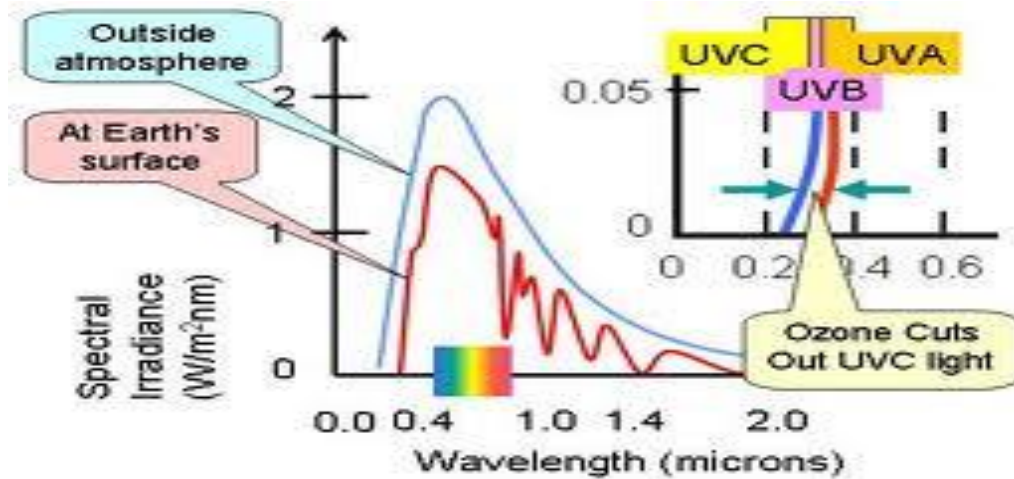
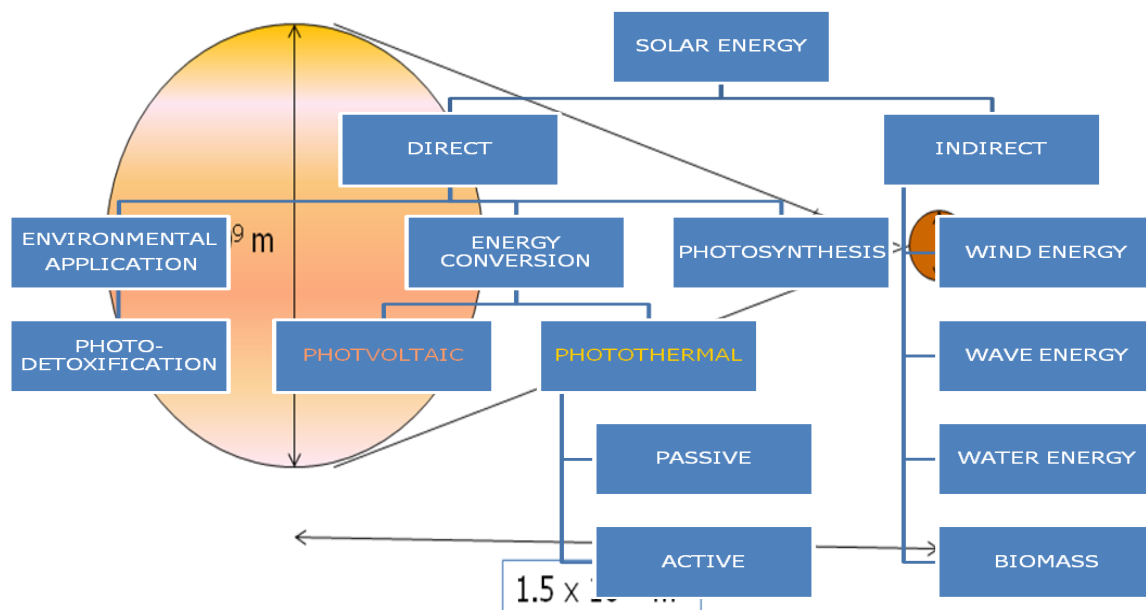


Fig 2: Components of extra-terrestrial Solar spectrum

Spectral Region	Range	Energy available
Ultra Violet	0.30 to 0.48 μm	7 %
Visible	0.48 to 0.76 μm	46 %
Infra red	0.76 μm onwards	47 %

Solar energy Utilization

Earth-Sun relation



Variation in solar constant

- Due to a small eccentricity(0.02) of earth's elliptical orbit the Earth-sun distance varies by 1.7% and results in $\pm 3\%$ variation in solar radiation reaching earth's outer atmosphere

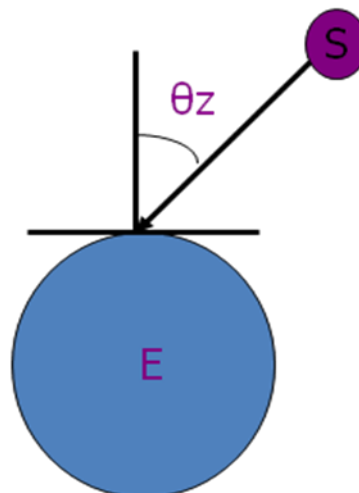
$$(1) \quad G_{on} = G_{sc} \left[1 + 0.033 \cos \frac{360n}{365} \right]$$

where n=day of the year, For January 1, n=1.

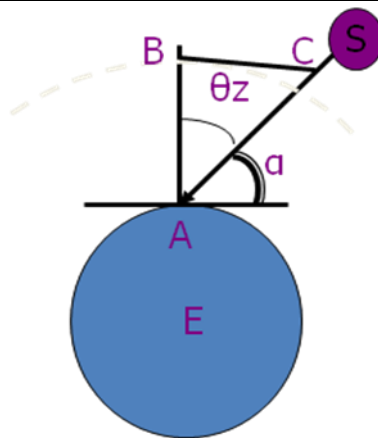
- Periodic variation of intrinsic solar radiation is about $\pm 1.5\%$
- Random variation because of sunspot activities is also there.

Sun, earth and solar radiation-Terms

- a. **Beam Radiation:** It is the radiation received directly from the sun without being scattered by earth's atmosphere It is also called Direct radiation. About 80% of total radiation on a clear day. Subscript 'b'
- b. **Diffuse Radiation:** The solar radiation received from the sun after its direction has been changed by scattering by atmospheric gases, and solid and liquid particulate matters. It is also called Sky radiation and is about 20% of the total radiation on a clear day. Most of it is in the shorter wavelength region. Subscript 'd'.
- c. **Total Solar Radiation:** It is the sum of beam and diffuse radiation on a given surface. If the surface is horizontal then total solar radiation is referred to as Global radiation. Subscript 'T'.
- d. **Zenith Angle(θ_z):** This is the angle between the beam radiation and the vertical line to the zenith. Its complementary angle is the altitude angle α , the angle between beam radiation and its horizontal projection.



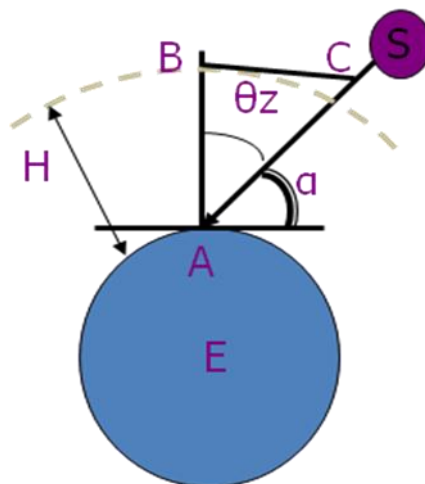
- e. **Air Mass(m, AM):** It is the ratio of the optical thickness of atmosphere traversed by beam radiation and the optical thickness of the atmosphere overhead.



$$m = AC/AB = \sec \theta_z = \operatorname{cosec} \alpha \quad (2)$$

Position of sun	Zenith angle	Value of Air Mass	Notation
Outside atmosphere		$m=0$	AM0
Sun is at zenith	$\theta_z = 0^\circ$	$m=1$	AM 1
Sun at zenith angle 60°	$\theta_z = 60$	$m=?$	AM ?
	Answer	$m=2$	AM2

- Relation (2) is valid for i) homogeneous atmosphere and ii) $\theta_z = 0-70^\circ$ only after this the earth's curvature becomes significant.
- For $\theta_z = 70^\circ$ $M = [\{(R/H) \cos \theta_z + 2(R/H) + 1\}^{1/2} - (R/H) \cos \theta_z]$
(3)
where R = earth's radius = 6370 km and $H=7991$ km



Comparative table of solar radiation at different airmass

AirMass	Sun's Position	Solar Irradiance (W/m^2)
---------	----------------	--

AM0	Extraterrestrial	1377
AM1	Sun Overhead	1105
AM1.5	Sun with $\theta_z = 48^\circ$	1000
AM2	Sun with $\theta_z = 60^\circ$	894

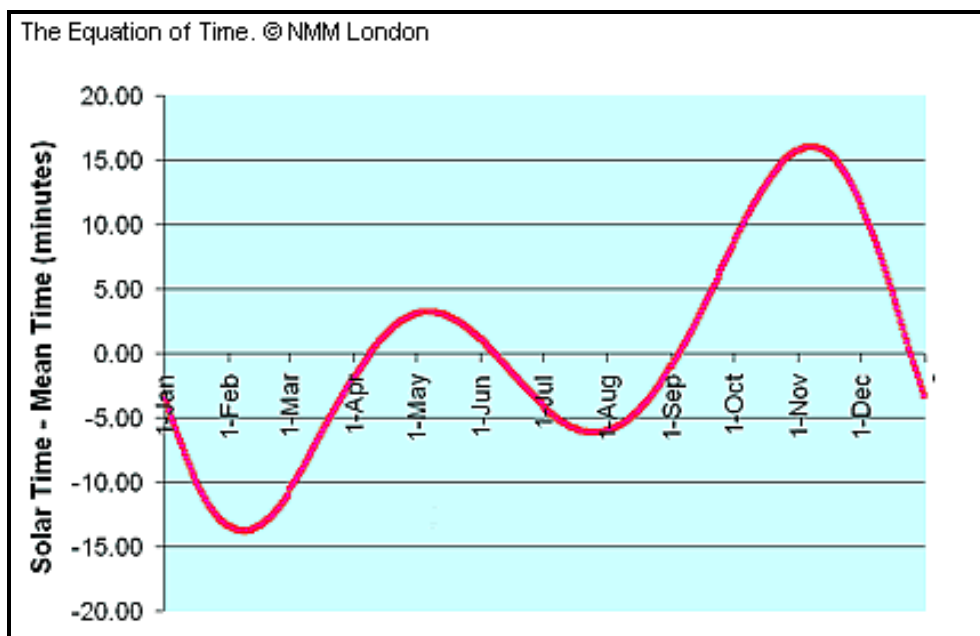
- f. Irradiance (G, W/m^2): The rate at which radiation is incident over an unit area of surface.
- g. Irradiation(I, J/m^2) The incident energy on an unit area of surface over an specified time(day, hour). Integrated irradiance. Insolation ?
- h. Radiosity(E, W/m^2) Rate at which radiant energy leaves a surface by combined emission, reflection and transmission. Emissive power ?
- i. Solar Time: Helps in knowing relation between time and position of sun wrt earth.

$$\text{Solar Time} = \text{Standard time} \pm 4 (L_{\text{st}} - L_{\text{loc}}) + E \quad (4)$$

$$E = 9.87 \sin 2B - 7.53 \cos -1.5 \sin B$$

$$B = 360(n-81)/364$$

$$\text{where } 1 \leq n \leq 365 \quad E = \pm 17 \text{ min}$$



Problem: What is the solar time corresponding to 10:30 am IST on February 02 at 75 E? Given $E = -13.5$ minutes.

$$\begin{aligned}
 \blacksquare \text{ Solar Time} &= 10:30 - 4(82.5 - 75) - 13.5 \\
 &= 10:30 - 4 \times 7.5 - 13.5 \\
 &= 9:46.5 \text{ AM}
 \end{aligned}$$

Direction and amount of beam Radiation

Direction: In terms of some known angles. These angles will be defined properly in the following section

Amount of solar radiation: Is it possible to determine it?

Yes, extra-terrestrial value with reasonable accuracy

But for this it is required to know about the related angles as amount of radiation is highly dependent on angle of incidence.

- Slope(β): angle between plane and horizontal with respect to earth. $0 \leq \beta \leq 180^\circ$.



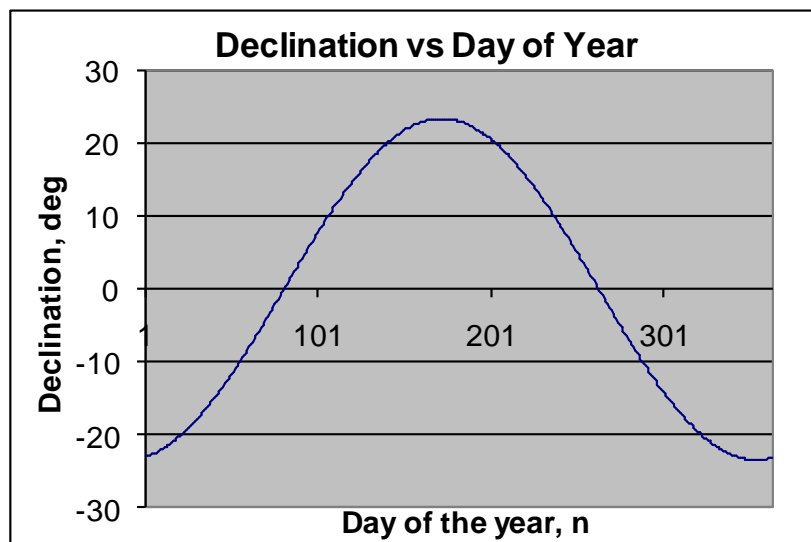
- Latitude(Φ): Angular Location of place with respect to equator in the direction north or south of it. North positive, Tezpur (26.70N,92.84E)
Here, $-90^\circ \leq \Phi \leq +90^\circ$

- Declination(δ): Angular position of sun w.r.t. plane of equator. Its value may be determined for a given day using equation (5). North of equator is taken as positive and south as negative.

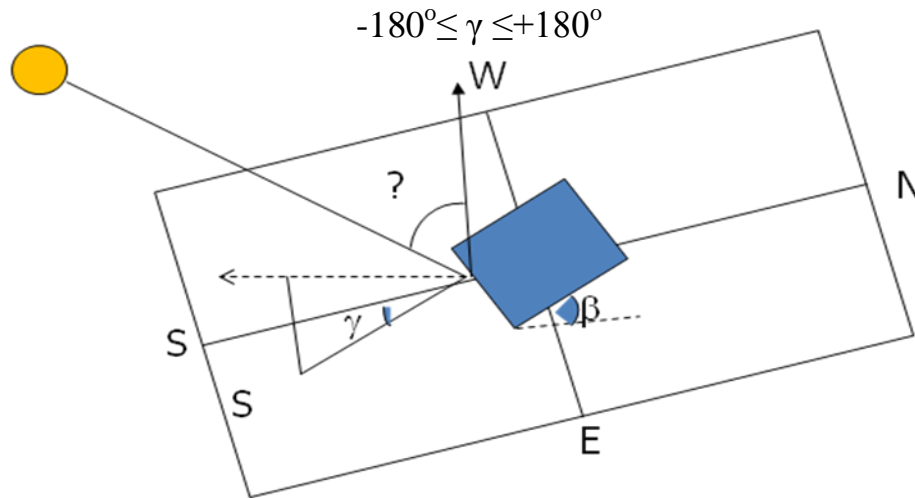
Here, $-23.45^\circ \leq \delta \leq +23.45^\circ$

$$\delta = 23.45 \sin\left(\frac{284+n}{365} 360\right) \quad (5)$$

Variation of equation (5) with the value of day of the year, n ($n=1$, January 1) is shown in the graph.



- Surface Azimuth Angle(γ): Deviation of the projection of the normal to the surface on a horizontal plane from the local meridian with zero due south. East –ve.



N.B.: Solar azimuth angle (γ_s) is the deviation of projection of beam radiation. Please note that the angle under question mark(?) is the zenith angle.

- Hour angle(ω): Angular displacement of sun with respect to observer's meridian and is related to earth's rotation on its axis. One hour= 15° . Morning –ve afternoon positive. At noon $\omega=0$
 $-180^\circ \leq \omega \leq +180^\circ$

What is the value of hour angle at 10AM(Solar Time)?

Ans: -30 deg

N.B.: Unless otherwise mentioned the time is always solar time.

- Angle of Incidence(θ): This is the angle between the beam radiation and the normal to the surface. In terms of other angles

$$\begin{aligned} \cos\theta &= \sin\delta \sin\phi \cos\beta \\ &\quad - \sin\delta \cos\phi \sin\beta \cos\gamma \\ &\quad + \cos\delta \cos\phi \cos\beta \cos\omega \\ &\quad + \cos\delta \sin\phi \sin\beta \cos\gamma \cos\omega \\ &\quad + \cos\delta \sin\beta \sin\gamma \sin\omega \end{aligned} \quad (6)$$

- Commonly used forms

Case(a): For surface sloped towards South $\gamma=0^\circ$ in Northern hemisphere
 or North $\gamma=180^\circ$ in Southern hemisphere

$$\begin{aligned} \cos\theta &= \sin\delta \sin\phi \cos\beta - \sin\delta \cos\phi \sin\beta \\ &\quad + \cos\delta \cos\phi \cos\beta \cos\omega \\ &\quad + \cos\delta \sin\phi \sin\beta \cos\omega \end{aligned} \quad (7)$$

Towards North ?

Case(b): For vertical surface ($\beta=90^\circ$) oriented in any direction($\gamma \neq 0^\circ, 180^\circ$), from (6)

$$\cos\theta = -\sin\delta \cos\phi \cos\gamma + \cos\delta \sin\phi \cos\gamma \cos\omega + \cos\delta \sin\gamma \sin\omega \quad (8)$$

Case(c): For vertical surface ($\beta=90^\circ$) facing south($\gamma=0^\circ$), from (6) or (7)

$$\cos\theta = -\sin\delta \cos\phi + \cos\delta \sin\phi \cos\omega \quad (9)$$

Case(d): For horizontal surface($\beta=0^\circ$) (sloped towards south $\gamma=0^\circ$ or North $\gamma=180^\circ$?). From eqn(7)

$$\cos\theta = \sin\delta \sin\phi + \cos\delta \cos\phi \cos\omega$$

Here $\theta = \theta_z$, therefore, $\cos\theta_z = \sin\delta \sin\phi + \cos\delta \cos\phi \cos\omega$
(10)

Case(e): Rewriting equation (7) we get a useful equation valid for northern hemisphere

$$(11) \quad \cos\theta = \sin\delta \sin(\phi - \beta) + \cos\delta \cos(\phi - \beta) \cos\omega$$

Problem : Calculate the zenith angle of sun for a place(19°N) at 9:30AM on February 13.

■ For feb 13, $n=44$, $\delta = -14^\circ$; for 9:30 AM solar time $\omega = -37.5^\circ$

$$\begin{aligned} \cos\theta_z &= \sin\delta \sin\phi + \cos\delta \cos\phi \cos\omega \\ &= \sin(-14)\sin(19) + \cos(-14)\cos(19)\cos(-37.5) \\ &= -0.24 \times 0.33 + 0.97 \times 0.95 \times 0.79 \\ &= -0.078 + 0.728 = 0.65 \\ \theta_z &= 49.5^\circ \end{aligned}$$

Problem: For a given place in Northern hemisphere solar beam radiation falls normally to a surface tilted at an angle β at solar noon. Prove that it is tilted at an angle $\beta = (\phi - \delta)$.

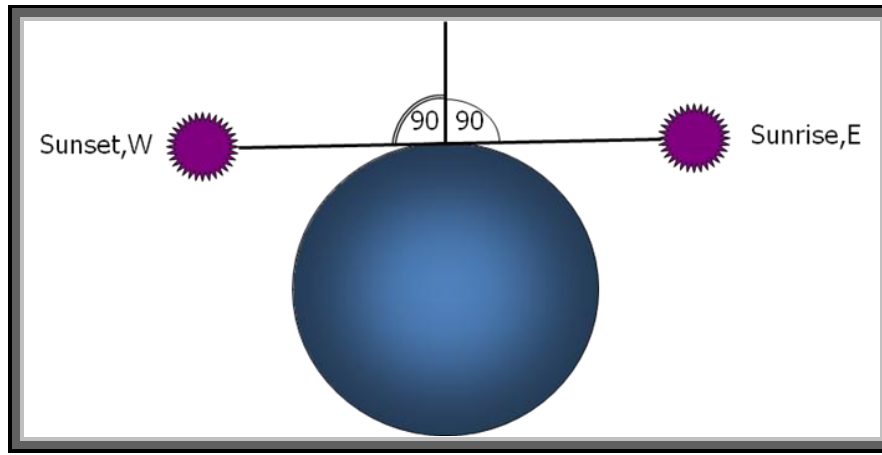
■ Surface tilted south $\gamma=0^\circ$. At solar noon $\omega=0$ and $\theta=0$.

$$\begin{aligned} \cos\theta &= \sin\delta \sin(\phi - \beta) + \cos\delta \cos(\phi - \beta) \cos\omega \\ \cos 0 &= \sin\delta \sin(\phi - \beta) + \cos\delta \cos(\phi - \beta) \cos 0 \\ \cos 0 &= \sin\delta \sin(\phi - \beta) + \cos\delta \cos(\phi - \beta) \\ \cos 0 &= \cos\{\delta - (\phi - \beta)\} \\ 0 &= \delta - (\phi - \beta) \\ \text{Hence } \beta &= \phi - \delta \end{aligned}$$

- Sunset or sunrise hour angle(ω_s) corresponds to $\theta_z = 90^\circ$. From eqn.(10)

$$\cos\omega_s = -\frac{\sin\phi \sin\delta}{\cos\phi \cos\delta}$$

$$\omega_s = \cos^{-1}(-\tan\phi \tan\delta)$$



- Number of daylight hours(N): Hour angle for the whole day= $2 \omega_s = 2 \cos^{-1}(-\tan \phi \tan \delta)$

$$N = (2/15) \cos^{-1}(-\tan \phi \tan \delta) \quad (13)$$

Eqn(13) is applicable for horizontal surface. For tilted surface

$$N = (2/15) \cos^{-1}\{-\tan(\phi - \beta) \tan \delta\} \quad (14)$$

- Expressing daily extraterrestrial insolation on a horizontal surface

Extraterrestrial solar irradiance on a horizontal surface,

$$G_o = G_{SC} \left[1 + 0.033 \cos \frac{360n}{365} \right] \cos \theta_z \quad (15)$$

where G_{SC} is solar constant and n =day of the year.

$$G_o = G_{SC} \left[1 + 0.033 \cos \frac{360n}{365} \right] (\cos \delta \cos \phi \cos \omega + \sin \delta \sin \phi) \quad (16)$$

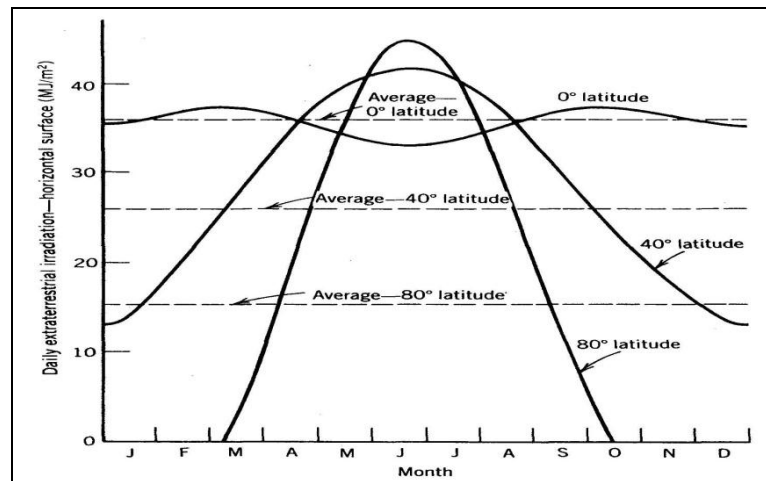
Integrating eqn(16) between sunrise and sunset i.e. daily extra-terrestrial insolation on a horizontal surface,

$$H_o = G_{SC} \left[1 + 0.033 \cos \frac{360n}{365} \right] \int_{-\omega_s}^{\omega_s} (\cos \delta \cos \phi \cos \omega + \sin \delta \sin \phi) d\omega$$

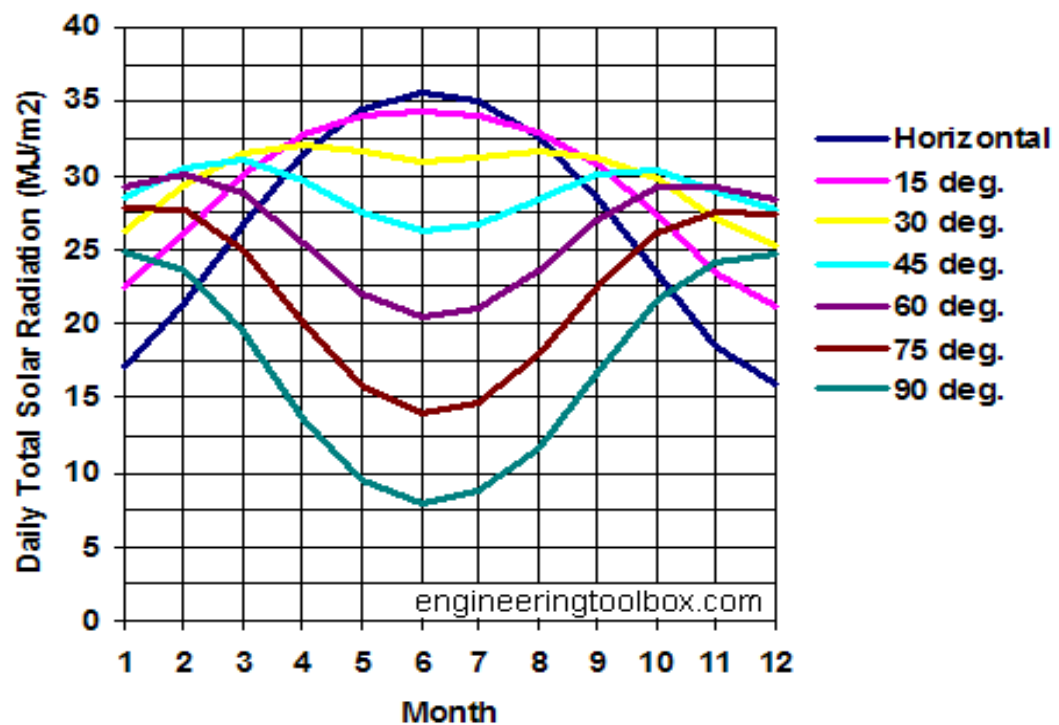
$$H_o = \frac{24 \times 3600}{\pi} G_{SC} \left[1 + 0.033 \cos \frac{360n}{365} \right] \int_0^{\omega_s} (\cos \delta \cos \phi \cos \omega + \sin \delta \sin \phi) d\omega$$

$$H_o = \frac{24 \times 3600}{\pi} G_{SC} \left[1 + 0.033 \cos \frac{360n}{365} \right] (\cos \delta \cos \phi \sin \omega_s + \omega_s \sin \delta \sin \phi) \quad (17)$$

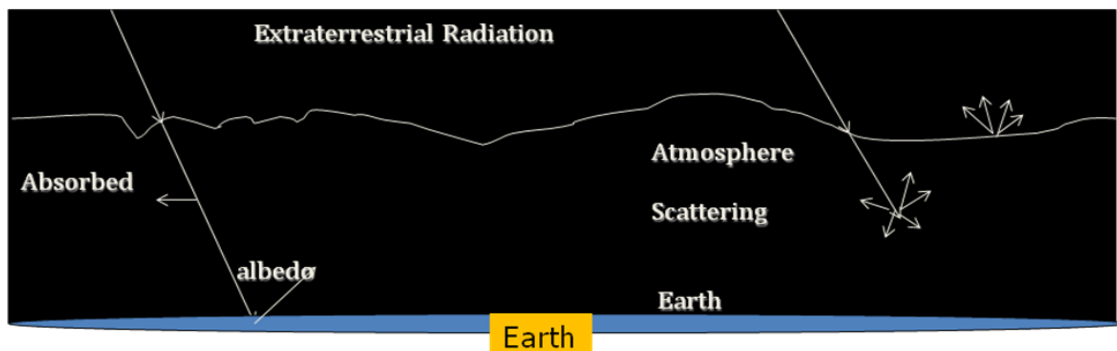
- Daily Extraterrestrial Insolation on horizontal surface



- Daily Extra-terrestrial Insolation with tilt angle β (Latitude 30deg)



Terrestrial solar radiation: Measurement and Calculation



- Terrestrial solar radiation is radiation available for use*
- Variation and attenuation in its values
 - Variation depending on time of the day, day of the year & place because of variation in Extra-terrestrial radiation
 - Attenuation because of scattering by air molecules, water vapour, and dust particles; absorption by ozone, Carbon dioxide, water and to a lesser extent by CO, O₂, CH₄, NO₂ etc. These meteorological and climatic parameters are variable.

N.B: Data of terrestrial solar radiation is always is given for horizontal surface unless otherwise mentioned.

Prediction/generation of terrestrial solar radiation data

- Not possible with reasonable degree of accuracy
- One of the following methods is used
 - By actual measurement using instruments on hourly or daily basis and representing it by Fourier type equations
 - Empirical Relation for Estimation of mean values of Radiation using average values of meteorological parameters
 - i. Estimation of average value using radiation data of a location in close proximity and with similar climate. It needs measured data of sunshine hours or cloudiness index
 - ii. Use extraterrestrial data and relate it with empirical equations for meteorological attenuating parameters such as - air mass, amount of precipitable water, dust particles, ozone layer etc.
- Radiation measurement using Instruments
 - Basis
 - a) Principle of measurement
 - b) Component of radiation measured
 - Types
 - a) Pyrheliometer
 - b) Pyranometer
 - c) Solarimeter
 - d) Actinometer
- Pyrheliometer: An instrument using a collimated detector for measuring solar radiation from sun and from a small portion of sky around it at normal incidence. Pyrheliometers are divided into two standards a) Primary Standard , and b) Secondary Standard

- Primary Standard: Abbot's Pyrheliometer, Angstrom compensation Pyrheliometer
- Secondary standard: Abbot Silver disc Pyrheliometer
- Abbot's Pyrheliometer
 - Single tube with absorbing cavity with cooling water around it.
 - Modified with two thermally identical absorbing cavities. One heated directly by solar radiation and the other electrically.
- Angstrom Compensation Pyrheliometer
 - Uses two blackened Manganin strips
 - Alloy : 86% copper, 12% manganese, and 2% nickel.
 - Virtually zero temperature coefficient of resistance(α) value and long term stability. Hence resistivity

$$\rho = \rho_o \{1 + \alpha(T - T_o)\}$$

$$\alpha = \frac{1}{\rho_o} \left(\frac{d\rho}{dT} \right) \approx 0$$

So resistivity is almost independent of temperature i.e. rise in temperature of such systems would have linear dependence on current. Temperature is dependent on radiation absorption equilibrium. The set-up is shown in the Fig3.

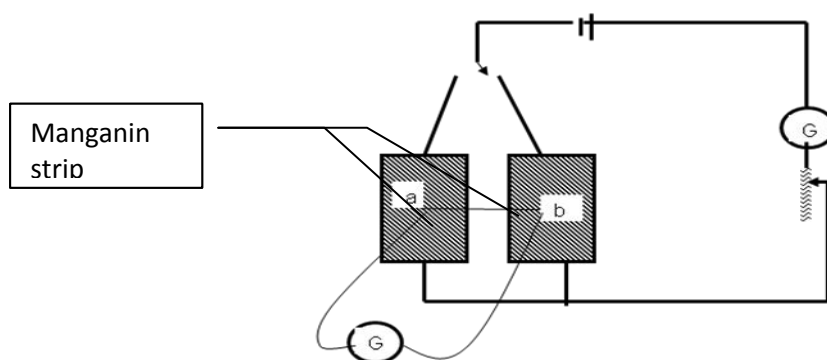
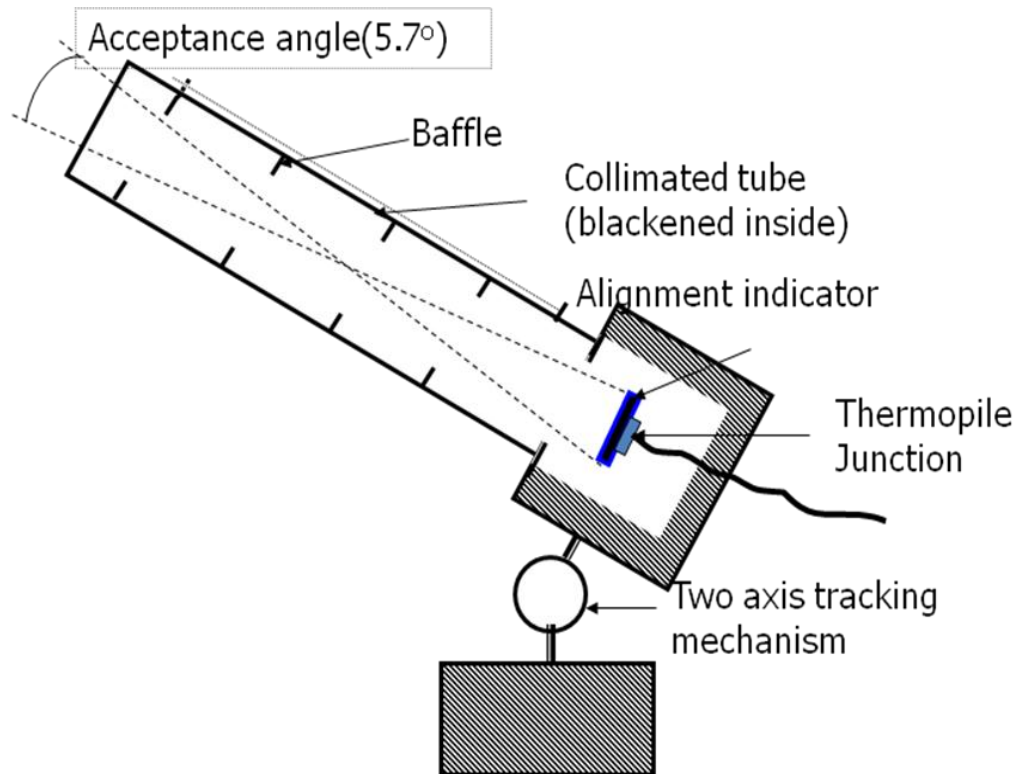


Fig 3 : Schematic for experimental set up for the temperature with respect to the radiation.

- Placed in a collimated tube one strip is heated by exposing to sun while the other is shaded and heated electrically to reach the same temperature. Three current values corresponding to first strip, second strip and again first strip heating are measured.
- Alternate the strips function to compensate for effects – i) Edge effects ii) non-uniform heating(losses)
- Average current is calculated, $I = i_1 + 2i_2 + i_3/4$, $V = \text{Known}$, $P = I \times V$

- Solar irradiance is found by equating the electrical energy to product of solar irradiance(G_{on}), strip area(A) and absorptance(α) of the strip.
- Drawbacks: Edge effects, Non-uniform heating
- Not fully primary because of problems in correction factors

- Abbot Silver Disc Pyrheliometer (Secondary Standard)



Abbot Silver Disc Pyrheliometer

Fig 4: Different parts of abbot Silver pyrheliometer



Fig.5: Photograph of Abbot's Silver Disc Pyrheliometer

- Working Principle: The black absorber heats-up after absorbing incident solar radiation. Its temperature rises till it reaches equilibrium. The hot end of thermopile is attached to the bottom of the absorber. Thermo-emf is calibrated to give solar beam irradiance. May be integrated to give hourly or daily values.
- Details:
 - Collimating tube made of Copper is provided with baffles and blackened from inside
 - Silver disc(38 mm dia, 7 mm thick) suspended at the end of collimating tube.
 - Silver disc is coated with Parson's black.
 - At the back of the disc the hot end of the thermopile is attached.
 - At any point the disc has an aperture angle of 5.7 degree i.e. about 0.0013 of hemisphere is seen by the silver.

- Operation:

Tube is always aligned in the direction of sun rays with two axis tracking mechanism. An alignment indicator is used to ensure proper alignment.

- Eppley Precision Pyranometer

A pyranometer is an instrument [Fig.6] which measures the the total hemispherical solar (beam+diffuse) radiation, usually on a horizontal surface. When shaded from beam radiation by a shading ring it can be used to measure diffuse radiation as well [Fig.7]. N.B.: It is a secondary standard calibrated against standard pyrheliometer on clear sky day by measuring total and diffuse radiation.

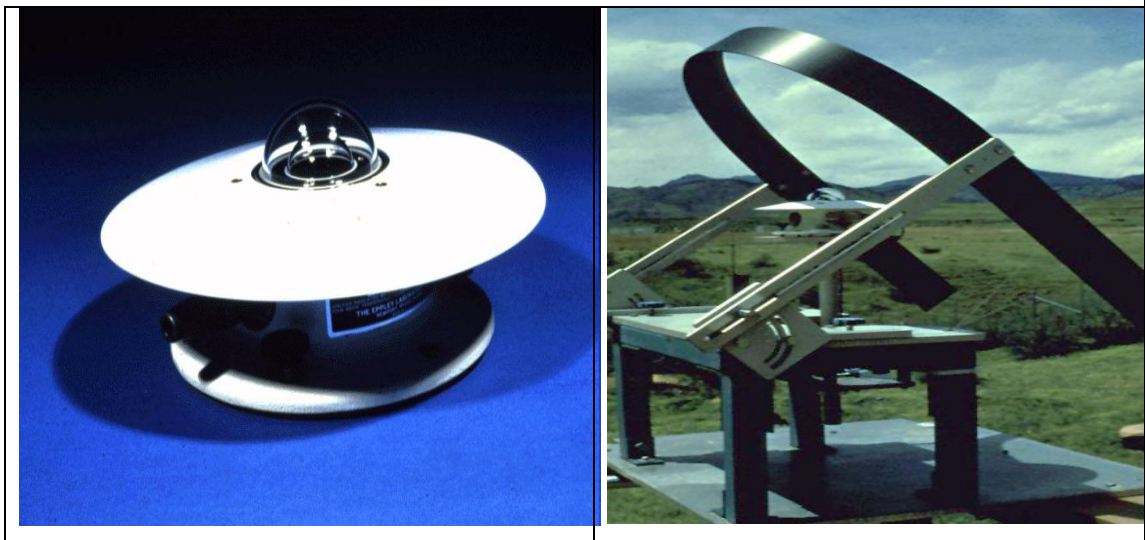


Fig.6: Photograph of pyranometer and shading ring

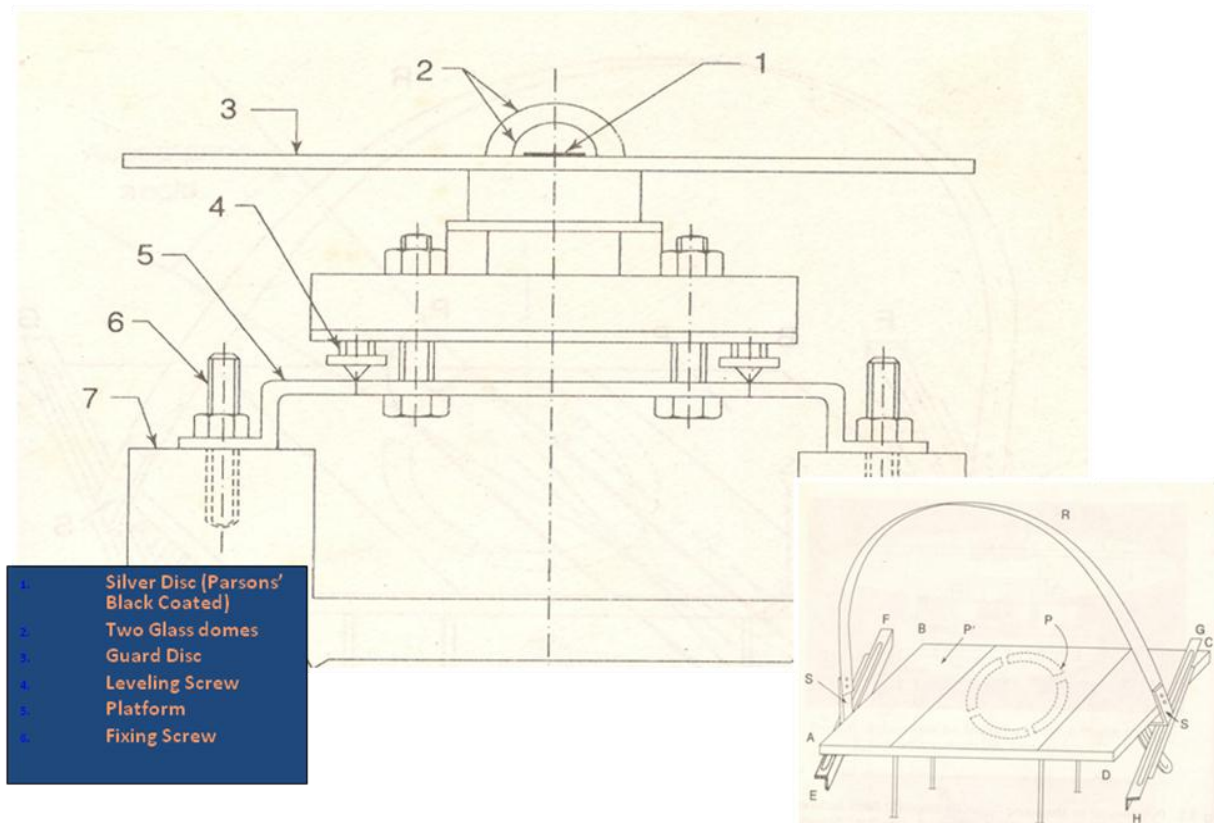
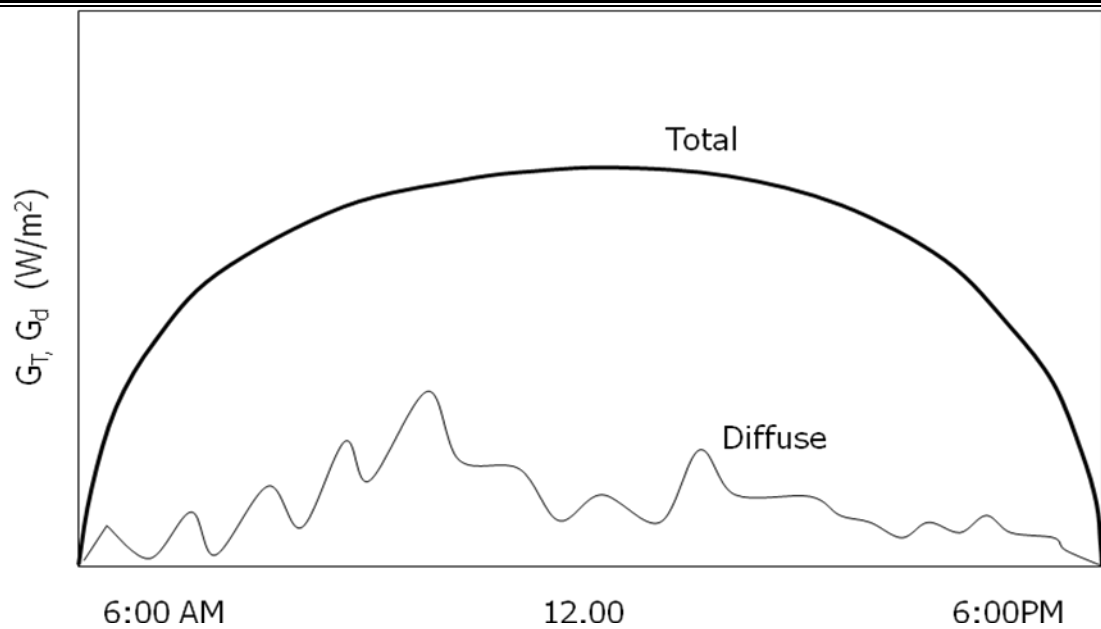


Fig 7: Schematic of Pyranometer and shading ring

- Working Principle: The black absorber heats-up after absorbing incident solar radiation. Its temperature rises till it reaches equilibrium. The hot end of thermopile is attached to the bottom of the absorber. Thermo-emf generated (0-10mV) is calibrated to measure the absorbed radiation. The instantaneous values may be integrated to give global radiation over a time.
- Details:
 - Blackened silver disc (dia 25 mm)
 - Hot junction of thermopile attached to the bottom.
 - Disc covered by two concentric hemispheric glass domes(dia 30 & 50 mm), Optically ground soda-lime glass, $\tau=0.90$. Why ?
 - Guard plate ?
 - Heavy base ?
 - Spirit level and leveling screws ?
- Measurement:
 - Thermopile e.m.f. is calibrated to give the value of radiation.
- Shading Ring:

- For measuring diffuse radiation Pyranometer is mounted at the centre of semi-circular (dia 450mm) shading ring(SR). The width of the ring is 50 mm. Its upper surface is coated dull white while inner surface is coated matt black.
 - SR's plane is in the plane of ecliptic of the sun across the sky. This keeps the black surface of the Pyranometer under shade from beam radiation during the day. Consequently Pyranometer measures only diffuse component.
 - SR is mounted on a platform on two sides of which two angle-iron arms with slots are fixed. On the carrying sliders in the slots the two ends of SR are fixed.
 -
 - Working:
 - The arms pivoted to the platform may be tilted around an axis passing through the centre of platform at an angle equal to latitude of the place.
 - The ring may be slid along the slots for fixing it according to the declination of the sun.
 - The platform may be rotated about vertical axis to take care of azimuth angle(due South in northern hemisphere).
 - Correction Factor:
 - A correction factor of 1.05 to 1.25 is needed to take care of the diffuse radiation blocked by the ring itself.
 - Detectors of Pyranometer as well as Pyrheleiometer
- Detectors are basically thermopile based on the principle of Seebeck effect. But coating and cover over them have an important role to play as
- Detector must have response independent of wavelength.
 - The detector's response must be independent of angle of incidence.
- Solar Radiation over a day



- Solarimeter

- Yellot's solarimeter: Based on Silicon PV cells. Spectral response is not linear due to inherent material property. So the instrument is calibrated as a function of the spectral distribution of solar radiation. CdS and Se cells are also used.

N.B. Plastic diffusers are used to avoid variation in calibration with the angle of incidence.

Spectral Response Graph

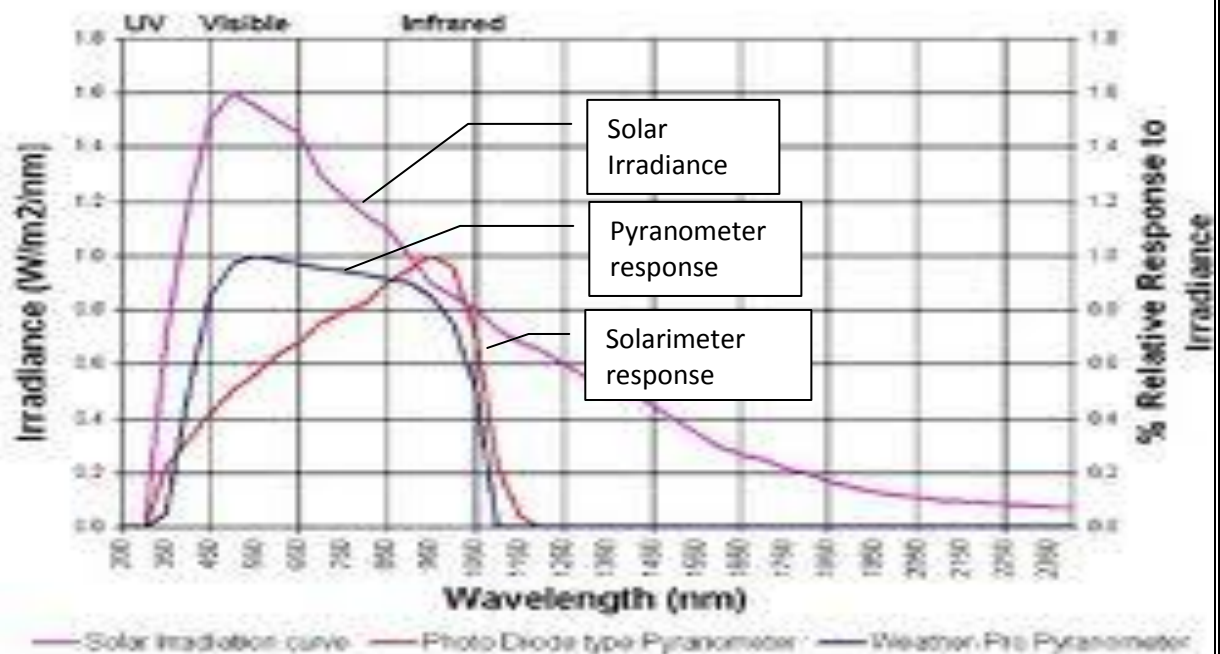


Fig.8: Solar Spectrum and Spectral response of Pyranometer and solarimeter

- Actinometer

- Two types: i) Potassium Ferrioxalate actinometer
ii) Uranyl Oxalate actinometer

- Used for photochemical studies
- Based on change in the oxidation states accompanied by change in colour of the solutions of the compounds.
- Change in colour is calibrated to give the amount (dose) of radiant exposure.
- Thus it gives the integrated value of the radiation which is absorbed unlike the others which give the value of incident radiation only.
- Sunshine Duration Recorder
 - Campbell-Stokes sunshine duration recorder [Fig.9]: It gives the hours of bright sunshine. It does not need external power and hence is quite useful.
 - Details:
 - Consists of a 10 cm dia spherical lens mounted concentrically with a spherical bowl.
 - At the focus specially treated papers of different sizes and shapes are fixed in a notch.
 - The burn mark length is calibrated to give the daylength.
 - Mounting:
 - Its azimuth angle is adjusted to due south.
 - Its focal axis connecting the treated paper is tilted at the latitude of the place.



Fig. 9. Photograph of Sunshine duration recorder and the calibrated strip

- Empirical estimation of available solar radiation (based on meteorological data)

If measured data for solar radiation is not available then it is possible to establish empirical relationship linking the radiation with meteorological parameters such as: Cloud cover, sunshine hours, precipitable water content, etc.

i) Monthly Mean Global Terrestrial Solar Radiation: Angstrom Relation

- Requires monthly mean sunshine duration hour (on a horizontal surface) data for the place

- The data can be measured using sunshine duration recorder (does not need electricity)

$$\frac{\bar{H}}{\bar{H}_c} = a' + b' \left(\frac{\bar{n}}{\bar{N}} \right) \quad (19)$$

Where a' and b' are empirical constants and

\bar{H} = Monthly mean daily radiation on a horizontal surface (J/m²) ?

\bar{H}_c = Monthly mean daily terrestrial clear sky for location & month
 \bar{n})

\bar{N} = Monthly mean daily actual bright sunshine hours on horizontal surface (hrs)
 = Monthly mean daily maximum possible bright sunshine hours on horizontal surface (hrs)

Here getting a clear day over a month for all the months is practically impossible. So it is difficult to estimate H_c =?

Page suggested a change. Use H_o in place of H_c .

$$\frac{\bar{H}}{\bar{H}_o} = a + b \left(\frac{\bar{n}}{\bar{N}_{\max}} \right) \quad (20)$$

where \bar{H}_o = Monthly mean daily maximum possible extraterrestrial radiation on a horizontal surface (J/m²) and , empirical constant a=0.30, b=0.34(for India)

For Pune, a=0.30, b=0.51 (monsoon)

a=0.41, b=0.34 (dry)

For Shillong, a=0.22, b=0.40

$$\frac{\bar{H}}{\bar{H}_o} = \bar{K}_T = \text{Monthly Clearness Index} \quad (21)$$

Solar radiation on a tilted surface

The measuring instruments give data on a horizontal surface. The same is true for empirical relations. But most of the solar systems are tilted at an angle with respect to the horizontal. So there is a need to calculate it on tilted surface. It is a sum of three components: beam, diffuse and albedo.

Tilt factor: for beam radiation for surface with $\gamma=0$

$$\text{For Diffi } r_b = \frac{\cos \theta}{\cos \theta_z} = \frac{\cos \delta \cos(\phi - \beta) \cos \omega + \sin \delta \sin(\phi - \beta)}{\sin \phi \sin \delta + \cos \phi \cos \delta \cos \omega} \quad (28) \text{uth angle}$$

$$r_d = \frac{1 + \cos \beta}{2} \quad (29)$$

For Albedo, assuming that the total radiation is reflected diffusively by the ground with reflectivity ρ , at any azimuth angle; $\rho = 0.2$ for normal ground and 0.7 for snow cover.

$$r_r = \rho \left(\frac{1 - \cos \beta}{2} \right) \quad (30)$$

- Hourly Insolation on a tilted surface =

$$I_T = I_b r_b + I_d r_d + (I_b + I_d) r_r \quad (31)$$

Dividing by I

$$\frac{I_T}{I} = \left(1 - \frac{I_d}{I} \right) r_b + \frac{I_d}{I} r_d + r_r \quad (32)$$

Eqn(32) can be used to calculate monthly mean hourly values i.e. I_T

$$\frac{\bar{I}_T}{\bar{I}} = \left(1 - \frac{\bar{I}_d}{\bar{I}} \right) \bar{r}_b + \frac{\bar{I}_d}{\bar{I}} \bar{r}_d + \bar{r}_r \quad (33)$$

where $\bar{r}_b = r_b, \bar{r}_d = r_d$ and $\bar{r}_r = r_r$

- Daily radiation on a tilted surface follow the similar relation (Liu and Jordan). However the hour angle needs to be averaged out over the day

$$\frac{H_T}{H} = \left(1 - \frac{H_d}{H} \right) R_b + \frac{H_d}{H} R_d + R_r \quad (34)$$

For south facing surface, $\gamma=0^\circ$

$$R_b = \frac{\cos \delta \cos(\phi - \beta) \cos \omega_{st} + \omega_{st} \sin \delta \sin(\phi - \beta)}{\cos \phi \cos \delta \cos \omega_s + \omega_s \sin \phi \sin \delta} \quad (35)$$

$$R_d = r_d = \frac{1 + \cos \beta}{2} \quad (36)$$

$$R_r = r_r = \rho \left(\frac{1 - \cos \beta}{2} \right) \quad (37)$$

In equn.(35) ω_{st} , and ω_s are sunset(sunrise) hour angle for tilted and horizontal surface. Eqn. (38) may be used to calculate monthly mean daily total radiation on a tilted surface if values for a representative day of month are known

$$\frac{\bar{H}_T}{\bar{H}} = \left(1 - \frac{\bar{H}_d}{\bar{H}}\right) \bar{R}_b + \frac{\bar{H}_d}{\bar{H}} \bar{R}_d + \bar{R}_r \quad (38)$$

$$\bar{R}_r = R_r = \rho \left(\frac{1 - \cos \beta}{2} \right) \quad (40)$$

$$R_d = r_d = \frac{1 + \cos \beta}{2} \quad (36)$$

$$R_r = r_r = \rho \left(\frac{1 - \cos \beta}{2} \right) \quad (37)$$

$$R_d = r_d = \frac{1 + \cos \beta}{2} \quad (36)$$

$$R_r = r_r = \rho \left(\frac{1 - \cos \beta}{2} \right) \quad (37)$$

$$\bar{R}_d = R_d = \frac{1 + \cos \beta}{2} \quad (39)$$

**UNIT-2: BASICS OF SOLAR THERMAL
CONVERSION**

This unit covers the basics of conversion of solar radiation flux to utilizable form. One of the utilizable forms is thermal energy which finds a number of applications in different sectors of human activities. Solar collectors are the systems used to convert solar energy to thermal energy. All these follow the same basic principle. It has been explained in detail using one such solar collector commonly known as flat plate collector system. The role of materials and interfaces, specially the selective coating on the absorbers, used in the flat plate and other such collectors have been discussed to understand the upper limit of performance of solar thermal collectors.

INTRODUCTION²

In spite of being Carnot-limited most of the current technologies are driven by thermal cycles. Hence solar thermal conversion is a logical route of utilization of solar energy. This technology utilizes the total spectrum of solar radiation. Thermodynamically the upper limit of achievable temperature by solar thermal conversion systems is about 6000°K i.e. sun's effective black body temperature. But practically a temperature upto 3500°C has been demonstrated using concentrators. Although useful, high temperature application of solar energy does not have favorable economics. Also about 25% of the thermal energy needs of industries are at 100°C which is a temperature at which the overall cost of solar thermal energy becomes comparable to conventional fossil fuel thermal energy. Further at this temperature the thermal conversion efficiency is relatively high.

This cost-effective solar driven technology may be used in water heating, air heating, space conditioning, etc. Most of these systems work in passive mode and do not need auxiliary energy systems. Larger systems may need some active energy support mainly in the form of pumps or blowers.

The heart of solar thermal systems, which collects; absorbs; and converts solar radiation, is termed as "Collector". Based on shape, special features, materials, working fluid, temperature, etc. a suitable prefix is added to this.

The major challenge in utilizing these collectors is their low efficiency at high temperatures and need of costly storage systems.

Some important applications of this technology are in green houses (crop conditioning/growing), crop drying, solar chick brooding (poultry), solar cooking, milk pasteurization, water distillation/purification, space heating, water heating, space cooling and refrigeration, passive architecture (windows), power generation, industrial process heat, etc. It may be seen that it may support most of the basic energy needs of human activity.

Classification of Solar Thermal Systems

² For this chapter knowledge of heat transfer and optical characteristics of materials is a prerequisite.

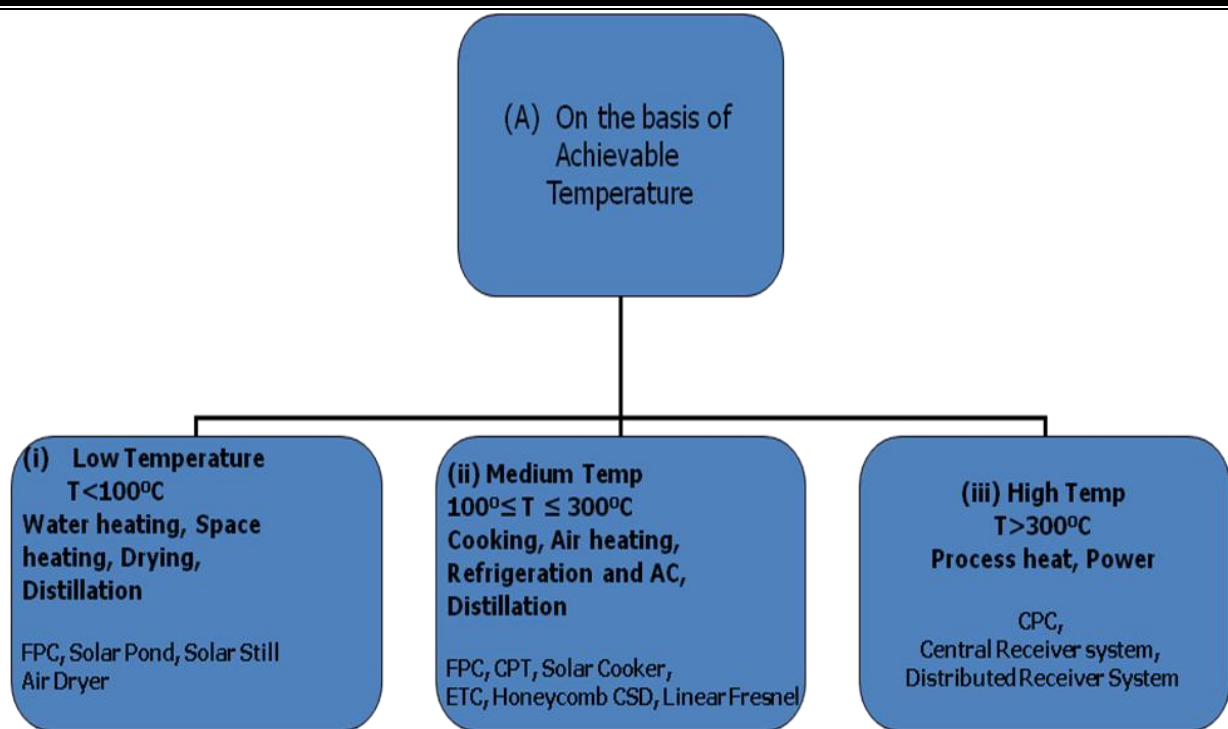


Fig 1: Classification of Solar thermal system on the basis of achievable temperature

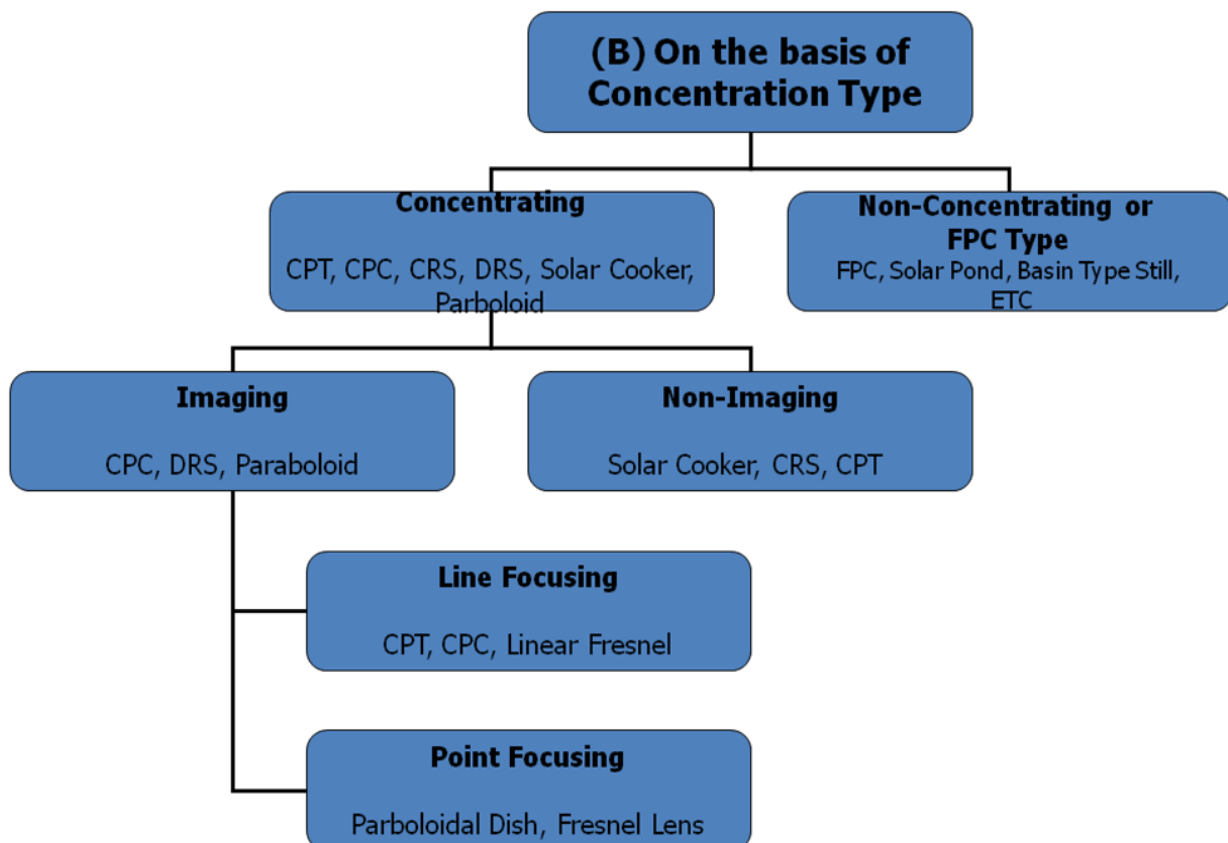


Fig 2: Classification of Solar thermal system on the basis of concentration type
Basic principle

The temperature of any surface rises on which solar radiation falls. The achievable efficiency depends upon the

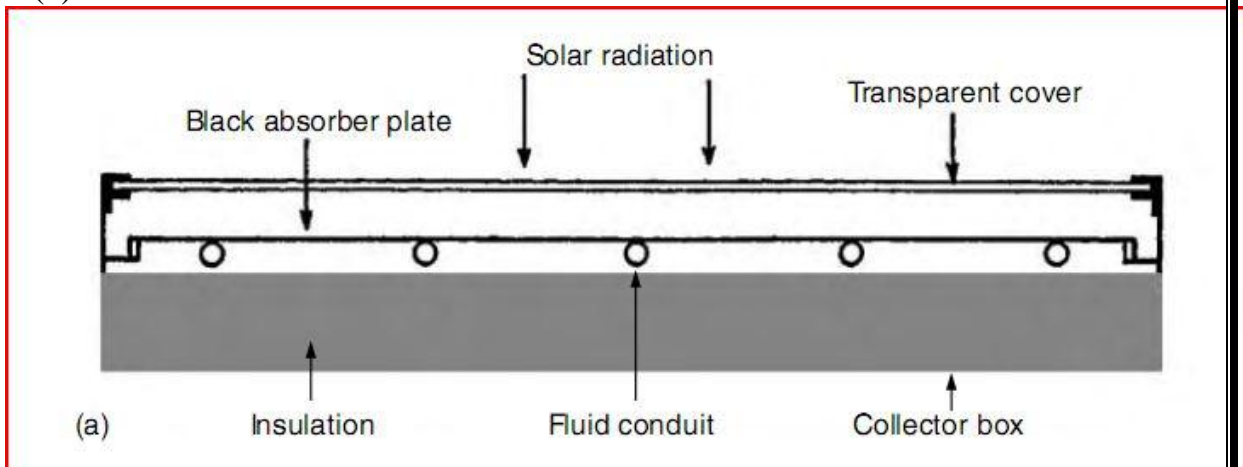
- absorption characteristics of the material of the surface,
- thermal Losses from the collector, and

c. energy extraction from the collector.

Flat Plate Collectors

A solar collector is the heart of any solar thermal system. Flat Plate Collectors or FPCs are one of the most important solar collectors. To understand different types of collectors the construction and working of FPCs is initially discussed. An FPC can easily achieve a temperature about 80°C above ambient temperature on a clear day with solar irradiance of about $600\text{W}/\text{m}^2$ or above. It uses both beam and diffuse components of solar radiation. It

(a)



(b)

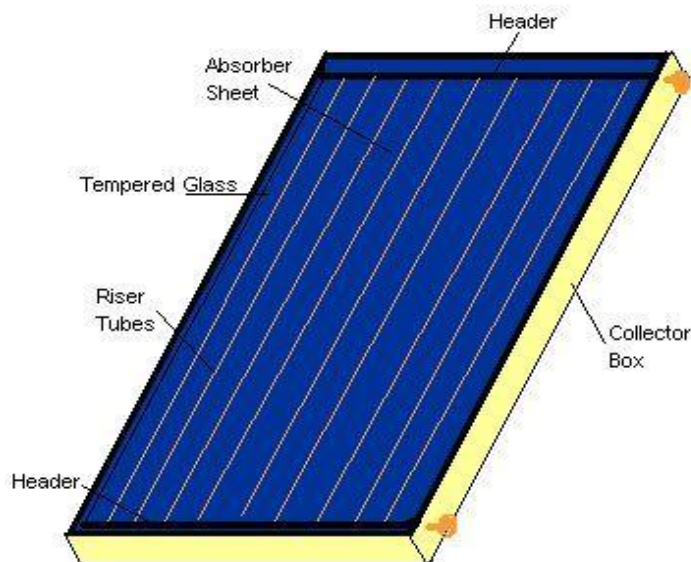


Fig 3: Basic part of a Flat plate collector

does not require tracking and requires little maintenance. Its thermal conversion efficiency is about 45% at 80°C . It may be used in applications like air heating, water heating, industrial process heating, passive air conditioning.

Basic parts of an FPC is shown in Fig 3:

A) Absorber plate

B) Transparent cover(s)(Glazing) of diathermous material

C) Bottom and side insulation

D) Tubes (in liquid FPC) or ducts (in air FPC) fixed under the absorber

E) Container(box or casing)

(A) Absorber plate:

It has two functions- i) to absorb solar energy, and ii) to transfer it in the form of heat to a working fluid like a heat exchanger.

Thus the desirable characteristics of an FPC are high thermal conductivity, adequate mechanical strength, good corrosion resistance, high solar absorptance, and low thermal emittance. The materials which qualify for this are copper, aluminium, steel(0.2 to 1mm thick), and polymers(1-mm thick). Out of these copper is preferred because of its relatively low corrosion resistance. Aluminum and steel on the other hand need chlorine, calcium and iron-free water. The absorber plate has black coating or pigmentation having high absorptance for solar radiation spectrum. The surface of the FPC may be flat, corrugated or grooved to enhance absorptance. It is normally 2m x 1m in size. Two dissimilar metals are not used in an absorber because the galvanic effect between dissimilar metals makes the joints unstable.

(B) Transparent cover:

The transparent cover is expected i) to reduce convection and re-radiation losses to the atmosphere and ii) to shield the absorber from weather(rains etc.) exposure. Hence the desirable characteristics are high solar transmittance, good mechanical strength, high durability, and non-degradability under adverse conditions.

Materials which fit into the criteria are glass(4-5mm thick) (preferably toughened, tempered), transparent Polymers like Teflon[®] (FEP, Poly fluoro-ethylene propylene), Tedlar[®] (PVF, Polyvinyl Fluoride), Mylar[®] (PET, Polyethylene Tetraphthalate) etc..

One or many transparent covers may be put over the absorber such that the absorber-cover spacing is about 8cm, and cover-cover spacing is between 1.5-3 cm. The variation depends upon the other design, material and operational parameters.

N.B.: Different types of sealant are used but silicone based sealant is preferred.

(C) Insulation:

Its main function is to reduce the losses from bottom and sides. In addition it is expected to support the structure. The insulation must have low thermal conductivity, should be non-degradable, should not degas, should be self-supporting, and should not sag (settle under its own load).

The most materials used for this purpose are glass wool, mineral wool, rock wool of 5-8 cm thickness. Please note that a reflecting sheet usually of aluminum foil is also used between absorber and insulator to reduce radiative thermal losses. A list of insulating and other related material is given in Table 1.

Table 1: Different type of insulating material used in Flat plate collector

Material	Conductivity,k (W/mK)	Material	Conductivity,k (W/mK)
Air	0.026 (at 20°C)	PUF (Poly urethane Foam)	0.024
Glass	1.05	Water	0.6(at 20°C)
Glasswool	0.04	Rockwool	0.02
Mineral wool	0.034	Thermocole	0.035(below 70°C)

(D) Tubes/Ducts/Manifolds:

Two sets of tubes are used in normal liquid collectors. The riser tubes which allow the heat to be transferred to the fluid in it and to make the fluid to flow up. Riser tubes are connected in parallel to two header tubes responsible for admitting or discharging the fluid in and out of FPC.

Desirable characteristics of the tubes are high thermal conductivity, matching thermal expansion property with that of the absorber and easy bonding with absorber plate. Material used are copper, galvanized iron(GI) tubes, stainless steel(SS) channel (normally in-built), polymeric channels(in-built). The size of the riser is 1-1.5 cm ID(Pitch 5-12 cm) and that of the header is 2-2.5cm ID.

N.B. Bonding may be soldered, brazed, welded, pressure-bonded, ultrasonically welded. Ultrasonic welding gives superior performance.

(E) Container:

Its basic functions are to protect absorber and insulator from dust and moisture and to support the FPC structure.

Material may be aluminum, steel, or fibre reinforced plastic(FRP). The normal size of container is 2m x 1m x 0.1m.

Working

Figure shows the physical arrangements of the major components of a conventional flat-plate collector with a liquid working fluid. The blackened absorber is heated by radiation admitted via the transparent cover. Thermal losses to the surroundings from the absorber are contained by the cover, which is opaque to the infrared radiation and by insulation provided under the absorber plate. Passages attached to the absorber are filled with a circulating fluid, which extracts energy from the hot absorber. The simplicity of the overall device makes for long service life.

The absorber is the most complex portion of the flat-plate collector, and a great variety of configurations are currently available for liquid and air collectors. Fig 4. Illustrates some of these concepts in absorber design for both liquid and air absorbers. The material used and their details have already been discussed. The absorber designs may also vary a lot. Bonded plates having internal passageways perform well as absorber plates because the

hydraulic passage ways can be designed for optimal fluid and thermal performance. Such collectors are called *roll-bond collectors*. Another common absorber consists of tubes soldered or brazed to a single metal sheet, and mechanical attachments of the tubes to the plate have also been employed. This type of collector is called a *tube-and-sheet collector*. *Heat pipe collectors* have also been developed, though these are not as widespread as the previous two types. The so-called *trickle type of flat-plate collector*, with the fluid flowing directly over the corrugated absorber plate, dispenses entirely with fluid passageways. *Evacuated Tubular collectors* have also been used because of the relative ease by which air can be evacuated from such collectors, thereby reducing convective heat losses from the absorber to the ambient air. The absorber in an air collector normally requires a larger surface than in a liquid collector because of the poorer heat transfer coefficients of the flowing air stream. Roughness elements and producing turbulence by way of devices such as expanded metal foil, wool, and overlapping plates have been used as a means for increasing the heat transfer from the absorber to the working fluid. Another approach to enhance heat transfer is to use packed beds of expanded metal foils or matrices between the glazing and the bottom plate. Accordingly the liquid and air collectors have variation in their characteristics(see Table)

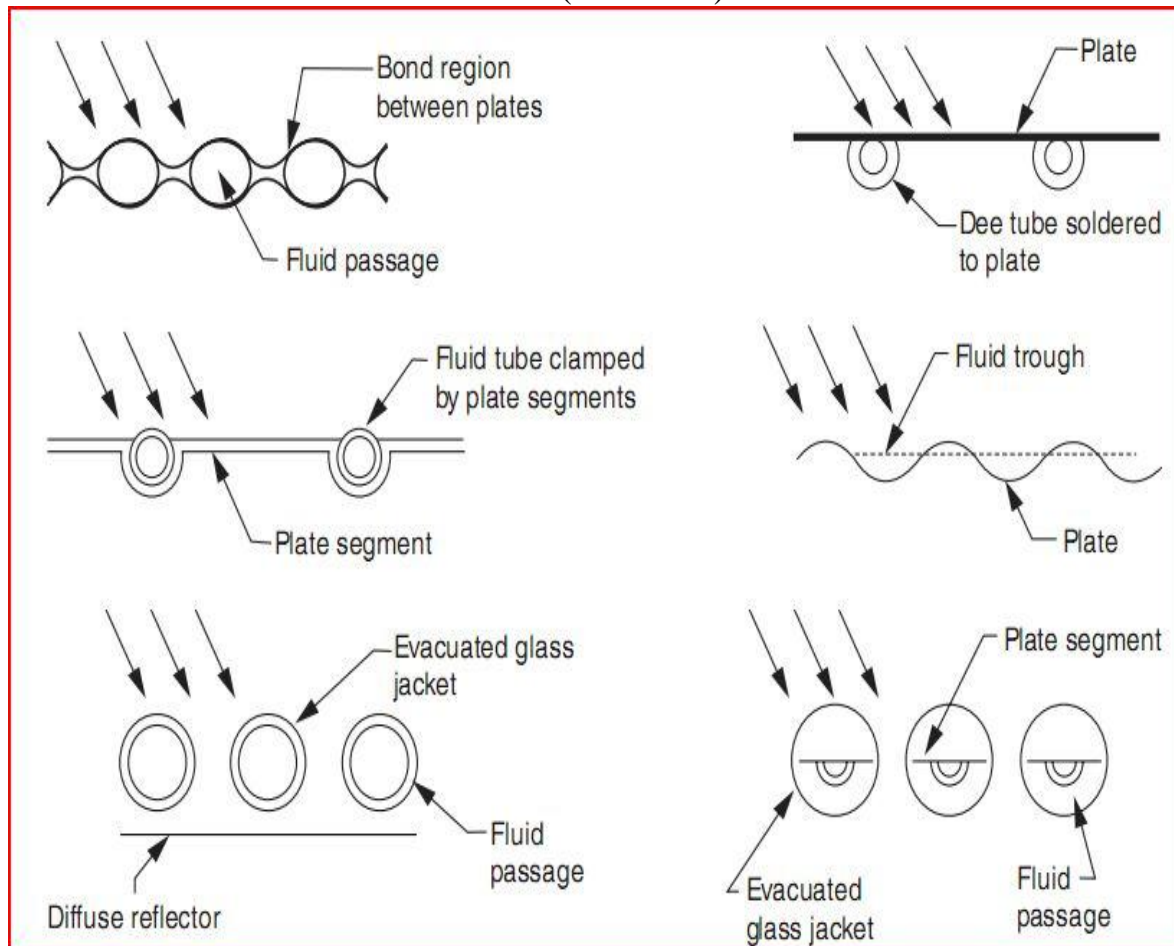


Fig 4: Absorber types with different shapes and bonding

Table 2: Variation in Liquid and air collector characteristics

<i>Characteristics</i>	<i>Liquid</i>	<i>Air</i>
Efficiency	Collectors generally more efficient for a given temperature difference	Collectors generally operate at slightly lower efficiency
System configuration	Can be readily combined with service hot-water and cooling systems	Space heat can be supplied directly but does not adapt easily to cooling. Can preheat hot-water
Freeze protection	May require antifreeze and heat exchangers that add cost and reduce efficiency	None needed
Maintenance	Precautions must be taken against leakage, corrosion and boiling	Low maintenance requirements. Leaks repaired readily with duct tape, but leaks may be difficult
Space Requirements	Insulated pipes take up nominal space and are more convenient to install in existing buildings	Duct work and rock storage units are bulky, but ducting is a standard HVAC installation technique
Operation	Less energy required to pump liquids	More energy required by blowers to move air; noisier operation
Cost	Collectors cost more	Storage costs more
State of the art	Has received considerable attention from solar industry	Has received less attention from solar industry

Energy Balance Equation for FPC

For evaluation of thermal performance of a solar thermal collector energy balance equation is developed. It includes the balance of solar energy absorbed, the portion utilized and the portion lost as optical and thermal losses. For an FPC of area A_c the useful energy is

$$\dot{Q}_u = A_c S - \dot{Q}_L - \frac{dQ_s}{dt} \quad (1)$$

$$\dot{Q}_u = A_c [S - U_L (T_{pm} - T_a)] - \frac{dQ_s}{dt} \quad (2)$$

The *Instantaneous Collector Efficiency* η_i is given as the ratio of useful energy gain and the incident solar energy

$$\eta_i = \frac{\dot{Q}_u}{A_c G_T} \quad (3)$$

τ is time period over which it is averaged.

$$\eta = \frac{\int_0^\tau \dot{Q}_u d\tau}{A_c \int_0^\tau G_T d\tau} \quad (4)$$

The detailed analysis of a collector is complicated because the temperature of the absorber across the risers and along the riser tubes are not constant shown in Fig

5.

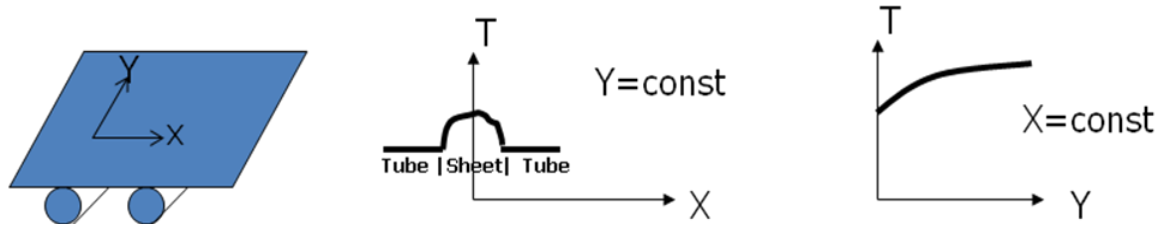


Fig 5: Temperature of collector across and along the riser tubes

But it is possible to simplify the problem without obscuring the physical situation. These are

- i) **The collector is under thermal steady state.**
- ii) Irradiation on the collector is uniform.
- iii) There is no absorption of solar energy by glass covers and heat flow through them is one-dimensional.
- iv) The temperature drop between top and bottom of the absorber plate is negligible
- v) There is one-dimensional heat flow through back and side insulations.
- vi) The sky may be considered to be black body for long-wave radiation at an equivalent sky temperature.
- vii) Properties are independent of temperature.
- viii) Losses are to the ambient.

Stagnation Temperature: If heat is not taken out through the absorber plate then a stage is reached when the solar energy absorbed is lost as heat to the environment. Then

Energy Gained = Energy Lost

$$\dot{Q}_L = A_c S \quad (5)$$

Here T_{pm} is the highest temperature the collector can attain. This can be one of the relative performance indicators.

Calculation of solar radiation absorbed (S):

where
$$S = G_b R_b (\tau\alpha)_b + G_d R_d (\tau\alpha)_d + G_T \rho (\tau\alpha)_d \quad (6)$$

$$\begin{aligned} \rho_d (\tau\alpha)_b &= \frac{\tau\alpha}{1 - (1 - \alpha)\rho_d} \quad (7) \\ &= 0.15 \text{ (1 glass cover)} \\ &= 0.22 \text{ (2 glass cover)} \\ &= 0.24 \text{ (3 glass cover)} \end{aligned} \quad (8)$$

However in equations $S = G_T (\tau\alpha)_{aver}$ or $G_T (\tau\alpha)$ is used where $(\tau\alpha)$ is weighted average across the solar spectrum for all the components.

$$(\tau\alpha)_d = (\tau\alpha)_b, \theta = 60^\circ \quad (9)$$

Calculation of overall heat loss factor (U_L):

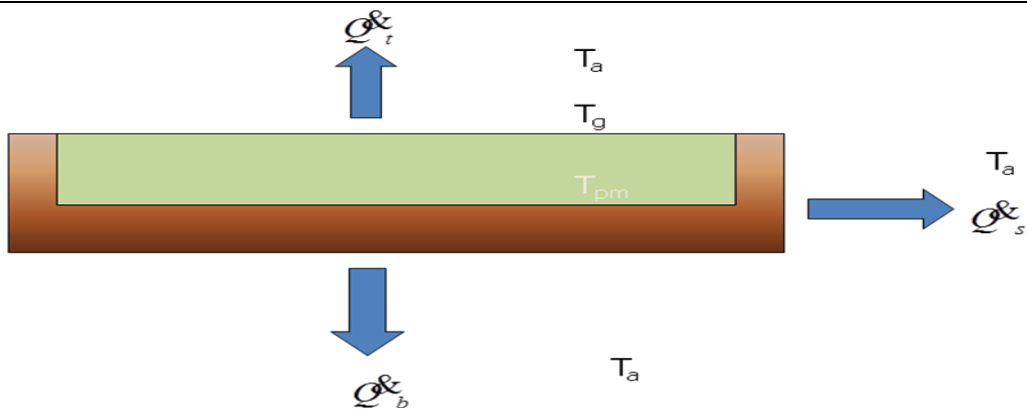


Fig 5: Heat loss through top, bottom and sides

Here overall rate of heat loss is

$$\dot{Q}_L = U_L A_C (T_{pm} - T_a) \quad (10)$$

$$\dot{Q}_L = \dot{Q}_t + \dot{Q}_b + \dot{Q}_s \quad (11)$$

where top, bottom and side losses are defined as

$$\dot{Q}_t = U_t A_C (T_{pm} - T_a) \quad (12)$$

$$\dot{Q}_b = U_b A_C (T_{pm} - T_a) \quad (13)$$

Substituting (12), (13), and (14) in (11) we get

$$U_L = U_t + U_b + U_s \quad (15)$$

Calculation of values of heat losses:

$$\dot{Q}_b = K_b A_b \frac{(T_{pm} - T_a)}{t_b} \quad (16)$$

Equating (16) and (17) with (13) and (14) respectively

$$\dot{Q}_b = U_b A_c (T_{pm} - T_a) = K_b A_b \frac{(T_{pm} - T_a)}{t_b} \quad (19)$$

$$U_b = \frac{K_b A_b}{A_c t_b} \quad (20)$$

Calculation of top heat loss factor(U_t):

U_t can be determined in two ways shown in Fig 6:

- By developing heat balance equation and solving them numerically
- By developing analytical/empirical relations for the purpose

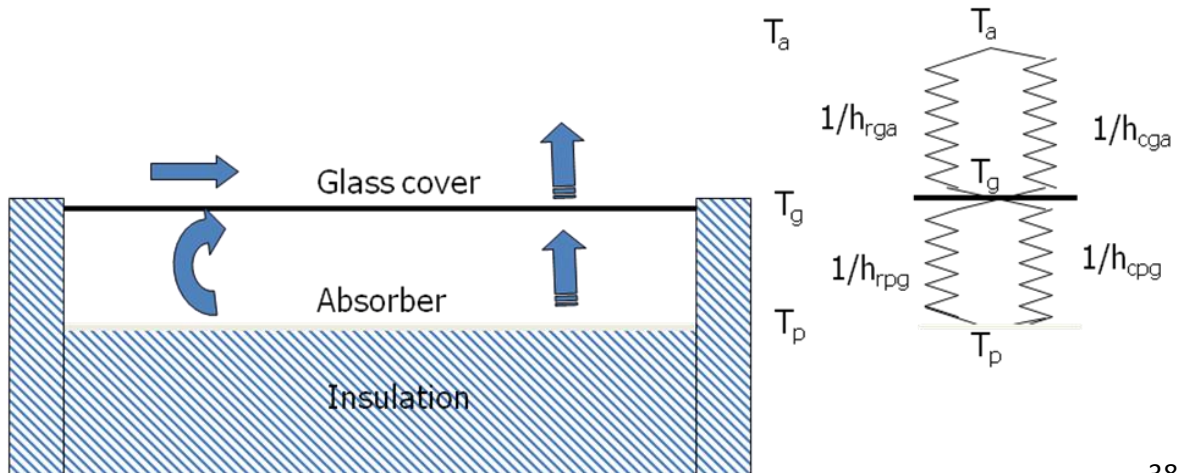


Fig 6: Top heat loss of Flate plate collector

$$\dot{Q}_{ga} = A_c \left[h_{cga} + h_{rga} \right] (T_g - T_a) \quad (22)$$

$$\dot{Q}_{pa} = A_c U_t (T_p - T_a) \quad (24)$$

$$U_t = \left[\frac{\dot{Q}_{pa}}{A_c (T_p - T_a)} \right] \quad (25)$$

Radiative heat transfer coefficient between absorber plate and glass cover

$$h_{rpg} = \frac{\sigma (T_{pm}^2 + T_g^2) (T_{pm} + T_g)}{\frac{1}{\varepsilon_p} + \frac{1}{\varepsilon_g} - 1} \quad (26)$$

Radiative heat transfer coefficient between glass cover and ambient

Radiative heat transfer coefficient between glass cover and sky i.e. assuming radiative heat loss from glass cover to the sky at sky temperature T_s

$$h_{rgs} = \frac{\sigma \varepsilon_g (T_g^4 - T_s^4)}{(T_g - T_a)} \quad (27)$$

$$\text{Swinbank's } h_{rgs} = \frac{\sigma \varepsilon_g (T_g^4 - T_s^4)}{(T_g - T_a)} \quad (28)$$

Convective heat transfer coefficient between glass cover and ambient is given in terms of wind heat transfer coefficient which according to McAdam's(1954) correlation is

$$h_{cga} = h_w = 5.7 + 3.8 V_w \quad (30)$$

$$= 8.55 + 2.56 V_w \text{ (Test et al 1981)} \quad (30a)$$

Convective heat transfer coefficient between plate and glass cover is given using KGT Hollands' relation for Nusselt number,

$$Nu = 1 + 1.44 \left[1 - \frac{1708}{Ra'} \right]^+ + \left[1 - \frac{(\sin 1.8\beta)^{1.6} 1708}{Ra'} \right]^+ \left[\left(\frac{Ra'}{1708} \right)^{1/3} - 1 \right]^+ \quad (31)$$

$$Nu = \frac{\text{Convective heat transfer coefficient}}{\text{Conductive heat transfer coefficient}} = \frac{h_c L}{k} \quad (32)$$

$$h_c = \frac{Nu \times k}{L} \quad (33)$$

where $h_c = h_{cpg}$

Empirical Relations for U_t :

i) One of the most popular relations is by Klein(1975)

$$U_t = \left[\frac{M}{\left(\frac{C}{T_{pm}} \right) \left(\frac{T_{pm} - T_a}{M + f} \right)^{0.33}} + \frac{1}{h_w} \right]^{-1} + \left[\frac{\sigma (T_{pm}^2 + T_a^2) (T_{pm} + T_a)}{\frac{1}{\varepsilon_p + 0.05M(1 - \varepsilon_p)} + \frac{(2M + f - 1)}{\varepsilon_c} - 1} \right] \quad (34)$$

where, $f=(1-0.04h_w+0.0005h_w^2(1+0.091M))$
 $C=365.9(1-0.00883\beta+0.0001298\beta^2)$
 M =number of glass cover
 T in K, h_w in W/m^2K and σ in W/m^2-K^4
and is valid for $320 \leq T_{pm} \leq 420$ K
 $260 \leq T_a \leq 310$ K
 $0.1 \leq \epsilon_p \leq 0.95$
 $1 \leq M \leq 3$
 $0 \leq \beta \leq 90^\circ$

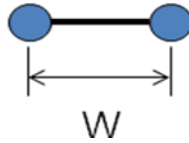
ii) The other more analytical correlation developed by Samdarshi and Mullick(1994) is

$$U_t^{-1} = \left[h_{cpg} + \frac{\sigma(T_{pm}^2 + T_g^2)(T_{pm} + T_g)}{\frac{1}{\epsilon_p} + \frac{1}{\epsilon_g} - 1} \right]^{-1} + (N-1) \left[h_{cgg} + \frac{\sigma(T_1^2 + T_N^2)(T_1 + T_N)}{2\epsilon_g^{-1} - 1} \right]^{-1}$$

where $\Delta T = (T_p - T_N)/N = (T_p - T_a)/(N+f)$; $T_N = T_a + (N+f)\Delta T$;
 $f = (5/h_w)^{1/2} + [h_w + \sigma \epsilon_g (T_N^2 + T_a^2)(T_N + T_a)]^{-1} + \frac{Nt_g}{k_g}$ (35)

Collector Efficiency Factor:

To calculate U_L T_{pm} must be known. But it is difficult to measure it with reasonable degree of accuracy. But T_{pm} may be related to T_f and inlet fluid temperature T_{fi} .



Consider plate at local fluid temperature T_f then useful energy gain rate per unit length of collector in flow direction

$$q'_u = WF'(S - U_L(T_f - T_a)) \quad (36)$$

$$\text{where } T_f = (T_{fi} + T_{fo})/2 \quad (37)$$

F' is the **Collector Efficiency Factor**

F' is defined as the ratio of useful energy gain to the useful energy gain that would occur if absorber plate is at local fluid temperature. In most geometries

$$F' = U_o/U_L \quad (38)$$

U_o = Heat transfer coefficient between fluid and ambient air

Some important points to be noted here is

- F' is constant for a collector design and fluid flow rate.
- It decreases with increase in W .
- It increases with absorber plate and tube thickness and thermal conductivity of their material.
- It decreases with increase in U_L .
- It has value between 0 – 1.

Collector Heat Removal Factor(F_R):

It is the ratio of actual useful energy gain of the collector to the useful energy gain that would occur if the whole absorber plate is at inlet fluid temperature.

$$F_R = \frac{\dot{m}C_p (T_{fo} - T_{fi})}{A_c [S - U_L (T_{fi} - T_a)]} \quad (39)$$

F_R can be expressed as

$$F_R = \frac{\dot{m}C_p}{A_c U_L} \left[1 - \exp \left(- \frac{A_c U_L F'}{\dot{m}C_p} \right) \right] \quad (40)$$

where C_p = Fluid's specific heat capacity

F' = Collector efficiency factor

It may be noted that

- F_R can never exceed F' .
- Its value ranges between 0-1.
- It is equivalent to conventional heat exchanger effectiveness.
- It is a measure of the thermal resistance encountered by absorbed solar radiation in reaching the collector fluid.

Collector Flow Factor(F'')

It is defined as the ratio of F_R and F' .

$$F'' = \frac{F_R}{F'} = \frac{\dot{m}C_p}{A_c U_L F'} \left[1 - \exp \left(- \frac{A_c U_L F'}{\dot{m}C_p} \right) \right] \quad (41)$$

It can be seen that F'' is a function of single dimensionless variable called *Collector Capacitance Rate* and is given by

$$\frac{\dot{m}C_p}{A_c U_L F'} \quad (42)$$

Hottel Whillier-Bliss(HWB) Equation:

Using the relation for F_R we have

$$\mathcal{Q}_u = F_R U_L [S - U_L (T_{fi} - T_a)] \quad (43)$$

It is one of the *most important equations* and is used for calculating energy gain in terms of known/measurable quantity i.e. fluid inlet temperature.

Hence efficiency

$$\eta = F_R U_L \left[(\tau\alpha)_e - \frac{U_L (T_{fi} - T_a)}{G} \right] \quad (44)$$

Problem: Calculate the hourly collector efficiency between 10-11 AM when $T_a=2^\circ\text{C}$, $I_T=3.92 \text{ MJ/m}^2$, $S=3.29 \text{ MJ/m}^2$, $U_L=8.0 \text{ W/m}^2$, $F'=0.841$. The flow rate through the collector is 0.03 kg/s and inlet fluid temperature $=40^\circ\text{C}$. Given $C_p=4190 \text{ J/kg/C}$, $A_c=2 \text{ sq.m}$.

$$F'' = \frac{F_R}{F'} = \frac{m\dot{C}_p}{A_c U_L F'} \left[1 - \exp\left(-\frac{A_c U_L F'}{m\dot{C}_p}\right) \right]$$

$$9.35 \text{ J/K}$$

$$\eta = \frac{Q_u}{A_c I_T} = \frac{q_u}{I_T} = \frac{F_R [S - U_L (T_{fi} - T_a)]}{I_T}$$

$$\eta=0.45$$

Parameters Affecting FPC Performance:

Classification of parameters

1. Design parameter: Number of Glass cover(N); Plate glass and glass-glass spacing(L); Solar absorptance of absorber(α_{solar}), Thermal emittance of absorber($\epsilon_{\text{thermal}}$), Transmittance of cover(τ), Collector heat removal factor (F_R), Insulation Thickness(t), Insulation conductivity(k).
2. Operational parameter: Tilt angle(β); Absorber temperature(T_p), Inlet fluid temperature(T_{fi})
3. Meteorological parameters: Ambient temperature(T_a), Incident flux(G_T), Wind velocity(v_w), Humidity(H)
4. Environmental parameters: Dust on the glass cover

Number of Glass Covers(N):

- Normally $N=1$ or 2

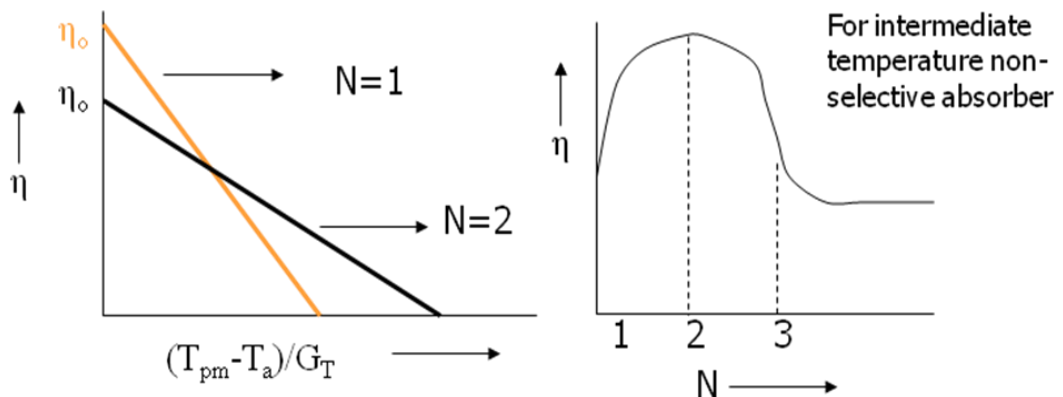


Fig 7: Efficiency for a selective and non-selective absorber system

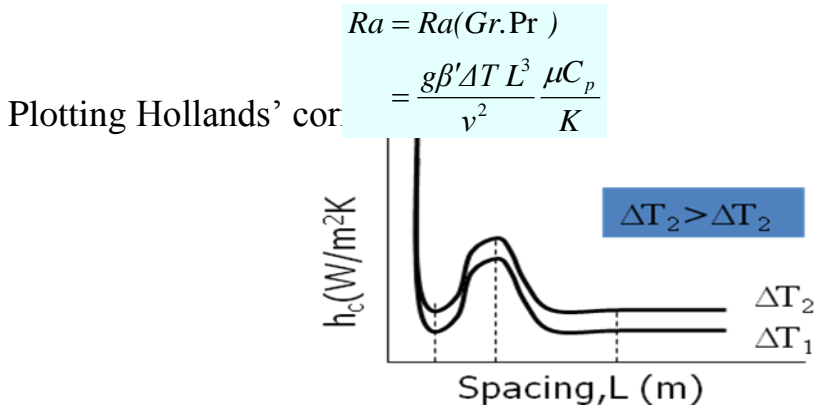
- With increase in N , U_L decreases but $(\tau\alpha)$ decreases. These increase and decrease are not identical/proportionate.
- So η goes through a maxima with N .

- For intermediate temperature non-selective absorber maximum efficiency is obtained by one or two glass covers.

NB: 1. For non-selective absorber double glazing gives better efficiency than single glazing.
2. For selective absorber single glazing is better

Absorber and Cover Spacing(L)

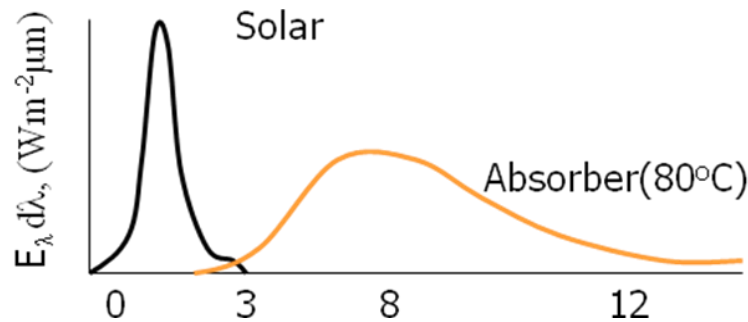
- The spacing between the absorber and the glass cover as well as between the glass covers governs the h_{cpg} , h_{cgg} .



Upto $R \cos\beta=1708$, the h value is in conduction regime between a and b i.e. $Nu=1$. Since value of h varies with T and β it is advisable to use larger spacing $L>5$ cm.

Selective properties of absorber(α, ϵ)

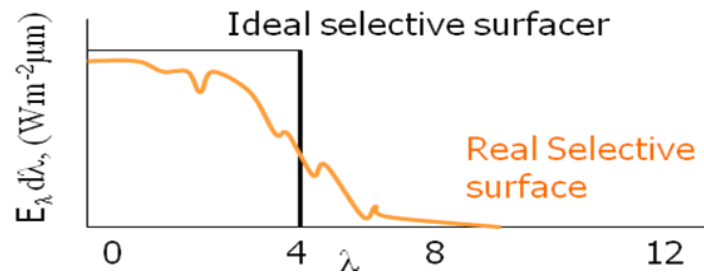
Absorber must have high α_{solar} and low $\epsilon_{thermal}$. At about $80^\circ C$ the emission spectrum of absorber does not overlap the solar radiation spectrum



- There is no overlap.
- Absorber plate maxima is at about $\lambda=8.3 \mu m$ at $80^\circ C$.
- So surface must have high α_{solar} i.e. for $\lambda<4 \mu m$ and low emissivity $\epsilon_{thermal}$ for $\lambda>4 \mu m$ i.e. a selective surface.
- Absorber must have high α_{solar} and low $\epsilon_{thermal}$. i.e.

$$\alpha_\lambda = \epsilon_\lambda = 1 \text{ for } \lambda > 4 \mu m$$

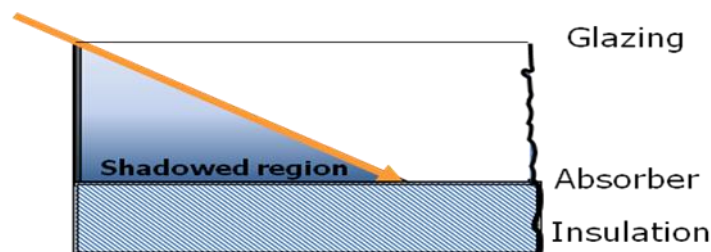
$$\alpha_\lambda = \epsilon_\lambda = 0 \text{ for } \lambda < 4 \mu m$$



Shading of absorber:

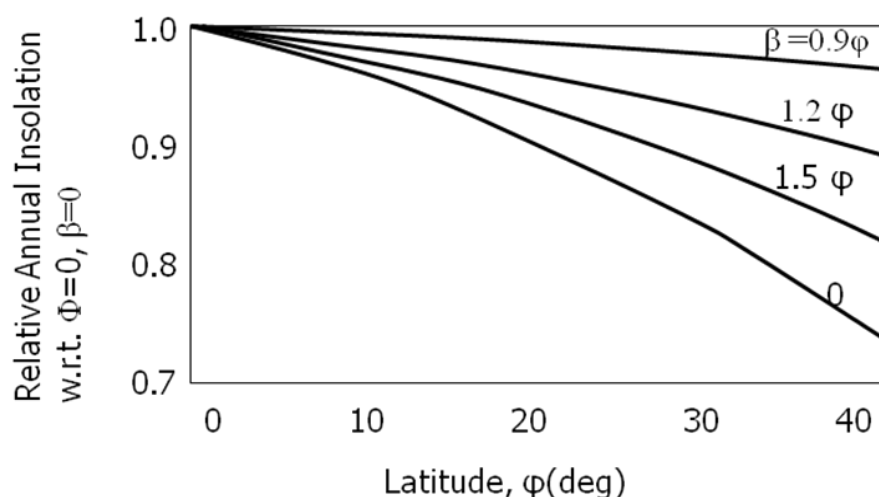
From convective heat transfer considerations L should be large. But it may result in shading during morning an evening hours.

- A spacing between covers by 2-3 cm results in a decrease in absorbed radiation by 3%; 5 cm- 5%.
- So S will become 0.97 and 0.95 respectively
- So reduction in convection losses is offset by loss in S .
- Inner walls may be made reflective.



Collector Tilt(β):

- Optimum value is $\beta = 0.9 \phi$ for variation in RAI is least for all latitudes.
- Upto $\phi = 30^\circ$ there is nt much variation in RAI for collector fixed at any angle.
- Surface azimuth angle $\gamma \pm 5^\circ$ does not have any affect.
- For heating application $\beta = \phi + 10^\circ$, or $\phi + 15^\circ$ for Northern hemisphere
- For cooling application $\beta = \phi - 10^\circ$, or $\phi - 15^\circ$ for Northern hemisphere

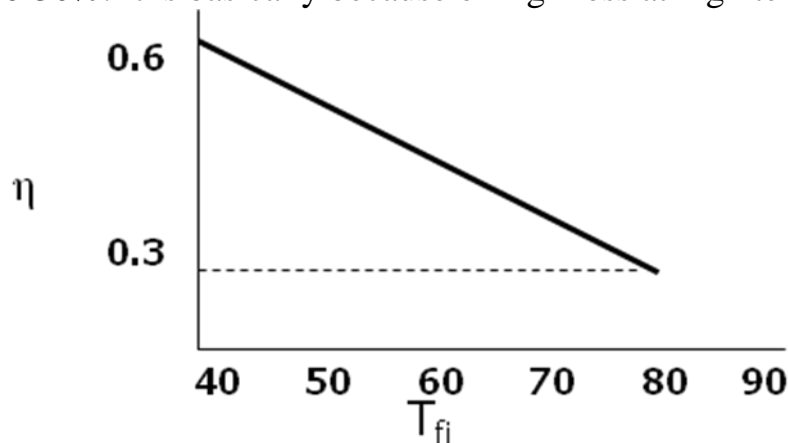


Optimum tilts may be calculated using the equation the expression given below. It has been derived assuming both beam and diffuse radiation.

where $\bar{H}_{bi} \beta_{opt} = \tan^{-1} \left[\frac{\sum_{i=1}^{12} \tan(\phi - \delta_i)}{\sum_{i=1}^{12} \bar{H}_{bi}} \right]$

Fluid Inlet

It can be seen that at high fluid inlet temperature the efficiency is low. For a typical range of temperature T - 40 – 90°C the efficiency ranges from 60-30%. It is basically because of high loss at high temperature.



Thermal Performance Test Procedure of F P C:

The schematic experimental test set up is shown in Fig.8.

- Standardized testing and rating procedures are needed for providing parameters which in turn provide an equitable basis for comparing the performance of different collectors for design and selection purpose
- Indoor or outdoor – Non-availability of ideal solar simulator indoors; Weather variability outdoors
- Open loop or Closed loop- Time and energy consumed.
- These have been developed by organization like ASHRAE, NBS, BIS, CSIRO

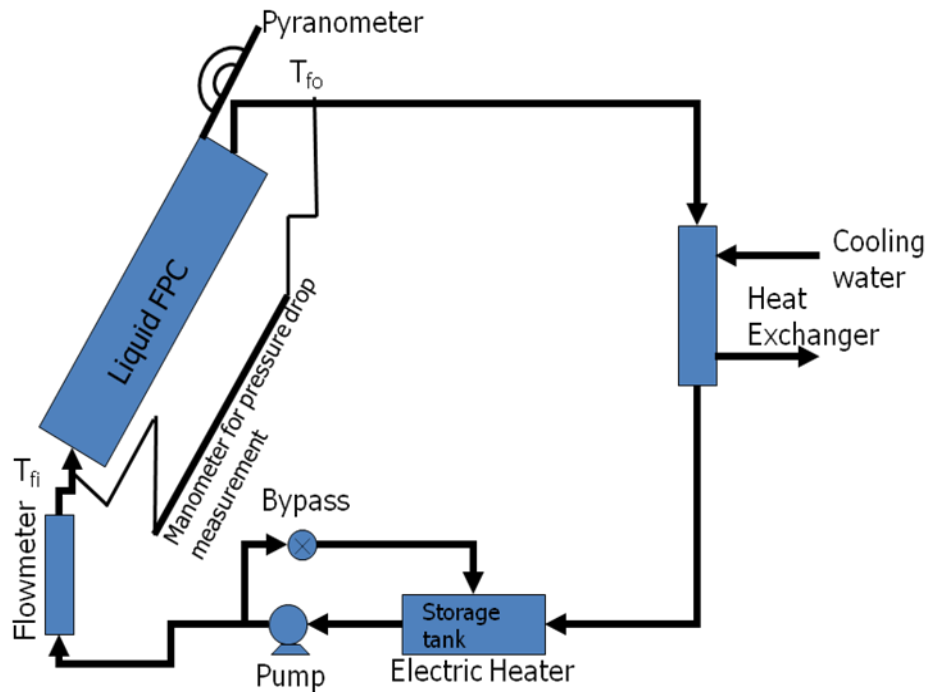


Fig 8: Schematic of experimental setup for a flat plate collector
Indian Test Standard (IS 12933 (Part 5)):

- Closed loop test procedure
- Collector, liquid pump, heat exchanger(HE) to remove heat, storage tank with electric heater, bypass valve
- HE , and storage tank with heater are used to control the inlet fluid temperature.

Procedure:

- i) For a given T_{fi} data is recorded under steady state condition.
- ii) Test is conducted symmetrically before and after solar noon. (e.g. 1100,1130,1230 and 1300 h Solar Time). This avoids any bias because of transient effect.
- iii) This is repeated for a minimum of four inlet temperatures on four different days (i.e. 16 data in total).
- iv) For each data set \dot{m} , T_{fi} , T_{fo} , G_T , T_a , Δp , and V_w are recorded.

Efficiency:

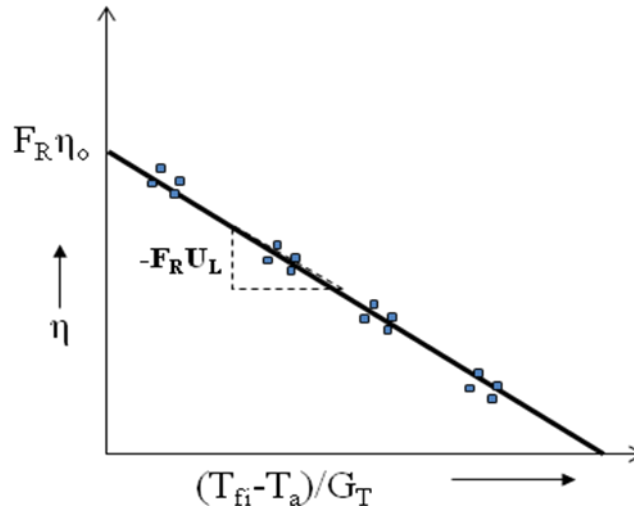
$$\eta_i = \frac{\dot{Q}_u}{A_c G_T} = \frac{\dot{m} C_p (T_{fo} - T_{fi})}{A_c G_T}$$

Conditions:

- Steady state – No deviation in experimental parameters for 15 minutes
- $G \pm 50 \text{ W/m}^2 > 600 \text{ W/m}^2$ ensures high beam component, θ within 15° .
- $T_a \pm 1^\circ$

- $\dot{m} \pm 1\%$ 0.02 kg/s/m^2
- $T_{fi} \pm 0.1^\circ\text{C}$
- $T_{fo} \pm 0.1^\circ\text{C}$
- V_w 3-6 m/s

Experimental plot:



Fitting in equation (44) we may get the values of the parameters, $F_R \eta_o$ and $F_R U_L$.

$$\eta = F_R U_L \left[(\tau\alpha)_e - \frac{U_L (T_{fi} - T_a)}{G} \right] \quad (44)$$

Problem $\eta_i = 0.572 - 4.796(T_{fi} - T_a) / G_T$ from the performance equation of a Flat plate collector.
Given

- So for this FPC, $F_R \eta_o = 0.572$ $F_R U_L = 4.796$

Other important parameters

- In liquid FPC \dot{m} does not appreciably affect the performance so other values may also be used. This is not true for air FPC, where performance for different \dot{m} values are different and are expected to be shown.
- In European test procedure η is plotted against $(\bar{T}_f - T_a) / \bar{G}_T$. The straight line provides $F' \eta_o$ and $F' U_L$ values.
- $G > 600 \text{ W/m}^2$ ensures high beam component, θ within 15° . Hence $(\tau\alpha)_{av}$ is effectively for normal incidence.
- Incidence angle modifier, $K_{\tau\alpha}$: For high θ ($>15^\circ$) ASHRAE 93-77 defines $K_{\tau\alpha}$ which is ratio of $\tau\alpha$ at any angle to that at normal incidence. So for $\theta > 60^\circ$ when $K_{\tau\alpha}$ shows dependence of $(\tau\alpha)_{av}$ on θ i.e. $K_{\tau\alpha}$ must be determined. The incidence angle modifier is defined as $K_{\tau\alpha} = (\eta_o / \eta_n)$.

The optical efficiency η_o depends on the collector configuration and varies with the angle of incidence as well as with the relative values of diffuse and beam radiation. For flat-plate collectors with 1 or 2 glass covers, $K_{\tau\alpha}$ is almost unchanged up to incidence angles of 60° , after which it abruptly drops to zero. A simple way to model the variation of $K_{\tau\alpha}$ with incidence angle for flat-plate collectors is to specify η_n , the optical efficiency of the collector at normal beam incidence, to assume the entire radiation to be beam, and to use the following expression for the angular dependence (ASHRAE 1978)

$$K_{\tau\alpha} = 1 + b_o \left(\frac{1}{\cos \theta} - 1 \right)$$

(45)

where θ is the solar angle of incidence on the collector plate (in degrees) and b_o is a constant called the incidence angle modifier coefficient. Plotting $K_{\tau\alpha}$ against $[(1/\cos \theta)-1]$ results in linear plots thus justifying the use of equation . We note that for one-glass and two-glass covers, approximate values of b_o are 0.10 and 0.17, respectively.

- Time Constant is another parameter which may be determined. It is a measure of heat capacity and heat loss factor of a collector.

Problem: How would the optical efficiency be effected at a solar incidence angle of 60° for a flat-plate collector with two glass covers? **Given:** $F_R \eta_n = 0.69$

- For two glass covers $b_o = 0.17$ and $K_{\tau\alpha} = 0.83$ for $\theta=60^\circ$. Hence $F_R \eta_o = F_R \eta_n K_{\tau\alpha} = 0.69 \times 0.83 = 0.57$

Selective Coatings:

Radiation-Matter Interaction

- Interaction is characterized by unique response based on -
Electronic structure of matter, and Lattice structure of matter
- Response is in the form of Reflectance spectra, Transmittance spectra, Absorption spectra, and Associated dispersion(frequency response)
- Response depth depends on frequency, Optical constants (RI, k) of medium and is confined to surface/interface of materials in absorbing and/or reflecting medium due to optically mismatched interface
- All materials show natural or intrinsic optical selectivity

Basically surfaces, thin films or coatings (single or multilayer) which yield a desired and selective suppression or enhancement of the spectral

dependence of reflectance, transmittance and absorptance are termed as **SELECTIVE**.

Characteristics:

- Must have long term stability at operating temperature.
- Stability to (recovery from) thermal shock (short term overheating) due to failure of extraction of heat from collector.
- Stability against corrosion
- Applicability to substrate material
- Reasonable cost
-

Techniques to achieve selectivity:

- Intrinsic solar selective materials
- Absorbing semiconductor and reflecting material
- Optical trapping by surface cavity or physical wavelength discrimination
- Optical interface effects by utilizing thin layers of metals and dielectrics
- Particulate coating composite film
- Quantum size effects
- Examples

SN	α_s	ϵ_{th}	Options
1.	High	High	Thick black alkyl resin paint
2.	High	Low	Thin Nickel black(Ni,Zn-S , alloy) on polished metal – Tabor Selective black; Black chrome; CuO/Cu; Al ₂ O ₃ /Al
3.	Low	High	White epoxy resin based paint (BaSO ₄)
4.	Low	Low	Al -foil

UNIT-3: SOLAR THERMAL SYSTEMS AND**APPLICATIONS**

Solar thermal systems have application specific designs and components. All these come with new challenges. Hence it is essential to study the specific features of each one of them keeping the basics discussed in earlier chapters in mind. A number of systems such as solar concentrators, evacuated tubular collectors (ETC), solar pond, solar water heaters, solar stills, solar dryers exist. The basic design of each one of them has been discussed in this chapter.

Solar Concentrators:*Introduction*

Solar concentrators are basically used to generate high temperature for a number of applications like distillation, process heat supply, and power generation. However it has been found attractive to generate electricity through thermal route due to low cost. There are two ways to produce electricity from the sun. First is by using the concentrating solar thermal system. This is done by focusing the heat from the sun to produce steam. The steam will drive a generator to produce electricity. This type of configuration is normally employed in solar power plants. The other way of generating electricity is through a photovoltaic (PV) cell. This technology will convert the sunlight directly into electricity. This technique is now being widely installed in the residential house and at remote places. It is also contributing to the significant increase in the development of Building Integrated Photovoltaic (BIPV) system.

However, despite numerous efforts done by the government and private sectors, solar energy only contributes to less than 1% of world's energy demand. Some of the main drawbacks for the solar technology are due to the high investment cost and long payback period. For an example, for an installation of a simple solar PV system, around 55 % of the total cost comes from the PV module. In terms of efficiency, only 15% to 30% of the sunlight is converted to electricity, depending on the type of semiconductor used in the PV. The highest efficiency recorded so far is by the Fraunhofer Institute for Solar Energy Systems, at

41.1%. If we could reduce the cost of the PV module, or minimise its usage in the solar cell, while maintaining the same amount of output, it is feasible and affordable to use the solar technology. Solar concentrator is the most favourable solution to this problem.

Concentrators can focus in either two or three dimensions. For the 2D case the concentration ratio is defined as:

$$C=D_{in}/D_{out}$$

where D_{in} is the diameter of the input aperture or collector and D_{out} is the diameter at the output of the concentrator. The output diameter usually corresponds to the diameter of the solar converter. The concentration ratio also determines the maximum collection angle and is determined by the Lagrange Invariant of the optical system. This relation states that the product of the refractive index ($n_{1,2}$), ray height (or diameter/2), and acceptance angle ($\theta_{1,2}$) is a constant:

$$n_1 D_1 \theta_1 = n_2 D_2 \theta_2$$

Solar concentrators

Overview

Solar concentrator is a device that allows the collection of sunlight from a large area and focusing it on a smaller receiver or exit. A conceptual representation of a solar concentrator used in harnessing the power from the sun to generate electricity is shown in Figure 1. The material used to fabricate the concentrator varies depending on the usage. For solar thermal, most of the concentrators are made from mirrors while for the BIPV system, the concentrator is either made of glass or transparent plastic. These materials are far cheaper than the PV material. The cost per unit area of a solar concentrator is therefore much cheaper than the cost per unit area of a PV material. By introducing this concentrator, not only the same amount of energy could be collected from the sun, the total cost of the solar cell could also be reduced. Arizona Public Service has concluded that the

most cost-effective PV for commercial application in the future will be dominated by high concentration collector incorporated by high-efficiency cell.

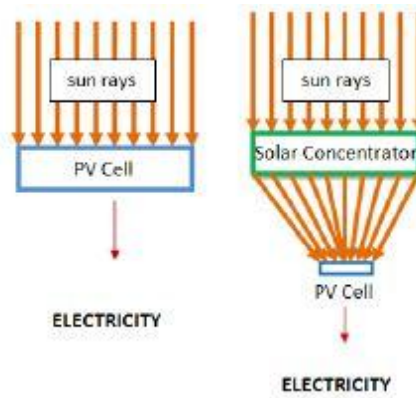


Figure 1: A Schematic representation of a solar concentrator

Some of the benefits and drawbacks of using the solar concentrators are summarised below.

Benefits:

1. Reduce the dependency on silicon cell
2. Increase the intensity of solar irradiance, hence increase the cell efficiency
3. Reduce the total cost of the whole system

Drawbacks:

1. Degrade the PV cell lifespan
2. Require mechanical tracking system
3. Need to cool down the PV to ensure the performance of the PV is optimum

2.2 Design of Solar Concentrator

For the past four decades, there have been a lot of developments involving the designs of the solar concentrators. This paper presents some of the distinguish designs which have shown significant contribution to the solar technology. They are:

- Parabolic Concentrator
- Hyperboloid Concentrator
- Fresnel Lens Concentrator

- Compound Parabolic Concentrator (CPC)
- Dielectric Totally Internally Reflecting Concentrator (DTIRC)
- Flat High Concentration Devices
- Quantum Dot Concentrator (QDC)

These concentrators can also be categorised according to their optical principles. In this paper, they are categorised into four groups, which is shown in Table 2:

Type	Description
Reflector	Upon hitting the concentrator, the sun rays will be reflected to the PV cell Example: <i>Parabolic Trough, Parabolic Dish, CPC Trough, Hyperboloid Concentrator.</i>
Refractor	Upon hitting the concentrator, the sun rays will be refracted to the PV cell. Example: <i>Fresnel Lens Concentrator</i>
Hybrid	Upon hitting the concentrator, the sun rays can experience both reflection and refraction before hitting to the PV cell. Example: <i>DTIRC, Flat High Concentration Devices</i>
Luminescent	The photons will experience total internal reflection and guided to the PV cell. Example: <i>QDC</i>

Table 1

Parabolic Concentrator

The two dimensional design of a parabolic concentrator is equals to a parabola. It is widely used as a reflecting solar concentrator. A distinct property that it has is that it can focus all the parallel rays from the sun to a single focus point, F as shown in Figure 2. It is not necessary to use the whole part of the parabola curve to construct the concentrator. Most of the parabolic concentrator employs only a truncated portion of the parabola.

Currently, there are two available designs of parabolic concentrator. One is by rotating the two dimensional design along the x-axis to produce a parabolic dish, and the other way is by having a parabolic trough. Both of the designs act as reflectors and are used mostly in concentrating solar power

system in big solar power plant. The EUCLIDES-THERMIE Plant in Tenerife, Canary Island employs the parabolic trough concentrators in the 480kW concentrator project. Although this concentrator could provide a high concentration, it requires larger field of view to maximise the sun energy collection. To obtain maximum efficiency, it needs a good tracking system, which is quite expensive. That is why this type of concentrator is not preferred in a small residential house.

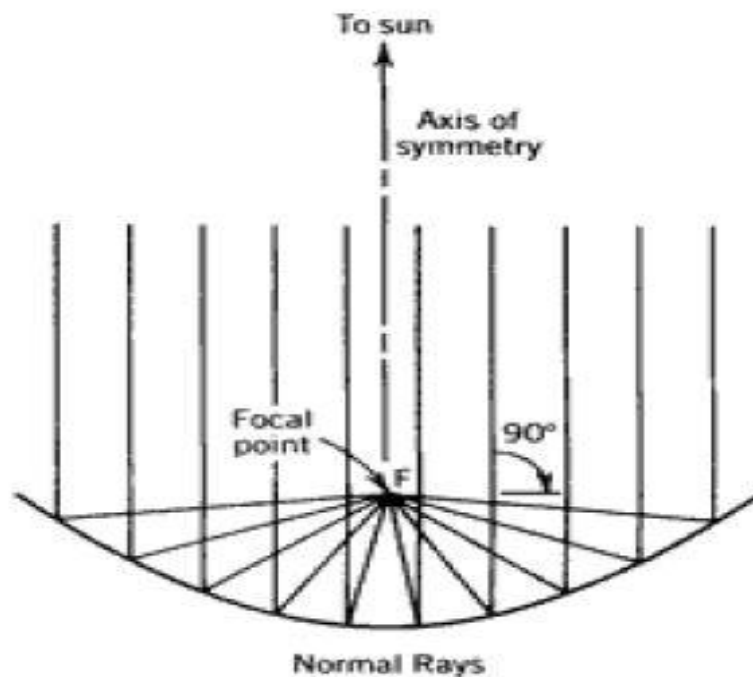


Figure 2: Parabolic Concentrator

Hyperboloid Concentrator

The general design of a hyperboloid concentrator is shown in Figure 3. It consists of two hyperbolic sections, AB and A'B'. The hyperboloid concentrator can be produced by rotating the two dimensional design along its symmetrical axis. The diameters of the entrance and exit aperture are labeled as d_1 and d_2 respectively. If the inside wall of the hyperbolic profile is considered as a mirror, the sun rays entering the concentrator from AA' will be reflected and focused to the exit aperture BB'.

The advantage of this concentrator is that it is very compact, since only truncated version of the concentrator needs to be used. Because of this factor, it

is mainly used as a secondary concentrator. An example of application of this concentrator has been developed by SolFocus, with the intention of reducing the cost of solar electricity. The design with Cassegranian-like architecture managed to produce 250W peak in a single Generation 1 solar panel. However, in most applications, it requires the usage of lenses at the entrance diameter AA' in order for the concentrator to work effectively.

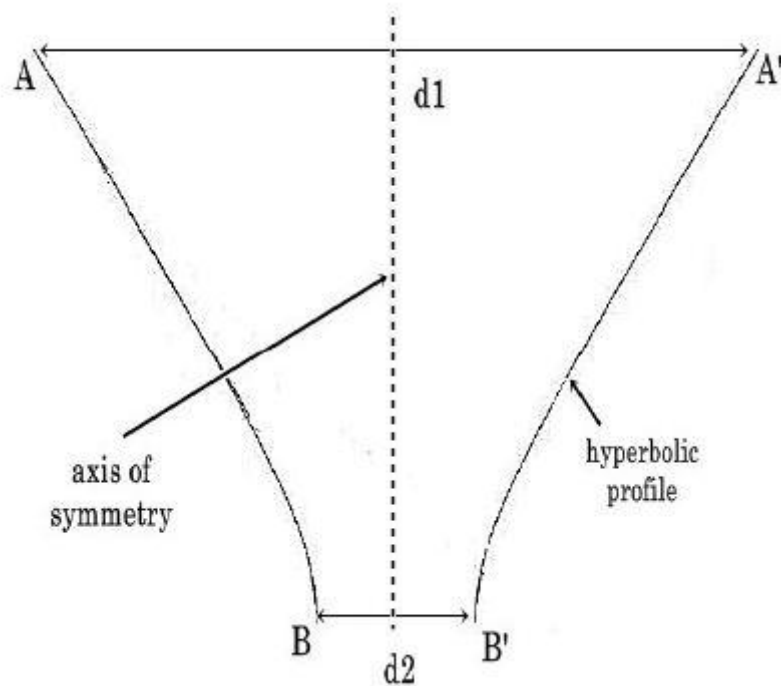


Figure 3: Hyperboloid Concentrator

Fresnel Concentrator

Fresnel lens function is similar to the conventional lens, by refracting the rays and focusing them at one focal point. It generally has two sections; a flat upper surface and a back surface that employs canted facets. The facet is an approximation of the curvature of a lens (see Figure 4). A good linear Fresnel lens could employ around 100 facets per millimeter.

There are two ways to use this concentrator; a point focus Fresnel lens or a line focus Fresnel lens. An application of this concentrator can be seen in the Sacramento Municipal Utility District, where the Fresnel lenses are used in the 30kW utility grid-connected plant. The advantage of a Fresnel lens over a conventional lens is that it is thinner and requires a lesser amount of material to fabricate. It also has the capability to separate the direct and diffuse light,

making it suitable to control the illumination and temperature of a building interior. One of the disadvantages of this concentrator will be due to the sharpness of the facet. An error in the manufacturing process could create a rounder shape at the edges of the facets, causing the rays improperly focused at the receiver.

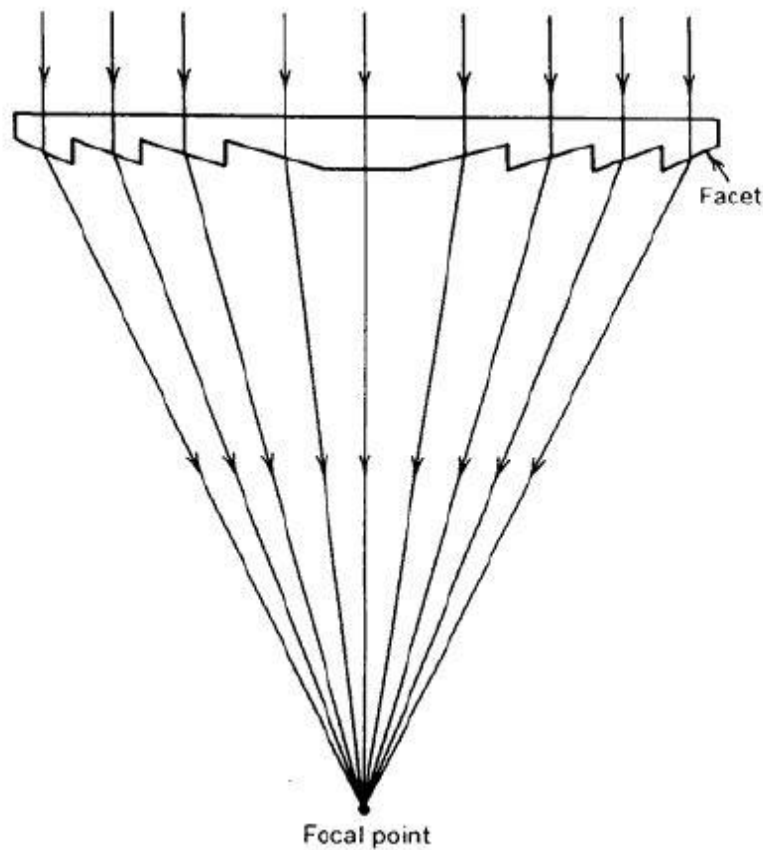


Figure 4: Fresnel Concentrator

Compound Parabolic Concentrator (CPC)

The basic concept of compound parabolic concentrator (CPC) has been developed and explained thoroughly by Welford and Winston. The geometry of a two dimensional CPC is shown in Figure 5(a). It consists of two segments of parabolas, AC and BD. A CPC can be divided into three parts; a planar entrance aperture, a totally internally reflecting side profile and an exit aperture. The entrance aperture of this CPC is of length CD. The CPC will have an acceptance angle of 2θ and will concentrate all the solar radiation at the exit aperture AB (see Figure 5(b)).

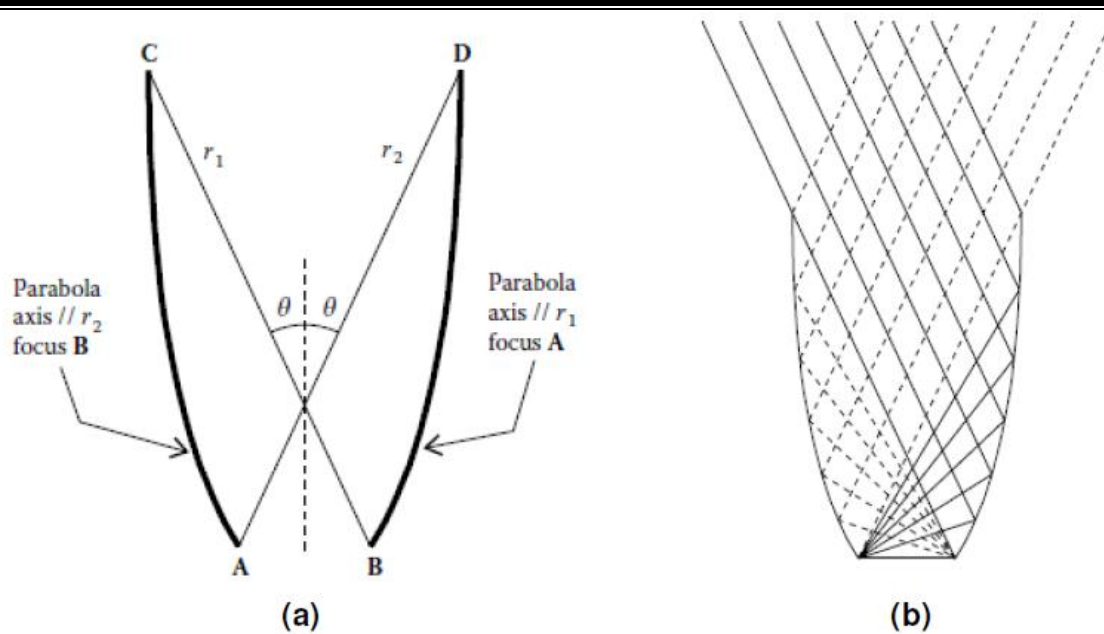


Figure 5: Different type of geometry for CPC

The total length of a CPC depends both on the exit aperture and the acceptance angle of the concentrator. By reducing the acceptance angle, the size of the concentrator will increase. The CPC can either be used as a three dimensional rotational symmetry concentrator or as a CPC trough concentrator. The later design is normally employed as a reflector in a solar power plant. SHAP S.p.A Solar Heat and Power is one of the companies that utilises the CPC trough design as its main commercial product in harnessing the solar power.

The main advantage of using a CPC is that it could offer a higher geometrical concentration gain with a narrow field of view. The disadvantages of the CPC trough concentrator will be the same as parabolic trough concentrator; it requires a good tracking system to maximise the collection of sun radiation.

Dielectric Totally Internally Reflecting Concentrator (DTIRC)

The first concept of DTIRC was introduced by Ning et al. in 1987. This new class of optical element has the capability to achieve concentrations close to the theoretical maximum limits. There are two ways to produce the DTIRC; maximum concentration method and phase conserving method. Although both methods will create almost identical structure, the first technique offers slightly higher concentration and therefore more suitable for solar application. DTIRC consists of three parts; a curved front surface, a totally internally reflecting side

profile and an exit aperture (see Figure 6). When the rays hit the front curved surface, they are refracted and directed to the side profile. Upon hitting the sidewall, they will be totally internally reflected to the exit aperture. The front aperture can be a hemisphere, but different designs such as parabola and eclipse have been developed recently.

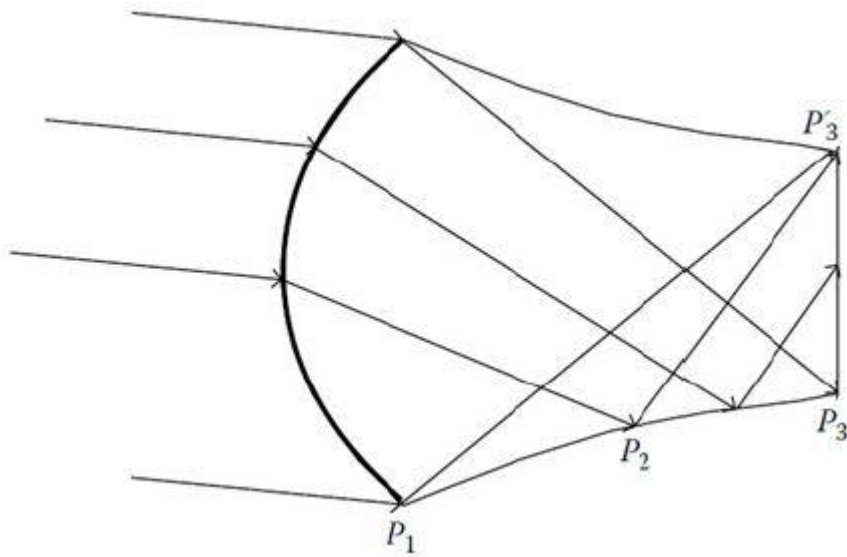


Figure 6: DTIRC concentrator

The geometrical concentration gain of a DTIRC depends on both acceptance angle and also the front arc angle. From Figure 7, it is concluded that the geometrical concentration gain is inversely proportional to the acceptance angle. Also, the front arc angle only gives very minimal effect on the geometrical gain.

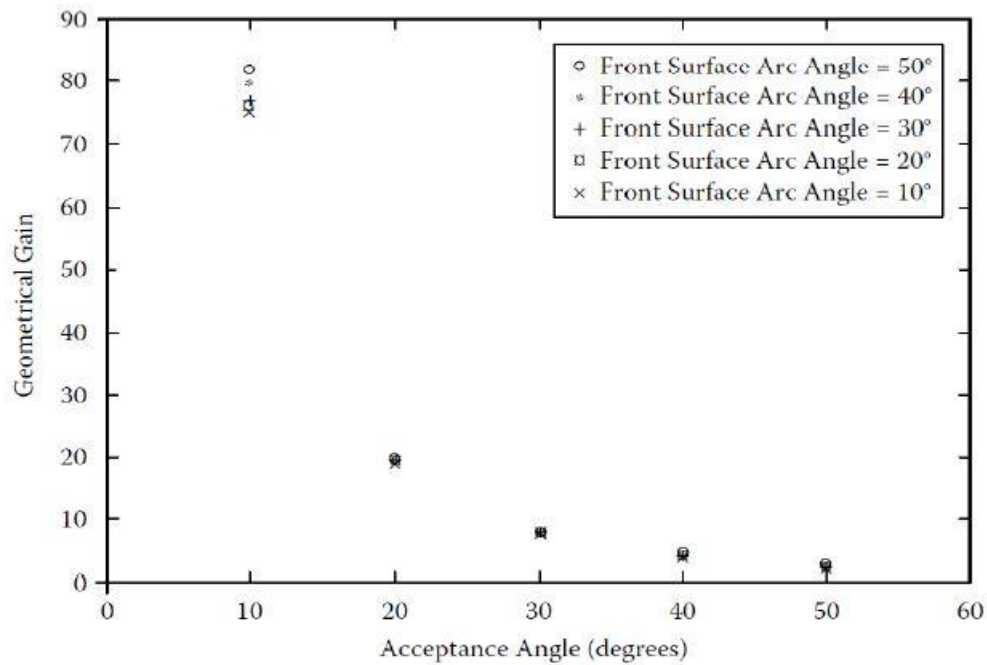


Figure 7: Dependence of geometrical concentration gain on acceptance angle

The advantage of DTIRC over CPC is that it offers higher geometrical concentration gain and smaller sizes. The disadvantage of a DTIRC is that it cannot efficiently transfer all of the solar energy that it collects into a lower index media. As a result, not all the sun rays are transmitted to the cell area. The DTIRC is available either as a three dimensional rotational symmetry concentrator or as a two dimensional optical extrusion, although the earlier design is more favourable. One of the examples is in the NASA flight demonstration program, where a DTIRC is used as the secondary concentrator for the solar thermal application in space

Flat High Concentration Devices

Instituto de Energia Solar, Universidad Politecnica de Madrid (UPM) in Spain, Minano and Benitez in particular, have successfully produced a different class of nonimaging concentrators. The concentrators are able to achieve theoretical maximum acceptance-angle-concentration. Currently, Light Prescription Innovators (LPI) is working closely with UPM to further develop and market these concentrators. Since 1995, there are five available designs; RR, XX, XR, RX and RXI. In this design, 'R' represents refraction, 'X' denotes reflection and 'I' means total internal reflection. Basically, an XR concentrator means that the

rays in this concentrator will first experience a reflection followed by refraction, before reaching the receiver of which a PV cell is attached.

For simplicity, we will restrict the discussion on the RXI design. Figure 8 shows a typical diagram of an RXI concentrator. It is devised using the Simultaneous Multiple Surface, also known as the Minano-Benitez design method. An RXI concentrator has three sections; an upper surface with a mirror at the centre, a lower surface made from mirror, and a receiver. Minano et. al. has shown that by using an RXI with rotational symmetry and the refractive index of the dielectric is 1.5, a concentrator with an acceptance angle of $\pm 2.70^\circ$ could achieve a concentration factor of 1000x. These concentrators have two major benefits; they are very compact and offer very high concentration. However, there are some disadvantages of this design. Due to the cell's position, it is difficult to create electrical connection and heat sinking. The cell dimension must be designed to be as minimal as possible to reduce shadowing effect.

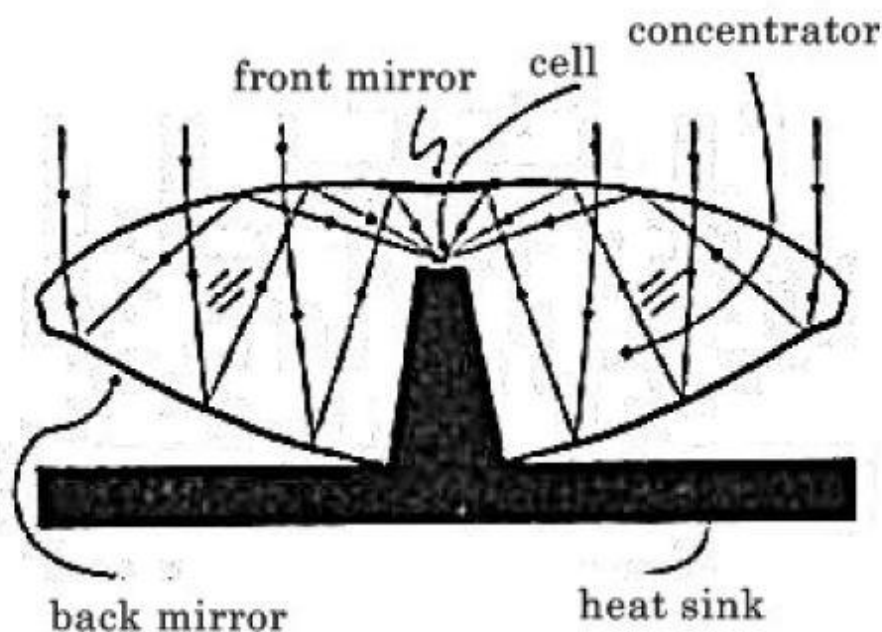


Figure 8: RXI concentrator

Quantum Dot Concentrator (QDC)

Quantum dot concentrator, (QDC) is a planar device that consists of three parts; a transparent sheet of glass or plastic made doped with quantum dots (QDs), reflective mirrors mounted on the three edges and back surface, and an exit

where a PV cell is attached (see Figure 9). When the sun radiation hits the surface of a QDC, a part of the radiation will be refracted by the fluorescent material and absorbed by the QDs. Photons are then reemitted in all direction and are guided to the PV cell via total internal reflection. The total geometrical concentration will be the ratio of the large surface area of glass to the area of PV cell. QDC major advantage is that it does not requires any tracking as other conventional concentrator. It can also make full use of both direct and diffuse solar radiation. However, the drawback of the QDC is that the development of QDC is restricted to high requirements on the luminescent dyes; i.e. high quantum efficiency, suitable absorption spectra and red shifts, and stability under illumination. Evident Technologies is one of the companies that sees the huge potential in this concentrator and has been marketing the quantum dot products to the consumers.

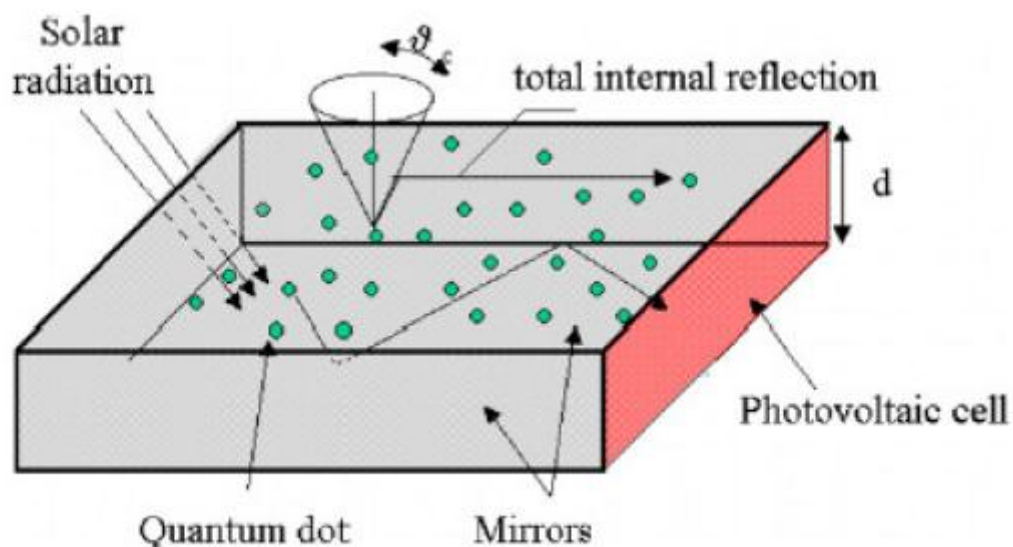


Figure 9: Quantum dot concentrator

To summarize the various design of the concentrator, Table 3 shows the comparison of each concentrator, showing the advantage and disadvantage of each design respectively.

Type of Concentrator	Advantage	Disadvantage
Parabolic Concentrator	<ul style="list-style-type: none"> • High concentration. 	<ul style="list-style-type: none"> • Requires larger field of view. • Need a good tracking system.
Hyperboloid Concentrator	<ul style="list-style-type: none"> • Compact 	<ul style="list-style-type: none"> • Need to introduce lens at the entrance aperture to work effectively.
Fresnel Concentrator	<ul style="list-style-type: none"> • Thinner than conventional lens. • Requires less material than conventional lens. • Able to separate the direct and diffuse light - suitable to control the illumination and temperature of a building interior. 	<ul style="list-style-type: none"> • Imperfection on the edges of the facets, causing the rays improperly focused at the receiver.
Compound Parabolic Concentrator	<ul style="list-style-type: none"> • Higher gain when its field of view is narrow. 	<ul style="list-style-type: none"> • Need a good tracking system.
Dielectric Totally Internally Reflecting Concentrator	<ul style="list-style-type: none"> • Higher gain than CPC. • Smaller sizes than CPC. 	<ul style="list-style-type: none"> • Cannot efficiently transfer all of the solar energy that it collects into a lower index media.
Flat High Concentration Devices (RR, XX, XR, RX, and RXI)	<ul style="list-style-type: none"> • Compact. • Very high concentration 	<ul style="list-style-type: none"> • Difficulty to create electrical connection and heat sinking due to the position of the cell. • The cell dimension must be designed to a minimum to reduce shadowing effect.
Quantum Dot Concentrator	<ul style="list-style-type: none"> • No tracking needed. • Fully utilise both direct and diffuse solar radiation 	<ul style="list-style-type: none"> • Restricted in terms of development due to the requirements on the luminescent dyes.

SOLAR WATER HEATERS

Solar water heater are systems to heat water up to about 80oC with an arrangement to store it for day long use. They are of various types depending on whether they are for domestic and/or industrial applications. Some of them are discussed here.

Closed-Loop and Open-Loop Systems

The two possible configurations of solar thermal systems with daily storage are classified as closed-loop or open-loop systems. Though different authors define these differently, we shall define these as follows. A closed-loop system has been defined as a circuit in which the performance of the solar collector is directly dependent on the storage temperature. Figure 11 gives a schematic of a closed-loop system in which the fluid circulating in the collectors does not mix with the fluid supplying thermal energy to the load. Thus, these two subsystems are distinct in the sense that any combination of fluids (water or air) is theoretically feasible (a heat exchanger, as shown in the figure, is of course imperative when the fluids are different). However, in practice, only water-water, water-air, or air-air combinations are used. From the point of system performance, the storage temperature normally varies over the day and, consequently, so does collector performance. Closed-loop system configurations have been widely used to date for domestic hot water and space heating applications. The flow rate per unit collector area is generally around 50 kg/(h m²) for liquid collectors. The storage volume makes about 5–10 passes through the collector during a typical sunny day, and this is why such systems are called multipass systems. The temperature rise for each pass is small, of the order of

28°C–58°C for systems with circulating pumps and about 10°C for thermosyphon systems. An expansion tank and a check valve to prevent reverse thermosyphoning at nights, although not shown in the figure, are essential for such system configurations.

Figure 10 illustrates one of the possible configurations of open-loop systems. Open-loop systems are defined as systems in which the collector performance is independent of the storage temperature. The working fluid may be rejected (or a heat recuperator can be used) if contaminants are picked up during its passage through the load. Alternatively, the working fluid could be directly recirculated back to the entrance of the solar collector field. In all these open-loop configurations, the collector is subject to a given or known inlet temperature specified by the load requirements. If the working fluid is water, instead of having a continuous flow rate (in which case the outlet temperature of the water will vary with isolation), a solenoid valve can be placed just at the exit of the collector, set so as to open when the desired temperature level of the fluid in the collector is reached. The water is then discharged into storage, and fresh water is taken into the collector. The solar collector will thus operate in a discontinuous manner, but this will ensure that the temperature in the storage is always at the desired level. An alternative way of ensuring uniform collector outlet temperature is to vary the flow rate according to the incident radiation. One can collect a couple of percent more energy than with constant rate single-pass designs. However, this entails changing the flow rate of the pump more or less continuously, which is injurious to the pump and results in reduced life. Of all the three variants of the open-loop configuration, the first one, namely the single-pass open-loop solar thermal system configuration with constant flow rate and without a solenoid valve, is the most common. As stated earlier, closed-loop systems are appropriate for domestic applications. Until recently, industrial process heat systems were also designed as large solar domestic hot-water systems with high collector flow rates and with the storage tank volume making several passes per day through the collectors. Consequently, the storage tank tends to be fairly well mixed. Also the tank must be strong enough to withstand the high pressure from the water mains. The open-loop single-pass configuration, wherein the required average daily fluid flow is circulated just once through the collectors with the collector inlet temperature at its lowest value, has been found to be able to deliver as much as 40% more yearly energy for industrial process heat applications than the multipass designs. Finally, in a closed-loop system where an equal amount of fresh water is introduced into storage whenever a certain amount of hot water is drawn off by the load, it is not possible to extract the entire amount of thermal energy contained in storage since the storage temperature is continuously reduced due to mixing. This partial depletion effect in the storage tank is not experienced in open-loop systems. The penalty in yearly energy delivery ranges typically from about 10% for daytime-only loads to around 30% for nighttime-only loads compared to a closed-loop multipass system where the storage is depleted every day. Other advantages of open-loop systems are (i) the storage tank need not be pressurized (and hence is less costly), and (ii) the pump size and parasitic power can be lowered. A final note of caution is required. The single-pass design is not recommended for

variable loads. The tank size is based on yearly daily load volumes, and efficient use of storage requires near-total depletion of the daily collected energy each day. If the load draw is markedly lower than its average value, the storage would get full relatively early the next day and solar collection would cease. It is because industrial loads tend to be more uniform, both during the day and over the year, than domestic applications that the single-pass open-loop configuration is recommended for such applications.

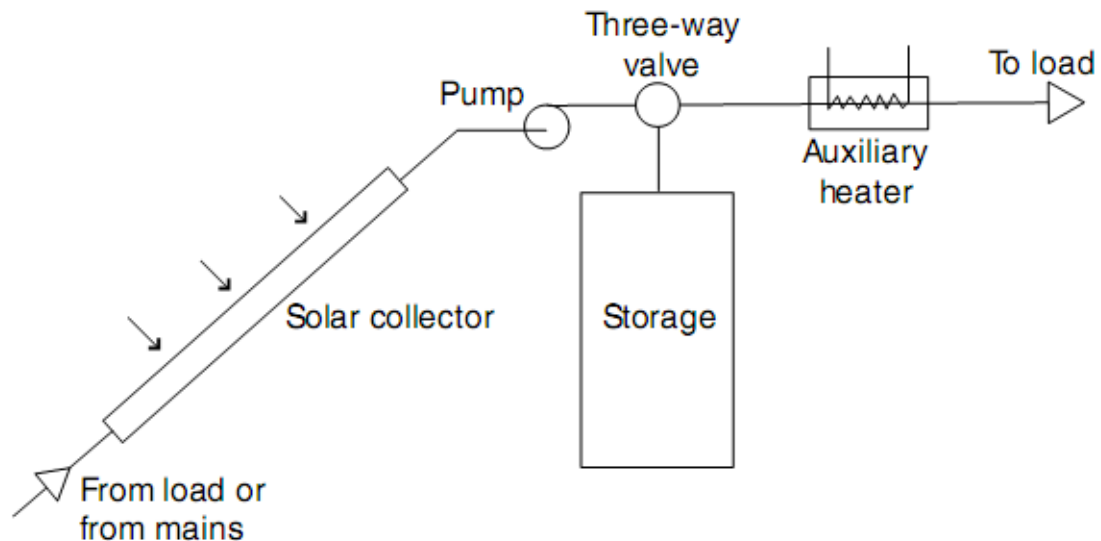


Fig10: An open-loop solar water heating system

Description of a Typical Closed-Loop System

Figure illustrates a typical closed-loop solar-supplemented liquid heating system. The useful energy is often (but not always) delivered to the storage tank via a collector-heat exchanger, which separates the collector fluid stream and the storage fluid. Such an arrangement is necessary either for antifreeze protection or to avoid corrosion of the collectors by untreated water containing gases and salts. A safety relief valve is provided because the system piping is normally nonpressurized, and any steam produced in the solar collectors will be let off from this valve. When this happens, energy dumping is said to take place.

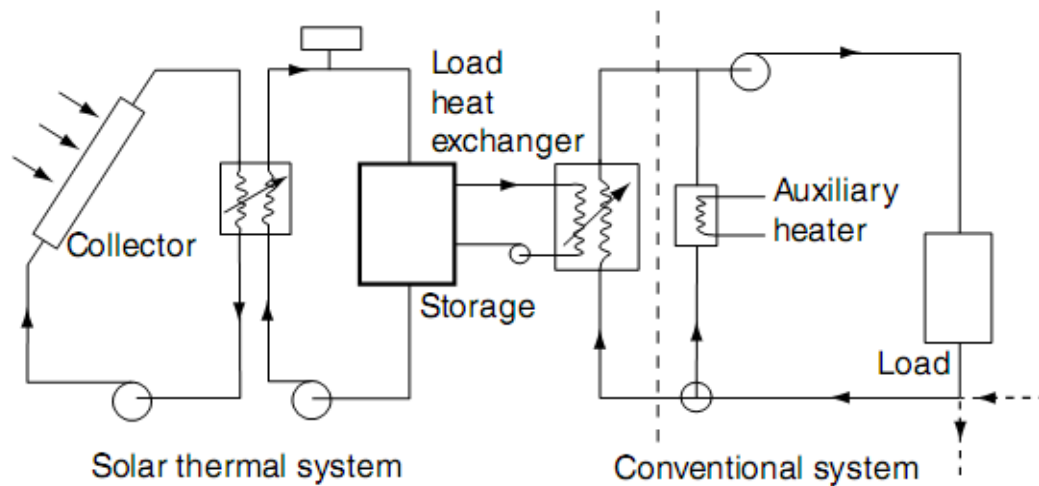


Fig 11: Closed-loop solar-supplemented liquid heating system

Fluid from storage is withdrawn and made to flow through the load-heat exchanger when the load calls for heat. Whenever possible, one should withdraw fluid directly from the storage and pass it through the load, and avoid incorporating the load-heat exchanger, since it introduces additional thermal penalties and involves extra equipment and additional parasitic power use. Heat is withdrawn from the storage tank at the top and reinjected at the bottom in order to derive maximum benefit from the thermal stratification that occurs in the storage tank. A bypass circuit is incorporated prior to the load heat exchanger and comes into play

1. when there is no heat in the storage tank (i.e., storage temperature T_s is less than the fluid temperature entering the load heat exchanger T_{xi})
2. when T_s is such that the temperature of the fluid leaving the load heat exchanger is greater than that required by the load (i.e., $T_{xo} > T_{Li}$, in which case the three-way valve bypasses part of the flow so that $T_{xo} = T_{Li}$). The bypass arrangement is thus a differential control device which is said to modulate the flow such that the above condition is met. Another operational strategy for maintaining $T_{xo} = T_{Li}$ is to operate the pump in a “bang-bang” fashion (i.e., by short cycling the pump). Such an operation is not advisable, however, since it would lead to premature pump failure.

An auxiliary heater of the topping-up type supplies just enough heat to raise T_{xo} to T_{Li} . After passing through the load, the fluid (which can be either water or air) can be recirculated or, in case of liquid contamination through the load, fresh liquid can be introduced. The auxiliary heater can also be placed in parallel with the load in which case it is called an all-or-nothing type. Although such an arrangement is thermally less efficient than the topping-up type, this type is widely used during the solar retrofit of heating systems because it involves little mechanical modifications or alterations to the auxiliary heater itself. It is obvious that there could also be solar-supplemented energy systems that do not include a storage element in the system. The operation of such systems is not very different from that of systems with storage, the primary difference being that whenever instantaneous solar energy collection exceeds load requirements (i.e., $T_{Co} > T_{Li}$), energy dumping takes place. It is obvious that by definition there

cannot be a closed-loop, no-storage solar thermal system. Solar thermal systems without storage are easier to construct and operate, and even though they may be effective for 8–10 h a day, they are appropriate for applications such as process heat in industry.

Active closed-loop solar systems as described earlier are widely used for service hot-water systems, that is, for domestic hot water and process heat applications as well as for space heat. There are different variants to this generic configuration. A system without the collector-heat exchanger is referred to as having collectors directly coupled to the storage tank. For domestic hot-water systems, the system can be simplified by placing the auxiliary heater (which is simply an electric heater) directly inside the storage tank. One would like to maintain stratification in the tank so that the coolest fluid is at the bottom of the storage tank, thereby enhancing collection efficiency. Consequently, the electric heater is placed at about the upper third portion of the tank so as to assure good collection efficiency while assuring adequate hot water supply to the load. A more efficient but expensive option is widely used in the United States: the double tank system, shown in Figure 12.

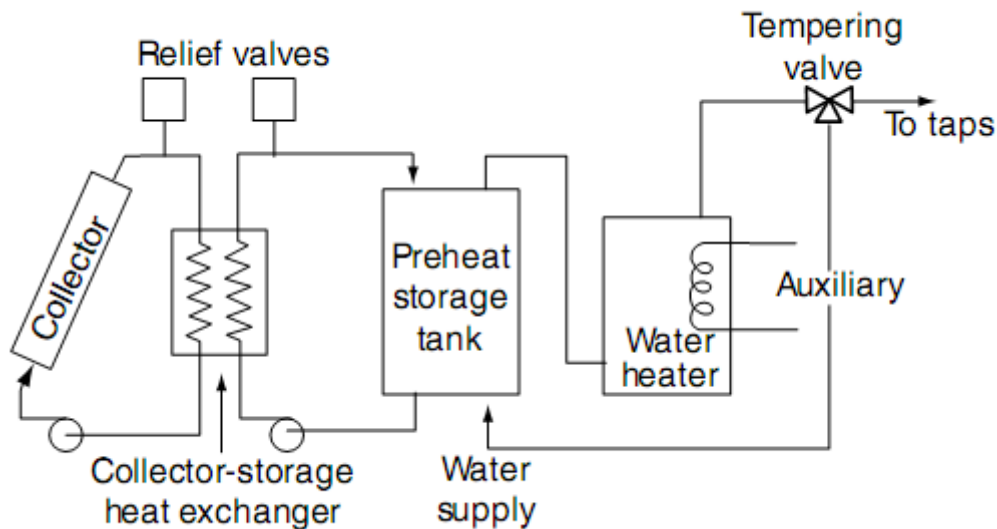


Fig12: Domestic hot water system with double tank arrangement

Here the functions of solar storage and auxiliary heating are separated, with the solar tank acting as a preheater for the conventional gas or electric unit. Note that a further system simplification can be achieved for domestic applications by placing the load heat exchanger directly inside the storage tank. In certain cases, one can even eliminate the heat exchanger completely. Another system configuration is the drain-back (also called drain-out) system, where the collectors are emptied each time the solar system shuts off. Thus the system invariably loses collector fluid at least once, and often several times, each day. No collector-heat exchanger is needed, and freeze protection is inherent in such a configuration. However, careful piping design and installation, as well as a two-speed pump, are needed for the system to work properly. The drain-back configuration may be either open (vented to atmosphere) or closed (for better corrosion protection). Long-term experience in the United States with the drain-

back system has shown it to be very reliable if engineered properly. A third type of system configuration is the drain-down system, where the fluid from the collector array is removed only when adverse conditions, such as freezing or boiling, occur. This design is used when freezing ambient temperatures are only infrequently encountered. Active solar systems of the type described above are mostly used in countries such as the United States and Canada. Countries such as Australia, India, and Israel (where freezing is rare) usually prefer thermosyphon systems. No circulating pump is needed, the fluid circulation being driven by density difference between the cooler water in the inlet pipe and the storage tank and the hotter water in the outlet pipe of the collector and the storage tank. The low fluid flow in thermosyphon systems enhances thermal stratification in the storage tank. The system is usually fail-proof, and a thermosyphon system performs better than several pumped service hot-water systems. If operated properly, thermosyphon and active solar systems are comparable in their thermal performance. A major constraint in installing thermosyphon systems in already existing residences is the requirement that the bottom of the storage tank be at least 20 cm or more higher than the top of the solar collector in order to avoid reverse thermosyphoning at night. To overcome this, spring-loaded one-way valves have been used, but with mixed success.

Controls

There are basically five categories to be considered when designing automatic controls: (i) collection to storage, (ii) storage to load, (iii) auxiliary energy to load, (iv) miscellaneous (i.e., heat dumping, freeze protection, overheating, etc.), and (v) alarms. The three major control system components are sensors, controllers, and actuating devices. Sensors are used to detect conditions (such as temperatures, pressures, etc.). Controllers receive output from the sensors, select a course of action, and signal a system component to adjust the condition. Actuated devices are components such as pumps, valves, and alarms that execute controller commands and regulate the system.

The sensors for the controls must be set, operated, and located correctly if the solar system is to collect solar energy effectively, reduce operating time, wear and tear of active components, and minimize auxiliary and parasitic energy use. Moreover, sensors also need to be calibrated frequently. For diagnostic purposes, it may be advisable to add extra sensors and data acquisition equipment in order to verify system operation and keep track of long-term system operation. Potential problems can be then rectified in time.

Though single-point temperature controllers or solar-cell-activated controls have been used for activated solar collectors, the best way to do so is by differential temperature controllers. Temperature sensors are used to measure the fluid temperature at collector outlet and at the bottom of the storage tank. When the difference is greater than a set amount, say 5°C, then the controller turns the pump on. If the pump is running and the temperature difference falls below another preset value, say 1°C, the controller stops the pump. The temperature deadband between switching-off and reactivating levels should be set with care, since too high a deadband would adversely affect collection efficiency and too low a value would result in short cycling of the collector pump. The number of on-off cycles at system start-up depends on solar intensity, fluid flow rate,

volume of water in the collector loop, and the differential controller setting. A similar phenomenon of cycling also occurs in the afternoon. However, the error introduced in solar collector long-term performance predictions by neglecting this cycling effect in the modeling equations is usually small.

Evacuated Tubular Collectors

One method of obtaining temperatures between 100 and 200°C is to use evacuated tubular collectors. The advantage in creating and being able to maintain a vacuum is that convection losses between glazing and absorber can be eliminated. There are different possible arrangements of configuring evacuated tubular collectors. Two designs are shown in Figure 13. The first is like a small flat-plate collector with the liquid to be heated making one pass through the collector tube. The second uses an all-glass construction with the glass absorber tube being coated selectively. The fluid being heated passes up the middle of the absorber tube and then back through the annulus. Evacuated tubes can collect both direct and diffuse radiation and do not require tracking. Glass breakage and leaking joints due to thermal expansion are some of the problems which have been experienced with such collector types. Various reflector shapes (like flat-plate, V-groove, circular, cylindrical, involute, etc.) placed behind the tubes are often used to usefully collect some of the solar energy, which may otherwise be lost, thus providing a small amount of concentration.

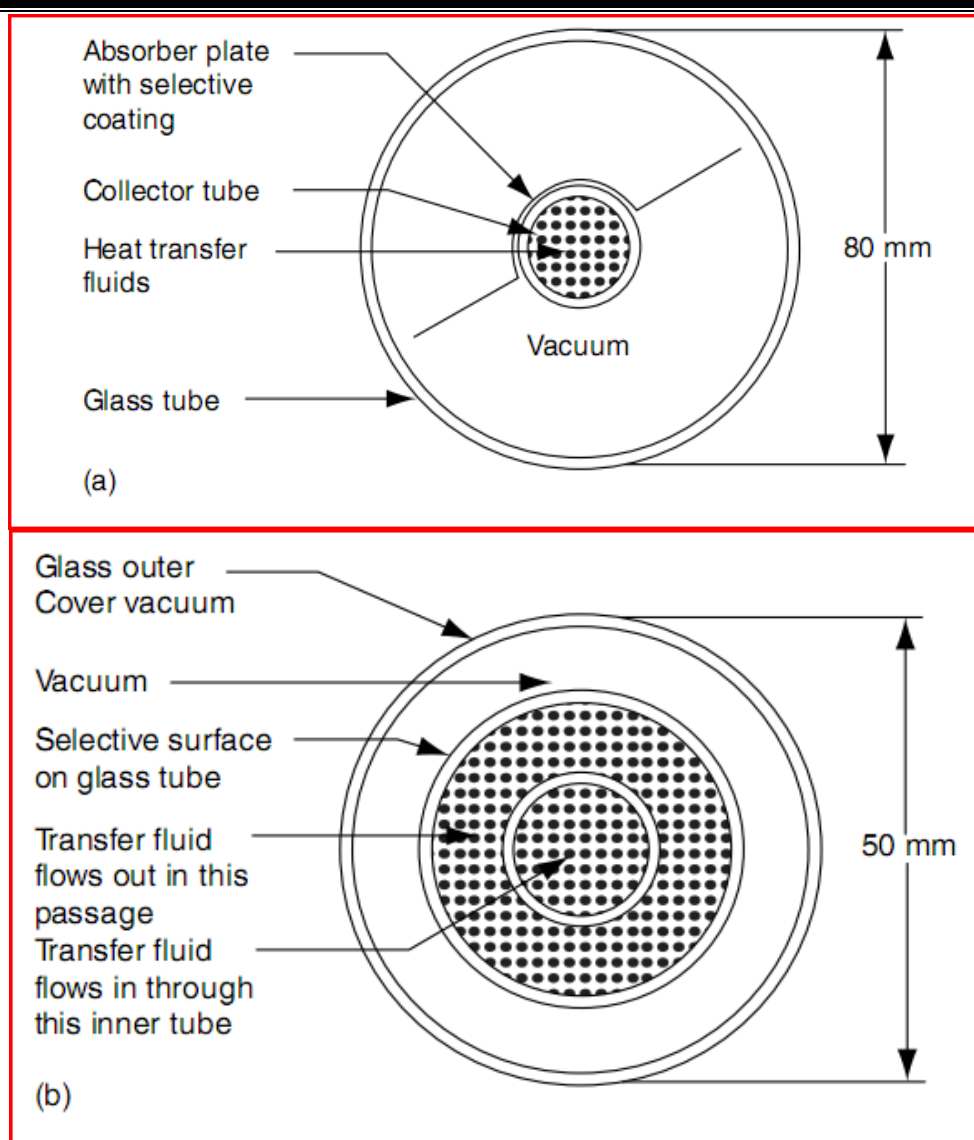


Fig 13: Evacuated tubular collectors.

and absorber can be eliminated. There are different possible arrangements of configuring evacuated tubular collectors. Two designs are shown in Figure 20.8. The first is like a small flat-plate collector with the liquid to be heated making one pass through the collector tube. The second uses an all-glass construction with the glass absorber tube being coated selectively. The fluid being heated passes up the middle of the absorber tube and then back through the annulus. Evacuated tubes can collect both direct and diffuse radiation and do not require tracking. Glass breakage and leaking joints due to thermal expansion are some of the problems which have been experienced with such collector types. Various reflector shapes (like flat-plate, V-groove, circular, cylindrical, involute, etc.) placed behind the tubes are often used to usefully collect some of the solar energy, which may otherwise be lost, thus providing a small amount of concentration.

Solar Pond

Introduction

Solar energy is an abundant and renewable energy source. The annual solar energy incident at the ground in India is about 20,000 times the current electrical energy consumption. The use of solar energy in India has been very

limited. This is because solar energy is a dilute energy source (average daily solar energy incident in India is $5 \text{ kWh/m}^2 \text{ day}$) and hence energy must be collected over large areas resulting in high initial capital investment; it is also an intermittent energy source. Hence solar energy systems must incorporate storage in order to take care of energy needs during nights and on cloudy days. This results in further increase in the capital cost of such systems. One way to overcome these problems is to use a large body of water for the collection and storage of solar energy. This concept is called a solar pond.

Principle of a solar pond

In a clear natural pond about 30% solar radiation reaches a depth of 2 meters. This solar radiation is absorbed at the bottom of the pond. The hotter water at the bottom becomes lighter and hence rises to the surface. Here it loses heat to the ambient air and, hence, a natural pond does not attain temperatures much above the ambient. If some mechanism can be devised to prevent the mixing between the upper and lower layers of a pond, then the temperatures of the lower layers will be higher than of the upper layers. This can be achieved in several ways. The simplest method is to make the lower layer denser than the upper layer by adding salt in the lower layers. The salt used is generally sodium chloride or magnesium chloride because of their low cost. Ponds using

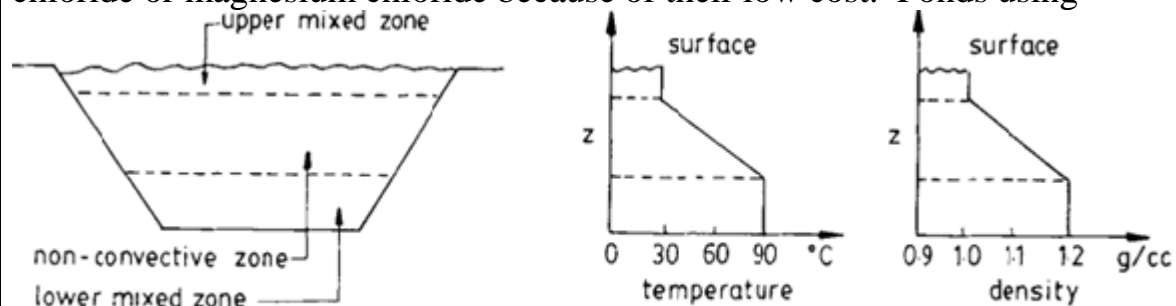


Fig 14: Different Zone in the solar pond

salts to stabilize the lower layers are called 'salinity gradient ponds'. There are other ways to prevent mixing between the upper and lower layers. One of them is the use of a transparent honeycomb structure which traps stagnant air and hence provides good transparency to solar radiation while cutting down heat loss from the pond. The honeycomb structure is made of transparent plastic material. One can also use a transparent polymer gel (cross-linked polyacrylamide) as a means of allowing solar radiation to enter the pond but cutting down the losses from the pond to the ambient. Typical temperature and density profiles in a large salinity gradient solar pond are shown in figure. We find that there are three distinct zones in a solar pond [Fig.14]. The lower mixed zone has the highest temperature and density and is the region where solar radiation is absorbed and stored. The upper mixed zone has the lowest temperature and density. This zone is mixed by surface winds, evaporation and nocturnal cooling. The intermediate zone is called the non-convective zone (or the gradient zone) because no convection occurs here. Temperature and density decrease from the bottom to the top in this layer, and it acts as a transparent insulator. It permits solar radiation to pass through but reduces the heat loss from the hot lower convective zone to the

cold upper convective zone. Heat transfer through this zone is by conduction only. The thicknesses of the upper mixed layer, the non-convective layer and the lower mixed layer are usually around 0.5, 1 m and 1 m, respectively.

Thermal performance

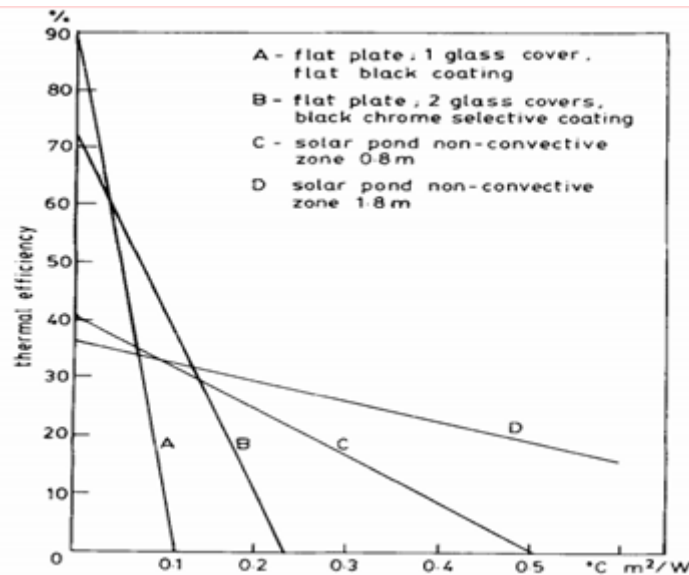
The thermal performance of a solar pond can be represented in a form similar to that used for conventional flat plate collectors. Assuming a steady state condition,

$$Q_u = Q_a - Q_e,$$

where Q_u = useful heat extracted, Q_a = solar energy absorbed, Q_e = heat losses.

Fig.15.

with
is



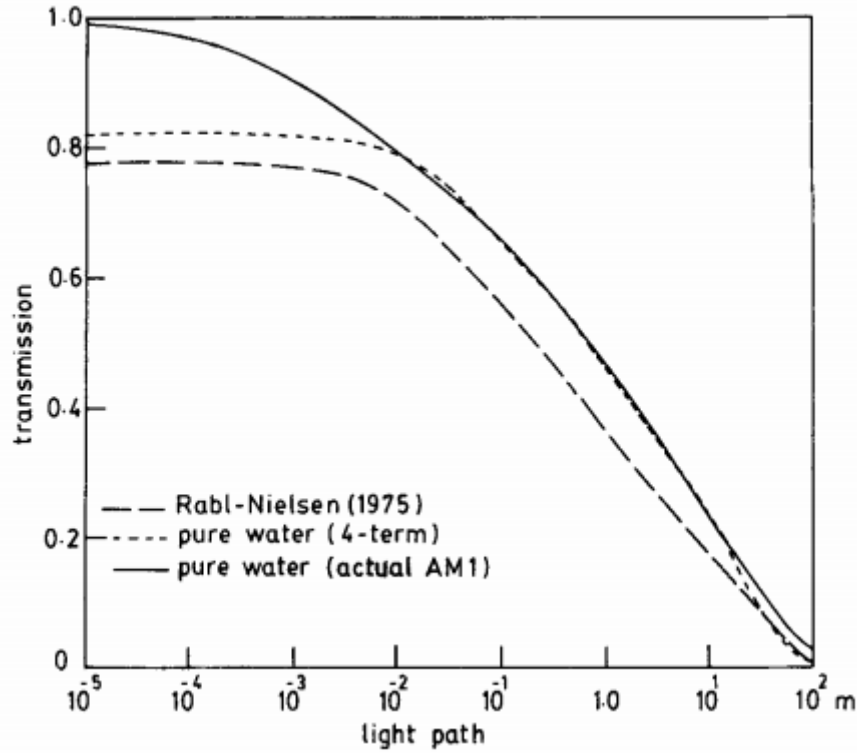
Variation of
thermal
efficiency
 T/I , where t
the
temperature
difference

between the storage zone and the ambient and I is the intensity of solar irradiation.

The thermal efficiency of a solar pond can be defined as $\eta = (Q_u/I)$ where I is the solar energy incident on the pond. Thermal efficiency can be written as $\eta = \eta_o - Q_e/I$, where η_o is called the optical efficiency of the pond (Q_a/I). We express $Q_e = U_o (T_s - T_a)$, where T_s is the pond storage-zone temperature, T_a is the ambient temperature and U_o is the overall heat-loss coefficient. If we neglect heat losses from the bottom and sides of the pond and assume that the temperature of the upper mixed layer is the same as the ambient, then $U_o = K_w/b$ where K_w is the thermal conductivity of water and b is the thickness of the gradient zone. Kooi (1979) has compared the efficiency of a solar pond with those of conventional flat plate collectors as shown in figure 15. We find that the thermal efficiency of a solar pond is higher than that of a flat plate collector when the operating temperatures are higher, and is in the range of 20 to 30% when the temperature difference is around 60°C. The thermal efficiency is strongly dependent upon the transparency of the pond which is influenced by the presence of algae and dust. Even if the solar pond is free of dust and algae, the absorption properties of pure water influence the transmission of solar radiation in the pond. The transmissivity of solar radiation in pure distilled water is shown in figure 16. We observe that about half the solar radiation is absorbed in the first 50cm of water. This is on account of strong infrared absorption bands in water. At a depth of 2 metres the transmission is about 40%. This sets the upper limit

on the thermal efficiency of a solar pond. The thickness of the gradient zone must be chosen depending on the temperature at which thermal energy is needed. If the thickness of the gradient zone is too high the transmission of solar radiation is reduced while if it is too small it causes high heat losses from the bottom to the top of the pond. The optimum value of the thickness depends on the temperature of the storage zone of the pond. Nielsen (1980) has provided a steady state analysis of a solar pond and has included the effect of solar radiation absorption in the gradient zone on the temperature profile.

Fig.16:
Variation



of

transmission of solar radiation with path length

In the steady state, the energy equation becomes

$$K(d^2T/dZ^2) = I(dz/dZ), \quad (1)$$

where K is the thermal conductivity of water and T is the fraction of solar radiation I reaching a depth Z .

This equation can be integrated to get

$$(dT/dZ) = \{I/K\} \{T(Z) - T(Z_1) + (dT/dZ)_{Z_2}\}, \quad (2)$$

where Z_2 is the interface between the gradient zone and storage zone. If $r/$ is the fraction of the incident solar energy which is extracted from the system as heat (including ground losses), then an energy balance of the storage zone gives

$$(dT/dZ)|_{Z_2} = \{I/K\} \{\tau(Z_2) - \eta\} \quad (3)$$

We can combine (2) and (3) to obtain the temperature profile in the gradient zone as

$$(dT/dZ) = \{I/K\} \{(\tau(Z) - \eta)\}$$

The temperature profile in the gradient zone for various values of η is shown in figure for $I = 200 \text{ W/m}^2$. Since T is proportional to I , the

above figure can also be used for other values of I by multiplying by an appropriate constant. The effect of ground-heat losses on the performance of a solar pond has been analysed. The ground heat-loss coefficient can be expressed as

$$U_g = K(1/D + bP/A),$$

where K is the ground conductivity. D is the depth of the water table, P and A are the pond perimeter and surface area and b is a constant whose value is around 0.9 (depending upon the side slope). The thermal efficiency of a steady state solar pond can now be written as

$$\eta = \frac{1}{Z_2 - Z_1} \left[\int_{Z_1}^{Z_2} \tau(Z) dZ - \frac{K_w \Delta T}{I} \right] - \frac{U_g \Delta T}{I},$$

where ΔT is the temperature difference between the storage zone and the upper mixed layer.

Note that the optical efficiency of the solar pond is dependent upon the mean transmittance in the gradient zone. This is because the radiation absorbed in the gradient zone is helpful in reducing the heat losses from the storage zone.

The steady-state analysis of a solar pond is useful in the sizing of the pond for a specific application. There will, however, be strong seasonal variation in the performance of the pond on account of seasonal variations in solar insolation, wind and temperature. A simple two-zone model for the simulation of the storage zone temperature of the pond has been proposed. The observed values of solar radiation, heat extraction and gradient zone thickness in the Bangalore solar pond were used in the simulation. The predictions of the storage zone temperature are compared with the observations. The predicted storage zone temperatures are in good agreement with observation. Predictions based on climatological variation of solar radiation show higher deviation.

Pond construction

The site selected for the construction of a solar pond should have the following attributes;

- (a) be close to the point where thermal energy from the pond will be utilized;
- (b) be close to a source of water for flushing the surface mixed-layer of the pond;
- (c) the thermal conductivity of the soil should not be too high;
- (d) the water table should not be too close to the surface.

To minimize heat losses and liner costs, the pond should be circular. Since a circular pond is difficult to construct, a square pond is normally preferred. In some cases, such as the Bangalore solar pond, the site constraints may force one to construct a rectangular pond with large aspect ratio. For large solar ponds (area > 10,000m²), the shape will not have a strong influence on cost or heat losses. The depth of the solar pond must be determined depending on the specific application. The usual thicknesses

of the surface, gradient and storage zone of the pond are 0.5, 1 and 1 m, respectively. If a particular site has low winds, one can reduce the thickness of the surface layer to 30 cm. If the temperature required for process heat applications is around 40°C (such as hatcheries) then the thickness of the gradient zone can be reduced to 0.5 m. Storage zone thickness higher than 1 m may be required to take care of long periods of cloudiness.

The excavation for a solar pond is similar to that for construction of water reservoirs. The side slope of the pond can vary between 1 : 1 to 1: 3 depending upon the type of soil. After the excavation and bunding is completed, and before a liner is laid, one must ensure that the area is free of sharp objects which may damage the liner when it is being laid.

In most solar ponds, a polymeric liner is used to prevent the leakage of salt. Some solar ponds in Israel, Australia and Mexico have not been lined. This is because at those sites the soil has low permeability. Since the leakage of salt from a solar pond can cause environmental pollution it is necessary to use a liner in most applications. Many types of polymeric liner have been used in solar ponds. Some of them are low-density polyethylene (LDPE), high-density polyethylene (HDPE), plasticized polyvinyl chloride, chlorinated polyethylene (CPE), chloro-sulphonated polyethylene (Hypalon), ethylene propylene diene monomer (EPDM) and polymer-coated polyester fabric (XR-5). These liners are available usually in 10m widths and hundreds of metres lengths, and are heat-sealed in the factory or in the field. Liners such as XR-5, EPDM and Hypalon can be used as exposed liners because they can resist ultraviolet degradation. Liners such as LDPE or HDPE undergo ultraviolet degradation and, hence, need to be covered with soil, brickwork or tiles. In the Bangalore solar pond three LDPE liners have been used. The topmost liner was used as sacrificial liner and replaced every two years. After the installation of the liner it can be tested for leaks by using a portable blower. If there are any pin holes or leakages at joints the liner will billow upwards. An inexpensive method to reduce leakage from pin holes is the use of Bentonite clay between adjacent LDPE liners. When Bentonite clay absorbs moisture it swells considerably and blocks further leakage. The use of alternate layers of LDPE and clay has been implemented at the 210,000m² solar pond at Bet Ha Arava in Israel. After the installation of the liner, it is useful to have a method for detection of any leakage of salt. Hull et al (1989) have shown that an accurate calculation of salt inventory in the pond will provide indication of leak as low as 1 mm per month.

After the liner is placed, the pond is filled with water to a depth equal to the thickness of the storage zone and half the gradient zone. Salt is directly dumped into the pond. The salt dissolves rapidly if the water in the pond is circulated through a pump and the water is directed as a jet into the pond. The concentration of the salt at the storage zone is between 200 to 300 kg/m³. Hence the salt inventory is between 1/3 to 1/2 ton per m². The normal method of establishing the gradient zone is by injection of fresh water. This method, is convenient and hence has been adopted in most solar pond installations in the world. Fresh water injection is initiated at the

interface between the storage zone and the gradient zone using a diffuser (see figure). The fresh water rises to the top and reduces the density of the layer above the injection point. For every 1 cm rise in water level, the diffuser is lifted by 2 cm. When the diffuser is at the same level as the water surface the establishment of the gradient zone is completed. More fresh water is added above the gradient zone to create an upper mixed layer with a thickness of 30 to 50 cm. The evolution Of density profile during the establishment of the gradient zone in the Miamisburg solar pond is shown in figure. After the establishment of the gradient zone, the pond begins to heat up if clear sky conditions prevail. The temperature in the storage zone of the Bangalore solar pond increased by 30°C within one month of the establishment of the gradient zone.

Pond stability

A solar pond will be statically stable if its density decreases with height from the bottom. A solar pond is subjected to various disturbances such as the wind blowing at the top surface and heating of the side walls. The criterion for dynamic stability of the pond is somewhat more stringent than that for static stability. This criterion can be obtained by perturbation analysis of the basic laws of conservation of mass, momentum and energy. The criterion for stability obtained from such an analysis can be written as

$$\beta_T \frac{\partial T}{\partial Z} < \beta_S \frac{\partial S}{\partial Z} \left[\frac{Sc + 1}{Pr + 1} \right]$$

where

$$\beta_T = -\frac{1}{\rho} \left[\frac{\partial \rho}{\partial T} \right] = \text{thermal expansion coefficient,}$$

$$\beta_S = +\frac{1}{\rho} \left[\frac{\partial \rho}{\partial S} \right] = \text{salinity expansion coefficient.}$$

Pr = Prandtl number,

Sc = Schmidt number.

For typical conditions encountered in a solar pond, this result can be simplified to

$$\frac{\partial S}{\partial Z} > 1.19 \frac{\partial T}{\partial Z},$$

where S is in kg/m³ and T in °C.

In order to prevent formation of internal convective zones within the gradient zone it is essential that the above criterion is satisfied at all points within the gradient zone. A safety margin of 2 is desirable. In the Bangalore solar pond, an internal convective zone was formed although the safety margin was above 2. This is believed to be on account of side wall heating. Side-wall heating can result in the formation of internal convective zones. In the Bangalore solar pond, the distance between the side

walls was as low as 9 m at the bottom of the gradient zone. The free convective boundary layers that formed on the side walls could have merged at the centre and led to the formation of internal convective zones. In large solar ponds, side-wall heating would not be able to initiate the formation of internal convective zones and hence a safety margin around 2 should be adequate. The thickness of the gradient zone (which provides insulation and hence reduces heat losses) can be reduced by the formation of internal convective zones or erosion of the boundaries of the gradient zone. Erosion of the gradient zone-surface zone interface occurs primarily on account of wind-induced mixing. The effect of wind-induced mixing can be reduced by using floating plastic nets or pipes. It is reported that mean-squared wind speeds exceeding $20 \text{ m}^2/\text{s}^2$ caused the erosion of the gradient zone at the rate of 1 cm/day, while for values below $10 \text{ m}^2/\text{s}^2$ there was no gradient erosion. Erosion of the gradient zone from below depends upon the density and temperature gradients at the gradient zone-storage zone interface. Nielsen (1983) has determined experimentally that the gradient zone-storage zone interface remains stationary if the salinity and temperature gradients satisfy the following relationship.

$$\frac{\partial S}{\partial Z} = A \left[\frac{\partial T}{\partial Z} \right]^{0.63},$$

where

$$A = 28(\text{kg}/\text{m}^4)(\text{m}/\text{K})^{0.63}.$$

If the actual salinity gradient is more than that given by the above criterion, the gradient zone will move downwards, while if it is less, the gradient zone will erode. To ensure that the gradient zone does not erode from above, the density of the surface layer must be kept as low as possible. The density of the surface layer increases on account of diffusion of salt from below and because of evaporation. Hence the surface layer must be flushed regularly with fresh water to keep the salinity below 5% (by weight).

Salt replenishment

On account of the gradient of concentration between the storage and the surface zones, there is a steady diffusion of salt through the gradient zone. The transport of salt through the gradient zone by diffusion can be expressed as

$$Q_m = [(S_l - S_u)D]/b,$$

where b = thickness of gradient zone, D = mass diffusion coefficient, and S_l, S_u = salinity in lower and upper mixed layers, respectively.

If the salinity in the storage zone is $300 \text{ kg}/\text{m}^3$ and in the surface zone is $20 \text{ kg}/\text{m}^3$, gradient zone thickness is 1 m and diffusion coefficient of salt is $3 \times 10^{-9} \text{ m}^2/\text{s}$, then the rate of transport of salt by diffusion will be about $30 \text{ kg}/\text{m}^2 \text{ year}$. In small solar ponds the salt transport can be as high as $60 \text{ kg}/\text{m}^2 \text{ year}$ because of additional salt transport through side-wall heating.

If the salt lost from the storage zone is not replenished regularly then there may be an erosion of the gradient zone from below or formation of internal convective zones. The normal method of salt

replenishment is by pumping the brine in the storage zone through a salt bed.

Solar pond applications

In the last thirty years more than sixty solar ponds have been built all around the world. The largest solar pond built so far is the 250,000m² pond at Bet Ha Arava in Israel. This pond has been used to generate 5 MWe (peak) power using an organic Rankine cycle. The heat stored in the solar pond can be used in a variety of applications. In Argentina, solar ponds are being used commercially for production of sodium sulphate using solution-refining techniques. The ore (rich in sodium sulphate) mined in the Andes Mountains is dissolved in a 400 m² solar pond constructed adjacent to the mines. The brine is removed and placed in a cooling pond at night where sodium sulphate crystallizes. Solar pond concepts have been used to prevent precipitation of magnesium sulphate in the salt works at the Great Salt Lake in Utah, USA. A 2000 m² solar pond has been constructed to provide hot water for a swimming pool in Miamisburg, Ohio, USA. A 3355m² solar pond at El Paso, Texas, has demonstrated the use of a solar pond for food processing, power generation and desalination. The feasibility of grain drying using a solar pond has been demonstrated at Montreal (Canada), Ohio (USA) and for heating greenhouses at Lisbon (Portugal). A 20,000m² solar pond in Italy has been used for desalination of sea water and producing 120 tonnes of fresh water per day. The major limitation of solar ponds for industrial applications is the fact that the temperature in the storage layer cannot go beyond 95°C. Many industries require process temperatures above 100°C. The use of an absorption heat pump in conjunction with a solar pond to generate steam is possible. If this approach is successful, it will open up new applications for thermal energy from solar ponds.

The Indian experience

The first solar pond in India was a 1200 m² pond built at the Central Salt and Marine Chemicals Research Institute in Bhavnagar, Gujarat, in 1970. This solar pond was based on bittern, which is a waste product during the production of sodium chloride from sea water. The second solar pond was a 100 m² circular pond built in Pondicherry in 1980. This pond used sodium chloride and was operational for two years. The LDPE liner used in this pond developed a leak and hence had to be replaced without too much loss of thermal energy. The third solar pond was a 1600m² solar pond built at Bhavnagar in 1980. This pond was based on bittern and hence had problems with the clarity of bittern. The fourth solar pond was a 240 m² solar pond commissioned at the Indian Institute of Science, Bangalore, in 1984. This pond has provided long-term data on continuous heat extraction from small solar ponds and has demonstrated the technical and economic viability of small solar ponds for low temperature process heat. Srinivasan (1985) has argued that low temperature process heat from small solar ponds can be used in hatcheries, hostels and dairies. A 400 m² solar pond has been constructed at Masur on the West Coast of India to supply hot water needs of a rural community. A 6000m² solar pond in Bhuj (Gujarat) and is used to supply hot water for a dairy. A 6000 m² solar pond is under construction at Pondicherry

for generation of 100 kWe (peak) power. The solar ponds at Masur and Bhuj experienced salt leakages on account of the failure of LDPE liners.

Conclusions

Solar pond technology has made tremendous progress in the last fifteen years. An excellent monograph is now available on the science and technology of salinity gradient solar ponds. This technology is cost effective for low temperature process heat needs of industry. The generation of electricity using solar ponds is not economically viable as yet. However, the new concerns regarding the environment and the safety of nuclear power plants and nuclear waste disposal may change the picture totally.

SOLAR DRYER

Food losses in the developing world are thought to be 50% of the fruits and vegetables grown and 25% of harvested food grain. Food preservation can reduce wastage of a harvest surplus, allow storage for food shortages, and in some cases facilitate export to high-value markets. Drying is one of the oldest methods of food preservation. Drying makes produce lighter, smaller, and less likely to spoil. This paper presents the background and possibilities of solar drying, focusing on the technical needs of small farmers in the developing world. (The important social and cultural implications of introducing a new technology are not addressed here). The background section explains the moisture content of foods, how moisture is removed, and the energy required for this drying process. The “Solar Drying Essentials” section discusses drier components, the drying process, and the capabilities of solar driers. The paper concludes with a classification of drier types, some criteria for selecting a drier, and references to further information.

Background

Preserving fruits, vegetables, grains, and meat has been practiced in many parts of the world for thousands of years. Methods of preservation include: canning, freezing, pickling, curing (smoking or salting), and drying. Food spoilage is caused by the action of molds, yeasts, bacteria, and enzymes. The drying process removes enough moisture from food to greatly decrease these destructive effects.

Moisture Content

The moisture content of fresh foods ranges from 20% to 90%. Foods require different levels of dryness for safe storage, as shown in Table 1. For example: the moisture content of rice must be reduced from 24% to 14% of the total weight. Therefore, drying 1,000 kg of rice requires the removal of 100 kg of water. Safe storage generally requires reducing the moisture content to below 20% for fruits, 10% for vegetables, and 10-15% for grains. If food is properly dried, no moisture will be visible when it is cut.

Table 1: Moisture contents.

Food	Initial	Desired	Moisture Content (Wet Basis)
------	---------	---------	---------------------------------

Rice	24%	14%
Maize	35%	15%
Potatoes	75%	13%
Apricots	85%	18%
Coffee	50%	11%

Moisture Absorption

The length of time required to dry food depends upon how quickly air absorbs moisture out of the food. Fast drying primarily depends upon three factors: the air should be warm, dry, and moving. The dryness of air is measured in terms of relative humidity (RH). If air is at 100% relative humidity, it has absorbed 100% of the water it can hold at that temperature. If air has a RH near 100%, it must be heated before it will be able to absorb moisture out of food.

Energy Requirements

The amount of energy that must be added in order to dry produce depends on the local climate. Air drops in temperature as it absorbs moisture from food, and thus supplies some energy for drying. Therefore, if the air is warm and dry enough, food will dry slowly without additional heating from fuel or the sun. However, additional heat shortens the drying process and yields a higher quality product. Under typical conditions 100kg of maize might be dried with roughly 3kg of kerosene, or with 10kg of biomass such as wood or rice husks. Alternatively, a 6m² solar collector will dry the maize over three sunny days, if the relative humidity is low. The size of solar collector required for a certain size of drier depends on the ambient temperature, amount of sun, and humidity.

Solar Drying Essentials: Solar Drier Components.

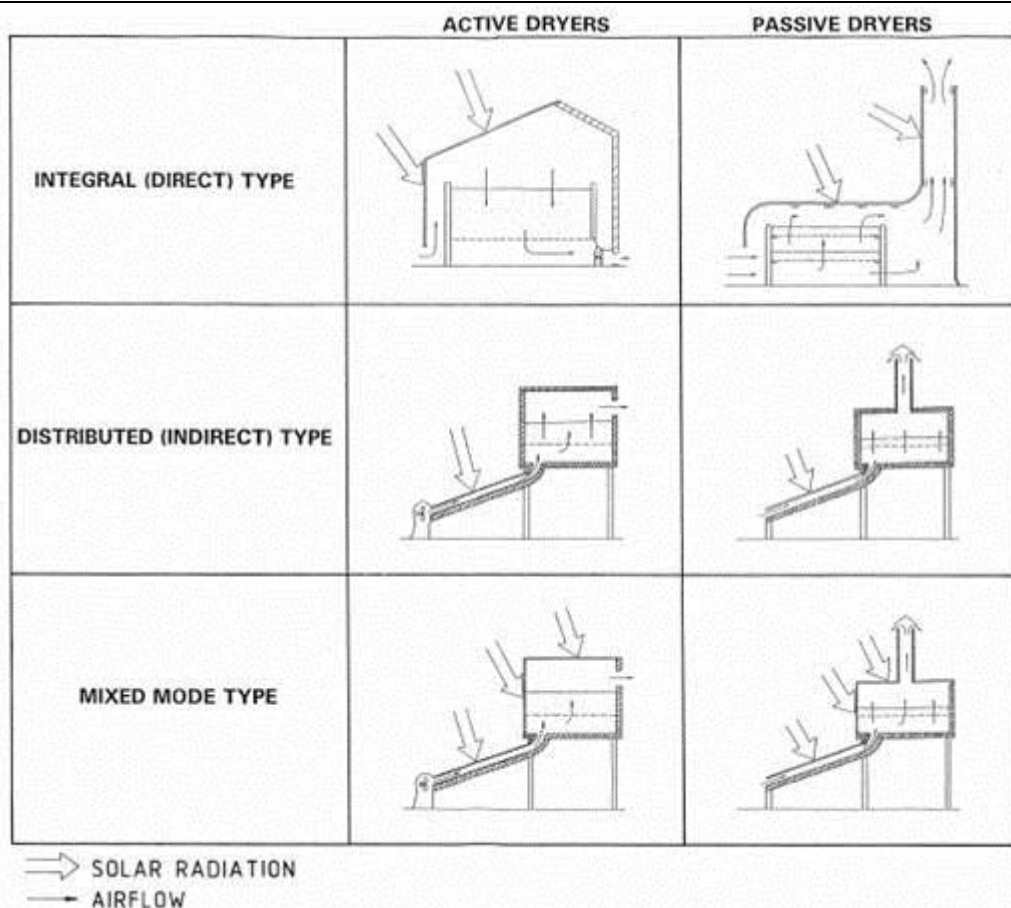


Fig.17: Different designs of solar driers

Solar driers may be viewed as three main components. Figures 17 shows one type of solar drier with each of these three components labeled. The drying chamber protects the food from animals, (with sawdust, for example) to increase efficiency. The trays should be safe for food contact; a plastic coating is best to avoid harmful residues in food. A general rule of thumb is that one m² of tray area is needed to lay out 10kg of fresh produce. The solar collector (or absorber) is often a dark colored box with a transparent cover. It raises the air temperature between 10 and 30°C above ambient. This may be separate from the drier chamber, or combined (as with direct driers). Often the bottom surface of the absorber is dark to promote solar absorption, and occasionally charred rice chaff serves this purpose. Glass is recommended for the absorber cover, although it is expensive and difficult to use. Plastic is acceptable if it is firm or supported by a rib such that it does not sag and collect water. Solar driers use one of two types of airflow systems; natural convection utilizes the natural principle that hot air rises, and forced convection driers force air through the drying chamber with fans. The effects of natural convection may be enhanced by the addition of a chimney in which exiting air is heated even more. Additionally, prevailing winds may be taken advantage of. Natural convection driers require careful use; stacking the product too high or a lack of sun can cause air to stagnate in the drier and halt the drying process. The use of forced convection can reduce drying time by three times and decrease the required collector area by 50%. Consequently, a drier using fans may achieve the same throughput as a natural convection drier with a collector six times as large. Fans may be powered with

utility electricity if it is available, or with a solar photovoltaic cell. For comparison, one study showed that the installation of three small fans and a photovoltaic cell was equivalent to the effect of a 12m chimney.

The Drying Process

Producing safe, high-quality dried produce requires careful procedures throughout the entire preservation process. Foods suffer only a slight reduction in nutrition and aesthetics if dried properly; however, incorrect drying can dramatically degrade food and brings the risk of food poisoning.

A process similar to the following seven steps is usually used when drying fruits and vegetables (and fish, with some modifications):

1. Selection (fresh, undamaged produce)
2. Cleaning (washing & disinfection)
3. Preparation (peeling, slicing, etc.)
4. Pre-treatment (e.g. sulfurizing, blanching, salting)
5. Drying
6. Packaging
7. Storage or Export

Only fresh, undamaged food should be selected for drying to reduce the chances of spoilage and help insure a quality product. After selection, it is important to clean the produce. This is because drying does not always destroy microorganisms, but only inhibits their growth. Fruits, vegetables, and meats generally require a pre-treatment before drying. The quality of dried fruits and vegetables is generally improved with one or more of the following pre-treatments: anti-discoloration by coating with vitamin C, de-waxing by briefly boiling and quenching, and sulfurization by soaking or fumigating. Fish is often salted. A small amount of chemical will treat a large amount of produce, and thus the cost for these supplies is usually small. However, potential problems with availability and the complexity of the process should be considered. The best pre-treatment procedure may be determined through a combination of experimentation and consulting literature on the subject. After selection, cleaning, and pre-treatment, produce is ready to place in the drier trays. Solar driers are usually designed to dry a batch every three to five days. Fast drying minimizes the chances of food spoilage. However, excessively fast drying can result in the formation of a hard, dry skin - a problem known as case hardening. Case hardened foods appear dry outside, but inside remain moist and susceptible to spoiling. It is also important not to exceed the maximum temperature recommended, which ranges from 35 to 45°C depending upon the produce. Learning to properly solar dry foods in a specific location usually requires experimentation. For strict quality control, the drying rate may be monitored and correlated to the food moisture content to help determine the proper drying parameters. After drying is complete, the dried produce often requires packaging to prevent insect losses and to avoid re-gaining moisture. It should cool first, and then be packaged in sanitary conditions. Sufficient drying and airtight storage

will keep produce fresh for six to twelve months. If possible, the packaged product should be stored in a dry, dark location until use or export. If produce is to be exported, it must meet the quality standards of the target country. In some cases this will require a chemical and microbiological analysis of dried samples in a laboratory.

Food drying requires significant labor for pre-treatment (except for grains), and minimal involvement during the drying process such as shifting food to insure even drying. Solar drying equipment generally requires little maintenance.

Capabilities of Solar Driers

Solar drying can preserve a variety of fruits, vegetables, grains, and some meat. It can also be used for cash crops such as coffee, herbs, cashew, and macadamia. Solar driers exist for treating timber, although they are not discussed here. Fruits are ideal for preservation by drying since they are high in sugar and acid, which act to preserve the dried fruit. Vegetables are more challenging to preserve since they are low in sugar and acid. Drying meat requires extreme caution since it is high in protein, which invites microbial growth. Fish drying, for example, requires thorough cleaning of the drier after each batch. Lists are available explaining which foods are suited to drying. For example, “Apples, apricots, coconuts, dates, figs, guavas, and plums are fruits that dry quite easily, while avocados, bananas, breadfruit, and grapes are more difficult to dry. Most legumes are easily dried, as well as chilies, corn, potatoes, cassava root, onion flakes, and the leaves of various herbs and spices. On the other hand, asparagus, beets, broccoli, carrots, celery, various greens, pumpkin, squash, and tomatoes are more difficult to dry successfully”.

Classification of Driers

Drying techniques may be divided into six general categories based on the way the food is heated (summarized in Table). Open-air, or unimproved, solar drying takes place when food is exposed to the sun and wind by placing it in trays, on racks, or on the ground. Although the food is rarely protected from predators and weather, in some cases screens are used to keep out insects, or a clear roof is used to shed rain. Direct sun driers enclose food in a container with a clear lid, such that sun shines directly on the food. In addition to the direct heating of the solar radiation, the green house effect traps heat in the enclosure and raises the temperature of the air. Vent holes allow for air exchange. Indirect sun driers heat fresh air in a solar collector separate from the food chamber, so the food is not exposed to direct sunlight. This is of particular importance for foods which lose nutritional value when exposed to direct sunlight. Mixed mode driers combine the aspects of direct and indirect types; a separate collector pre-heats air and then direct sunlight adds heat to the food and air. Hybrid driers combine solar energy with a fossil fuel or biomass fuel such as rice husks. (It is interesting to note that a harvest of 1000 kg of rice yields 200 kg of husks, and requires burning only 25 kg of husks to be dried) (Hislop, 1992). Fueled driers use conventional fuels or utility supplied electricity for heat and ventilation.

Table: Classification of food driers.

<i>Classification</i>	<i>Description</i>

Open-Air	Food is exposed to the sun and wind by placing in trays, on racks, or on the ground. Food is rarely protected from predators and the weather.
Direct Sun	Food is enclosed in a container with a clear lid allowing sun to shine directly on the food. Vent holes allow for air circulation.
Indirect Sun	Fresh air is heated in a solar heat collector and then passed through food in the drier chamber. In this way the food is not exposed to direct sunlight.
Mixed Mode	Combines the direct and indirect types; a separate collector pre-heats air and direct sunlight adds heat to the food and air.
Hybrid	Combines solar heat with another source such as fossil fuel or biomass.
Fueled	Uses electricity or fossil fuel as a source of heat and ventilation

Comparing Solar Drying with Other Options.

A first step when considering solar drying is to compare it with other options available. In some situations open-air drying or fueled driers may be preferable to solar. If either of these is already used in a certain location, solar drying will only be successful if it has a clear advantage over the current practice. Table lists the primary benefits and disadvantages of solar drying when compared with traditional open-air drying, and then with the use of fueled driers.

<i>Type of Drying</i>	<i>Benefits(+)</i>	<i>Disadvantages(-)</i>
Solar vs. Open-air	<ul style="list-style-type: none"> + Can lead to better quality dried products, and better market prices + Reduces losses and contamination from insects, dust, and animals + Reduces land required (by roughly 1/3) + Some driers protect food from sunlight, better preserving nutrition & color + May reduce labor required + Faster drying time reduces chances of spoilage + More complete drying allows longer storage + Allows more control (sheltered from rain, for example) 	<ul style="list-style-type: none"> - More expensive, may require importing some materials - In some cases, food quality is not significantly improved - In some cases, market value of food will not be increased
Solar vs. Fueled	<ul style="list-style-type: none"> + Prevents fuel dependence + Often less expensive + Reduced environmental impact (consumption of non-renewables) 	<ul style="list-style-type: none"> - Requires adequate solar radiation - Hot & dry climates preferred (usually RH below 60% needed) - Requires more time - Greater difficulty controlling process, may result in lower quality product

The above comparison will assist in deciding among solar, open-air, and fueled driers. The local site conditions will also play an important role in this decision. Some indications that solar driers may be useful in a specific location include:

- Conventional energy is unavailable or unreliable (making fuel driers unattractive)
- Plenty of sunshine
- Dry climate (relative humidity below 60%)
- Quality of open-air dried products needs improvement
- Land is extremely scarce (making open-air drying unattractive)

- Introducing solar drying technology will not have harmful socio-economic effects

In addition to local conditions, the type of product to be dried plays a role in the decision process. For example, in some locations traditional open-air drying may be suitable for coffee, whereas fruit would largely be lost to predators. High-value cash crops often require consistent high quality without risking lost produce, and thus the use of fuel driers may be best.

The uses of solar dried products might include: self-consumption, local sale, large markets, and export. Therefore, the potential market for solar dried foods is often another important consideration. Preservation always slightly reduces nutrition and aesthetics, and therefore dried foods are only desirable if fresh is not available. Even where fresh is not available, consumer acceptance may be problematic if dried foods are not already on the market. Existing infrastructure may be available to facilitate marketing dried produce. The expected market price will influence how much can be invested in a drier. Unfortunately, higher quality from solar driers doesn't always bring higher market prices than open-air drying. In some cases local markets are not willing to pay extra for higher quality solar dried products. In some cases a centralized operation is more economical than numerous small driers, due to economies of scale. The appropriate amount of centralization is different for simple natural convection driers than for more sophisticated forced convection driers. Natural convection may be more effective with multiple small driers rather than one large unit. This is because the construction of small driers is simpler, and independent operation allows more flexibility. However, for forced convection driers, economies of scale favor centralization to maximize use of the ventilation equipment.

Some useful criteria for selecting a solar drier. If the use of solar driers appears favorable, the next step is to consider which type of solar drier to use. Table presents four general categories of solar driers along with advantages and disadvantages of each.

Table : Advantages and disadvantages of the four types of solar food driers.

<i>Classification</i>	<i>Advantages</i>	<i>Disadvantages</i>
Direct Sun	+ least expensive + simple	- UV radiation can damage food
Indirect Sun	+ products protected from UV + less damage from temperature extremes	- more complex and expensive than direct sun
Mixed Mode	+ less damage from temperature extremes	- UV radiation can damage food - more complex and expensive than direct sun
Hybrid	+ ability to operate without sun reduces chance of food loss + allows better control of drying + fuel mode may be up to 40x faster than solar	

Choosing a solar drier is a subjective decision, and is heavily dependent upon local conditions and the product to be dried. The following aspects should be considered when selecting a drier:

- Can the drier be made from locally available materials & skills?
- What are the purchase & maintenance costs?
- What is the drying capacity?
- What range of foods can be dried?
- What is the drying time required?
- What is the quality of the dried product?
- Is the drier adaptable to local conditions?

Solar drying has the potential to improve the quality of life in some areas. The decision of whether solar, open-air, or fueled driers are best may be made according to the criteria in Table. If solar drying is the best option, Table 6 and the selection criteria given may be used to choose a drier. Once a particular drier has been chosen, it may be purchased (if available) or constructed. Experience shows that the best configuration of a solar drier is different for each location, and therefore successful food drying usually requires a period of experimentation and adjustments at the local site.

Solar Still

Introduction

There is an important need for clean, pure drinking water in many developing countries. Often water sources are brackish (i.e. contain dissolved salts) and/or contain harmful bacteria and therefore cannot be used for drinking. In addition, there are many coastal locations where seawater is abundant but potable water is not available. Pure water is also useful for batteries and in hospitals or schools. Distillation is one of many processes that can be used for water purification. This requires an energy input, as heat, solar radiation can be the source of energy. In this process, water is evaporated, thus separating water vapour from dissolved matter, which is condensed as pure water. Solar water distillation is a solar technology with a very long history and installations were built over 2000 years ago, although to produce salt rather than drinking water. Documented use of solar stills began in the sixteenth century. An early large-scale solar still was built in 1872 to supply a mining community in Chile with drinking water. Mass production occurred for the first time during the Second World War when 200,000 inflatable plastic stills were made to be kept in life-crafts for the US Navy.

There are a number of other approaches to water purification and desalination, such as photovoltaic powered reverse-osmosis, for which small-scale commercially available equipment is available. These are not considered here. In addition, if treatment of polluted water is required rather than desalination, slow sand filtration is a good option.

Energy requirements for water distillation:

The energy required to evaporate water is the latent heat of vaporisation of water. This has a value of 2260 kilojoules per kilogram (kJ/kg). This means that to produce 1 litre (i.e. 1kg since the density of water is 1kg/litre) of pure water by distilling brackish water requires a heat input of 2260kJ. This does not allow for the efficiency of the heating method, which will be less than 100%, or for any recovery of latent heat that is rejected when the water vapour is condensed. It should be noted that, although 2260kJ/kg is required to evaporate water, to pump a kg of water through 20m head requires only 0.2kJ/kg. Distillation is therefore normally considered only where there is no local source of fresh water that can be easily pumped or lifted.

How a simple solar still operates

Figure 18 shows a single-basin still. The main features of operation are the same for all solar stills. The incident solar radiation is transmitted through the glass cover and is absorbed as heat by a black surface in contact with the water to be distilled. The water is thus heated and gives off water vapour. The vapour condenses on the glass cover, which is at a lower temperature because it is in contact with the ambient air, and runs down into a gutter from where it is fed to a storage tank

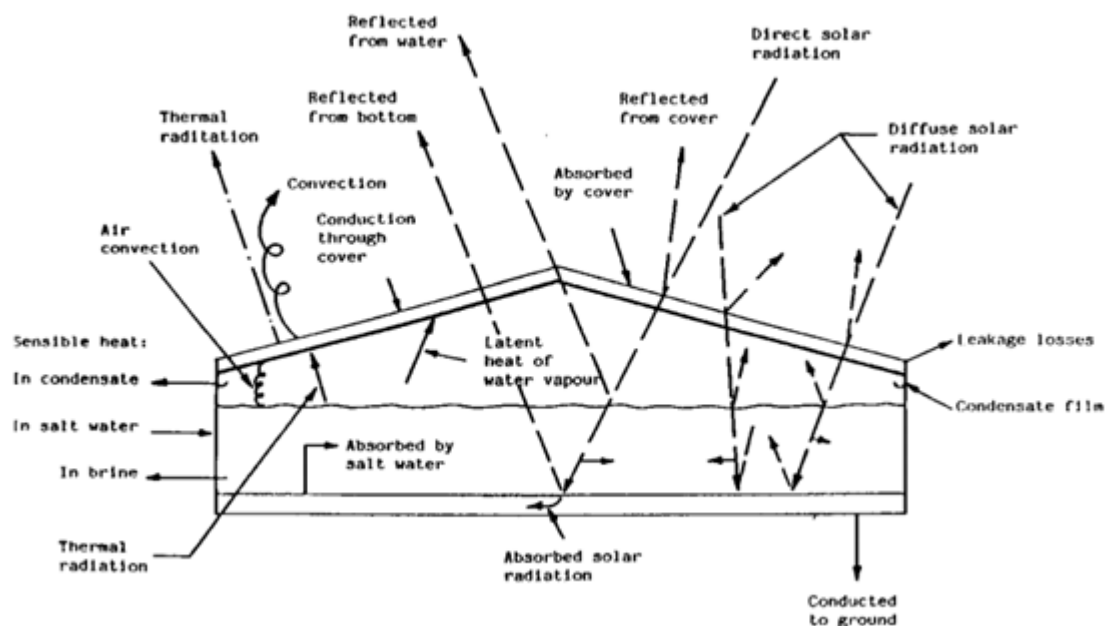


Fig.18. Design objectives for an efficient solar still

For high efficiency the solar still should maintain:

- a high feed (undistilled) water temperature
- a large temperature difference between feed water and condensing surface
- low vapour leakage.

A high feed water temperature can be achieved if:

- a high proportion of incoming radiation is absorbed by the feed water as heat. Hence low absorption glazing and a good radiation absorbing surface are required
- heat losses from the floor and walls are kept low

- the water is shallow so there is not so much to heat.

A large temperature difference can be achieved if:

- the condensing surface absorbs little or none of the incoming radiation
- condensing water dissipates heat which must be removed rapidly from the condensing surface by, for example, a second flow of water or air, or by condensing at night.

Design types and their performance

Single-basin stills have been much studied and their behavior is well understood [Fig.19]. Efficiencies of 25% are typical. Daily output as a function of solar irradiation is greatest in the early evening when the feed water is still hot but when outside temperatures are falling. Material selection is very important. The cover can be either glass or plastic. Glass is considered to be best for most long-term applications, whereas a plastic (such as polyethylene) can be used for short-term use.

Sand concrete or waterproofed concrete are considered best for the basin of a long-life still if it is to be manufactured on-site, but for factory-manufactured stills, prefabricated ferro-concrete is a suitable material.

Multiple-effect basin stills have two or more compartments. The condensing surface of the lower compartment is the floor of the upper compartment. The heat given off by the condensing vapour provides energy to vaporize the feed water above. Efficiency is therefore greater than for a single-basin still typically being 35% or more but the cost and complexity are correspondingly higher.

Wick stills - In a wick still, the feed water flows slowly through a porous, radiation-absorbing pad (the wick). Two advantages are claimed over basin stills. First, the wick can be tilted so that the feed water presents a better angle to the sun (reducing reflection and presenting a large effective area). Second, less feed water is in the still at any time and so the water is heated more quickly and to a higher temperature. Simple wick stills are more efficient than basin stills and some designs are claimed to cost less than a basin still of the same output.

Emergency still - To provide emergency drinking water on land, a very simple still can be made. It makes use of the moisture in the earth. All that is required is a plastic cover, a bowl or bucket, and a pebble.

Hybrid designs - There are a number of ways in which solar stills can usefully be combined with another function of technology. Three examples are given:

- Rainwater collection. By adding an external gutter, the still cover can be used for rainwater collection to supplement the solar still output.
- Greenhouse-solar still. The roof of a greenhouse can be used as the cover of a still.
- Supplementary heating. Waste heat from an engine or the condenser of a refrigerator can be used as an additional energy input.

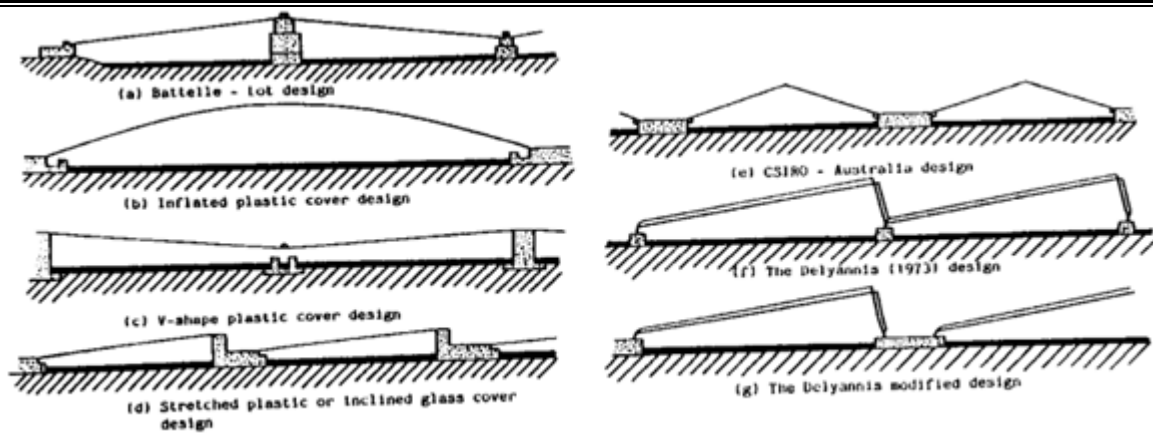


Fig.19. Simple type of solar still

Output of a solar still

An approximate method of estimating the output of a solar still is given by:

$$Q = (E \times G \times A) / 2.3$$

where:

Q = daily output of distilled water (litres/day)

E = overall efficiency

G = daily global solar irradiation (MJ/m²)

A = aperture area of the still ie, the plan areas for a simple basin still (2)

In a typical country the average, daily, global solar irradiation is typically 18.0 MJ/m² (5 kWh/m²). A simple basin still operates at an overall efficiency of about 30%. Hence the output per square metre of area is:

$$\begin{aligned} \text{daily output} &= (0.30 \times 18.0 \times 1) / 2.3 \\ &= 2.3 \text{ litres (per square metre)} \end{aligned}$$

The yearly output of a solar still is often therefore referred to as approximately one cubic metre per square metre.

Experience

Despite a proliferation of novel types, the single-basin still remains the only design proven in the field.

The cost of pure water produced depends on:

- the cost of making the still
- the cost of the land
- the life of the still
- operating costs
- cost of the feed water
- the discount rate adopted
- the amount of water produced.

The life of a glass still is usually taken as 20 to 30 years but operating costs can be large especially to replace broken glass.

Performance varies between tropical locations but not significantly. An average output of 2.5-3.0 l/m²/day is typical, that is, about 1m³/m²/year.

Would a solar still suit your needs?

Human beings need 1 or 2 litres of water a day to live. The minimum requirement for normal life in developing countries (which includes cooking, cleaning and washing clothes) is 20 litres per day (in the industrialised world 200 to 400 litres per day is typical). Yet some functions can be performed with salty water and a typical requirement for distilled water is 5 litres per person per day. Therefore 2m² of still are needed for each person served.

Solar stills should normally only be considered for removal of dissolved salts from water. If there is a choice between brackish ground water or polluted surface water, it will usually be cheaper to use a slow sand filter or other treatment device. If there is no fresh water then the main alternatives are desalination, transportation and rainwater collection. Unlike other techniques of desalination, solar stills are more attractive, the smaller the required output. The initial capital cost of stills is roughly proportional to capacity, whereas other methods have significant economies of scale. For the individual household, therefore, the solar still is most economic.

For outputs of 1m³/day or more, reverse osmosis or electrodialysis should be considered as an alternative to solar stills. Much will depend on the availability and price of electrical power. For outputs of 200 m³/day or more, vapour compression or flash evaporation will normally be least cost. The latter technology can have part of its energy requirement met by solar water heaters.

In many parts of the world, fresh water is transported from another region or location by boat, train, truck or pipeline. The cost of water transported by vehicles is typically of the same order of magnitude as that produced by solar stills. A pipeline may be less expensive for very large quantities. Rainwater collection is an even simpler technique than solar distillation in areas where rain is not scarce, but requires a greater area and usually a larger storage tank. If ready-made collection surfaces exist (such as house roofs) these may provide a less expensive source for obtaining clean water.

The single-basin still is the only design proven in the field. Multi-effect stills have the potential to be more economic but it would be as well to gain experience first with a single-basin still.

UNIT-4: SOLAR THERMAL ENERGY CONVERSION

Solar thermal energy may be converted for use through application-specific system designs. Specific designs and operating principles of these systems for cooling & refrigeration, passive applications and power generations form the structure of this chapter. Storage is an integral part of any solar system design and operation. It is discussed separately to give the reader an overview.

A. Solar Cooling and Refrigeration

In some ways, solar energy is better suited to space cooling and refrigeration than to space heating. The seasonal variation of solar energy is extremely well-suited to the space-cooling requirements of buildings. The principal factors affecting the temperature in a building are the average quantity of radiation received and the environmental air temperature. Because the warmest seasons of the year correspond to periods of high insolation, solar energy is most available when comfort cooling is most needed. Moreover, the efficiency of solar collectors increases with increasing insolation and increasing environmental temperature. Consequently, in the summer, the amount of energy delivered per unit surface area of collector can be larger than that in winter.

Solar cooling using various refrigeration cycles is technically feasible and has been demonstrated several times over past few decades. However, application of these systems has not become popular due to the unfavorable economics. The most widely used methods applied to solar cooling and air conditioning are vapor compression cycles, absorption-cooling cycles, and desiccant cooling. The vapor compression refrigeration cycle is probably the most widely used refrigeration cycle. The vapor compression refrigeration cycle requires energy input into the compressor which may be provided as electricity from a photovoltaic system or as mechanical energy from a solar driven heat engine. Referring to Figure 1 we see that the compressor raises the pressure of the refrigerant, which also increases the temperature.

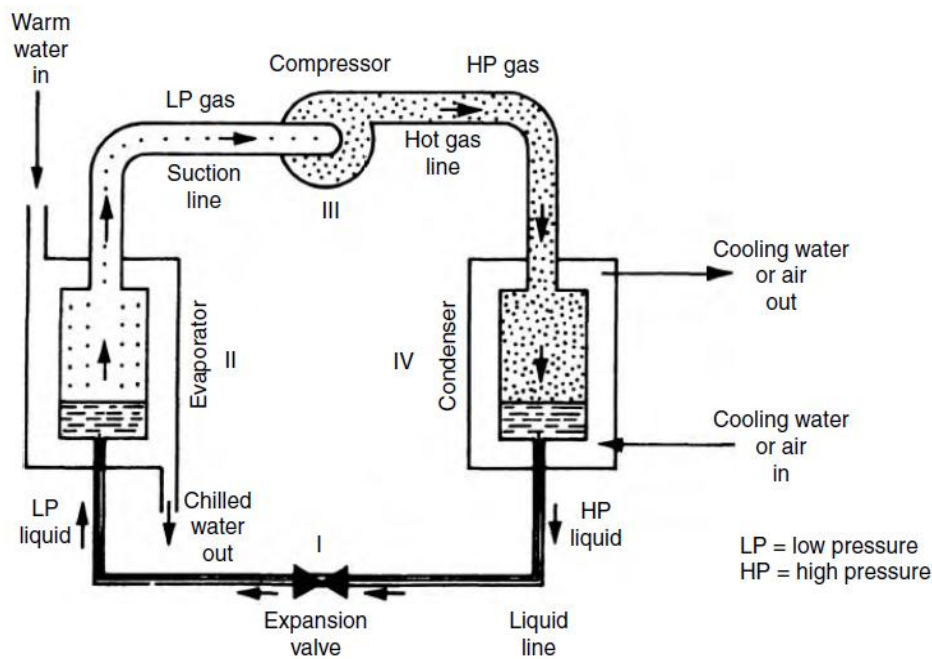


Fig: 1. A schematic diagram showing a typical vapor compression refrigeration cycle.

The compressed high-temperature refrigerant vapor then transfers heat to the ambient environment in the condenser, where it condenses to a high-pressure liquid at a temperature close to the environmental temperature. The liquid refrigerant is then passed through the expansion valve where the pressure is suddenly reduced, resulting in a vapor–liquid mixture at a much lower temperature. The low temperature refrigerant is then used to cool air or water in the evaporator where the liquid refrigerant evaporates by absorbing heat from the medium being cooled. The cycle is completed by the vapor returning to the compressor. If water is cooled in the evaporator, the device is usually called a chiller. The chilled water could then be used to cool air in a building. In an absorption system, the refrigerant is evaporated or distilled from a less volatile absorbent, the vapor is condensed in a water- or air-cooled condenser, and the resulting liquid is passed through a pressure-reducing valve to the cooling section (evaporator) of the unit. The refrigerant from the evaporator flows into the absorber, where it is reabsorbed in the stripped absorbing liquid and pumped back to the heated generator. The heat required to evaporate the refrigerant in the generator can be supplied directly from solar energy as shown in Figure 2.

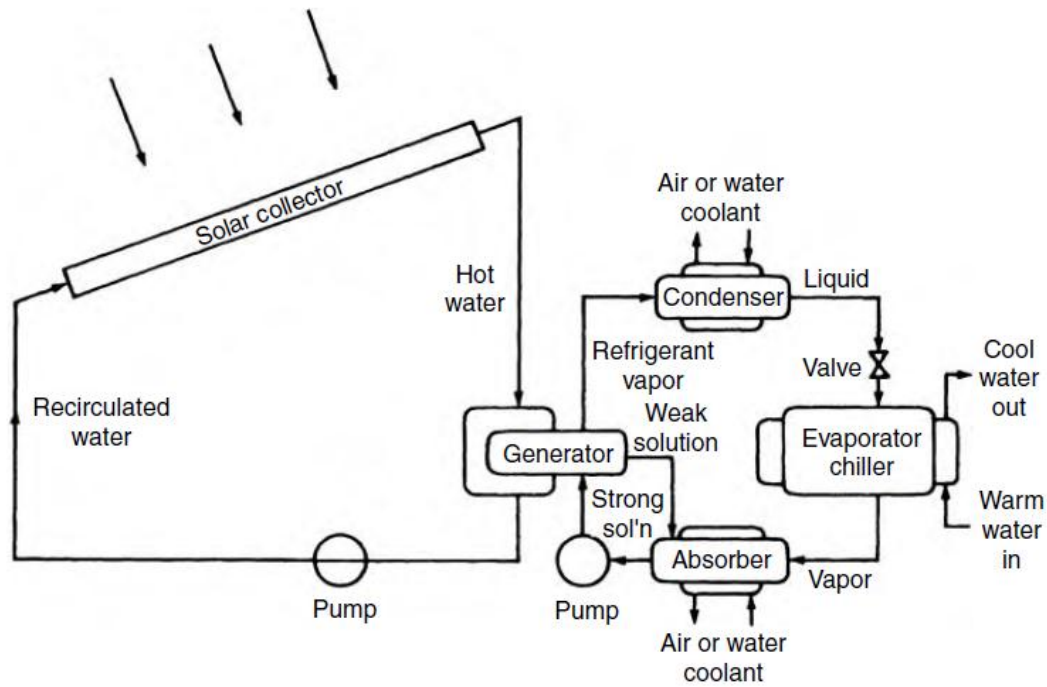


Fig: 2. Arrangement of a solar driven absorption cycle.

In humid climates, removal of moisture from the air represents a major portion of the air-conditioning load. In such climates, desiccant systems can be used for dehumidification, in which solar energy can provide most of the energy requirements. There are several passive space cooling techniques that are described elsewhere. The present section covers the active solar cooling techniques based on vapor compression and vapor-absorption refrigeration cycles and desiccant humidification.

Vapor Compression Cycle

The principle of operation of a vapor compression refrigeration cycle can be illustrated conveniently with the aid of a pressure–enthalpy diagram as shown in Figure 20.64. The ordinate is the pressure of the refrigerant in N/m^2 absolute, and the abscissa its enthalpy in kJ/kg . The roman numerals in Figure correspond to the physical locations in the schematic diagram of Figure 1. Process I is a throttling process in which hot liquid refrigerant at the condensing pressure p_c passes through the expansion valve, where its pressure is reduced to the evaporator pressure, p_e . This is an isenthalpic (constant enthalpy) process in which the temperature of the refrigerant decreases. In this process, some vapor is produced and the state of the mixture of liquid refrigerant and vapor entering the evaporator is shown by point A. Because the expansion process is isenthalpic, the following relation holds:

$$h_{ve}f + h_{lc}(1 - f) = h_{lc}, \quad (1)$$

where f is the fraction of mass in vapor state, subscripts “v” and “l” refer to vapor and liquid states, respectively, and “c” and “e” refer to states corresponding to condenser and evaporator pressures, respectively.

Process II represents the vaporization of the remaining liquid. This is the process during which heat is removed from the chiller. Thus, the specific refrigeration effect (per kilogram of refrigerant flow), q_r , is

$$q_r = h_{ve} - h_{lc}, \text{ in kJ/kg.}$$

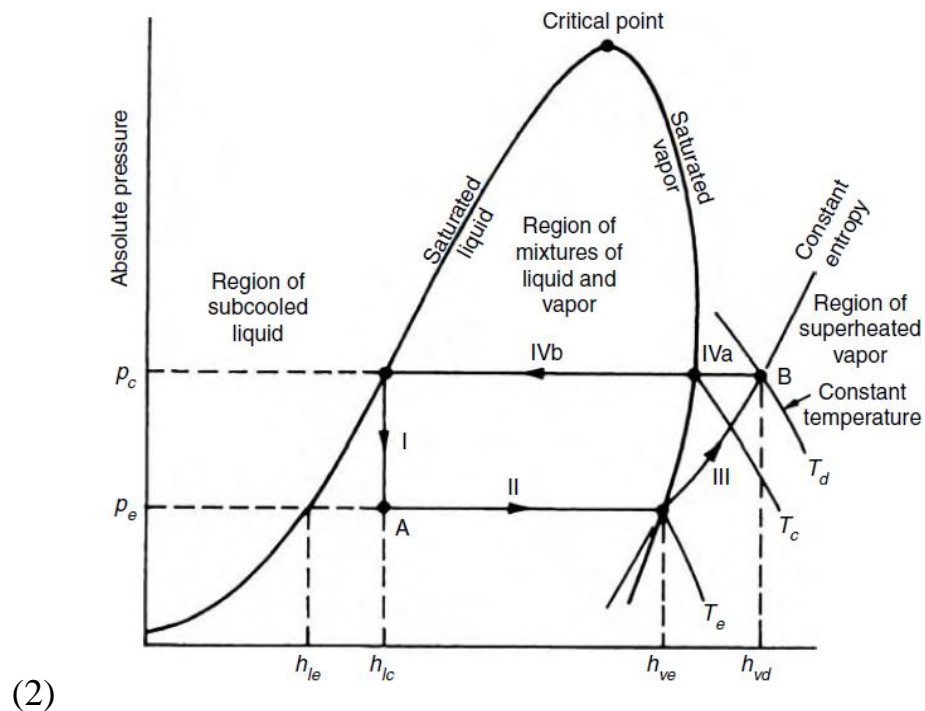


Fig.3. The thermodynamic state processes of the vapor compression refrigeration cycle shown on a pressure–enthalpy (p–h) diagram.

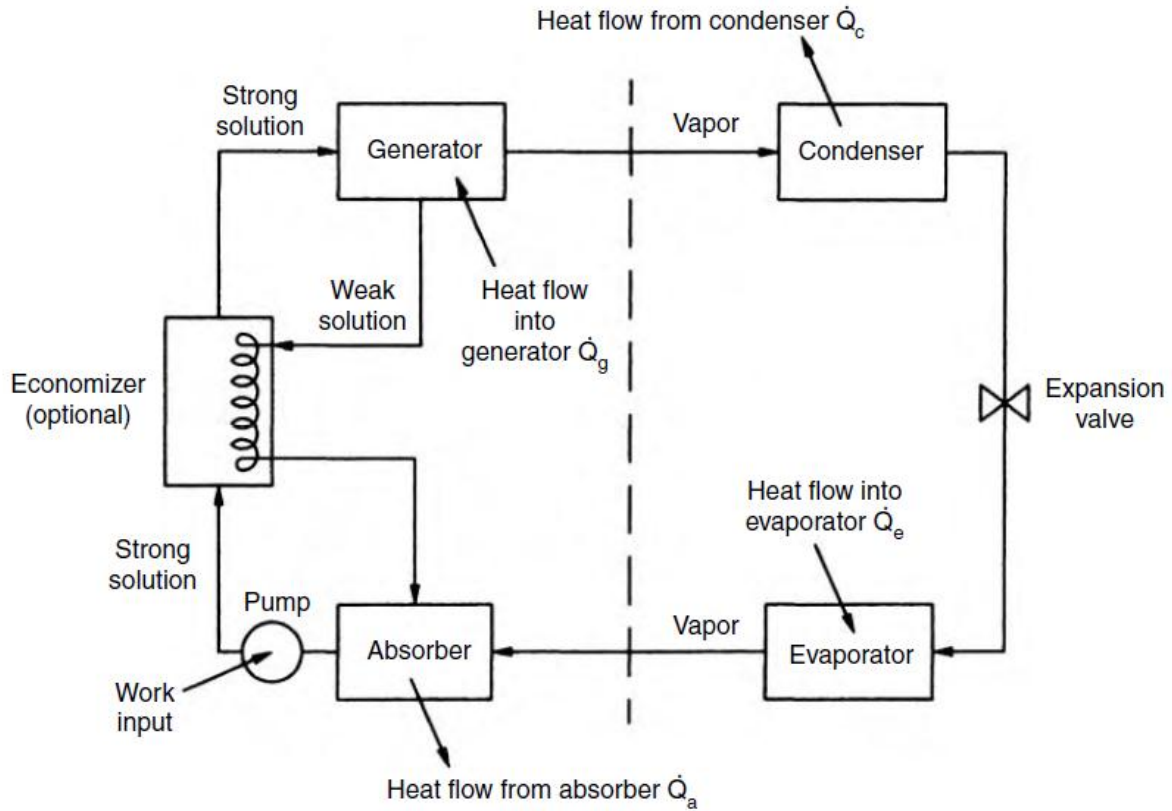


Fig: 4 A typical absorption refrigeration cycle.

In the United States, it is still common practice to measure refrigeration in terms of tons. One ton is the amount of cooling produced if 1 ton of ice is melted over a period of 24 h. One ton of cooling is equivalent to 3.516 kW, or 12,000 Btu/h. Process III in Figure 3 represents the compression of refrigerant from pressure p_e to pressure p_c . The process requires work input from an external source, which may be obtained from a solar-driven expander turbine or a solar electrical system. In general, if the heated vapor leaving the compressor is at the condition represented by point B in Figure 3, the work of compression is

$$W_c = \dot{m}_r(h_{vd} - h_{ve}). \quad (3)$$

In an idealized cycle analysis, the compression process is usually assumed to be isentropic. Process IV represents the condensation of the refrigerant. Actually, sensible heat is first removed in sub-process IVa as the vapor is cooled at constant pressure from T_d to T_c and latent heat is removed at the condensation temperature T_c corresponding to the saturation pressure, p_c , in the condenser. The heat transfer rate in the condenser, Q_c , is

$$\dot{Q}_c = \dot{m}_r(h_{vd} - h_{lc}). \quad (4)$$

This heat must be rejected to the environment, either to cooling water or to the atmosphere if no water is available. The overall performance of a refrigeration machine is usually expressed as the coefficient of performance that is defined as the ratio of the heat transferred in the evaporator, Q_e , to the shaft work supplied by the compressor:

$$\text{COP} = \frac{\dot{Q}_r}{W_c} = \frac{h_{ve} - h_{lc}}{h_{vd} - h_{ve}}. \quad (5)$$

Absorption Air Conditioning

Absorption air conditioning is compatible with solar energy because a large fraction of the energy required is thermal energy at temperatures that solar collectors can easily provide. Low- and medium-temperature solar collectors have been used to drive several absorption air conditioning systems. Although single-effect absorption refrigeration systems can be run using solar heated hot water at 80°C, higher temperatures are preferred for better refrigeration cycle performance. The key difference between a conventional gas fired absorption chiller and one used for solar applications is the larger heat transfer area required to make the cycle work using the lower driving temperatures available in solar applications. Figure.4 shows a schematic of an absorption refrigeration system. Absorption refrigeration differs from vapor compression air conditioning only in the method of compressing the refrigerant (left of the dashed line in Figure 20.65). In absorption air conditioning systems, the pressurization is accomplished by first dissolving the refrigerant in a liquid (the absorbent) in the absorber section, then pumping the solution to a high pressure with a liquid pump. The low-boiling refrigerant is then driven from solution by the addition of heat in the generator. By this means, the refrigerant vapor is compressed without the large input of high-grade shaft work that the vapor compression cycle demands.

The effective performance of an absorption cycle depends on the two materials that comprise the refrigerant–absorbent pair. Desirable characteristics for the refrigerant–absorbent pair are as follows:

1. Absence of a solid-phase sorbent
2. A refrigerant more volatile than the absorbent so that separation from the absorbent occurs easily in the generator
3. An absorbent that has a strong affinity for the refrigerant under conditions in which absorption takes place
4. A high degree of stability for long-term operations
5. Nontoxic and nonflammable fluids for residential applications; this requirement is less critical in industrial refrigeration
6. A refrigerant that has a large latent heat so that the circulation rate can be kept low
7. A low fluid viscosity that improves heat and mass transfer and reduces pumping power
8. Fluids that do not have long-term environmental effects

Lithium bromide–water (LiBr–H₂O) and ammonia–water (NH₃–H₂O) are the two pairs that meet most of the requirements and have been used commercially in several applications. In the LiBr–H₂O system, water is the refrigerant and

LiBr is the absorbent, whereas in the ammonia–water system, ammonia is the refrigerant and water is the absorbent. Because the LiBr–H₂O system has a high-volatility ratio, it can operate at lower pressures and therefore, at the lower generator temperatures achievable by flat-plate collectors. A disadvantage of this system is that LiBr has a tendency to crystallize in the stream returning from the generator. Crystallization is avoided by careful system design and by the use of additives. Furthermore, because the refrigerant is water, the system evaporator cannot be operated at or below the freezing point of water. Therefore, the LiBr–H₂O system is operated at evaporator temperatures of 5°C or higher. Using a mixture of LiBr with some other salt as the absorbent can overcome the crystallization problem. The ammonia–water system has the advantage that the evaporator can be maintained at very low temperatures. However, for temperatures much below 0°C, water vapor must be removed from ammonia as much as possible to prevent ice crystals from forming. This requires a rectifying column after the boiler.

Also, ammonia is a safety code group B2 fluid (ASHRAE Standard 34-1992) that restricts its use indoors. Consequently, the ammonia–water system cannot use a direct expansion (DX) evaporator. Other refrigerant–absorbent pairs include :

- † Ammonia–salt
- † Methylamine–salt
- † Alcohol–salt
- † Ammonia–organic solvent
- † Sulfur dioxide–organic solvent
- † Halogenated hydrocarbons–organic solvent
- † Water–alkali nitrate
- † Ammonia–water–salt

If the pump work is neglected, the COP of an absorption air conditioner can be calculated from Figure.4:

$$\text{COP} = \frac{\text{cooling effect}}{\text{heat input}} = \frac{\dot{Q}_e}{\dot{Q}_g} \quad (6)$$

The COP values for absorption air conditioning range from 0.5 for a small, single-stage unit to 0.85 for a double-stage, steam-fired unit. Another figure of merit for absorption systems is the ratio of the cooling effect to work supplied to the system (circulation pumps, fans, etc.).

Explicit procedures for the mechanical and thermal design as well as the sizing of the heat exchangers are presented in standard heat transfer texts. In large commercial units, it may be possible to use higher concentrations of LiBr, operate at a higher absorber temperature, and thus save on heat-exchanger costs. In a solar-driven unit, this approach would require concentrator-type or high-efficiency flat-plate solar collectors.

Ammonia–Water Systems

The main difference between an ammonia–water system and a water–lithium bromide system is that a small amount of absorbent (water) also evaporates along with the refrigerant (ammonia) in the vapor generator. Therefore, ammonia–water systems use a rectifier (also called a dephlagmator) after the generator to condense as much water vapor out of the vapor mixture as possible. Figure 5 shows a schematic of an $\text{NH}_3\text{--H}_2\text{O}$ absorption refrigeration system.

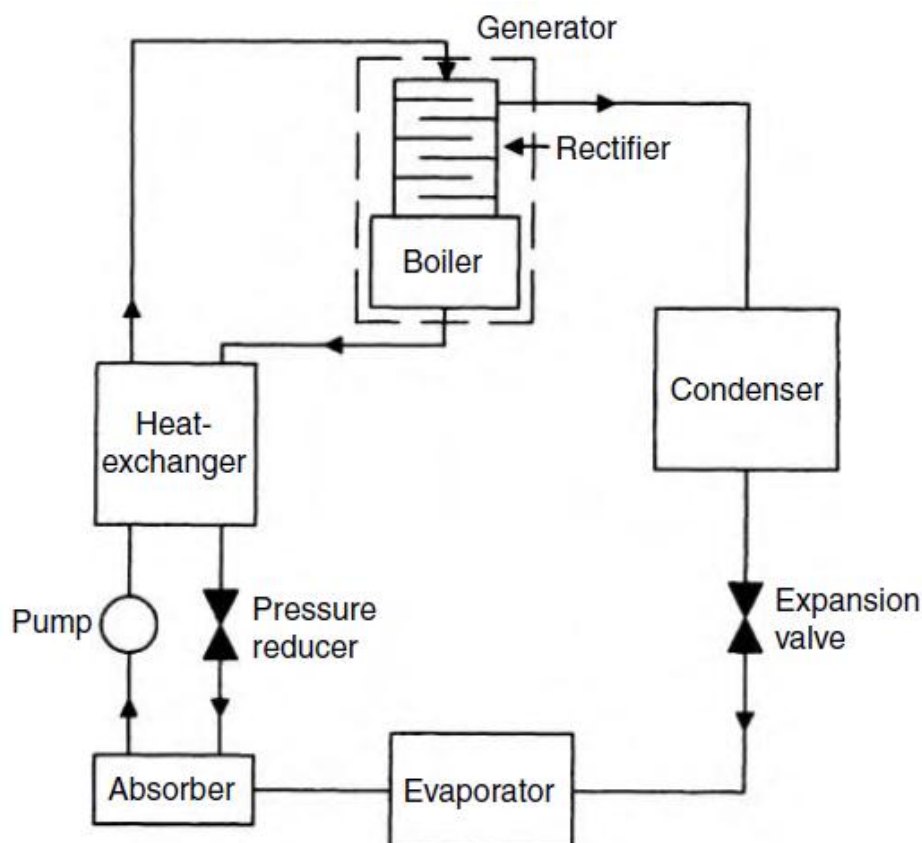


Fig. 5: A diagram showing the arrangement of components for an ammonia-absorption cycle.

Because ammonia has a much lower boiling point than water, a very high fraction of ammonia and a very small fraction of water are boiled off in the boiler. The vapor is cooled as it rises in the rectifier by the countercurrent flow of the strong $\text{NH}_3\text{--H}_2\text{O}$ solution from the absorber; therefore, some moisture is condensed. The weak ammonia–water solution from the boiler goes through a pressure-reducing valve to the absorber, where it absorbs the ammonia vapor from the evaporator. The high-pressure ammonia from the rectifier is condensed by rejecting heat to the atmosphere. It may be further sub-cooled before expanding in a throttle valve. The two-phase low temperature ammonia from the throttle valve provides refrigeration in the evaporator. The vapor from the evaporator is recombined with the weak ammonia solution in the absorber. Operating pressures are primarily controlled by the ambient air temperature for

an air-cooled condenser, the evaporator temperature, and the concentration of the ammonia solution in the absorber.

Multi-effect Systems

A major price component in designing absorption systems is the solar collector field. To improve the economics of a solar absorption system, the efficiency of the solar collectors must be improved in addition to the COP of the absorption system, thus reducing the required collector area. A single-effect absorption system has a typical efficiency of around 0.7. For higher COP, double-effect systems are used. Double-effect systems typically operate at higher temperatures than single-effect systems requiring higher concentration solar collectors to provide the heat input. An example of a typical double-effect lithium bromide system is shown in Figure.6 .

A double-effect lithium bromide cycle has two generators at two different pressure levels. Vapor is generated using the solar heat source in the first generator. This vapor is condensed in the second generator and the heat of condensation is used to produce more vapor (this arrangement is known as a condenser-coupled system). Thus the double-effect absorption cycle is a triple pressure cycle. A double effect ammonia–water system is configured slightly differently (absorber-coupled), but still uses the same

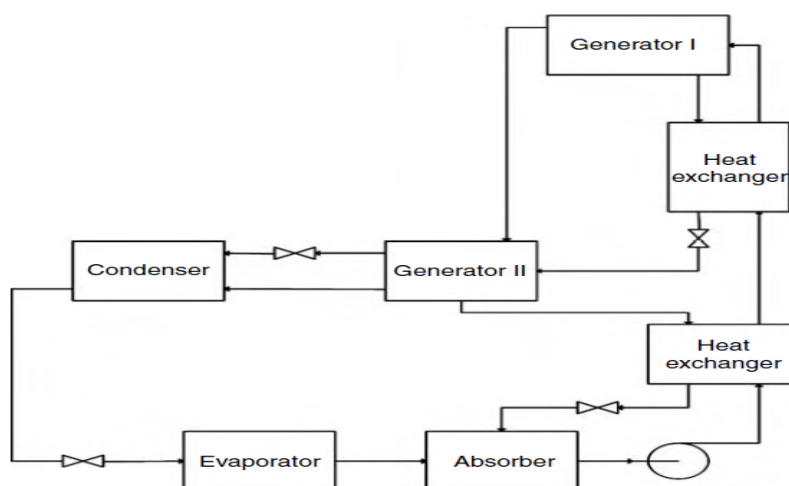


Fig. 6: A schematic diagram of a condenser coupled double-effect absorption cooling cycle.

principle of internal heat recovery to produce more refrigerant vapor than is possible in a single-effect system. However, it requires a much higher driving temperature (140°C or higher) to operate efficiently.

Solar Desiccant Dehumidification

In hot and humid regions of the world experiencing significant latent cooling demand, solar energy may be used for dehumidification using liquid or solid desiccants. Researchers compared a number of strategies for ventilation air conditioning for Miami, Florida, and found that a conventional vapor compression system could not even meet the increased ventilation requirements

of ASHRAE Standard 62-1989. By pretreating the ventilation air with a desiccant system, proper indoor humidity conditions could be maintained and significant electrical energy could be saved. A number of researchers have shown that a combination of a solar desiccant and a vapor compression system can save from 15 to 80% of the electrical energy requirements in commercial applications such as supermarkets.

In a desiccant air conditioning system, moisture is removed from the air by bringing it in contact with the desiccant, followed by sensible cooling of the air by a vapor compression cooling system, vapor absorption vapor pressure. When the vapor pressure in air is higher than on the desiccant surface, moisture is transferred from the air to the desiccant until an equilibrium is reached as shown in Figure.7. To regenerate the desiccant for reuse, the desiccant is heated, which increases the water vapor pressure on its surface. If air with lower vapor pressure is brought into contact with this desiccant, the moisture passes from the desiccant to the air.

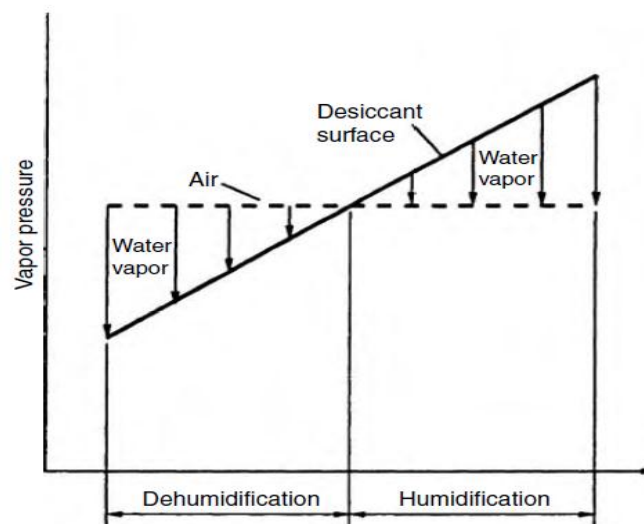


Figure.7 Vapor pressure vs. temperature and water content for desiccant and air.

Two types of desiccants are used: solids such as silica gel and lithium chloride, or liquids such as salt solutions and glycols. The two solid desiccant materials that have been used in solar systems are silica gel and molecular sieves, a selective absorber. Figure.8. shows the equilibrium absorption capacity of several substances. Note that molecular sieves has the highest capacity up to 30% humidity, and silica gel is optimal between 30 and 75%, the typical humidity range for buildings.

Dehumidification

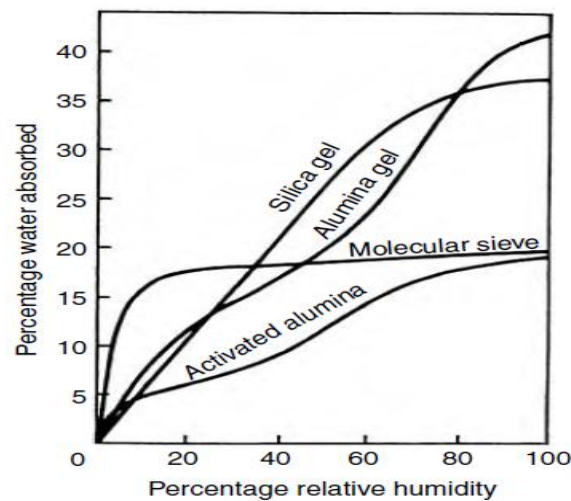


Figure. 8. Equilibrium capacities of common water absorbents.

Figure. 9. is a schematic diagram of a desiccant cooling ventilation cycle (also known as the Pennington cycle), which achieves both dehumidification and cooling. The desiccant bed is normally a rotary wheel of a honeycomb-type substrate impregnated with the desiccant. As the air passes through the rotating wheel, it is dehumidified while its temperature increases (processes 1 and 2) due to the latent heat of condensation. Simultaneously, a hot air stream passes through the opposite side of the rotating wheel, which removes moisture from the wheel. The hot and dry air at state 2 are cooled in a heat exchanger wheel to condition 3 and further cooled by evaporative cooling to condition 4. Air at condition 3 may be further cooled by vapor compression or vapor absorption systems instead of evaporative cooling. The return air from the conditioned space is cooled by evaporative cooling (processes 5 and 6), which in turn cools the heat exchanger wheel. This air is then heated to condition 7. Using solar heat, it is further heated to condition 8 before going through the desiccant wheel to regenerate the desiccant. A number of researchers have studied this cycle, or an innovative variation of it, and have found thermal COPs in the range of 0.5–2.

Liquid-Desiccant Cooling System

Liquid desiccants offer a number of advantages over solid desiccants. The ability to pump a liquid desiccant makes it possible to use solar energy for regeneration more efficiently. It also allows several small dehumidifiers to be connected to a single regeneration unit. Because a liquid desiccant does not require simultaneous regeneration, the liquid may be stored for regeneration later when solar heat is available. A major disadvantage is that the vapor pressure of the desiccant itself may be enough to cause some desiccant vapors to mix with the air. This disadvantage, however, may be overcome by proper choice of the desiccant material.

A schematic of a liquid desiccant system is shown in Figure.10 Air is brought into contact with concentrated desiccant in a countercurrent flow in a dehumidifier. The dehumidifier may be a spray column or packed bed. The

packings provide a very large area for heat and mass transfer between the air and the desiccant. After dehumidification, the air is sensibly cooled before entering the conditioned space. The dilute desiccant exiting the dehumidifier is regenerated by heating and exposing it to a countercurrent flow of a moisture-scavenging air stream. Liquid desiccants commonly used are aqueous solutions of lithium bromide, lithium chloride, calcium chloride, mixtures of these solutions, and triethylene glycol (TEG) (see Table-1). Vapor pressures of these common desiccants are shown in Figure.11 as a function of concentration and temperature, based on a number of references .

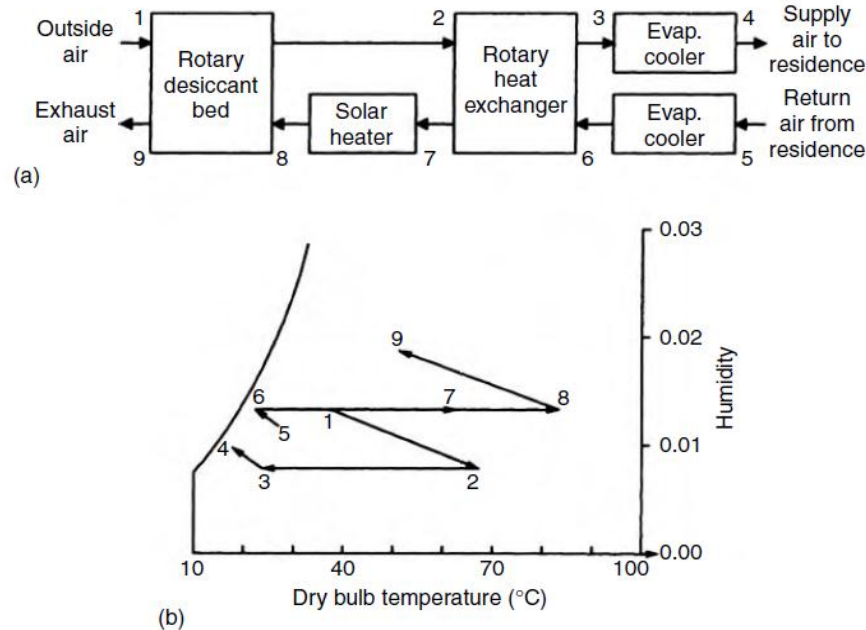


Figure. 9. Schematic of a desiccant cooling ventilation cycle, (a) schematic of air flow, (b) the process on a psychrometric chart.

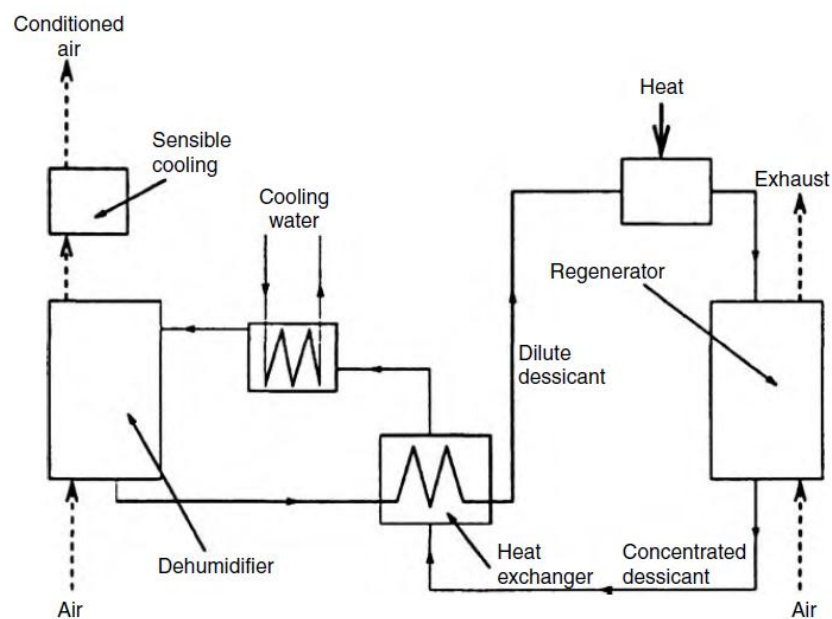


Figure.10. A conceptual liquid-desiccant cooling system. Although salt solutions and TEG have similar vapor pressures, the salt solutions are corrosive and have higher surface tension. The disadvantage of TEG is that it

requires higher pumping power because of its higher viscosity. Based on an extensive numerical modeling and on experimental studies, they have presented correlations. The performance of a packed-bed dehumidifier or a regenerator may be represented by a humidity effectiveness, ε_y , defined as the ratio of the actual change in humidity of the air to the maximum possible for the operating conditions

$$\varepsilon_y = \frac{Y_{in} - Y_{out}}{Y_{in} - Y_{eq}}, \quad (7)$$

where Y_{in} and Y_{out} are the humidity ratios of the air inlet and outlet, respectively, and Y_{eq} is the humidity ratio in equilibrium with the desiccant solution at the local temperature and concentration (Figure. 12). In addition to the humidity effectiveness, an enthalpy effectiveness, ε_H , is also used as a performance parameter :

$$\varepsilon_H = \frac{H_{a,in} - H_{a,out}}{H_{a,in} - H_{a,eq}}, \quad (8)$$

where $H_{a,in}$, $H_{a,out}$, and $H_{a,eq}$ are the enthalpies of the air at the inlet and outlet, and in equilibrium with the desiccant, respectively. The correlation for ε_y and ε_H is as follows:

$$\varepsilon_y, \varepsilon_H = 1 - C_1(L/G)^a (H_{a,in}/H_{L,out})^b (aZ)^c, \quad (9)$$

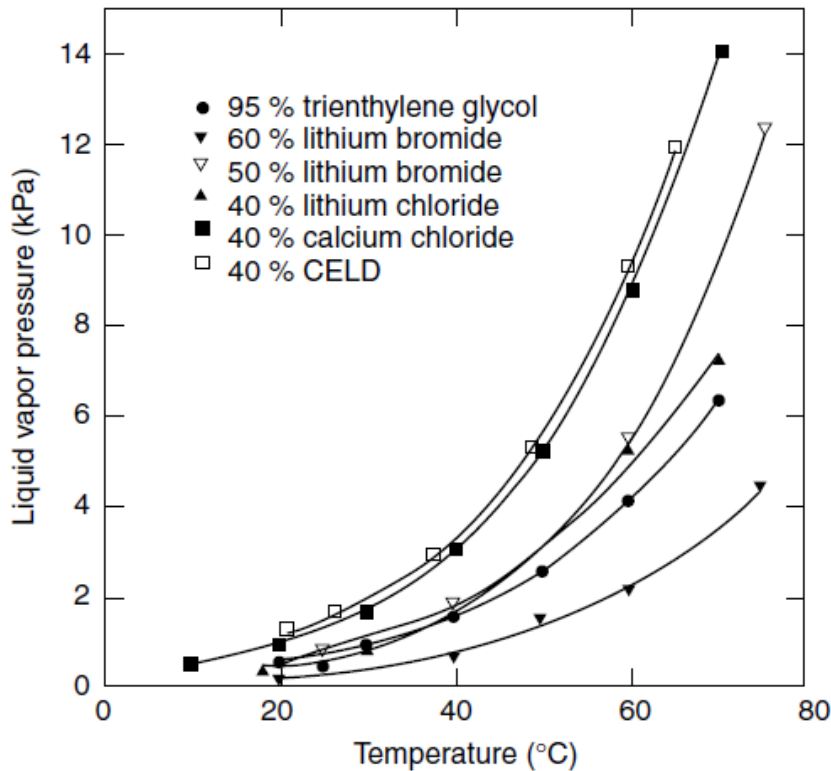


Figure.11: Vapor pressures of liquid desiccants.

Table.1 : Physical Properties of Liquid Desiccants at 25°C

Desiccant	Density, $\rho \times 10^{-3}$ (kg/m ³)	Viscosity, $\mu \times 10^3$ (Ns/m ²)	Surface Tension, $\gamma \times 10^3$ (N/m)	Specific Heat, c_p (kJ/kg °C)	Reference
95% by weight triethylene glycol	1.1	28	46	2.3	Thornbloom and Nimmo (1996)
55% by weight lithium bromide	1.6	6	89	2.1	Gordon and Ralston (1986); Oberg and Goswami (1998a, 1998b)
40% calcium chloride	1.4	7	93	2.5	Gordon and Ralston (1986); Siddiqui (1993); Spear and Judge (1997)
40% by weight lithium chloride	1.2	9	96	2.5	Gordon and Ralston (1986)
40% by weight CELD	1.3	5	—	—	Cyprus Foote Mineral Company

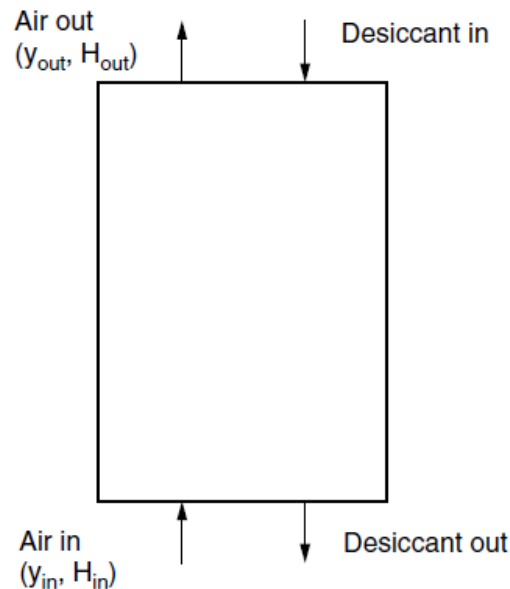


Figure.12 : Exchange of humidity and moisture between desiccant and air in the tower.

Although liquid-desiccant cooling systems are not an off-the-shelf variety currently on the market, there are a number of examples of their use, especially in hybrid combinations with conventional vapor compression systems. In a hybrid system, the liquid desiccant would remove moisture from the air, allowing the vapor compression system to be downsized. Hybrid systems are especially useful in their ability to maintain comfort conditions in hot and humid climates, where conventional high-efficiency systems usually have trouble maintaining low humidity. A house that typically requires a 5-ton conventional air conditioning unit in Florida could use a hybrid system consisting of a desiccant tower of height 1.1 m, and a vapor compression system of 2 ton. and has a simple payback period would be 9.5 years. The payback period is high mainly because the solar regeneration system is not utilized throughout the year.

For applications where the system can be used year-around, the payback period would be much shorter. For a commercial application in a supermarket where the hybrid desiccant system and the solar regeneration system would be used throughout the year, the payback period would be less.

B. Passive Solar Heating, and Cooling

Introduction

Passive systems are defined, quite generally, as systems in which the thermal energy flow is by natural means: by conduction, radiation, and natural convection. A passive heating system is one in which the sun's radiant energy is converted to heat upon absorption by the building. The absorbed heat can be transferred to thermal storage by natural means or used to directly heat the building. Passive cooling systems use natural energy flows to transfer heat to the environmental sinks: the ground, air, and sky. If one of the major heat transfer paths employs a pump or fan to force flow of a heat transfer fluid, then the system is referred to as having an active component or subsystem. Hybrid systems—either for heating or cooling—are ones in which there are both passive and active energy flows. The use of the sun's radiant energy for the natural illumination of a building's interior spaces is called daylighting. Daylighting design approaches use both solar beam radiation (referred to as sunlight) and the diffuse radiation scattered by the atmosphere (referred to as skylight) as sources for interior lighting, with historical design emphasis on utilizing skylight.

Distinction Between a Passive System and Energy Conservation

A distinction is made between energy conservation techniques and passive solar measures. Energy conservation features are designed to reduce the heating and cooling energy required to thermally condition a building: the use of insulation to reduce either heating and cooling loads, and the use of window shading or window placement to reduce solar gains, reducing summer cooling loads. Passive features are designed to increase the use of solar energy to meet heating and lighting loads, plus the use of ambient “coolth” for cooling. For example, window placement to enhance solar gains to meet winter heating loads and/or to provide daylighting is passive solar use, and the use of a thermal chimney to draw air through the building to provide cooling is also a passive cooling feature.

Passive Solar Heating Design Fundamentals

Passive heating systems contain the five basic components of all solar systems, as described in the previous chapter on Active Solar Systems. Typical passive realizations of these components are:

1. Collector: windows, walls and floors

2. Storage: walls and floors, large interior masses (often these are integrated with the collector absorption function)
3. Distribution system: radiation, free convection, simple circulation fans
4. Controls: moveable window insulation, vents both to other inside spaces or to ambient
5. Backup system: any non-solar heating system

The design of passive systems requires the strategic placement of windows, storage masses, and the occupied spaces themselves. The fundamental principles of solar radiation geometry and availability are instrumental in the proper location and sizing of the system's "collectors" (windows). Storage devices are usually more massive than those used in active systems and are frequently an integral part of the collection and distribution system.

Types of Passive Heating Systems

A commonly used method of cataloging the various passive system concepts is to distinguish three general categories: direct, indirect, and isolated gain. Most of the physical configurations of passive heating systems are seen to fit within one of these three categories. For direct gain(Figure.13), sunlight enters the heated space and is converted to heat at absorbing surfaces. This heat is then distributed throughout the space and to the various enclosing surfaces and room contents. For indirect gain category systems, sunlight is absorbed and stored by a mass interposed between the glazing and the conditioned space. The conditioned space is partially enclosed and bounded by this thermal storage mass, so a natural thermal coupling is achieved. Examples of the indirect approach are the thermal storage wall, the thermal storage roof, and the northerly room of an attached sunspace. In the thermal storage wall , sunlight penetrates the glazing and is absorbed and converted to heat at a wall surface interposed between the glazing and the heated space. The wall is usually masonry (Trombe wall) or containers filled with water (water wall), although it might contain phasechange material. The attached sunspace is actually a two-zone combination of direct gain and thermal storage wall. Sunlight enters and heats a direct gain southerly "sunspace" and also heats a

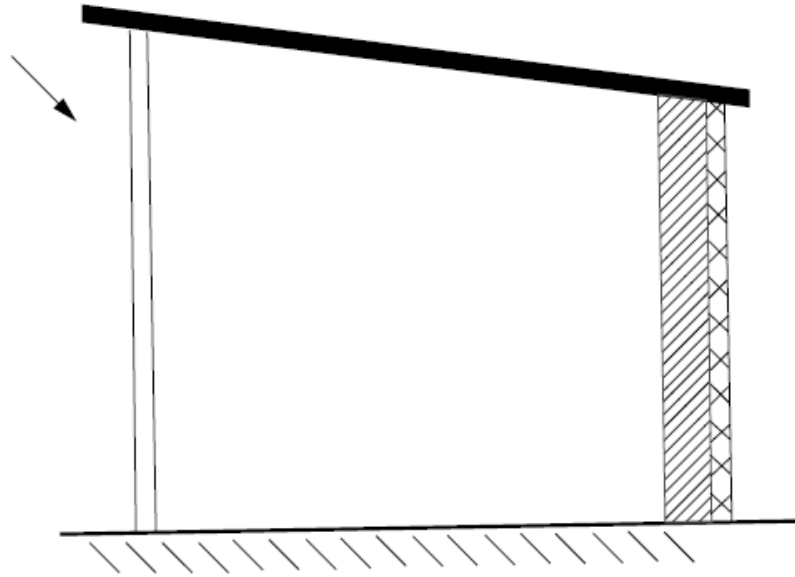


Fig.13 Direct gain.

mass wall separating the northerly buffered space, which is heated indirectly. The “sunspace” is frequently used as a greenhouse, in which case, the system is called an “attached greenhouse.” The thermal storage roof is similar to the thermal storage wall except that the interposed thermal storage mass is located on the building roof.

The isolated gain category concept is an indirect system, except that there is a distinct thermal separation (by means of either insulation or physical separation) between the thermal storage and the heated space. The convective (thermosyphon) loop, as depicted in Figure , is in this category and, while often used to heat domestic water, is also used for building heating. It is most akin to conventional active systems in that there is a separate collector and separate thermal storage. The thermal storage wall, thermal storage roof, and attached sunspace approaches can also be made into isolated systems by insulating between the thermal storage and the heated space.

Fundamental Concepts for Passive Heating Design

Figure 16 is an equivalent thermal circuit for the building illustrated in Figure 14 of the Trombe wall type system. For the heat transfer analysis of the building, three temperature nodes can be identified: room temperature, storage wall temperature, and the ambient temperature. The circuit responds to

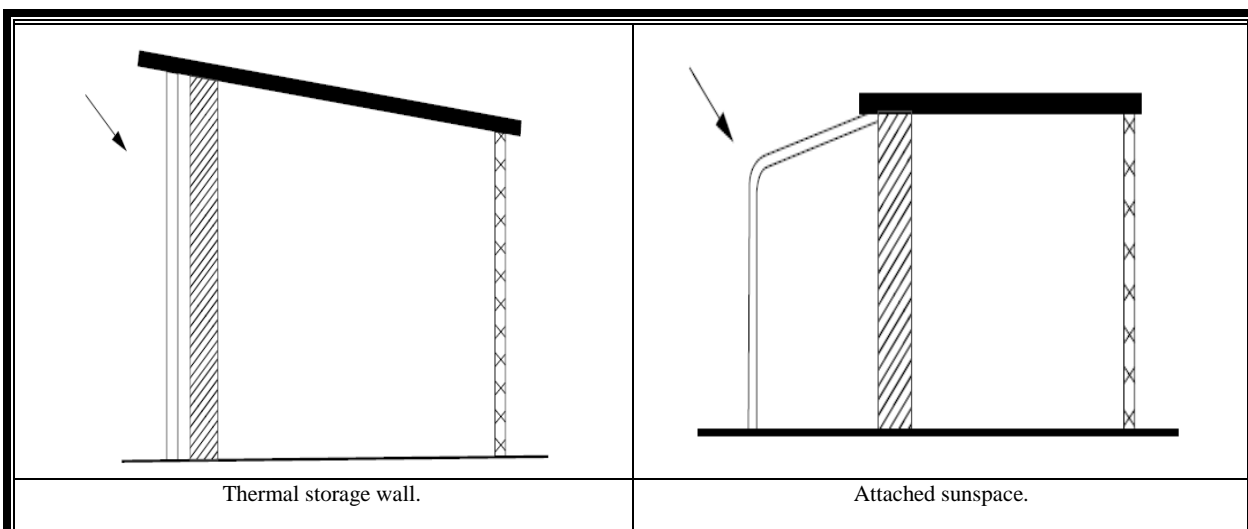


Figure. 14: Trombe wall type system

climatic variables represented by a current injection I_s (solar radiation) and by the ambient temperature T_a . The storage temperature, T_s , and room temperature, T_r , are determined by current flows in the equivalent circuit. By using seasonal and annual climatic data, the performance of a passive structure can be simulated and the results of many such simulations correlated to give the design approaches described below.

Passive Design Approaches

Design of a passive heating system involves selection and sizing of the passive feature type(s), determination of thermal performance, and cost estimation. Ideally, a cost/performance optimization would be performed by the designer. Owner and architect ideas usually establish the passive feature type, with general size and cost estimation available. However, the thermal performance of a passive heating system has to be calculated. There are several “levels” of methods that can be used to estimate the thermal performance of passive designs. First-level methods involve a rule of thumb and/or generalized calculation to get a starting estimate for size and/or annual performance. A second-level method involves climate, building, and passive system details, which allow annual performance determination, plus some sensitivity to passive system design changes. Third-level methods involve periodic calculations (hourly, monthly) of performance and permit more detailed variations of climatic, building, and passive solar system design parameters. These three levels of design methods have a common basis in that they all are derived from correlations of a multitude of computer simulations of passive systems. As a result, a similar set of defined terms is used in many passive design approaches:

† A_p , solar projected area, m^2 the net south-facing passive solar glazing area projected onto a vertical plane

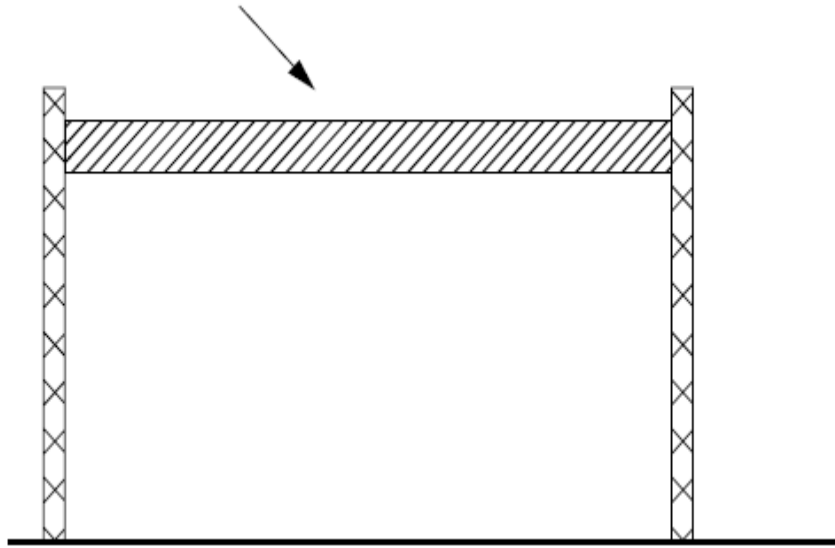


Figure. 15: Thermal storage roof.

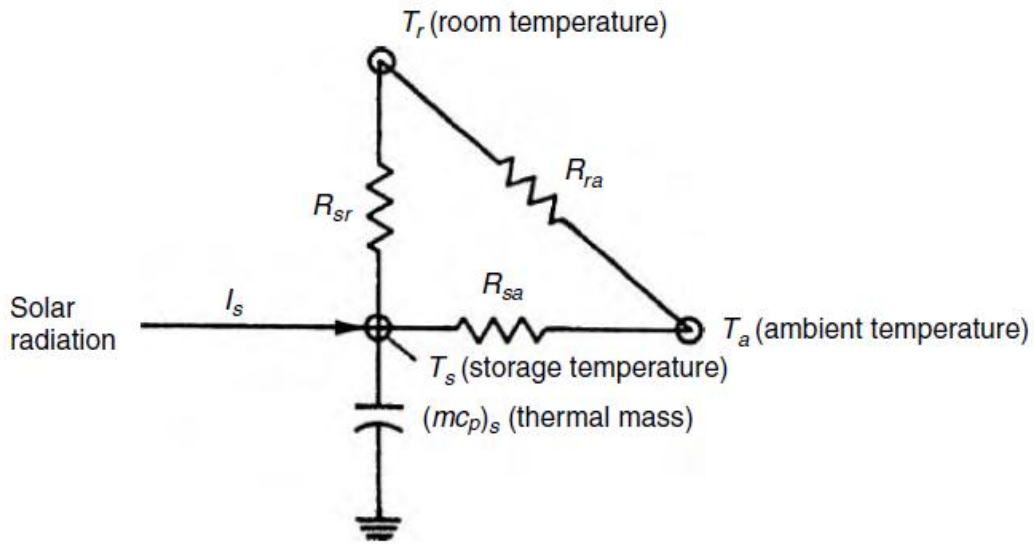


Figure.16. Equivalent thermal circuit for passively heated solar building

† NLC, net building load coefficient, kJ/CDD: net load of the nonsolar portion of the building per degree day of indoor–outdoor temperature difference. The CDD and FDD terms refer to Celsius and Fahrenheit degree days, respectively

† Qnet, net reference load, Wh (Btu): heat loss from nonsolar portion of building as calculated by Qnet NLC Number of degree days :

$$Q_{\text{net}} = \text{NLC} \times (\text{Number of degree days}).$$

(10)

† LCR, load collector ratio, kJ/m² CDD : ratio of NLC to A_p,

$$\text{LCR} = \text{NLC}/A_p$$

(11)

† SSF, solar savings fraction, %: percentage reduction in required auxiliary heating relative to net reference load,

$$SSF = 1 - \frac{\text{Auxiliary heat required } (Q_{aux})}{\text{Net reference load } (Q_{net})} \quad (12)$$

Therefore, using Equation the auxiliary heat required, Q_{aux} , is given by

$$Q_{aux} = (1 - SSF) \times NLC \times (\text{Number of degree days}). \quad (13)$$

The amount of auxiliary heat required is often a basis of comparison between possible solar designs as well as being the basis for determining building energy operating costs. Thus, many of the passive design methods are based on determining SSF, NLC, and the number of degree days in order to calculate the auxiliary heat required for a particular passive system by using Equation.

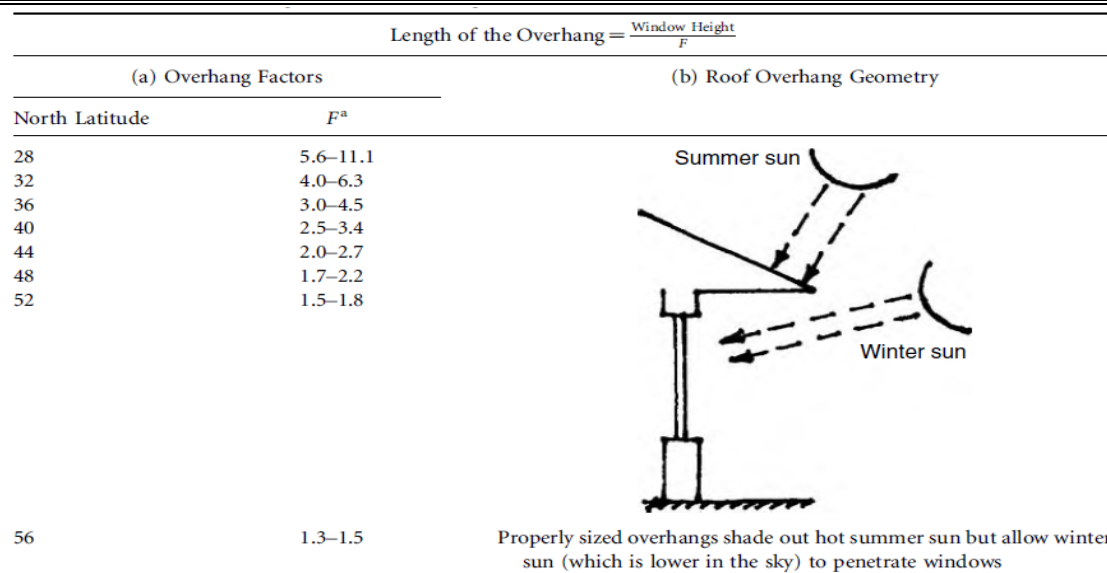
Passive Space Cooling Design Fundamentals

Passive cooling systems are designed to use natural means to transfer heat from buildings, including convection/ventilation, evaporation, radiation, and conduction. However, the most important element in both passive and conventional cooling design is to prevent heat from entering the building in the first place. Cooling conservation techniques involve building surface colors, insulation, special window glazings, overhangs and orientation, and numerous other architectural/engineering features.

Solar Control

Controlling the solar energy input to reduce the cooling load is usually considered a passive (versus conservation) design concern because solar input may be needed for other purposes, such as daylighting throughout the year and/or heating during the winter. Basic architectural solar control is normally “designed in” via the shading of the solar windows, where direct radiation is desired for winter heating and needs to be excluded during the cooling season. The shading control of the windows can be of various types and “controllability,” ranging from drapes and blinds, use of deciduous trees, to the commonly used overhangs and vertical louvers. A rule of thumb design for determining proper south-facing window overhang for both winter heating and summer shading is presented in Table. 2

Table.2: Overhang factors for designing south facing window overhang for summer and winter



Natural Convection/Ventilation

Air movement provides cooling comfort through convection and evaporation from human skin. ASHRAE (1989) places the comfort limit at 798F for an air velocity of 50 ft./min (fpm), 828F for 160 fpm, and 858F for 200 fpm. To determine whether or not comfort conditions can be obtained, a designer must calculate the volumetric flow rate, Q , which is passing through the occupied space. Using the cross-sectional area, A_x , of the space and the room air velocity, V_a , required, the flow is determined by

$$Q = A_x V_a \quad (14)$$

The proper placement of windows, “narrow” building shape, and open landscaping can enhance natural wind flow to provide ventilation. The air flow rate through open windows for wind-driven ventilation is given by ASHRAE :

$$Q = C_v A_w V_w \quad (15)$$

where Q is air flow rate (m^3/s), A_w is free area of inlet opening (m^2), V_w is wind velocity (m/s), and C_v is effectiveness of opening that is equal to 0.5–0.6 for wind perpendicular to opening, and 0.25–0.35 for wind diagonal to opening.

The stack effect can induce ventilation when warm air rises to the top of a structure and exhausts outside, while cooler outside air enters the structure to replace it. Figure. 17 illustrates the solar

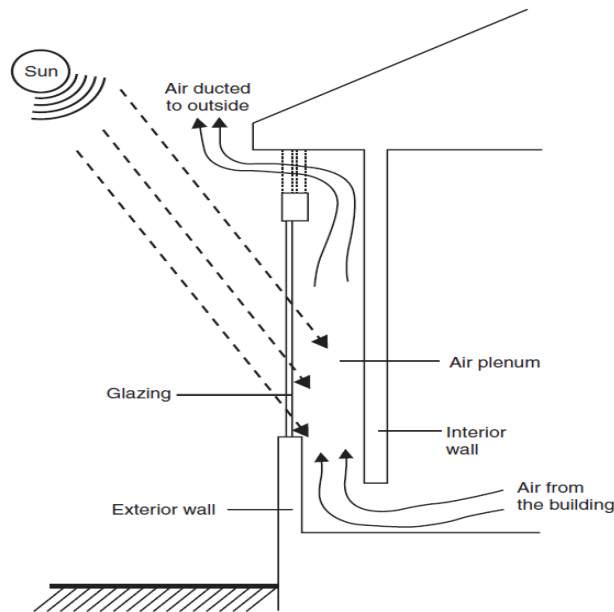


Figure. 17: The stack-effect/solar chimney concept to induce convection/ventilation.

chimney concept, which can easily be adapted to a thermal storage wall system. The greatest stack-effect flow rate is produced by maximizing the stack height and the air temperature in the stack, as given by

$$Q = 0.116 A_j \sqrt{h(T_s - T_o)} \quad (16)$$

where Q is stack flow rate (m^3/s), A_j is the area of inlets or outlets, whichever is smaller (m^2), h is the inlet to outlet height (m), T_s is the average temperature in stack ($^{\circ}\text{C}$), and T_o is the outdoor air temperature ($^{\circ}\text{C}$). If inlet or outlet area is twice the other, the flow rate will increase by 25%, and by 35% if the areas' ratio is 3:1 or larger .

Table. 3 Ground Reflectivities

Material	ρ (%)
Cement	27
Concrete	20–40
Asphalt	7–14
Earth	10
Grass	6–20
Vegetation	25
Snow	70
Red brick	30
Gravel	15
White paint	55–75

Source: From Murdoch, J. B., *Illumination Engineering—From Edison's Lamp to the Laser*, Macmillan, New York, 1985.

Example

A two-story (5-m) solar chimney is being designed to produce a flow of $0.25 \text{ m}^3/\text{s}$ through a space. The preliminary design features include a 25 cm, 1.5 m inlet, a 50 cm, 1.5 m outlet, and an estimated 35°C average stack temperature on a sunny 308C day. Can this design produce the desired flow?

Solution. Substituting the design data into Equation

$$\begin{aligned} Q &= 0.116(0.25 \times 1.5)[5(5)]^{1/2} \\ &= 0.2 \text{ m}^3/\text{s}. \end{aligned} \quad (17)$$

Because the outlet area is twice the inlet area, the 25% flow increase can be used:

$$Q = 0.2(1.25) = 0.25 \text{ m}^3/\text{s} \quad (18)$$

(Answer: Yes, the proper flow rate is obtained).

Evaporative Cooling

When air with less than 100% relative humidity moves over a water surface, the evaporation of water causes both the air and the water itself to cool. The lowest temperature that can be reached by this direct evaporative cooling effect is the wet-bulb temperature of the air, which is directly related to the relative humidity, with lower wet-bulb temperature associated with lower relative humidity. Thus, dry air (low relative humidity) has a low wet-bulb temperature and will undergo a large temperature drop with evaporative cooling, while humid air (high relative humidity) can only be slightly cooled evaporatively. The wet-bulb temperature for various relative humidity and air temperature conditions can be found via the “psychrometric chart” available in most thermodynamic texts. Normally, an evaporative cooling process cools the air only part of the way down to the wet-bulb temperature. To get the maximum temperature decrease, it is necessary to have a large water surface area in contact with the air for a long time, and interior ponds and fountain sprays are often used to provide this air-water contact area. The use of water sprays and open ponds on roofs provides cooling primarily via evaporation. The hybrid system involving a fan and wetted mat, the “swamp cooler,” is by far the most widely used evaporative cooling technology. Direct, indirect, and combined evaporative cooling system design features are described in ASHRAE.

Nocturnal and Radiative Cooling Systems

Another approach to passive convective/ventilative cooling involves using cooler night air to reduce the temperature of the building and/or a storage mass. Thus, the building/storage mass is prepared to accept part of the heat load during the hotter daytime. This type of convective system can also be combined with evaporative and radiative modes of heat transfer, utilizing air and/or water as the convective fluid. Work in Australia investigated rock storage beds that were

chilled using evaporatively cooled night air. Room air was then circulated through the bed during the day to provide space cooling. The use of encapsulated roof ponds as a thermal cooling mass has been tried by several investigators and is often linked with nighttime radiative cooling.

All warm objects emit thermal infrared radiation; the hotter the body, the more energy it emits. A passive cooling scheme is to use the cooler night sky as a sink for thermal radiation emitted by a warm storage mass, thus chilling the mass for cooling use the next day. The net radiative cooling rate, Q_r , for a horizontal unit surface (ASHRAE) is

$$Q_r = \varepsilon \sigma (T_{\text{body}}^4 - T_{\text{sky}}^4), \quad (19)$$

where Q_r is the net radiative cooling rate, W/m^2 , ε is the surface emissivity fraction (usually 0.9 for water), σ is $5.67 \times 10^{-8} \text{ W/m}^2 \text{ K}^4$, T_{body} is the warm body temperature, Kelvin (Rankine), and T_{sky} is the effective sky temperature, Kelvin (Rankine).

Example : Estimate the overnight cooling possible for a 10 m^2 , 85°C water thermal storage roof during July in Tezpur.

Solution. Assume the roof storage unit is black with $\varepsilon=0.9$. From $T_{\text{air}} - T_{\text{sky}}$ is approximately 6°C for Tezpur. From weather data, the July average temperature is 39°C with a range of 10°C . Assuming night temperatures vary from the average down to half the daily range ($10/2$), then the average night time temperature is chosen as $39 - (1/2)(10/2) = 36^\circ\text{C}$. Therefore, $T_{\text{sky}} = 36 - 10 = 26^\circ\text{C}$. From Equation

$$Q_r = 0.9(5.67 \times 10^{-8})[(273+85)^4 - (273+26)^4] \quad (20)$$

For a 10-h night and 10 m^2 roof area, Total radiative cooling = $Q_r(10 \text{ h})(10 \text{ m}^2)$.

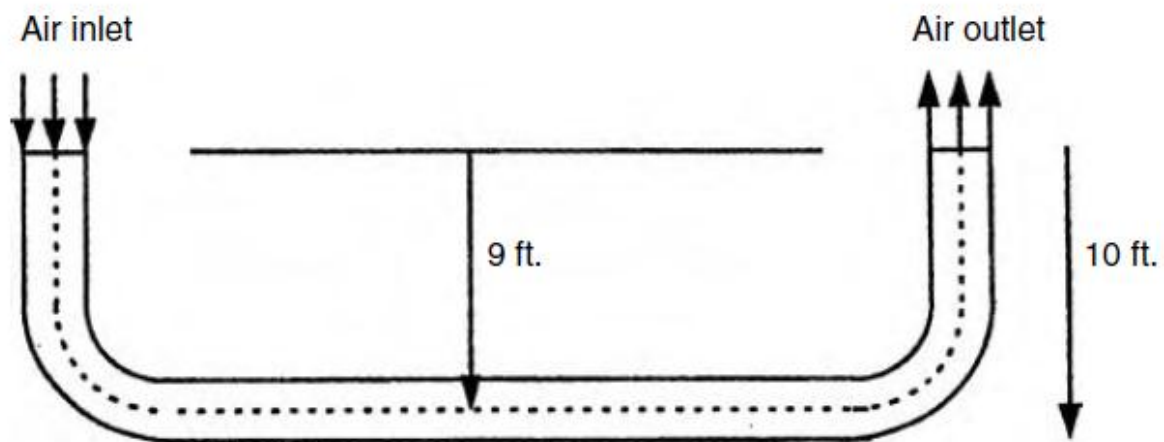


Figure. 18: Open loop underground air tunnel system.

Note that this does not include the convective cooling possible, which can be approximated (at its maximum rate) for still air (ASHRAE) by

$$\text{Maximum total } Q_{\text{conv}} = hA(T_{\text{roof}} - T_{\text{air}})(\text{Time}) = 5(129)(85 - 26)(10) \text{ J} \quad (21)$$

This is a maximum since the 85°C storage temperature will drop as it cools; this is also the case for the radiative cooling calculation. However, convection is seen to usually be the more dominant mode of nighttime cooling.

Earth Contact Cooling (or Heating)

Earth contact cooling or heating is a passive summer cooling and winter heating technique that utilizes underground soil as the heat sink or source. By installing a pipe underground and passing air through the pipe, the air will be cooled or warmed depending on the season. A schematic of an open loop system and a closed loop air-conditioning system are presented in Figure 18 and Figure 19, respectively. The use of this technique can be traced back to 3000 BC when Iranian architects designed some buildings to be cooled by natural resources only. In the nineteenth century, Wilkinson designed a barn for 148 cows where a 500-ft. long underground passage was used for cooling during the summertime. Since that time, a number of experimental and analytical studies of this technique have

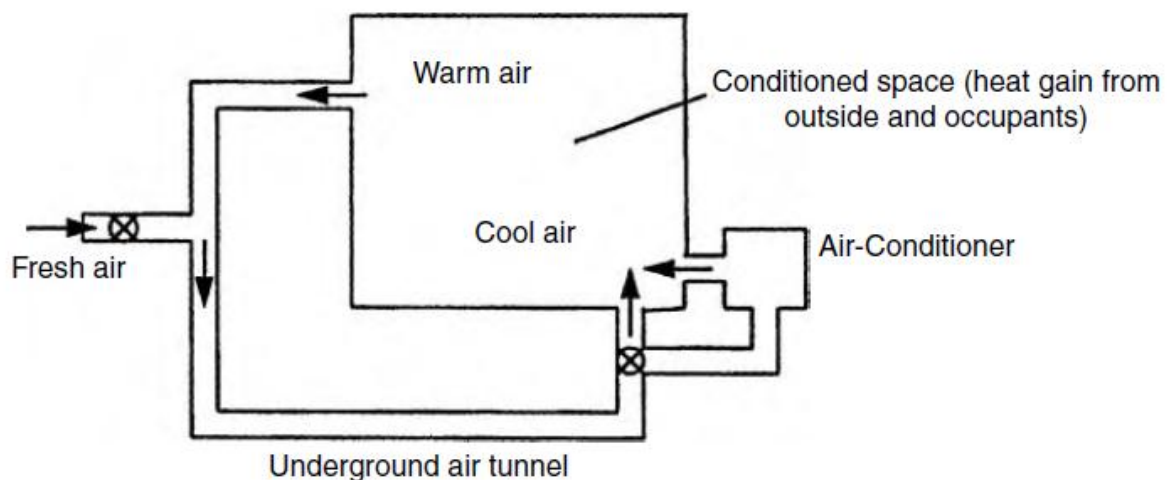


Figure. 19: Schematic of closed loop air-conditioning system using air-tunnel.

continued to appear in the literature.

C. Heat storage and heat transfer fluids (HTF)

Thermal energy storage can be stored as a change in internal energy of a material as sensible heat, latent heat and thermochemical or combination of these. An overview of major technique of storage of solar thermal energy is shown in Fig. 20

Sensible heat storage

In sensible heat storage (SHS), thermal energy is stored by raising the temperature of a solid or liquid. SHS system utilizes the heat capacity and the change in temperature of the material during the process of charging and discharging. The amount of heat stored depends on the specific heat of the medium, the temperature change and the amount of storage material

$$Q = \int_{T_i}^{T_f} m C_p dT$$

$$= m C_{ap} (T_f - T_i) \quad (22)$$

The sensible heat storage capacity of some selected solid–liquid materials is shown in Table 4. Water appears to be the best SHS liquid available because it is inexpensive and has a high specific heat. However above 100 °C, oils, molten salts

and liquid metals, etc. are used. For air heating applications rock bed type storage materials are used.

Table. 4: A list of selected solid-liquid material for sensible heat storage

A list of selected solid–liquid materials for sensible heat storage

Medium	Fluid type	Temperature range (°C)	Density (kg/m ³)	Specific heat J/kg K)
Rock		20	2560	879
Brick		20	1600	840
Concrete		20	1900–2300	880
Water		0–100	1000	4190
Caloria HT43	Oil	12–260	867	2200
Engine oil	Oil	Up to 160	888	1880
Ethanol	Organic liquid	Up to 78	790	2400
Propanal	Organic liquid	Up to 97	800	2500
Butanol	Organic liquid	Up to 118	809	2400
Isotunaol	Organic liquid	Up to 100	808	3000
Isopentanol	Organic liquid	Up to 148	831	2200
Octane	Organic liquid	Up to 126	704	2400

Latent heat storage

Latent heat storage (LHS) is based on the heat absorption or release when a storage material undergoes a phase change from solid to liquid or liquid to gas or vice versa. The storage capacity of the LHS system with a PCM medium is given by

$$Q = \int_{T_i}^{T_m} m C_p dT + m a_m \Delta h_m + \int_{T_m}^{T_f} m C_p dT$$

$$Q = m [C_{sp} (T_m - T_i) + a_m \Delta h_m + C_{lp} (T_f - T_m)] \quad (23)$$

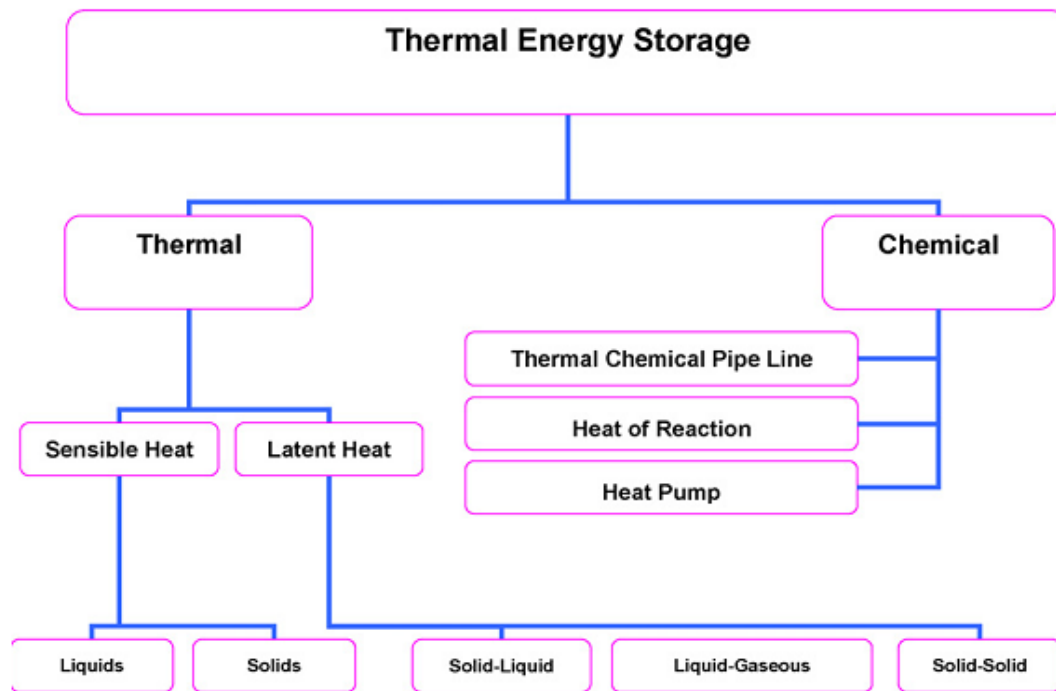


Figure.20: Different types of thermal storage of solar energy.

Thermochemical energy storage

Thermochemical systems rely on the energy absorbed and released in breaking and reforming molecular bonds in a completely reversible chemical reaction. In this case, the heat stored depends on the amount of storage material, the endothermic heat of reaction, and the extent of conversion.

$$Q = a_r m \Delta h_r \quad (24)$$

Amongst above thermal heat storage techniques, latent heat thermal energy storage is particularly attractive due to its ability to provide high-energy storage density and its characteristics to store heat at constant temperature corresponding to the phase-transition temperature of phase change material (PCM). Phase change can be in the following form: solid–solid, solid–liquid, solid–gas, liquid–gas and vice versa.

In solid–solid transitions, heat is stored as the material is transformed from one crystalline to another. These transitions generally have small latent heat and small volume changes than solid–liquid transitions. Solid–solid PCMs offer the advantages of less stringent container requirements and greater design flexibility. Most promising materials are organic solid solution of pentaerythritol (m.p. 188 °C, latent heat of fusion 323 kJ/kg), pentaglycerine (m.p. 81 °C, latent heat of fusion 216 kJ/kg), Li_2SO_4 (m.p. 578, latent heat of fusion 214 kJ/kg) and KHF_2 (m.p. 196 °C, latent heat of fusion 135 kJ/kg) [1]. Trombe wall with these materials could provide better performance than a plain concrete Trombe wall. Solid–gas and liquid–gas transition through have higher latent heat of phase

transition but their large volume changes on phase transition are associated with the containment problems and rule out their potential utility in thermal-storage systems.

Large changes in volume make the system complex and impractical. Solid–liquid transformations have comparatively smaller latent heat than liquid–gas. However, these transformations involve only a small change (of order of 10% or less) in volume. Solid–liquid transitions have proved to be economically attractive for use in thermal energy storage systems. PCMs themselves cannot be used as heat transfer medium. A separate heat transfer medium must be employed with heat exchanger in between to transfer energy from the source to the PCM and from PCM to the load. The heat exchanger to be used has to be designed specially, in view of the low thermal diffusivity of PCMs in general. The volume changes of the PCMs on melting would also necessitate special volume design of the containers to house PCM. It should be able to absorb these volume changes and should also be compatible with the PCM used. Any latent heat energy storage system therefore, possess at least following three components:

- (i) a suitable PCM with its melting point in the desired temperature range,
- (ii) a suitable heat exchange surface, and
- (iii) a suitable container compatible with the PCM.

The development of a latent heat thermal energy storage system hence, involves the understanding of three essential subjects: phase change materials, containers materials and heat exchangers. A wide range of technical options available for storing low temperature thermal energy is shown in Fig.

Latent heat storage materials

Phase change materials (PCM) are “Latent” heat storage materials. The thermal energy transfer occurs when a material changes from solid to liquid, or liquid to solid. This is called a change in state, or “Phase.” Initially, these solid–liquid PCMs perform like conventional storage materials, their temperature rises as they absorb heat. Unlike conventional (sensible) storage materials, PCM absorbs and release heat at a nearly constant temperature. They store 5–14 times more heat per unit volume than sensible storage materials such as water, masonry, or rock. A large number of PCMs are known to melt with a heat of fusion in any required range. However, for their employment as latent heat storage materials these materials must exhibit certain desirable thermodynamic, kinetic and chemical properties. Moreover, economic considerations and easy availability of these materials has to be kept in mind. The PCM to be used in the design of thermal-storage systems should possess desirable thermophysical, kinetics and chemical properties which are as follows (Figure.21):

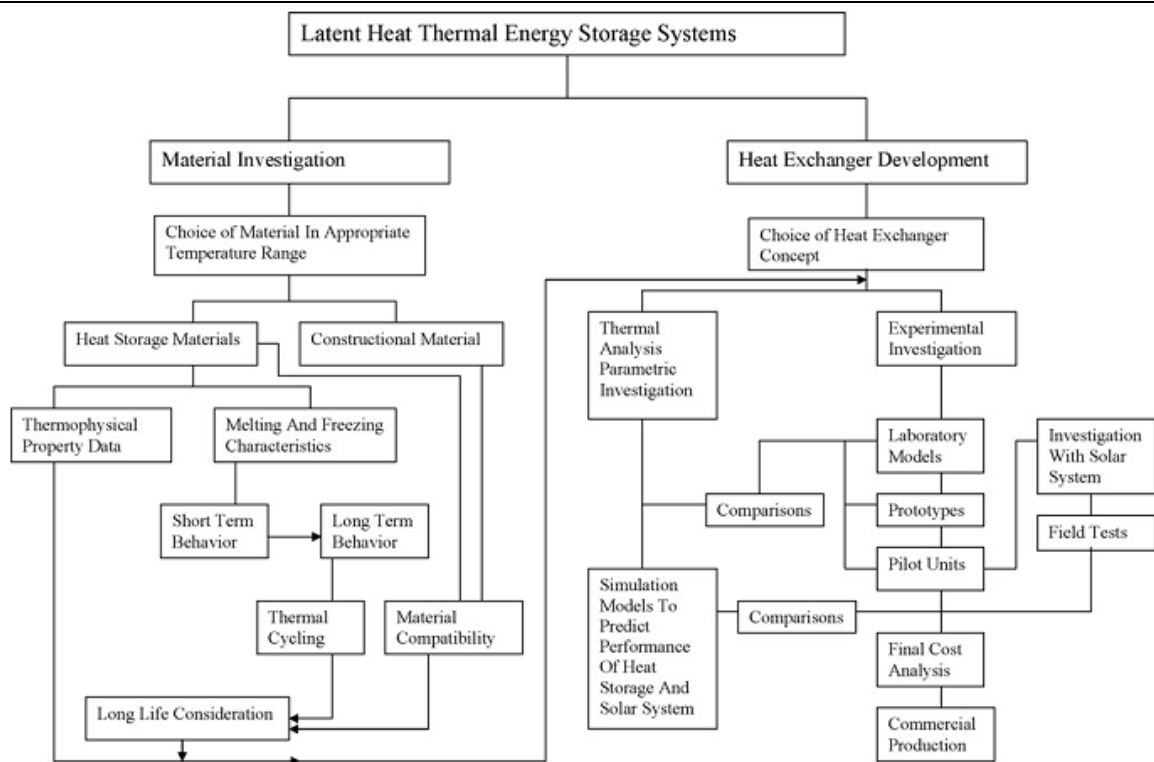


Figure.21: Flow chart showing different stages involved in the development of a latent heat storage system.

Thermal properties

- (i) Suitable phase-transition temperature.
- (ii) High latent heat of transition.
- (iii) Good heat transfer.

Selecting a PCM for a particular application, the operating temperature of the heating or cooling should be matched to the transition temperature of the PCM. The latent heat should be as high as possible, especially on a volumetric basis, to minimize the physical size of the heat store. High thermal conductivity would assist the charging and discharging of the energy storage.

Physical properties

- (i) Favorable phase equilibrium.
- (ii) High density.
- (iii) Small volume change.
- (iv) Low vapor pressure.

Phase stability during freezing melting would help towards setting heat storage and high density is desirable to allow a smaller size of storage container. Small volume changes on phase transformation and small vapor pressure at operating temperatures to reduce the containment problem.

Kinetic properties

- (i) No supercooling.
- (ii) Sufficient crystallization rate.

Supercooling has been a troublesome aspect of PCM development, particularly for salt hydrates. Supercooling of more than a few degrees will interfere with proper heat extraction from the store, and 5–10 °C supercooling can prevent it entirely.

Chemical properties

- (i) Long-term chemical stability.
- (ii) Compatibility with materials of construction.
- (iii) No toxicity.
- (iv) No fire hazard.

PCM can suffer from degradation by loss of water of hydration, chemical decomposition or incompatibility with materials of construction. PCMs should be non-toxic, non-flammable and non-explosive for safety.

Economics

- (i) Abundant.
- (ii) Available.
- (iii) Cost effective.

Low cost and large-scale availability of the phase change materials is also very important.

Classification of PCMs

A large number of phase change materials (organic, inorganic and eutectic) are available in any required temperature range. A classification of PCMs is given in Fig.22. There are a large number of organic and inorganic chemical materials, which can be identified as PCM from the point of view melting temperature and latent heat of fusion. However, except for the melting point in the operating range, majority of phase change materials does not satisfy the criteria required for an adequate storage media as discussed earlier. As no single material can have all the required properties for an ideal thermal-storage media, one has to use the available materials and try to make up for the poor physical property by an adequate system design. For example metallic fins can be used to increase the thermal conductivity of PCMs, supercooling may be suppressed by introducing a nucleating agent or a 'cold finger' in the storage material and incongruent melting can be inhibited by use of suitable thickness. In general inorganic compounds have almost double volumetric latent heat storage capacity (250–400 kg/dm³) than the organic compounds (128–200 kg/dm³). For their very different thermal and chemical behavior, the properties of each subgroup which affects the design of latent heat thermal energy storage systems using PCMs of that subgroup are discussed in detail below.

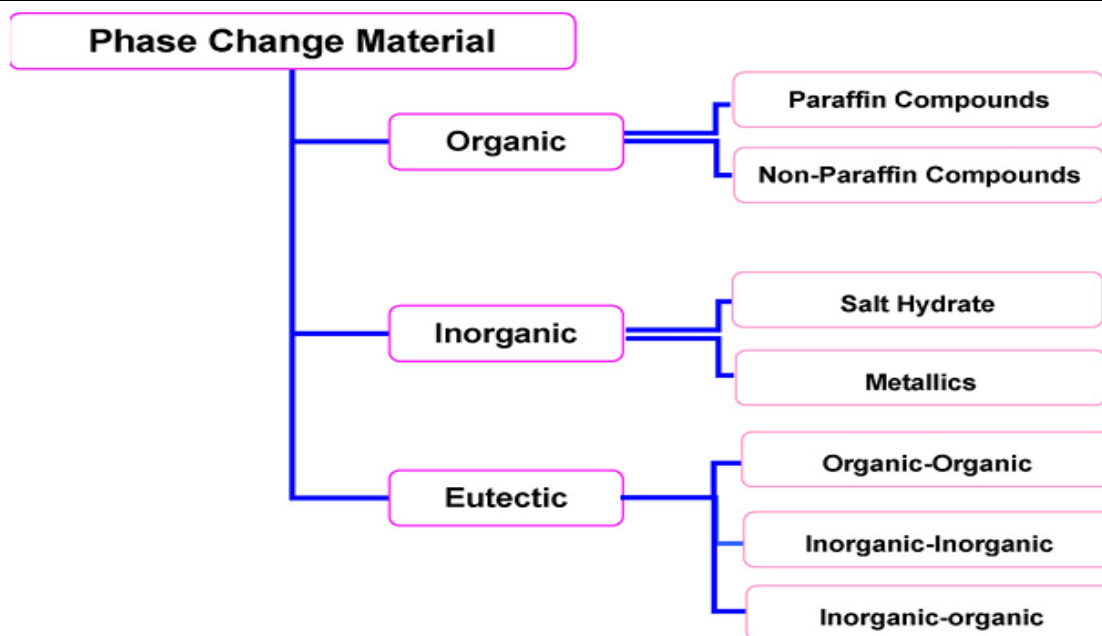


Fig.22 Classification of PCMs

Organic phase change materials

Organic materials are further described as paraffin and non- paraffins. Organic materials include congruent melting means melt and freeze repeatedly without phase segregation and consequent degradation of their latent heat of fusion, self nucleation means they crystallize with little or no supercooling and usually non-corrosiveness.

Paraffins

Paraffin wax consists of a mixture of mostly straight chain n- alkanes $\text{CH}_3\text{--}(\text{CH}_2)\text{--CH}_3$. The crystallization of the $(\text{CH}_2)\text{--}$ chain release a large amount of latent heat. Both the melting point and latent heat of fusion increase with chain length. Paraffin qualifies as heat of fusion storage materials due to their availability in a large temperature range. Due to cost consideration, however, only technical grade paraffins may be used as PCMs in latent heat storage systems. Paraffin is safe, reliable, predictable, less expensive and non-corrosive. They are chemically inert and stable below 500°C , show little volume changes on melting and have low vapor pressure in the melt form. For these properties of the paraffins, system-using paraffins usually have very long freeze–melt cycle. Table.5 lists thermal properties of some technical grade paraffins, which are essentially, paraffin mixtures and are not completely refined oil. The melting point of alkane increases with the increasing number of carbon atoms. Apart from some several favorable characteristic of paraffins, such as congruent melting and good nucleating properties. They show some undesirable properties such as: (i) low thermal conductivity, (ii) non-compatible with the plastic container and (iii) moderately flammable. All these undesirable effects can be partly eliminated by slightly modifying the wax and the storage unit. Some selected paraffins are shown in Table along-with their melting point, latent heat

of fusion and groups. PCMs are categorized as: (i) group I, most promising; (ii) group II, promising; and (iii) group III, less promising.

Table. 5: Physical properties of some paraffin's
Physical properties of some paraffin's

Paraffin ^a	Freezing point/ range (°C)	Heat of fusion (kJ/kg)	Group ^b
6106	42–44	189	I
P116 ^c	45–48	210	I
5838	48–50	189	I
6035	58–60	189	I
6403	62–64	189	I
6499	66–68	189	I

^a Manufacturer of technical Grade Paraffin's 6106, 5838, 6035, 6403 and 6499: Ter Hell Paraffin Hamburg, FRG.

^b Group I, most promising; group II, promising; group III, less promising; — insufficient data.

^c Manufacturer of Paraffin's P116: Sun Company, USA.

Non-paraffins

The non-paraffin organic are the most numerous of the phase change materials with highly varied properties. Each of these materials will have its own properties unlike the paraffin's, which have very similar properties. This is the largest category of candidate's materials for phase change storage. An extensive survey of organic materials has been conducted with identification of a number of esters, fatty acids, alcohol's and glycol's suitable for energy storage. These organic materials are further subgroups as fatty acids and other non-paraffin organic. These materials are flammable and should not be exposed to excessively high temperature, flames or oxidizing agents. Some of the features of these organic materials are as follows: (i) high heat of fusion, (ii) inflammability, (iii) low thermal conductivity, (iv) low flash points, (v) varying level of toxicity, and (vi) instability at high temperatures.

Fatty acids have high heat of fusion values comparable to that of paraffin's. Fatty acids also show reproducible melting and freezing behavior and freeze with no supercooling. The general formula describing all the fatty acid is given by $\text{CH}_3(\text{CH}_2)_{2n}\text{COOH}$ and hence, qualify as good PCMs. Their major drawback, however, is their cost, which are 2–2.5 times greater than that of technical grade paraffin's. They are also mild corrosive. Some fatty acids of interest to low temperature latent heat thermal energy storage applications and are tabulated in Table 4.

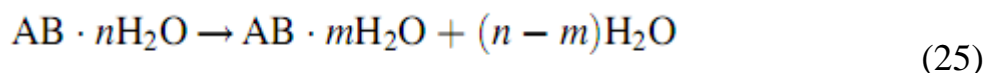
Inorganic phase change materials

Inorganic materials are further classified as salt hydrate and metallics. These phase change materials do not supercool appreciably and their heats of fusion do not degrade with cycling.

Salt hydrates

Salt hydrates may be regarded as alloys of inorganic salts and water forming a typical crystalline solid of general formula AB

$n\text{H}_2\text{O}$. The solid–liquid transformation of salt hydrates is actually a dehydration of hydration of the salt, although this process resembles melting or freezing thermodynamically. A salt hydrates usually melts to either to a salt hydrate with fewer moles of water, i.e.



or to its anhydrous form



At the melting point the hydrate crystals breakup into anhydrous salt and water, or into a lower hydrate and water. One problem with most salt hydrates is that of incongruent melting caused by the fact that the released water of crystallization is

not sufficient to dissolve all the solid phase present. Due to density difference, the lower hydrate (or anhydrous salt) settles down at the bottom of the container. Most salt hydrates also have poor nucleating properties resulting in supercooling of the liquid before crystallization beings. One solution to this problem is to add a nucleating agent, which provides the nuclei on which crystal formation is initiated. Another possibility is to retain some crystals, in a small cold region, to serve as nuclei. Salt hydrates are the most important group of PCMs, which have been extensively studied for their use in latent heat thermal energy storage systems. The most attractive properties of salt hydrates are: (i) high latent heat of fusion per unit volume, (ii) relatively high thermal conductivity (almost double of the paraffin's), and (iii) small volume changes on melting. They are not very corrosive, compatible with plastics and only slightly toxic. Many salt hydrates are sufficiently inexpensive for the use in storage.

Three types of the behavior of the melted salts can be identified: congruent, incongruent and semi-congruent melting. (i) Congruent melting occurs when the anhydrous salt is completely soluble in its water of hydration at the melting temperature. (ii) Incongruent melting occurs when the salt is not entirely soluble in its water of hydration at the melting point. (iii) Semi-congruent melting the liquid and solid phases in equilibrium during a phase transition is of different melting composition because of conversion of the hydrate to a lower-hydrated material through loss of water. The major problem in using salt hydrates, as PCMs is the most of them, which are judged suitable for use in thermal storage, melts incongruently. As n moles of water of hydration are not sufficient to dissolves one mole of salt, the resulting solution is supersaturated at the melting temperature. The solid salt, due to its higher density, settles down at the bottom of the container and is unavailable for recombination with water during the

reverse process of freezing. This results in an irreversible melting–freezing of the salt hydrate goes on decreasing with each charge–discharge cycle. Another important problem common to salt hydrates is that of supercooling. At the fusion temperature, the rate of nucleation is generally very low. To achieve a reasonable rate of nucleation, the solution has to be supercooled and hence energy instead of being discharged at fusion temperature is discharged at much lower temperature.

Other problem faced with salt hydrates is the spontaneous of salt hydrates with lower number of water moles during the discharge process. Adding chemicals can prevent the nucleation of lower salt hydrates, which preferentially increases the solubility of lower salt hydrates over the original salt hydrates with higher number of water moles.

The problem of incongruent melting can be tackled by one of the following means: (i) by mechanical stirring, (ii) by encapsulating the PCM to reduce separation, (iii) by adding of the thickening agents which prevent setting of the solid salts by holding it in suspension, (iv) by use of excess of water so that melted crystals do not produce supersaturated solution, (v) by modifying the chemical composition of the system and making incongruent material congruent. To overcome the problem of salt segregation and supercooling of salt hydrates, scientists of General Electric Co., NY suggested a rolling cylinder heat storage system. The system consists of a cylindrical vessel mounted horizontally with two sets of rollers. A rotation rate of 3 rpm produced sufficient motion of the solid content (i) to create effective chemical equilibrium, (ii) to prevent nucleation of solid crystals on the walls, and (iii) to assume rapid attainment of axial equilibrium in long cylinders. Some of the advantages of the rolling cylinder method as listed are: (i) complete phase change, (ii) latent heat released was in the range of 90–100% of the theoretical latent heat, (iii) repeatable performance over 200 cycles, (iv) high internal heat transfer rates, (v) freezing occurred uniformly. A list of salt hydrates is given in Table .6

Table.6: Melting point and latent heat of fusion: salt hydrates

Melting point and latent heat of fusion: salt hydrates

Material	Melting point (°C)	Latent heat (kJ/kg)	Group ^a
K ₂ HPO ₄ ·6H ₂ O	14.0	109	II
FeBr ₃ ·6H ₂ O	21.0	105	II
Mn(NO ₃) ₂ ·6H ₂ O	25.5	148	II
FeBr ₃ ·6H ₂ O	27.0	105	II
CaCl ₂ ·12H ₂ O	29.8	174	I
LiNO ₃ ·2H ₂ O	30.0	296	I
LiNO ₃ ·3H ₂ O	30	189	I
Na ₂ CO ₃ ·10H ₂ O	32.0	267	II
Na ₂ SO ₄ ·10H ₂ O	32.4	241	II
KFe(SO ₄) ₂ ·12H ₂ O	33	173	I
CaBr ₂ ·6H ₂ O	34	138	II
LiBr ₂ ·2H ₂ O	34	124	I
Zn(NO ₃) ₂ ·6H ₂ O	36.1	134	III
FeCl ₃ ·6H ₂ O	37.0	223	I
Mn(NO ₃) ₂ ·4H ₂ O	37.1	115	II
Na ₂ HPO ₄ ·12H ₂ O	40.0	279	II

Metallics

This category includes the low melting metals and metal eutectics. These metallics have not yet been seriously considered for PCM technology because of weight penalties. However, when volume is a consideration, they are likely candidates because of the high heat of fusion per unit volume. They have high thermal conductivities, so fillers with added weight penalties are not required. The use of metallics poses a number of unusual engineering problems. A major difference between the metallics and other PCMs is their high thermal conductivity. A list of some selected metallics is given in Table. Some of the features of these materials are as follows: (i) low heat of fusion per unit weight (ii) high heat of fusion per unit volume, (iii) high thermal conductivity, (iv) low specific heat and (v) relatively low vapor pressure.

Eutectics

A eutectic is a minimum-melting composition of two or more components, each of which melts and freeze congruently forming a mixture of the component crystals during crystallization. Eutectic nearly always melts and freezes without segregation since they freeze to an intimate mixture of crystals, leaving little opportunity for the components to separate. On melting both components liquefy simultaneously, again with separation unlikely. Some segregation PCM compositions have sometimes been incorrectly called eutectics, since they are minimum melting. Because of the components undergoes a peritectic reaction during phase transition, however, they should more properly be termed peritectics. Freezing point of the mixture of tetradecane (m.p. 5.3°C) and

hexadecane (m.p. 17.9 °C) is shown in Fig. The eutectic point of laboratory grade hexadecane–tetradecane mixture occurs at approximately 91.67% of tetradecane, and its phase change temperature is approximately 1.7°C.

D. Solar Thermal Power generation

Of the 162 PW of solar radiation reaching the Earth, 86 PW hit its surface in the form of direct (75%) and diffused light (25%). The energy quality of diffused radiation is lower (75.2% of exergy content instead of 93.2% for direct light), with consequences on the amount of work that can be extracted from it. 38PW hit the continents and a total exergy of 0.01TW is estimated to be destroyed during the collection and use of solar radiation for energy services. This estimation includes the use of photovoltaics and solar thermal plants for the production of electricity and hot water. Similar estimates are shown for wind energy (0.06TW), ocean thermal gradient (not yet exploited for energy production), and hydroelectric energy (0.36TW).

The market share of solar energy is still low. Current electricity generation from PVs is only of the order of 2.6GW compared to 36.3GW for all renewable energies, hydroelectric power excluded. Developed countries are steadily increasing their investments in solar power plants, and projections for 2030 give an enhancement of solar electricity generation up to 13.6GW (80% of which will be from photovoltaics, and the rest (2.4GW) from solar thermal plants). However, this amount will not exceed 6% of the total electricity production from non-hydro renewable energies. It is worth noting that passive solar technologies for water heating, not included in these statistics, represent a fairly large amount of power. International energy agency estimates a power production of 5.3GW in 2002 and an increase up to 46GW by 2030.

The major causes of the slow deployment of solar technologies are:

- The current relative high capital cost per kW installed compared with other fossil fuel based and renewable technologies;
- The intermittent nature of the energy input, and hence the requirement for energy storage systems to match the energy supply with the electricity demand and to decrease the capital cost. In a medium term, energy storage will be a key requirement for intermittent renewable energies to become more competitive versus fossil fuels.

The solar-to-electric efficiency of solar thermal technologies varies largely depending upon the solar flux concentration factor, the temperature of the thermal intermediary, and the efficiency of the thermal cycle for the production of mechanical work and electricity. Parabolic troughs and power towers reach peak efficiencies of about 20%. Dish-Stirling systems are the most efficient, with ~30% solar-to-electric demonstrated efficiency. The performance of these systems is highly influenced by the plant availability. In the case of parabolic troughs and power towers, thermal storage increases the annual capacity factor from typically 20% to 50% and 75%, respectively.

A wide variety of solar technologies have the potential to become a large component of the future energy portfolio. Passive technologies are used for indoor lighting and heating of buildings and water for domestic use. Also,

various active technologies are used to convert solar energy into various energy carriers for further utilization:

- Photovoltaics directly convert photon energy into electricity. These devices use inorganic or organic semiconductor materials that absorb photons with energy greater than their bandgap to promote energy carriers into their conduction band. Electron-hole pairs, or excitons for organic semiconductors, are subsequently separated and charges are collected at the electrodes for electricity generation.
- Solar thermal technologies convert the energy of direct light into thermal energy using concentrator devices. These systems reach temperatures of several hundred degrees with high associated exergy. Electricity can then be produced using various strategies including thermal engines (e.g. Stirling engines) and alternators, direct electron extraction from thermionic devices, Seebeck effect in thermoelectric generators, conversion of IR light radiated by hot bodies through thermophotovoltaic devices, and conversion of the kinetic energy of ionized gases through magnetohydrodynamic converters.

Photon-to-Thermal-to-Electric Energy Conversion

In this section we analyze solar thermal technologies that produce electricity through concentration of solar energy for the production of heat and subsequent conversion into electric current. There are a number of options available at different stages of development 16. The most developed technologies are the parabolic dish, the parabolic trough, and the power tower. The parabolic dish is already commercially available. This system is modular and can be used in single dish applications (with output power of the order of 25kWe) or grouped in dish farms to create large multi-megawatt plants (see for example the 500MW solar dish farm project in Victorville, California [92]). Parabolic troughs are a proven technology and will most likely be used for deployment of solar energy in the near-term. Various large plants are currently in operation (California - 354MW) or in the planning process in the USA and in Europe. Power towers, with low cost and efficient thermal storage, promise to offer dispatchable, high capacity factor power plants in the future. Together with dish/engine systems, they offer the opportunity to achieve higher solar-to-electric efficiencies and lower cost than parabolic trough plants (see Table.7), but uncertainty remains as to whether these technologies can achieve the necessary capital cost reductions.

Table.7 : Characteristics of major solar thermal electric power systems

	Parabolic Trough	Power Tower	Dish/Engine
Size ^(a)	30-320MW	10-200MW	5-25kW
Approximate operating temperature	400°C	600°C	750°C
Annual capacity factor ^(a)	23-50%	20-77%	25%
Peak Efficiency	20% ^(b)	23%	29.4% ^(b)
Net annual efficiency ^(a)	11 ^(b) -16%	7 ^(b) -20%	12-25%
Cost [\$/W] ^(a)	4.0-2.7	4.4-2.5	12.6-1.3
Cost [\$/W _p] ^{(a) (c)}	4.0-1.3	2.4-0.9	12.6-1.1

(a) Value range indicates changes over the 1997-2030 time frame

(b) Demonstrated values; other values are estimated or predicted

(c) \$/W_p removes the effect of thermal storage (or hybridization for dish/engine)

All these technologies involve a thermal intermediary and thus can be readily hybridized with fossil fuel combustion and in some cases adapted to utilize thermal storage. The primary advantage of hybridization and thermal storage is that the technologies can provide dispatchable power and operate during periods when solar energy is not available. In particular, thermal storage allows an increase in the annual capacity factor of a solar plant of 50% or more. Hybridization and thermal storage can enhance the economic value of the electricity produced and reduce its average cost.

Parabolic troughs

Parabolic trough systems use single-axis tracking parabolic mirrors to focus sunlight on thermally efficient receiver tubes that contain a heat transfer fluid (HTF). The receiver tubes are usually metallic and embedded into an evacuated glass tube that reduces heat losses. A special high-temperature coating additionally reduces radiation heat losses. The working fluid (e.g. thermo oil) is heated to $\sim 400^{\circ}\text{C}$ and pumped through a series of heat exchangers to produce superheated steam which powers a conventional turbine generator (Rankine cycle) to produce electricity. It is also possible to produce superheated steam directly using solar collectors. This makes the thermo oil unnecessary, and also reduces costs because the relatively expensive thermo oil and the heat exchangers are no longer needed. However, direct steam generation (DSG) is still in the prototype stage and more research is required to solve the thermo-mechanical issues related to working pressures above 100 bar and the presence of a two-phase fluid in the receivers. The efficiency of a solar thermal power plant is the product of the collector efficiency, field efficiency and steam-cycle efficiency. The collector efficiency depends on the angle of incidence of the sunlight and the temperature in the absorber tube, and can reach values up to 75%. Field losses are usually below 10%. Altogether, solar thermal trough power plants can reach annual efficiencies of about 15%; the steam-cycle efficiency of about 35% has the most significant influence. Central receiver systems such as solar thermal tower plants can reach higher temperatures and therefore achieve higher efficiencies.

Current research in parabolic trough systems aims at improving performance and lifetime and at reducing manufacturing, operation, and maintenance costs with improved designs. These activities concern all critical components of the system, namely the support and tracking structure, the reflector (glass mirrors, polymeric reflectors and other alternative reflectors), and the receiver tubes (absorbers, glass/metal seals, etc.).

Power towers

In a power tower plant, hundreds of two-axis tracking heliostats are installed around a tower where they focus sunlight with concentrations ranging from 100 to 10,000 suns. The absorber is located on the top of the tower and can reach temperatures from 200°C to 3000°C . Hot air or molten salt are usually used to transport the heat from the absorber to a steam generator where superheated steam is produced to drive a turbine and an electrical generator. Power towers are suited for large-output applications, in the 30 to 400MW_e range, and need to be large to be economical. Thermal storage can be easily integrated with this

type of solar systems, allowing the enhancement of the annual capacity factor from 25% to 65% and the stabilization of the power output through fluctuations in solar intensity until the stored energy is depleted. Since the early 1980s, power towers were built in Russia, Italy, Spain, Japan, France, and the USA, with power outputs ranging from 0.5MWe to 10MWe (Solar Two, Southern California) and using various combinations of heat transfer fluids (steam, air, liquid sodium, molten nitrate, molten nitrate salt) and storage media (water/steam, nitrate salt/water, sodium, oil/rock, ceramic). The Solar Two plant has proven the feasibility of molten-salt power towers, achieving turbine operation at full capacity for three hours after sunset thanks to the two-tank (290°C/570°C) molten salt storage system (with a capacity of 110MWh). The main design challenge for this system was identifying the materials that work with molten salt, since this fluid has relatively high freezing point (220°C), low viscosity, wets metal surfaces extremely well, and is corrosive. Solar Tres, Spain is the first commercial power tower and is a follow-up of the technologies developed for Solar Two. Its size is three fold larger, the electrical power output is 15MW_e, and the thermal storage capacity 600MWh (16 hours). The efficiency of a solar-powered steam turbine electric generator used in the power tower concept is a critical function of the temperature T_R of the receiver, which is influenced not only by the incident energy but also of several factors including the heliostat optical performance, the mirror cleanliness, the accuracy of the tracking system, and wind effects. For an ambient temperature of 340K, the efficiency is 35% for $T_R = 800K$ and 62% for $T_R = 3000K$. Solar Two achieved 13% peak efficiency with $T_R = 570^\circ C$ (the efficiency expected for a commercial plant is 23%). The development of heat transfer fluids working at high temperature is a key issue for increasing the overall efficiency of power towers.

Various thermal storage options are currently being considered for parabolic troughs and power towers. Some of them have already been demonstrated but many need further research, particularly concerning the optimization of the HTF materials. Here are some among the most significant technologies: The development of new heat transfer fluids (HTFs) is crucial for increasing the operating temperature of a solar thermal plant, and hence the efficiency of the steam cycle. Stability at high temperature, low flammability, low vapor pressure at high temperature, low corrosivity in standard materials, low freezing point, high boiling point, and low cost are the main required characteristics.

- Concrete – This system would use a HTF in the solar field and pass it through an array of pipes imbedded in concrete. The highest uncertainty is the long-term stability of the concrete material itself after thousands of charging cycles.
- Indirect two-tank molten-salt – In current applications, a synthetic oil (e.g. biphenyl-diphenyl oxide) is used as HTF in the solar field and for heating molten salt through a heat exchanger in the thermal storage system. Two separate tanks are used for this system. The excess heat of the solar collector field heats up the molten salt, which is pumped from the cold to the hot tank. If the solar collector field cannot produce enough heat to drive the turbine, the molten salt is

pumped back from the hot to the cold tank, and heats up the heat transfer fluid. The molten salt, as it was used in the Solar-Two solar tower pilot demonstration plant, is a binary mixture of 60% sodium nitrate (NaNO_3) and 40% potassium nitrate (KNO_3) salt. The feasibility of this system was proven and the concept seems to have low technological risk despite the relatively high freezing point ($\sim 225^\circ\text{C}$) of the salt.

- Thermocline storage – Thermoclines use a single storage tank. A low-cost filler material (e.g. quartzite and silica sand) acts as the primary thermal storage medium and replaces approximately two-thirds of the molten salt that would be needed in a two-tank system. With the hot and cold fluid in a single tank, the thermocline storage system relies on thermal buoyancy to maintain thermal stratification. The thermocline is the region of the tank between the two temperature resources, with a temperature difference of about 60°C . Thermoclines can maintain their integrity over a three-day no-operation period.
- Molten-salt HTF – Using a lower temperature molten salt as the HTF in the solar field allows the same fluid to be used in both the solar field and the thermal storage field, leading to significant cost reduction for the thermal storage, especially when used in the thermocline configuration. This also allows the solar field to be operated at higher outlet temperatures, increasing the power cycle efficiency and further reducing the cost of thermal storage. Major technical barriers to this option include the challenges of high freezing temperature salts (of the order of 120°C) and with higher operating temperatures leading to higher heat losses and requiring new materials and components.
- Organic molten-salt HTF – Organic salts, or ionic liquids, have the advantage of being liquid at room temperature. Additionally they can be synthesized to have specific properties desirable for solar applications, namely low freezing point, high thermal stability, low corrosivity, good heat transfer and thermal properties, and low cost. The development of organic salts is relatively new and more research is required to optimize all these characteristics, particularly to lower the materials cost.

Alternative systems for converting thermal energy into electricity have been explored, such as liquid metal magnetohydrodynamic generators (LMMHD). These systems were first investigated in the early 1980s and offer significant increases in the system thermal efficiency over the 33% considered attainable with conventional turbo-machinery. With sodium at a temperature of 650°C , the theoretical efficiency is 39.5%. A peak efficiency of 46.5% is predicted for lithium at 760°C . The thermodynamic efficiency at maximum power, with an ambient temperature of 300K and a blackbody source temperature of 6000K, is 64% and occurs at a receiver optimal temperature of 2900K. Additional potential advantages are that the sodium/steam heat exchanger is eliminated in liquid metal systems, and, where LMMHD systems employ the same working fluid as the solar receiver, no recirculating pump is required as pumping power is provided directly by the cycle.

Dish-engine systems

Dish-engine systems can be used to generate electricity in the kilowatts range. A parabolic concave mirror concentrates sunlight; the two-axis tracked mirror must follow the sun with a high degree of accuracy in order to achieve high efficiencies. At the focus is a receiver which is heated up over 700°C. The absorbed heat drives a thermal engine which converts the heat into motive energy and drives a generator to produce electricity. If sufficient sunlight is not available, combustion heat from either fossil fuels or biofuels can also drive the engine and generate electricity. The solar-to-electric conversion efficiency of dish-engine systems can be as high as 30%, with large potential for low-cost deployment. For the moment, the electricity generation costs of these systems are much higher than those for trough or tower power plants, and only series production can achieve further significant cost reductions for dish-engine systems. A number of prototype dish-engine systems are currently operating in Nevada, Arizona, Colorado, and Spain. High levels of performance have been established; durability remains to be proven, although some systems have operated for more than 10,000 hours.

Most research and development efforts aim at incrementally enhancing the reliability, performance, and cost-effectiveness of all major components of these systems: concentrators, receivers, and engines. The development of high-efficiency low-cost thermal engines or alternative heat-to-electric conversion systems is the most critical requirement for these systems to become economical. Various thermodynamic cycles have been considered for dish-engine systems. Stirling and open Brayton (gas turbine) cycles have shown the best performances to date. Stirling engines have a potential for high efficiency and external heating makes them easily adaptable to solar dishes. Modern, high-performance Stirling engines use hydrogen or helium working gas at temperatures over 700°C and pressures as high as 20MPa, resulting in thermal-to-electric conversion efficiencies of about 40%. The main disadvantage of these types of engines is their manufacturing cost, mainly determined by the materials used for the hot part heat exchanger (stainless steel, high-temperature alloys or ceramic materials) and by the design of the cooling system. In a dish-Brayton system, solar heat is used to replace or supplement the fuel at the entrance of the gas turbine. Current designs include pressure ratios of ~2.5, turbine inlet temperatures of about 850°C, and recuperation of waste heat, with predicted efficiencies over 30%. Dish-Brayton systems are still at an early stage of development. Alternative dish systems replace the thermal engine with high-efficiency (>30%) multijunction photovoltaic cells working with concentrated sunlight (see section on photovoltaics), or with thermoelectric or thermionic devices for direct current extraction from the high temperature receiver. Thermoelectrics can convert thermal energy into electrical energy through the Seebeck effect. Theoretical efficiency limits are below 30% of the Carnot efficiency $\Delta T/T_{\text{high}}$ for figure of merit (ZT) values <1. The challenge in designing efficient thermoelectric materials is enhancing electrical conductivity (e.g. by using crystalline, high-bandgap, heavily doped semiconductors) while minimizing thermal conductivity, as described in the “phonon-glass electron-single-crystal” (PGEC) concept by G.A. Slack. Lattice thermal conductivity, the

major contribution to thermal conductivity, can be minimized by increasing the phonon scattering by introducing heavy atoms, disorder, large unit cells, clusters, and rattling atoms. Using these principles, a variety of high ZT materials have been developed with different operation temperature ranges. Skutterudite material systems and complex chalcogenide structures are some representative examples of such materials. Low-dimensional (nanostructured) thermoelectric materials have high potential for achieving figure of merit values of 2 and higher. In fact, quantum and size effects may enhance the Seebeck coefficient and the electrical conductivity, while boundary phonon scattering would lead to a large reduction in thermal conductivity. In contrast with thermoelectric devices, electron transport in thermionic converters is not diffusive but ballistic, the emitter and collector electrodes being physically separated to prevent thermal diffusion along a solid lattice. Thermionics are an old technology that was widely developed from the 1950's to the mid-1970's. The development efforts were virtually abandoned because of the lack of electrode materials with combined low working functions ($\sim 1\text{eV}$) and low vapor pressures (for long-term stability); the lowperformance (heat-to-electric conversion efficiency $<10\%$) and the high operating temperatures ($>1400\text{K}$); and the technical challenges related to manufacturing devices with an interelectrode spacing $<10\mu\text{m}$ needed to decrease the negative-space-charge effect in vacuum thermionic converters. High-pressure cesium diode thermionic converters with refractory-metal electrodes (having low vapor pressure) showed better performances, with output-power densities ranging from $1\text{W}/\text{cm}^2$ to $30\text{W}/\text{cm}^2$ and efficiencies from 5% to 20% with emitter temperatures T_E between 1500K and 2000K, the theoretical efficiency limit for thermionic conversion being 30% (0.65η Carnot for emitter and collector temperatures of 1800K and 900K, respectively). The development of nanotechnologies led to realizing devices with interelectrode spacing as small as 1-10nm, allowing tunneling of hot electrons and thus higher conversion efficiencies. As in the case of thermoelectric devices, extensive research efforts are focused on low temperature applications such as cooling at temperatures below room temperature or power generation from waste heat at temperatures $<400\text{-}500\text{K}$. For high temperature applications, effective high-energy electron selectivity, and decreasing the large (up to 50%) power losses caused by the charge-space effect, are among the main fundamental issues that are currently being addressed to enhance the efficiency of thermionics.

Solar chimneys

In contrast with the previously described thermal technologies, solar chimneys convert into electricity not only direct normal irradiance but global irradiance. A solar chimney power plant has a high chimney, up to 1000m, and is surrounded by a large collector roof up to 130m in diameter, that consists of glass or resistive plastic supported on a framework. Towards its centre, the roof curves upwards to join the chimney, creating a funnel. The sun heats up the ground and the air underneath the collector roof, and the heated air follows the roof until it reaches the chimney. There, it flows at high speed (35mph) through the chimney and drives multiple wind turbines at its bottom. The ground under the collector roof behaves as a storage medium, and can even heat up the air for a significant

time after sunset. The efficiency of the solar chimney power plant is below 2%, and depends mainly on the height of the tower. However, the whole power plant is not without other uses, as the outer area under the collector roof can also be utilized as a greenhouse for agricultural purposes. As with trough and tower plants, the minimum economical size of solar chimney power plants is also in the multi-megawatt range. A 1,000m tall pilot solar chimney of 200MW is planned for construction in Australia in 2006. Solar chimneys use well-known technologies, so research and development is needed in design and construction rather than in fundamental physics.

UNIT-5: BASICS OF SOLAR PHOTOVOLTAICS

This unit is a prelude to the unit-6. It mainly covers the basic principle of solar photovoltaic conversion. Starting with the basics of solar photovoltaics it dwells upon the technology for fabrication. The new generation excitonic solar cells such as DSSC, Organic solar cells in addition to the technology for enhancement of efficiency and reduction of cost of solar PV output is discussed to enable the readers to understand the course of technological development in solar cells.

[A] PRINCIPLE OF PHOTOVOLTAIC CONVERSION OF SOLAR CELL**1. INTRODUCTION**

Every day across the globe, the sun shines down on the earth. The energy in the photons from the sun can be converted to electrical energy. The term for this process is the 'Photovoltaic Effect'.

Since the first commercially available solar panel in the 1960's, photovoltaic (PV) technology has continued to be explored and developed throughout the world (Pratt & Schaeffer 51). The constant development of this technology has resulted in an increasing level of efficiency and PV panels that are more affordable than ever before, though still initially expensive. Today, humans continue to search for new ways to make photovoltaic technology a viable option for everyone throughout the world. Since most of us are not studying the atomic level of this technology, we can help in other ways - by gaining an understanding and spreading that understanding of photovoltaics, as well as by helping others to gain access to solar, or photovoltaic, systems.

This article explores the components of a photovoltaic system, describes their role and importance, and works as a beginning guide to those wishing to invest in a photovoltaic system.

2. PHOTOVOLTAIC EFFECT

The photovoltaic effect is the creation of a voltage (or a corresponding electric current) in a material upon exposure to light. Though the photovoltaic effect is directly related to the photoelectric effect, the two processes are different and should be distinguished. In the photoelectric effect, electrons are ejected from a material's surface upon exposure to radiation of sufficient energy. The photovoltaic effect is different in that the generated electrons are transferred between different bands (i.e. from the valence to conduction bands) within the material, resulting in the buildup of a voltage between two electrodes shown in Fig 1.

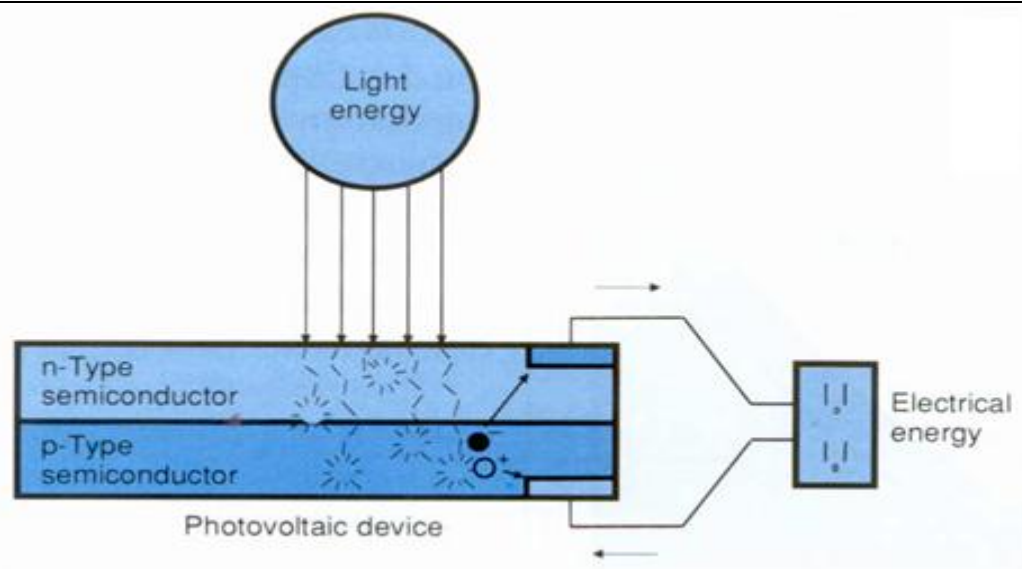


Fig 1: Photovoltaic conversion process

2.1. PHOTOVOLTAIC SYSTEM COMPONENTS

Photovoltaic system components are shown in Fig 2. It consists of following components.

i. Cell

Thin squares, discs, or films of semiconducting material which generate voltage and current when exposed to sunlight.

ii. Panel or Module

Configuration of PV cells laminated between a clear superstrate (glazing) and an encapsulating substrate.

iii. Array

One or more panels wired together at a specific voltage.

iv. Charge Controller

Regulates battery voltage and controls the charging rate, or the state of charge, for batteries.

v. Deep-Cycle Battery

Type of battery (Direct Current electrical energy storage device) that can be discharged to a large fraction of capacity many times without damaging the battery.

vi. Inverter

Changes direct current (DC) to alternating current (AC).

vii. Load

Any electrical component within a circuit that draws power from that circuit.

<http://pubs.acs.org/doi/abs/10.1021/ja202836s?mi=s7yd8w&af=R&pageSize=20&publication=40001010&searchText=photocatalysis>

3. SOLAR CELLS

Photovoltaics are best known as a method for generating electric power by using solar cells to convert energy from the sun into electricity. The photovoltaic effect refers to photons of light knocking electrons into a higher state of energy to create electricity. The term photovoltaic denotes the unbiased operating mode of a photodiode in which current through the device is entirely due to the transduced light energy. Virtually all photovoltaic devices are some type of photodiode.

The solar cell is the smallest practical element that harnesses the photovoltaic effect to generate electricity. Solar cells produce direct current electricity from sun light, which can be used to power equipment or to recharge a battery. The first practical application of photovoltaics was to power orbiting *satellites* and other *spacecraft*, but today the majority of photovoltaic modules are used for grid connected power generation. In this case an inverter is required to convert the DC to AC. There is a smaller market for off-grid power for remote dwellings, boats, recreational vehicles, electric cars, roadside emergency telephones, remote sensing, and cathodic protection of pipelines.

- **Cover glass** – required for protection to the environment.

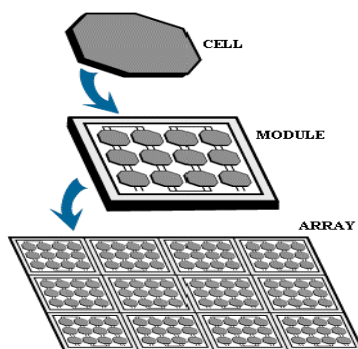


Fig 2: System component of PV system

- **Anti-reflecting coating** - a type of optical coating applied to the surface of lenses and other optical devices to reduce reflection.
- **Contact grid** – the front contact to the load.
- **N-type SI** - are a type of extrinsic semiconductor where the dopant atoms are capable of providing extra conduction electrons to the host material (*e.g. phosphorus in silicon*). This creates an excess of negative (n-type) electron charge carriers.

- A **P-type semiconductor** (P for *Positive*) is obtained by carrying out a process of doping, that is adding a certain type of atoms to the semiconductor in order to increase the number of free charge carriers (in this case positive). (e.g. boron or aluminium)
- **Back contact** – the back contact to the load

When the cell is illuminated, electron-hole pairs are produced by the interaction of the incident photons with the atoms of the cell. The electric field created by the cell junction causes the photon-generated-electron-hole pairs to separate, with the electrons drifting into the n-region of the cell and the holes drifting into the p-region. Figure 2.1 shows the I-V characteristics of a typical PV cell. Note that the amounts of current and voltage available from the cell depend upon the cell illumination level. In the ideal case, the I-V characteristic equation is

$$I = I_{\ell} - I_o \left(e^{\frac{qV}{kT}} - 1 \right) \quad (1)$$

where I is the component of cell current due to photons, $q = 1.6 \times 10^{-19}$ coul, $k = 1.38 \times 10^{-23}$ j/K and T is the cell temperature in K. To determine the open circuit voltage of the cell, the cell current is set to zero and (1) is solved for V_{oc} , yielding the result

$$V_{OC} = \frac{kT}{q} \ln \frac{I_{\ell} + I_o}{I_o} \cong \frac{kT}{q} \ln \frac{I_{\ell}}{I_o}, \quad (2)$$

Multiplying the cell current by the cell voltage yields the cell power. In order to obtain as much energy as possible from the rather costly PV cell, it is desirable to operate the cell to produce maximum power. Referring to Figure 3, note that there is one point on the cell I-V characteristic where the cell produces maximum power. Note also that the voltage at which maximum power occurs is dependent upon the cell illumination level. The maximum power point can be obtained by plotting a set of hyperbolas defined as $IV = \text{constant}$, and noting the power associated with the hyperbola that is tangent to the cell I-V curve at only one point, as opposed to missing the curve or intersecting the curve in two points. The maximum power point may also be determined by differentiating the cell power equation and setting the result equal to zero. After finding the voltage for which this condition is satisfied, and checking to verify that this voltage represents a maximum, the maximum power point is known.

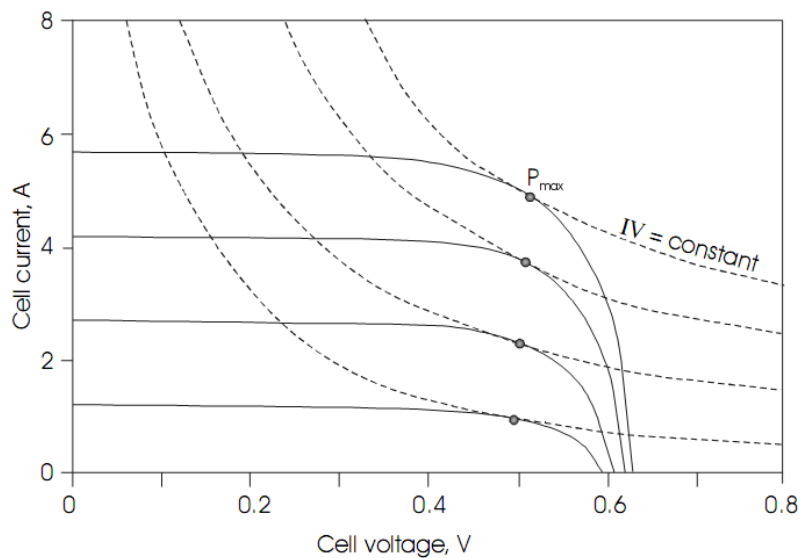


Fig 3. I-V Characteristic of a PV cell

The maximum power point is also readily found by simply plotting cell power vs. cell voltage, as shown in Figure 3. If I_m represents the cell current at maximum power, and if V_m represents the cell voltage at maximum power, then the cell maximum power can be expressed as

$$(3) \quad P_{\max} = I_m V_m = FF I_{SC} V_{OC},$$

where FF is defined as the cell fill factor. The fill factor is a measure of the quality of the cell. Cells with large internal resistance will have smaller fill factors, while the ideal cell will have a fill factor of unity. Note that a unity fill factor suggests a rectangular cell I-V characteristic. Such a characteristic implies that the cell operates as either an ideal voltage source or as an ideal current source. Although a real cell does not have a rectangular characteristic, it is clear that it has a region where its operation approximates that of an ideal voltage source and another region where its operation approximates that of an ideal current source.

The photocurrent developed in a PV cell is dependent on the intensity of the light incident on the cell. The photocurrent is also highly dependent on the wavelength of the incident light. It is noted that terrestrial sunlight approximates the spectrum of a 5800 K blackbody source. PV cells are made of materials for which conversion to electricity of this spectrum is as efficient as possible. Depending on the cell technology, some cells must be thicker than others to maximize absorption. Cells are often coated with an antireflective coating to minimize reflection of sunlight away from the cells.

4. THE PV MODULE

In order to obtain adequate output voltage, PV cells are connected in series to form a PV module. Since PV systems are commonly operated at multiples of 12 volts, the modules are typically designed for optimal operation

in these systems. The design goal is to connect a sufficient number of cells in series to keep V_m of the module within a comfortable range of the battery/system voltage under conditions of average irradiance. If this is done, the power output of the module can be maintained close to maximum. This means that under full sun conditions, V_m should be approximately 16–18 V. Since V is normally about 80% of V_{oc} , this suggests designing the module to have a V_{oc} of about 20 volts. With silicon single cell open-circuit voltages typically in the range of 0.5– 0.6 volts, this suggests that a module should consist of 33–36 cells connected in series. With each individual cell capable of generating approximately 2–3 watts, this means the module should be capable of generating 70–100 watts. When connecting a module into a system, one consideration is what happens when the module is not illuminated. This can happen at night, but can also happen during the day if any cell or portion of a cell is shaded by any means. Under nighttime conditions, when none of the cells are generating appreciable photocurrent, it is necessary to consider the module as a series connection of diodes that may be forward biased by the system storage batteries. For example, suppose the module consisted of 33 cells, each of which has a reverse saturation current of 10^{-10} A. Suppose also that the system battery voltage is 12.8 volts, and that this voltage is uniformly distributed across the series cells. This means that each cell will have 0.388 volts across it in the forward bias direction.

5. THE PV ARRAY

If higher voltages or currents than are available from a single module are required, modules must be connected into arrays. Series connections result in higher voltages, while parallel connections result in higher currents. When modules are connected in series, it is desirable to have each module's maximum power production occur at the same current. When modules are connected in parallel, it is desirable to have each module's maximum power production occur at the same voltage. Thus, when mounting and connecting modules, the installer should have this information available for each module.

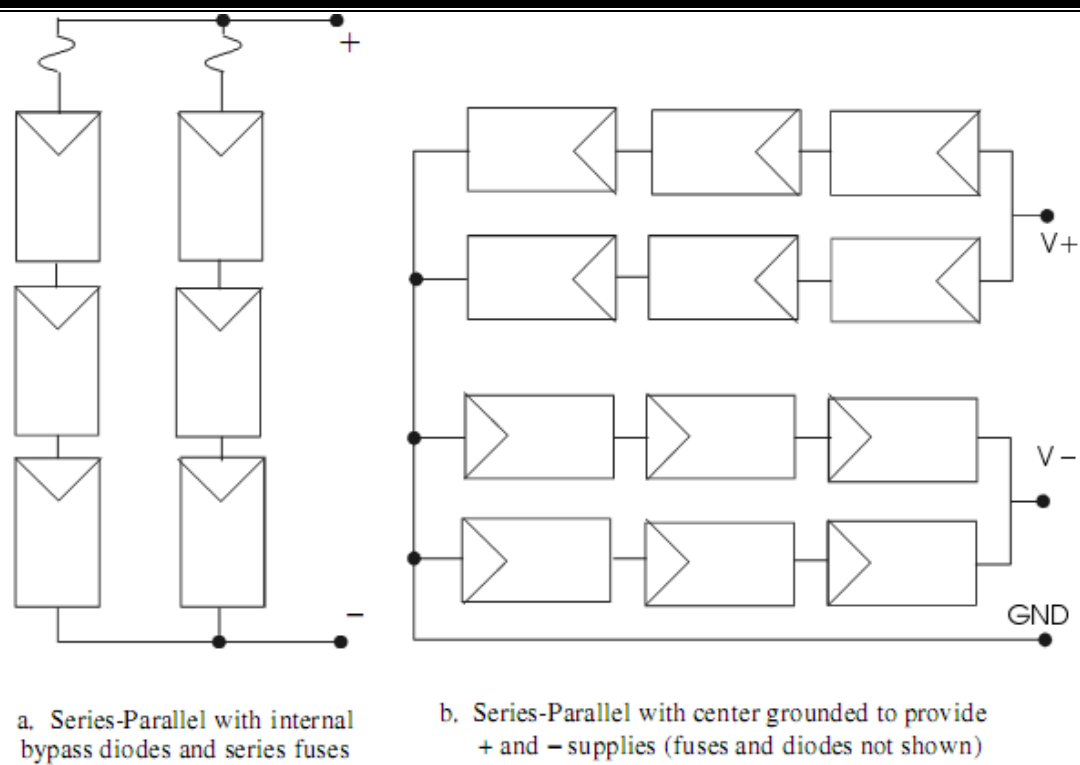


Fig 4. . Module Configuration

Figure 4. shows two common module configurations. In Figure 4.a, modules are connected in series-parallel. In the parallel connection of Figure 4.a, fuses are connected in series with each series string of modules, so that if any string should fail, any excess current from the remaining series strings that might otherwise flow in the reverse direction through the failed string will be limited by the fuse in the failed string. In Figure 4.b, the modules are connected to produce both positive and negative voltages with respect to ground. If three sets of modules are connected in this manner, the combined output conveniently feeds the input of a 3-phase inverter system. A 15 kW 3-phase system sometimes uses three 5 kW inverters and three arrays of modules connected to produce approximately ± 250 volts under maximum power conditions.

6. THE SUN AND PV ARRAY ORIENTATION

The total solar radiation is composed of components, direct or beam, diffuse and reflected. In regions with strong direct components of sunlight, it may be advantageous to have a PV array mount that will track the sun. Such tracking mounts can improve the daily performance of a PV array by more than 20% in certain regions. In cloudy regions, tracking is less advantageous. The position of the sun in the sky can be uniquely described by two angles—the azimuth, γ , and the altitude, α . The azimuth is the deviation from true south. The altitude is the angle of the sun above the horizon. When the altitude of the sun is 90° , the sun is directly overhead. Another convenient, but redundant, angle, is the hour angle, ω . Because the earth rotates 360° in 24 h, it rotates $15^\circ/\text{h}$. The sun thus appears to move along its arc 15° toward the west each hour. The hour angle is 0° at solar noon, when the sun is at its highest point in the sky during a given day. In

this handbook, we have a sign convention such that the hour angle and the solar azimuth angle are negative before noon and positive after noon. For example, at 10:00 a.m. solar time, the hour angle will be -30° . A further important angle that is used to predict sun position is the declination, δ . The declination is the apparent position of the sun at solar noon with respect to the equator. When $\delta=0$, the sun appears overhead at solar noon at the equator. This occurs on the first day of fall and on the first day of spring. On the first day of northern hemisphere summer (June 21), the sun appears directly overhead at latitude, L , of 23.45° north of the equator. On the first day of winter (December 21), the sun appears directly overhead at latitude of 23.45° south of the equator. At any other latitude, the altitude, $\alpha=90^\circ-[L-\delta]$ when the sun is directly south, (or north) i.e., at solar noon. At solar noon, the sun is directly south for $L>d$ and directly north for $L<d$. Note that if L is negative, it refers to the southern hemisphere. Several important formulas for determining the position of the sun (Messenger and Ventre 2004; Markvart 1994) include the following, where n is the day of the year with January 1 being day 1:

$$\delta = 23.45^\circ \sin \frac{360[n - 80]}{365}, \quad (4)$$

$$\omega = \pm 15^\circ (\text{hours from local solar noon})$$

$$\sin \alpha = \sin \delta \sin L + \cos \delta \cos L \cos \omega, \quad (5)$$

$$\cos \gamma = \frac{\cos \delta \sin \omega}{\cos \alpha}. \quad (6)$$

Solution of Equation 5 through Equation 6 shows that for optimal annual performance of a fixed PV array, it should face directly south and should be tilted at an angle approximately equal to the latitude, L . For best summer performance, the tilt should be at $L-15^\circ$ and for best winter performance, the array should be tilted at an angle of $L+15^\circ$. Although Equation 4 through Equation 6 can be used to predict the location of the sun in the sky at any time on any day at any location, they cannot be used to predict the degree of cloud cover. Cloud cover can only be predicted on a statistical basis for any region, and thus the amount of sunlight available to a collector will also depend upon cloud cover. The measure of available sunlight is the peak sun hour (p_{sh}). If sunlight intensity is measured in kW/m^2 , then if the sunlight intensity is integrated from sunrise to sunset over 1 m^2 of surface, the result will be measured in kWh. If the daily kWh/m is divided by the peak sun intensity, which is defined as 1 kW/m^2 , the resulting units are hours. Note that this hour figure multiplied by 1 kW/m^2 results in the daily kWh/m². Hence, the term peak sun hours, because the p_{sh} is the number of hours the sun would need to shine at peak intensity to produce the daily sunrise to sunset kWh. Obviously the p_{sh} is

also equivalent to kWh/m²/day. For locations in the United States, the National Renewable Energy Laboratory publishes p_{sh} for fixed and single-axis tracking PV arrays at tilts of horizontal, latitude-15°, latitude, latitude+15°, and vertical. NREL also tabulates data for double axis trackers. These tables are extremely useful for determining annual performance of a PV array.

7. SYSTEM CONFIGURATIONS

Figure 5. Illustrates four possible configurations for PV systems. Perhaps the simplest system is that of Figure 6.a, in which the output of the PV module or array is connected directly to a DC load. This configuration is most commonly used with a fan or a water pump, although it is likely that the water pump will also use a linear current booster (LCB) between the array and the pump motor. Operation of the LCB will be explained later. The configuration of Figure 5.b includes a charge controller and storage batteries so the PV array can produce energy during the day that can be used day or night by the load. The charge controller serves a dual function. If the load does not use all the energy produced by the PV array, the charge controller prevents the batteries from overcharge. While flooded lead acid batteries require overcharging about once per month, frequent overcharging shortens the life of the batteries. As the batteries become discharged, the charge controller disconnects the load to prevent the batteries from over discharge. Normally PV systems incorporate deep discharge lead-acid batteries, but the life of these batteries is reduced significantly if they are discharged more than 80%. Modern charge controllers typically begin charging as constant current sources. In the case of a PV system, this simply means that all array current is directed to the batteries. This is called the “bulk” segment of the charge cycle. After the battery voltage reaches the bulk voltage, which is an owner programmable value, as determined by the battery type and the battery temperature, the charging cycle switches to a constant voltage mode, commonly called the absorption mode. During the absorption charge mode, the charge controller maintains the bulk charge voltage for a preprogrammed time, again depending upon manufacturers’ recommendations. During the absorption charge, battery current decreases as the batteries approach full charge. At the end of the absorption charge period, the charging voltage is automatically reduced to the “float” voltage level, where the charging current is reduced to a “trickle” charge. Because quality charge controllers are microprocessor controlled, they have clock circuitry so that they can be programmed to automatically subject the batteries to an “equalization” charge approximately once a month. The equalization mode applies a voltage higher than the bulk voltage for a preset time to purposely overcharge the batteries. This process causes the electrolyte to bubble, which helps to mix the electrolyte as well as to clean the battery plates. Equalization is recommended only for flooded lead-acid batteries. Sealed varieties can be seriously damaged if they are overcharged.

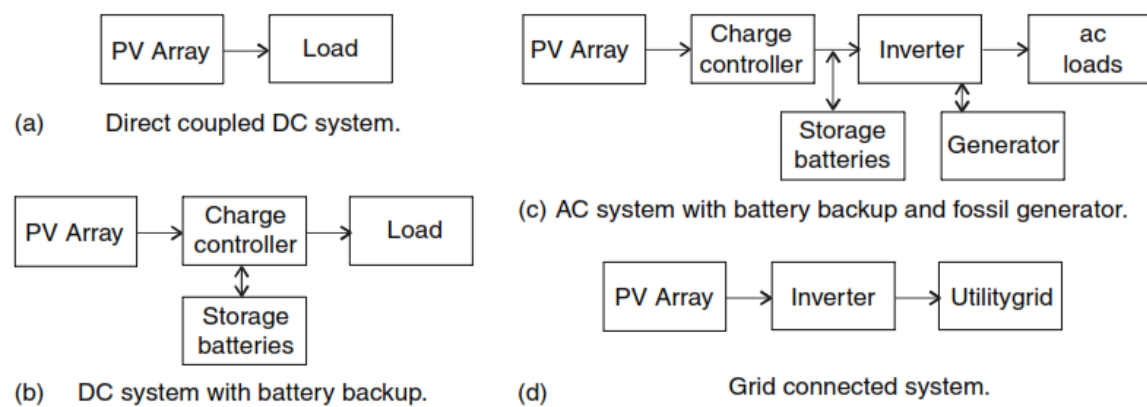


Fig 5: Possible Configuration of PV system

[B] TECHNOLOGY FOR FABRICATION OF PHOTOVOLTAIC DEVICES

Introduction

PV cells are generally made either from crystalline silicon, sliced from ingots or castings, from grown ribbons or thin film, deposited in thin layers on a low-cost backing.

The performance of a solar cell is measured in terms of its efficiency at turning sunlight into electricity. A typical commercial solar cell has an efficiency of 15% about one-sixth of the sunlight striking the cell generates electricity. Improving solar cell efficiencies while holding down the cost per cell is an important goal of the PV industry.

Crystalline silicon technology:

Crystalline silicon cells are made from thin slices cut from a single crystal of silicon (monocrystalline) or from a block of silicon crystals (polycrystalline), [Fig.1], their efficiency ranges between 11% and 19%. This is the most common technology representing about 90% of the market today.

Three main types of crystalline cells can be distinguished:

- Monocrystalline (Mono c-Si)
- Polycrystalline (or Multicrystalline) (multi c-Si)
- Ribbon sheets (ribbon-sheet c-Si)

In the process of converting Solar Light into Electricity, one of the major components used is the Solar Panel. These are the devices which absorb sunlight and thus facilitating any further process. Any cell which is able to convert Sunlight into Electricity is often termed as the Photovoltaic Cell. These types of cells are made with semiconducting materials such as Germanium or Silicon so that they can withstand heat. Normally, most of the current day solar panels are made with Silicon. Then based on the arrangement of these silicon cells, the

solar panels can be further divided into two types -Amorphous and Crystalline. Crystalline Solar Panels are those in which the Photovoltaic cells are arranged in repetitive units while Amorphous Panels are those in which the cells are arranged in a randomized manner. Usually, the efficiency is more in crystalline cells as they have a repeating structure but the amorphous ones are cheaper as you don't have to spend much time and effort in arranging the most renowned and effective Solar Panels are the Crystalline Silicon ones. In these types, a rather pure form of silicon along with high quality crystals has to be used in order to produce maximum efficiency. The structure of Silicon is complex. On the outer surface, it has four electrons and in order to obtain a stable gas configuration, it has to form two bonds with neighboring atoms which it does. Now, when light or heat is applied externally over this configuration, it will break it. So, when sunlight is incident over the Silicon Crystalline solar panel, it will break the stable configuration of the panel resulting in the formation of electron vacancies. The presence of these vacancies give rise to a condition called as Intrinsic Conductivity. It becomes impossible for the electron to conduct electricity in such a condition. So, the vacancy produced in the structure has to be satisfied by mixing it with a suitable material like Boron or Phosphorous which has the structure to satisfy such a condition. If phosphorous is added, the doping (mixing impurities in order to make the material conductive) process is called as n-doping on the other hand, if Boron is added, the process is called as p-doping. The n-doping is more effective than the p-doping. In n-doping, the electron will be allowed to move freely thus creating the ability to transfer charges. But in the p-doping, the vacancy filled will be regenerated in a new place causing further intrinsic conduction. If both the p area and the n area are brought together, the structure will be known as the p-n junction, this junction facilitates the movement of n-ions to the positive and p ions to the negative region forming an electric field in the process. This electric field can be withdrawn and it can be used to power out houses. So, technically this p-n junction is called as the Solar Cell in this case. This junction is arranged repetitively on your rooftops in order to absorb sunlight.

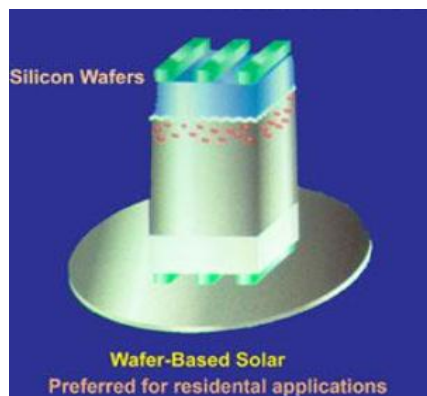


Fig 1: wafer based si-solar cell

Amorphous silicon a-(Si,Ge):H

Amorphous silicon, a-(Si,Ge):H, is the only thin-film technology that already has a substantial market share (15%, Maycock 1999), and it is generally believed to be the first thin-film technology that can compete with x-Si. The discussion on a-(Si,Ge):H will be based on three possible production methods: batch deposition on a glass superstrate, roll-to-roll deposition on a flexible substrate (e.g. steel as done by United Solar; see Yang, 1998; Nath, 1998; Guha,

1997), and roll-to-roll on a temporary superstrate (Helianthos by AKZO-Nobel; see Middelma, 1998; Schropp, 1998). For the evaluation table, the triple junction on a flexible substrate will be used mainly. About 40% of the NOZ-PV solar-cell R&D funding was attributed to a-(Si,Ge):H in 1999.

Thin Film technology:

Thin film modules are constructed by depositing extremely thin layers of photosensitive materials onto a low-cost backing such as glass, stainless steel or plastic [Fig.2]. Thin Film manufacturing processes result in lower production costs compared to the more material-intensive crystalline technology, a price advantage which is counterbalanced by lower efficiency rates (from 4% to 11%). However, this is an average value and all Thin Film technologies do not have the same efficiency. Four types of thin film modules (depending on the active material used) are commercially available at the moment:

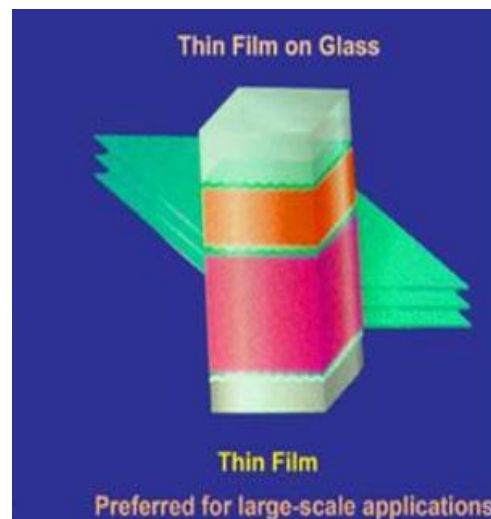


Fig 2: Thin film amorphous silicon solar cell

- Amorphous silicon (a-Si)
- Cadmium telluride (CdTe)
- Copper Indium / gallium Diselenide /disulphide (CIS, CIGS)
- Multi junction cells (a-Si/m-Si)

In 2002, the highest reported efficiency for solar cells based on thin films of CdTe is 18%, which was achieved by research at Sheffield Hallam University, although this has not been confirmed by an external test laboratory. The US national renewable energy research facility NREL achieved an efficiency of 19.9% for the solar cells based on copper indium gallium selenide thin films, also known as CIGS. These CIGS films have been grown by physical vapour deposition in a three-stage co-evaporation process. In this process In, Ga and Se are evaporated in the first step; in the second step it is followed by Cu and Se co-evaporation and in the last step terminated by In, Ga and Se evaporation

again. In 2008, in an article from Scientific American chemist Paul Alivisatos states that, "Newer materials use smaller, cheaper crystals, such as copper-indium-gallium-selenide, that can be shaped into flexible films called thin films. Thin film solar technology, is not as good as silicon in turning light into electricity. Thin-film crystalline silicon (f-Si) covers a broad technological field, which is usually divided in two main routes:

- High-temperature replacement of thick, expensive, silicon by a thin ($< 50\text{ }\mu\text{m}$) silicon film on a low-cost substrate
- Low-temperature the use of micro crystalline silicon $< 5\text{ }\mu\text{m}$ in an amorphous silicon-like or amorphous silicon-based structure.

A lot of research has been done on the high-temperature approach, as it has the potential to result in large-grain material with an efficiency close to that of multicrystalline silicon. The silicon film on substrate can be processed into cells with conventional mc-Si technology. The only film silicon produced on a pilot scale is operated by Astro Power. The low-temperature route results in a microcrystalline silicon film. The technology closely resembles that of amorphous silicon. Tandems are often made with both micro crystalline and amorphous silicon. In particular, the results of the Japanese company Kaneka ($>10\%$) received a lot of attention. In addition, a number of intermediate routes are being developed, based on the growth of large grain material at low temperatures using plasma-assisted, ion-assisted, or liquid-assisted growth. Clearly there are many options for making thin-film silicon, although no favoured approach has been chosen yet. With the reliability and efficiency character of x-Si compared with the nature of f-Si, it is believed that specific thin film developments have a high potential. This could be the reason for the amount of attention given on this technology world-wide. About 15% of the NOZ-PV solar-cell R&D funding was attributed to f-Si in 1999.

Cu(In,Ga)(Se,S)

Although Cu(In,Ga)(Se,S)_2 is not being investigated in the current NOZ-PV programme, it is an important material to incorporate in this evaluation. Many R&D and industry groups worldwide are investigating it. Besides, commercial Cu(In,Ga)(Se,S)_2 modules have entered the market (Siemens Solar shipped 300 kWp in 1999, Maycock, 2000) with top efficiencies of over 11% (Eikelboom, 1999; Karg, 2000). Moreover, with respect to the other technologies currently being developed, Cu(In,Ga)(Se,S)_2 represents an entirely different set of material properties and processing techniques.

CdTe

Like Cu(In,Ga)(Se,S) , CdTe is also not included in the current NOZ-PV programme. In 1999 CdTe was mainly produced for consumer electronics (by Matsushita; with a production of around 1.5 MWp, it constituted less than 1% of the total shipped PV volume, Maycock 1999). Several industries (e.g. BP Solarex, Antec, First Solar; Maycock 1999) have plans to start larger scale CdTe

production for outdoor applications. It is widely accepted that CdTe is a promising thin-film technology. Special attention will be given to the possible toxicity of CdTe with respect to the use of Cd, especially in relation to Dutch legislation.

Dye solar cells and organic solar cells

Actually, organic solar cells are a set of several different technologies, ranging from the wellknown dye-sensitised solar cells (DSC, dye cell) via the antenna cell, and molecular organic solar cells to bulk heterojunction solar cells and completely polymeric devices. Because it is believed that the dye cell is closest to market introduction, this type will be evaluated separately. The other possible organic solar cell concepts will be evaluated in less detail. About 20% of the NOZ-PV solar cell R&D funding was attributed to organic solar cells in 1999.

Comparison of commercial PV

Other cell types

There are several other types of photovoltaic technologies developed today starting to be commercialized or still at the research level, the main ones are:

Concentrated photovoltaic:

Some solar cells are designed to operate with concentrated sunlight. These cells are built into concentrating collectors that use a lens to focus the sunlight onto the cells. The main idea is to use very little of the expensive semiconducting PV material while collecting as much sunlight as possible. Concentrating photovoltaic systems use a large area of lenses or mirrors to focus sunlight on a small area of photovoltaic cells. High concentration means a hundred or more direct sunlight is focused. Most commercial producers are developing systems that concentrate between 400 and 1000 suns. Nearly all concentration systems need a one axis or more often two axis tracking system for high precision, since most systems only use direct sunlight and need to aim at the sun with errors of less than 3 degrees. The primary attraction of CPV systems is their reduced usage of semiconducting material which is expensive and currently in short supply. Additionally, increasing the concentration ratio improves the performance of general photovoltaic materials. Efficiencies are in the range of 20 to 30%. Despite the advantages of CPV technologies their application has been limited by the costs of focusing, sun tracking and cooling equipment.

Flexible cells:

Based on a similar production process to thin film cells, when the active material is deposited in a thin plastic, the cell can be flexible. This opens the

range of applications, especially for Building integration (roofs-tiles) and end-consumer applications

Problems

1. What is the Photovoltaic Effect? How solar light converted to electricity by a solar cell? Describe with schematic diagram.
2. What are the basic components of a photovoltaic system?
3. What are the basic components of a solar cell? Give their requirement in light energy conversion in a solar cell.
4. What is a PV Array? How the modules have to connect to get a high PV Array current?
5. Why sun tacking is necessary in a PV system? What is the declination angle? For high PV efficiency what should be declination angle?
6. What are the main Photovoltaic devices fabrication technologies?
7. Give a brief description about the commercially available thin film technologies.
8. What is concentrated photovoltaic? What is the advantages and disadvantages of a concentrated photovoltaic.

**UNIT-6: SOLAR PHOTOVOLTAIC ENERGY CONVERSION
AND UTILIZATION**

This unit is a sequel to the unit-5 which mainly covers the material aspect of solar photovoltaic conversion. Starting with the basics of solar photovoltaics this unit lays the foundation for its integration with the utilities. Based on the utilities the balance of system requirements are described view of the the specific needs for off-grid and grid-connected systems. Organic PV cells have been discussed to let the reader know the recent developments in the course of development of a low cost new generation cells. The need of electrochemical system in off-grid system makes it pertinent to understand the working dynamics of batteries which is discussed in detail. The primary purpose of a battery is to generate electricity by reaction of chemicals stored inside it. The need to power instruments from toys to satellites are varied. This chapter takes care of this special need.

A: Applications of solar cells in PV power generation systems**Solar Photovoltaic Power System**

The photovoltaic effect is the electrical potential developed between two dissimilar materials when their common junction is illuminated with radiation of photons. The photovoltaic cell, thus, converts light directly into electricity. The PV effect was discovered in 1839 by French physicist Becquerel. It remained in the laboratory until 1954, when Bell Laboratories produced the first silicon solar cell. It soon found application in the U.S. space programs for its high power capacity per unit weight. Since then it has been an important source of power for satellites. Having developed maturity in the space applications, the PV technology is now spreading into the terrestrial applications ranging from powering remote sites to feeding the utility lines.

The PV cell:

The physics of the PV cell is very similar to the classical p-n junction diode Figure.1. When light is absorbed by the junction, the energy of the absorbed photons is transferred to the electron system of the material, resulting in the creation of charge carriers that are separated at the junction. The charge carriers may be electron-ion pairs in a liquid electrolyte, or electron hole pairs in a solid semiconducting material. The charge carriers in the junction region create a potential gradient, get accelerated under the electric field and circulate as the current through an external circuit. The current squared times the resistance of the circuit is the power converted into electricity. The remaining power of the photon elevates the temperature of the cell. The origin of the photovoltaic potential is the difference in the chemical potential, called the Fermi level, of the electrons in the two isolated materials. When they are joined, the junction approaches a new thermodynamic equilibrium. Such equilibrium can be achieved only when the Fermi level is equal in the two materials. This occurs by the flow of electrons from one material to the other until a voltage difference is

established between the two materials which have the potential just equal to the initial difference of the Fermi level. This potential drives the photocurrent.

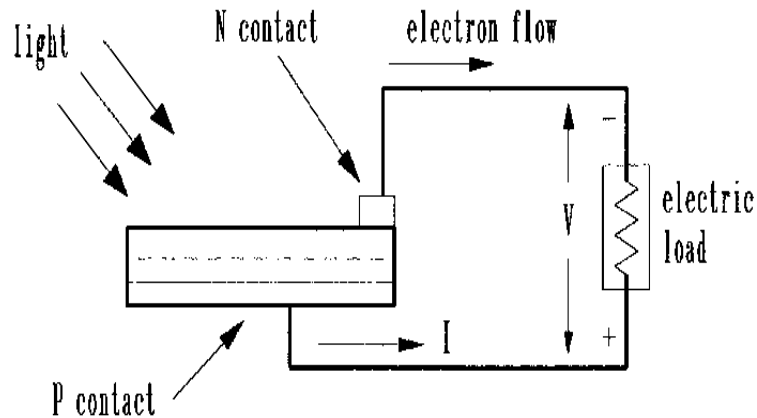


Figure.1: Photovoltaic effect converts the photon energy into voltage across the p-n junction.[2]

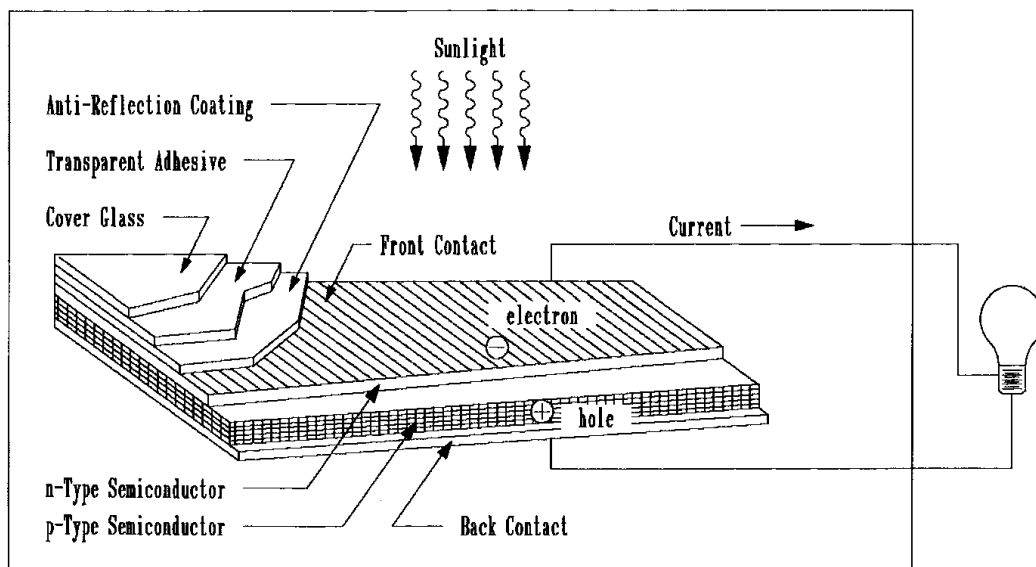


Figure.2: Basic construction of PV cell with performance enhancing features (current collecting mesh, anti-reflective coating and cover glass protection).[2]

Figure.2 shows the basic cell construction. For collecting the photocurrent, the metallic contacts are provided on both sides of the junction to collect electrical current induced by the impinging photons on one side. Conducting foil (solder) contact is provided over the bottom (dark) surface and on one edge of the top (illuminated) surface. Thin conducting mesh on the remaining top surface collects the current and lets the light through. The spacing of the conducting fibers in the mesh is a matter of compromise between maximizing the electrical conductance and minimizing the blockage of the light. In addition to the basic elements, several enhancement features are also included in the construction. For example, the front face of the cell has anti-reflective coating to absorb as much light as possible by minimizing the reflection. The mechanical protection is provided by the cover-glass applied with a transparent adhesive.

PV System Components:

The array by itself does not constitute the pv power system. We must also have a structure to mount it, point to the sun, and the components that accept the DC power produced by the array and condition the power in the form that is usable by the load. If the load is AC, the system needs an inverter to convert the DC power into AC, generally at 50 or 60 Hz.

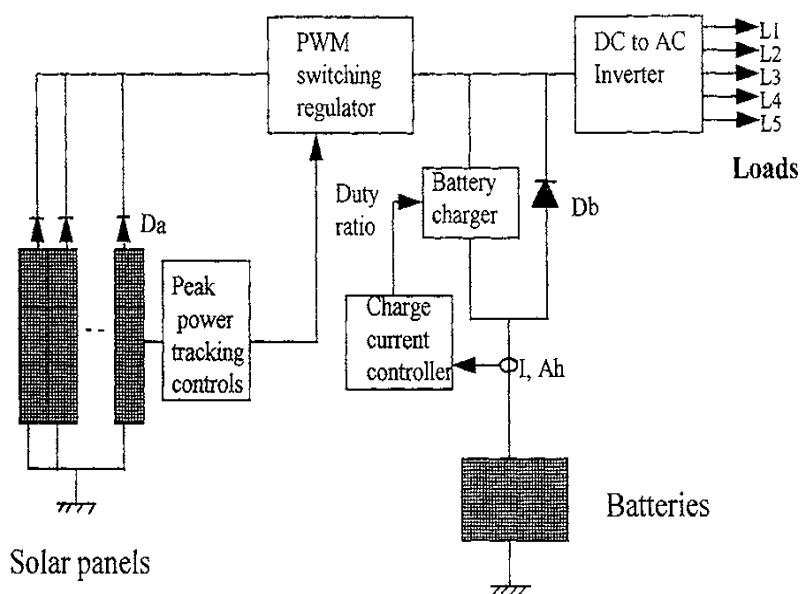


Figure.3: Photovoltaic power system showing major components[2]

Figure.3 shows the necessary components of a stand-alone PV power system. The peak power tracker senses the voltage and current outputs of the array and continuously adjusts the operating point to extract the maximum power under the given climatic conditions. The output of the array goes to the inverter, which converts the DC into AC. The array output in excess of the load requirement is used to charge the battery. The battery charger is usually a DC-DC buck converter. If excess power is still available after fully charging the battery, it is shunted in dump heaters, which may be space or room heaters in a stand-alone system. When the sun is not available, the battery discharges to the inverter to power the loads. The battery discharge diode D_b is to prevent the battery from being charged when the charger is opened after a full charge or for other reasons. The array diode is to isolate the array from the battery, thus keeping the array from acting as load on the battery at night. The mode controller collects the system signals, such as the array and the battery currents and voltages, keeps track of the battery state of charge by book keeping the charge/discharge ampere-hours, and commands the charger, discharge converter, and dump heaters on or off as needed. The mode controller is the central controller for the entire system. In the grid-connected system, dump heaters are not required, as all excess power is fed to the grid lines. The battery is also eliminated, except for small critical loads, such as the start up controls and the computers. The DC power is first converted into AC by the inverter, ripples are filtered and then only the filtered power is fed into the grid lines.

For PV applications, the inverter is a critical component, which converts the array DC power into AC for supplying the loads or interfacing with the grid. A new product recently being introduced into the market is the AC-PV modules, which integrates an inverter directly in the module, and is presently available in a few hundred watts capacity. It provides utility grade 60Hz power directly from the module junction box. This greatly simplifies the PV system design.

Photovoltaic cells and systems have a wide variety of application:

- space (e.g. satellites and space stations)
- navigational aids and warning devices (e.g. coded light beacons)
- telecommunications (e.g. microwave repeater stations, remote area radio telephones, emergency call boxes)
- railway crossing, road and emergency signage
- cathodic protection (e.g. corrosion prevention for pipe lines)
- consumer products requiring less than 10 mW (e.g. calculators and watches)
- battery charging (e.g. boats, campervans, lights, power systems of all types and even cars)
- educational (e.g. TV in developing countries)
- refrigeration (e.g. for medicines and vaccines in remote areas)
- water pumping (e.g. for irrigation and domestic water supplies)
- water purification, an increasingly important application in both developing and industrialised countries
- solar powered vehicles (e.g. golf carts, solar cars, boats on reservoirs where petroleum products and noisy motors are restricted)
- lighting (e.g. billboards, street and garden lights, security lighting, emergency warning lights)
- remote monitoring (e.g. weather, pollution, highway conditions, water quality, river heights and flow rates)
- remote meter reading
- gas flow metering
- direct drive applications (e.g. ventilation fans, toys)
- electric fences (e.g. to keep dingos and kangaroos out or stock in) remote gates
- remote community power supplies
- remote homestead and household power supplies (usually in a hybrid system)
- power for residential or commercial use where there is grid connection
- power for sectionalising switches along remote sections of electricity grids
- ‘distributed photovoltaics’—numerous appropriately-sized arrays feeding into distribution power grids at dispersed sites
- central power plants.

Off-grid systems (Stand-Alone System):

The major application of the stand-alone power system is in remote areas where utility lines are uneconomical to install due to terrain, the right-of way difficulties or the environmental concerns. Even without these constraints, building new transmission lines is expensive. A 230 kV line costs about \$1 million per mile. For remote villages farther than two miles from the nearest transmission line, a stand-alone system could be more economical.

The solar power outputs can fluctuate on an hourly or daily basis. The stand-alone system must, therefore, have some means of storing energy, which can be used later to supply the load during the periods of low or no power output. Alternatively, the PV can also be with diesel engine generator in remote areas or with fuel cells in urban areas.

The typical PV stand-alone system consists of a solar array and a battery connection as shown in Figure.4. The array powers the load and charges the battery during daytime. The battery powers the load after dark. The inverter converts the DC power of the array and the battery into 60 or 50 Hz power. Inverters are available in a wide range of power ratings with efficiency ranging from 85 to 95 percent. The array is segmented with isolation diodes for improving the reliability. In such designs, if one string of the solar array fails, it does not load or short the remaining strings. Multiple inverters, such as three inverters each with 35 percent rating rather than one with 105 percent rating, are preferred. If one such inverter fails, the remaining two can continue supplying essential loads until the failed one is repaired or replaced. The same design approach also extends in using multiple batteries. Most of the stand-alone PV systems installed in developing countries provide basic necessities, such as lighting and pumping water.

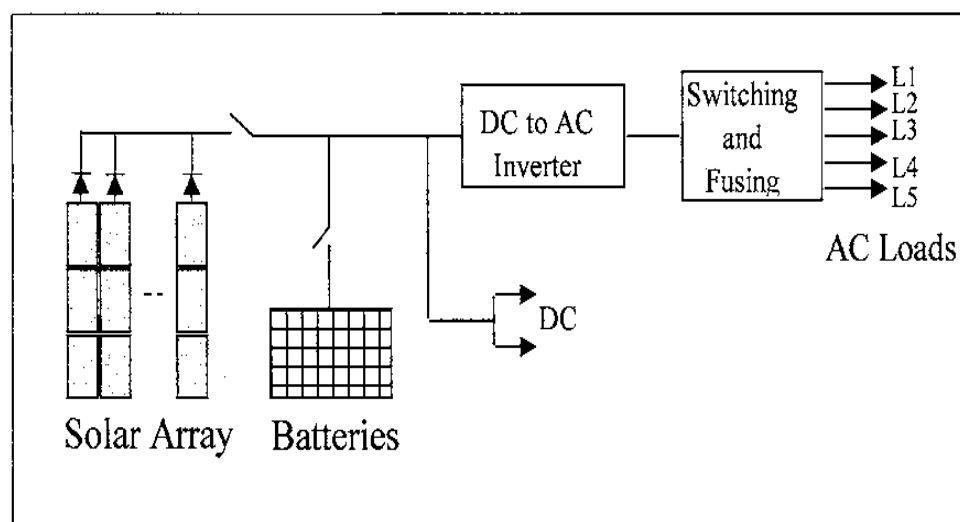


Figure.4: Photovoltaic stand-alone power system with battery[2]

Grid connected systems:

The photovoltaic power systems have made a successful transition from small stand-alone sites to large grid-connected systems. The utility interconnection brings a new dimension in the renewable power economy by pooling the temporal excess or the shortfall in the renewable power with the connecting grid. This improves the overall economy and the load availability of the renewable plant; the two important factors of any power system. The grid supplies power to the site loads when needed, or absorbs the excess power from the site when available. One kWh meter is used to record the power delivered to the grid, and another kWh meter is used to record the power drawn from the grid. The two meters are generally priced differently.

Figure.5 is a typical circuit diagram of the grid-connected photovoltaic power system. It interfaces with the local utility lines at the output side of the inverter as shown. A battery is often added to meet short term load peaks. In recent years, large building-integrated photovoltaic installations have made significant advances by adding the grid-interconnection in the system design.

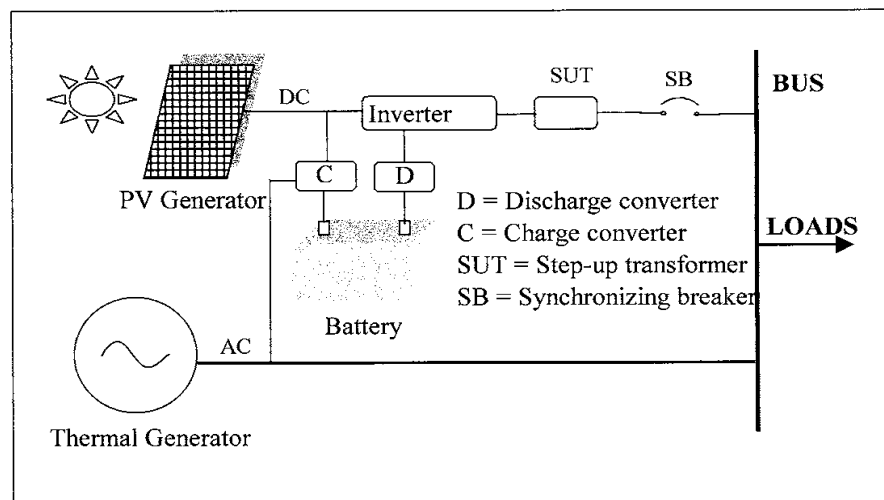


Figure.5: Electrical schematic of the grid-connected photovoltaic system[2]

Synchronizing with Grid:

The synchronizing breaker in Figures.6 has internal voltage and phase angle sensors to monitor the site and grid voltages and signal the correct instant for closing the breaker. As a part of the automatic protection circuit, any attempt to close the breaker at an incorrect instant is rejected by the breaker. Four conditions which must be satisfied before the synchronizing switch will permit the closure are as follows:

- the frequency must be as close as possible with the grid frequency, preferably about one-third of a hertz higher.
- the terminal voltage magnitude must match with that of the grid, preferably a few percent higher.
- the phase sequence of the two three-phase voltages must be the same.
- the phase angle between the two voltages must be within 5 degrees.

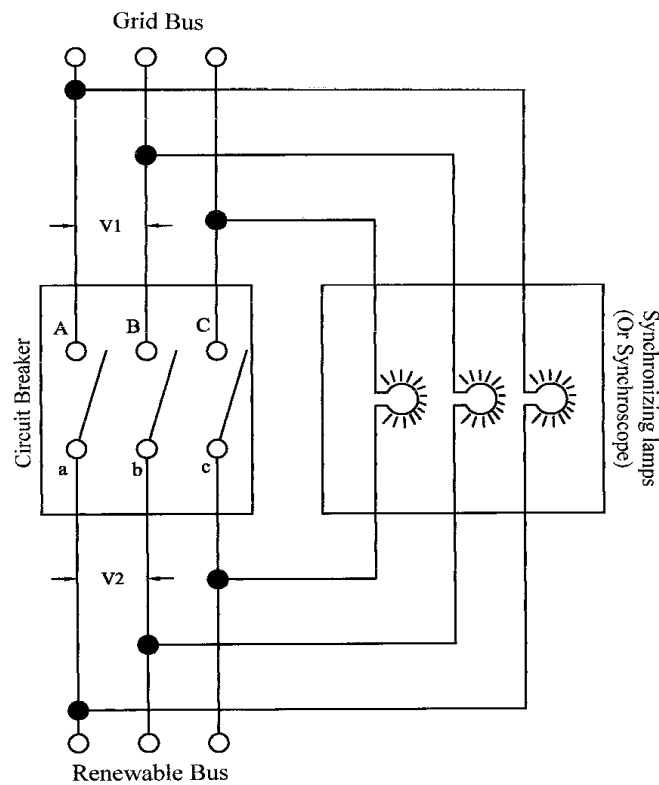


Figure.6: Synchronizing circuit using three synchronizing lamps or the synchroscope.[2]

B: ORGANIC PHOTOVOLTAIC SOLAR CELL

Introduction

Enthusiasm for solar cell technology originates from its superior viability as an energy source. Society is finally starting to acknowledge the environmental damage inflicted by the current usage of nonrenewable energy sources. Former vice president Al Gore, who has been leading a global warming awareness campaign, has been nominated for the 2007 Nobel Peace Prize. The knowledge that energy needs will only increase leads researchers and investors to explore innovative, environmentally friendly energy sources such as wind turbines, biogas, and solar cells. Nanotechnology-based “cleantech,” as the science of environmentally responsible energy sources has been dubbed, is expected to be one of the largest sinks for venture capital in the coming decade.

Solar cells are an exciting clean tech technology. Analyses of clean tech efforts to reduce or eliminate use of nonrenewable energy sources such as coal and oil indicate that photovoltaic energy converters are more reasonable than wind turbines and biofuels. Unlike wind turbines, solar cells employ no moving parts. Such solid-state devices are noiseless, don’t interfere with flight paths as wind turbines do, and require almost no maintenance once installed. To power society in the future, biofuels would require more arable land than is currently available (unless far more efficient fuel-driven technologies are invented). The lower power density of biofuels requires three to four orders of magnitude more land area than oil fields for equal power production. The environmental and

socioeconomic damage from displacement of natural crops with biofuel crops and fertilizer runoff pollution could be worse than the consequences of using nonrenewable energy. The most productive solar alternative is Brazilian ethanol from sugar cane, at $0.45\text{W}/\text{m}^2$. Corn ethanol only has a power density of only $0.22\text{W}/\text{m}^2$. To provide the amount of power the United States consumed in the beginning of this century for fueled transportation alone, an area of land equal to all of the United States' arable land would have to be replaced with sugar cane, or twice the United States' total arable land would have to be utilized for corn ethanol production (12 Gha). Of course, the growing conditions in the U.S. aren't as fertile and insolated as in Brazil; biofuel crops would be grown around equator zones. Based on lessons learned in the past, it is best to supply our energy from within the borders of our countries to reduce such a fundamental dependency on other nations. If the U.S. relied instead on solar energy, without disturbing current arable land, unutilized insolated areas such as roof tops and deserts could provide all the U.S.'s power needs. Global power consumption by the year 2050 is estimated to be 30TW; the sun provides earth with 89,000TW at the surface. All the U.S.'s energy needs could be provided by installing the common commercial 15% efficient solar cells into the unused desert areas of Nevada.

By these figures, one might deduce that the ultimate advantage of solar cells amongst other clean tech options is that solar energy is solely capable of providing all human society's energy needs (if we are to eventually convert to 100% renewable energy) Wind turbines and biofuels could not provide global energy needs without serious environmental impact (such as displacing all of our cities and arable land with biofuel crops). Solar cells remain too expensive to commercially replace other technologies except in the cases where they are greatly subsidized (as in California). Solar cells today span three generations of technology. First generation solar cells are those seen as flat silicon panels on rooftops; these comprise 87% of the current solar cell market today. First generation solar cells operate using a single P-N junction. Second generation solar cells operate using multiple (tandem) P-N junctions that cover a wider spectrum for better efficiencies; but because of the high cost of these additional photolithographic steps, the first generation technology remains more practical when weighing both efficiency and cost. Finally, everything else that does not rely on P-N junctions is (at least for the time being) considered third generation solar cell technology. This includes photoelectrochemical cells, polymer cells, and nanocrystalline material cells. All three could be organic solar cells.

Having set the case for solar cells, it can be postulated that amongst solar cell technologies, organic solar cells (a member of the 3 generation solar cell class) have the potential to supersede the current inorganic semiconductor solar cells, and hence become the most important source of power for society by the end of this century. This may seem counterintuitive since the best production-scale organic solar cell ($\eta=3\%$) is still four times less efficient than the cost-effective inorganic cell used for 87% of rooftop applications ($\eta=12\%$). The best performer of current solar cell technology, rated at nearly 41% efficiency, is

based on first-generation, photolithography-intensive, clean room fabricated inorganic semiconductor heterostructures. These heterostructures are made from silicon to take advantage of the existing silicon-CMOS infrastructure for cost savings and throughput. Silicon, being the second most abundant element (after oxygen) in the earth's crust, would seem to be the ideal material for solar cells; however, the electronic grade silicon wafer substrate necessary for fabricating inorganic solar cells is expensive. The optimism and investment in organic materials research is due to the unique properties of organic materials. These include the potential for self-assembling nanostructures, resulting in cost effective fabrication and high structural efficiency, and the ability to be fabricated in thin, flexible films. Organic films can be printed onto flexible sheet rolls. This allows organic solar cells, unlike the current inorganic solar cells, to be commercially printed without need for expensive clean room environments and lithographic tools. Additionally, such thin films require less material. In addition to reducing material costs, this ensures that there is enough Indium (In) and other rarer materials to meet the world's energy needs using organic solar cells. (As will be discussed in the Device Design and Fabrication section, Indium is one of the most common organic solar cell ingredients.) For perspective, Indium is about as abundant as silver. Researchers at Stanford's February 24th Solar Cell workshop working with inorganics claim that Indium is in too short of a supply to build enough organic solar cells to meet society's energy needs. Researchers working with organics claim that there is enough Indium provided we use thin film or alternate organic cell technologies.

Operation Principles

General operation principles for organic solar cells

The following operation principles apply to most organic solar cells. Photons (sunlight) must be absorbed in the active region of the device. Other regions of the device facing insolation must be transparent; this can be accomplished by use of a transparent substrate (usually glass) and a diffuse cathode matrix to allow sunlight to penetrate into the active region. The external quantum efficiency, η_{EQE} (1), is this ability to couple light into the active region, and is affected by the reflectivity of the layers adjacent to the active region R and the internal quantum efficiency

$$\eta_{EQE} = (1 - R) \eta_{IQE} \quad (1)$$

The active region must efficiently absorb photons (maximize absorption efficiency, η), generating photocurrent when an electron-hole exciton pair are broken apart between P and N type materials (exciton dissociation efficiency = η). The diffusion lengths of excitons are short, on the order of 10-30 nanometers. Therefore it is important for the bulk heterostructure material to consist of nanostructures that, in addition to increasing the surface area between P and N regions, provide conductive channels every 10-30 nanometers (maximizing exciton diffusion efficiency, η_{EDCT} , to a dissociation site). This can be accomplished, for example, by extremely conductive nanorods (increasing charge collection efficiency, η). With bandgap matching coatings, nanorods can provide both current transport mechanism and donor material

interfacing with an acceptor fill matrix. The cumulative internal quantum efficiency of the solar cell, η_{CC} , (2) is given in terms of the absorption efficiency of light within the active region of the solar cell (η_{IQE}), the exciton diffusion efficiency to a dissociation site (η), the charge transfer efficiency (efficiency of dissociation of an exciton into a free electron and hole pair, η_{ED}), and the charge collection efficiency

$$\eta_{IQE} = \eta_A \eta_{ED} \eta_{CT} \eta_{CC} \quad (2)$$

The power conversion efficiency, η (3), is given by the fill factor (FF), open circuit voltage (V_{OC}), the short circuit current density (I), and the incident power density (P).

$$\eta_P = \frac{V_{OC} J_{sc} FF}{P_{INC}} \quad (3)$$

A process called “photodoping” can enhance the charge transfer efficiency. Molecules such as buckminsterfullerene (a.k.a. buckyballs/C) increase photocurrent with increasing light intensity (Fig.1). This enhancement is best used with light concentrators to maximize this effect while reducing expensive chip area.

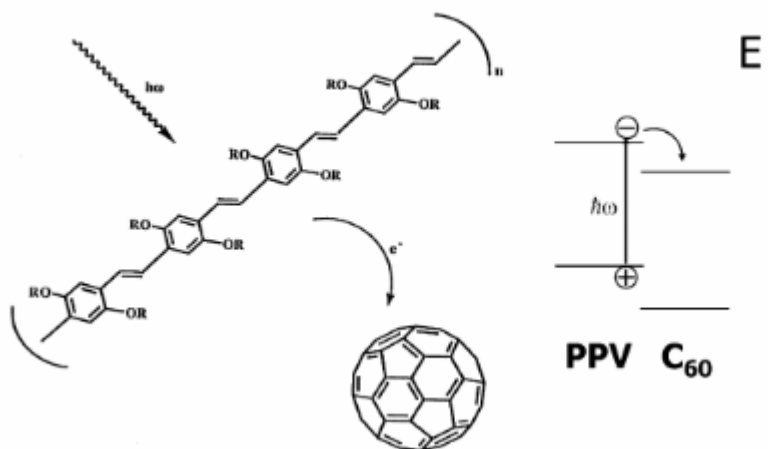


Fig 1: Illustration of photoinduced charge transfer (left) with sketch of energy level scheme (right)

Current Challenges

It was stated earlier that organic solar cell technology could supersede first and second generation solar cells (inorganic/ PN junction based technologies). However, in the current state, inorganic technology outperforms organics; the best efficiencies for commercial production organic and inorganic cells are 3% and 12%, respectively. In fact, organic solar cell technology was dormant for the first 30 years; only with recent advances during the last decade in nanoscience has it become interesting. Fundamentally, organics make excellent

absorbers (usually two orders of magnitude more absorption than inorganic counterparts) that are hindered by poor current transport. Therefore, the most critical research advances will be concerning current transport and cost effective fabrication before organic solar cells become competitive functionally and economically.

Current Collection and Transport

Current transport is the primary weakness of organic materials. New nanostructures are in development to alleviate this. As described in the Operation Principles section, current transport relies on organic bonds. This can be enhanced by “photodoping” with molecules that increase photocurrent with increasing light intensity. These are best used with light concentrators to maximize this effect while reducing expensive chip area. Additionally, the splitting of excitons by incident light to generate current (electron/hole pairs split into independent current carriers) is the primary mechanism of energy transfer from light to electricity. The excitons must be harvested within a diffusion length or they will recombine before any useful current can be extracted. These diffusion lengths are extremely short and so devices must have an exciton generation site, which can be formed by the interface between a p and n type material, every ten or twenty nanometers. Such a low-dimensional material interface structure is critical to current collection efficiency. Researchers are using nanostructured materials to accomplish such high surface area between P and N type bulk heterojunctions.

In addition to current collection, high-surface area bulk heterojunctions can be tailored to enhance conduction of the collected current to device anodes/cathodes. Conduction in organic materials relies is limited by distributed pi bonds. To increase transport to the anode and cathode, inherently conductive nanostructures are being explored, such as nanorods. These aligned structures conduct excellently, decreasing resistive losses and boosting efficiency. Disordered structures such as nanoporous materials provide less direct and therefore more resistive current paths, but can be filled with complementary polymers to achieve high-surface area P-N heterojunctions without as much processing complexity.

Cost effective processing

Silicon-based CMOS has garnered over 90% percent of today’s semiconductor market (up from 50% in 1980) because although electronic-grade silicon and other materials are very expensive, monolithically integrated device processing has become refined and high-throughput. There is enormous infrastructure build upon silicon-CMOS processing, including chip fabrication plants, design tools, and research. Organic solar cell devices generally cannot take advantage of the cost and throughput advantages of this mainstream fabrication. Organic solar cells often require materials incompatible with silicon-

CMOS processing. These materials are either banned in silicon-CMOS processing areas due to threat of contamination, or require unique processing due to nanostructure designs. This usually includes processing steps to fabricate and incorporate nanostructures such as nanorods, nanoporous materials, or nanocrystals. Screen printing methods promise to fulfill both high-volume production and cost requirements .

Device Design and Fabrication

Organic Solar Cell Design Overview

Organic solar cells can be generally described in five layers as shown in Fig.2. The first layer, the solar cell substrate, can be made of a heat-resistant transparent substrate such as glass, or flexible materials such as polyester. Whereas conventional solar cells allow light to enter through a conductive grid anode on

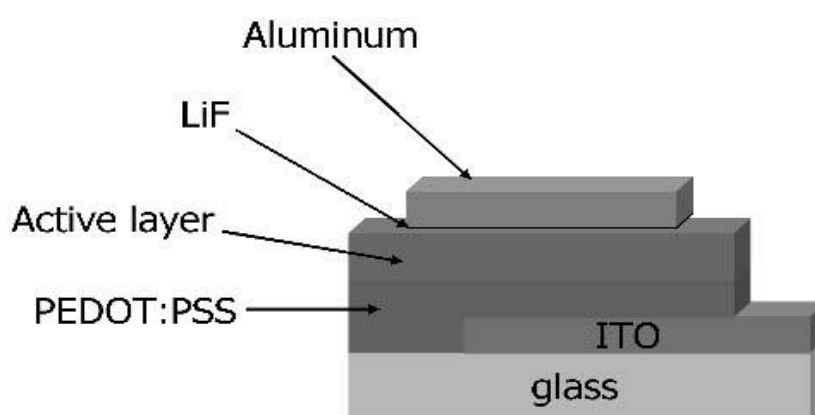


Fig 2: Design of a organic solar cell

the opposite end as the substrate, organic devices generally admit light through a transparent substrate top layer coated with Indium Tin Oxide (ITO), for example, which forms the cathode and second layer. ITO is a commercially available glass coating and is widely used as the conductive electrode second layer of organic solar cells because of its transparency in thin films and carrier injection properties that can be enhanced using film treatments. ITO allows for carrier injection into the organic layer of the solar cell. After deposition, oxygen plasma treatment using RF or microwave sources is one of the most effective methods to effectively increase the ITO work function, which allows an increase in hole injection between ITO and the hole transport layer (HTL). One of the challenges for researchers today is to quantitatively understand the effect of the plasma electrons and oxygen ions effect on the electrode-organic layer interface electronic properties.

Between the cathode material and active layer, a layer of poly (3, 4 ethylenedioxythiophene)-poly (styrenesulfonate) (PEDOT-PSS) can be deposited to form the third layer. PEDOT-PSS forms a hole transporting, exciton-blocking, and smoothing layer. Additionally it prevents oxygen and cathode material from diffusing into the active region. Any unwanted material in

the active region could form device degrading trap sites. The fourth layer of organic solar cells is a donor/acceptor-blend active layer. A dye-sensitized solar cell (DSSC) could be chosen to exemplify organic solar cell active layer structure because it is currently the most efficient and stable excitonic solar cell. Other types of organic solar cells, including organic and hybrid organic-inorganic types, use the same general device structure but with a different active layer scheme. Active layers usually employ some sort of nanomaterial to maximize surface area between donor and acceptor regions; nanoporous materials, nanocrystals, and aligned nano rods are all variations to suit this purpose. All variations have been attempted by many researchers and can be tuned for different enhancements. A LiF layer is deposited to make a good metallic contact. After this layer, the anodic fifth layer is deposited. The anode can be made from any conducting material; aluminum, gold, silver, and even calcium can be employed. In practice, a layer of lithium fluoride can serve as a protective barrier between the active and anodic layers.

Current Fabrication Techniques

The most economically promising way to fabricate organic solar cells is screen printing. Silicon Valley startup companies such as Nanosolar have popularized this technique by demonstrating the high throughput and cost savings benefits of printing devices roll-to roll. Screen printing utilizes wetprocessing rather than traditional deposition/photolithography. Other wetprocessing techniques include any solution processing. Organic molecules, monomers or polymers, must often be processed in solvent. Unlike other wetprocessing techniques such as doctor-blading, inkjet printing, and spin-coating, screenprinting allows cost savings by tapping into existing printing infrastructure. Wetprocessing is important to organic treatment because the active layers of organic devices are usually made of large molecules that cannot be deposited by vacuum deposition (as in traditional monolithically fabricated solar cell production). However, this is not a disadvantage. Unlike silicon-CMOS processing that is used to make the existing, inorganic semiconductor solar cells, organic solar cells which can be fabricated by printing techniques do not require expensive vacuum-environments, depositions, various lithography steps, high heat environments, and other energy expensive steps. The reduced amount of energy necessary to produce inorganic solar cells decreases the amount of time inorganic solar cells must be used before installation costs and production energy usages are recouped.

Applications

Flexible screen printed devices can be laid over large surface areas. They are durable and because they are printed in mass using cheaper materials and processing, low efficiency could be compensated for by inexpensively increasing light collection area. Lithographically produced devices can be used with concentrators to increase efficiency. Concentrators have a twofold function: to reduce the necessary area of solar cells, which are far more expensive than

plastic light condensers, and to boost efficiency. Efficiency of organic solar cells can be boosted by increasing light intensity with condensers due to a photodoping effect. For example, buckminsterfullerene (C_{60}), mixed with other organic materials, will increase photoconductivity when illuminated. The more concentrated the light that reaches the solar cell, the better the quantum efficiency due to this effect. Therefore, concentrators can help reduce the overall cost and increase efficiency (and can also be applied to inorganic solar cells).

C: ELECTROCHEMICAL ENERGY STORAGE BATTERIES

Introduction:

Electricity is more versatile in use because it is a highly ordered form of energy that can be converted efficiently into other forms. For example, it can be converted into mechanical form with efficiency near 100 percent or into heat with 100 percent efficiency. The heat energy, on the other hand, cannot be converted into electricity with high efficiency, because it is a disordered form of energy in atoms. For this reason, the overall thermal to electrical conversion efficiency of a typical fossil thermal power plant is under 40 percent.

A disadvantage of electricity is that it cannot be easily stored on a large scale. Almost all electrical energy used today is consumed as it is generated. This poses no hardship in conventional power plants, where the fuel consumption is varied with the load requirements. The photovoltaic and wind, being intermittent sources of power, cannot meet the load demand all of the time, 24 hours a day, 365 days of the year. The energy storage, therefore, is a desired feature to incorporate with power systems, which significantly improve the load availability, a key requirement for any power system.

The present and future energy storage technology, has considered electrochemical battery as the most widely used device for energy storage in a variety of applications.

Batteries:

The battery stores energy in the electrochemical form, and is the most widely used device for energy storage in a variety of applications. The electrochemical energy is a semi-ordered form of energy, which is in between the electrical and thermal forms. It has one-way conversion efficiency of 85 to 90 percent. A battery is a device that converts the chemical energy contained in its active materials directly into electric energy by means of an electrochemical oxidation-reduction (redox) reaction. In the case of a rechargeable system, the battery is recharged by a reversal of the process. This type of reaction involves the transfer of electrons from one material to another through an electric circuit. In a non-electrochemical redox reaction, such as rusting or burning, the transfer of electrons occurs directly and only heat is involved. As the battery electrochemically converts chemical energy into electric energy, it is not subject,

as are combustion or heat engines, to the limitations of the Carnot cycle dictated by the second law of thermodynamics. Batteries, therefore, are capable of having higher energy conversion efficiencies.

While the term “battery” is often used, the basic electrochemical unit being referred to is the “cell.” A battery consists of one or more of these cells, connected in series or parallel, or both, depending on the desired output voltage and capacity.

The cell consists of three major components:

1. The anode or negative electrode—the reducing or fuel electrode—which gives up electrons to the external circuit and is oxidized during the electrochemical reaction.
2. The cathode or positive electrode—the oxidizing electrode—which accepts electrons from the external circuit and is reduced during the electrochemical reaction.
3. The electrolyte—the ionic conductor—which provides the medium for transfer of charge, as ions, inside the cell between the anode and cathode. The electrolyte is typically a liquid, such as water or other solvents, with dissolved salts, acids, or alkalis to impart ionic conductivity. Some batteries use solid electrolytes, which are ionic conductors at the operating temperature of the cell.

The most advantageous combinations of anode and cathode materials are those that will be lightest and give a high cell voltage and capacity. Such combinations may not always be practical, however, due to reactivity with other cell components, polarization, difficulty in handling, high cost, and other deficiencies.

Classification of Batteries:

Depending on their capability of being electrically recharged electrochemical batteries are classified as:

- the primary battery, which converts the chemical energy into the electrical energy. The electrochemical reaction in the primary battery is non-reversible, and the battery after discharge is discarded. For this reason, it finds applications where high energy density for one time use is needed.
- the secondary battery, which is also known as the rechargeable battery. The electrochemical reaction in the secondary battery is reversible. After a discharge, it can be recharged by injecting direct current from an external source. This type of battery converts the chemical energy into electrical energy in the discharge mode. In the charge mode, it converts the electrical energy into chemical energy. In both the charge and the discharge modes, a small fraction of energy is converted into heat, which is dissipated to the surrounding medium.

The round trip conversion efficiency is between 70 and 80 percent.

- the reserve battery, which is used to meet extremely long or environmentally severe storage requirements that cannot be met with an active battery designed for the same performance characteristics. These batteries are used, for example, to deliver high power for relatively short periods of time, in missiles, and other weapon systems.

Operation of Batteries:

Discharge

The operation of a battery during discharge is also shown schematically in Fig. 1. When the cell is connected to an external load, electrons flow from the anode, which is oxidized, through the external load to the cathode, where the electrons are accepted and the cathode material is reduced. The electric circuit is completed in the electrolyte by the flow of anions (negative ions) and cations (positive ions) to the anode and cathode, respectively.

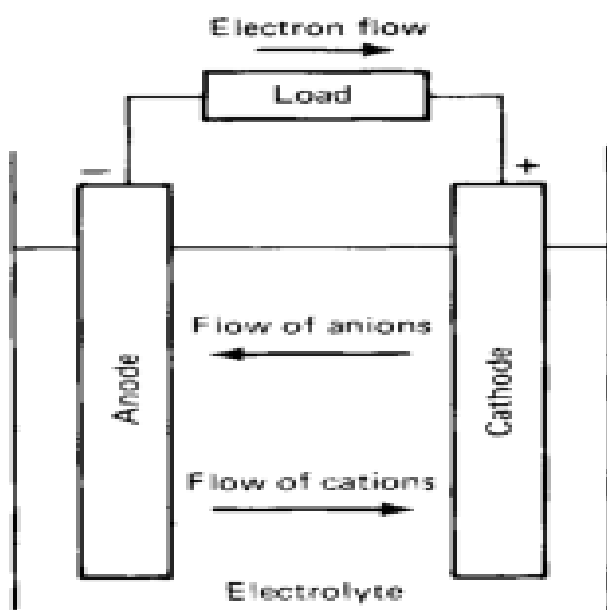
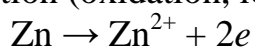


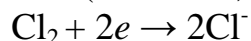
Figure.1: Electrochemical operation of a cell (discharge).[2]

The discharge reaction can be written, assuming a metal as the anode material and a cathode material such as chlorine (Cl_2), as follows:

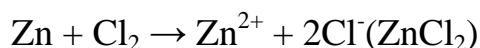
Negative electrode: anodic reaction (oxidation, loss of electrons)



Positive electrode: cathodic reaction (reduction, gain of electrons)



Overall reaction (discharge):

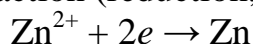


Charge

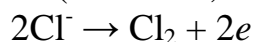
During the recharge of a rechargeable or storage battery, the current flow is reversed and oxidation takes place at the positive electrode and reduction at the negative electrode, as shown in Fig.2. As the anode is, by definition, the

electrode at which oxidation occurs and the cathode the one where reduction takes place, the positive electrode is now the anode and the negative the cathode. In the example of the Zn/ Cl₂ cell, the reaction on charge can be written as follows:

Negative electrode: cathodic reaction (reduction, gain of electrons)



Positive electrode: anodic reaction (oxidation, loss of electrons)



Overall reaction (charge):

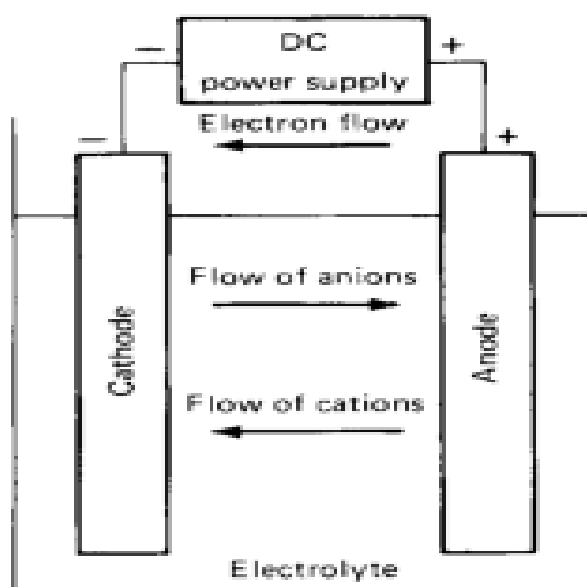
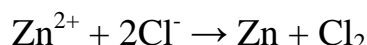


Figure.2: Electrochemical operation of a battery (charge).[2]

Types of Batteries:

Major types of batteries available today are as follows:

- lead-acid (Pb-acid).
- nickel-cadmium (NiCd).
- nickel-metal hydride (NiMH).
- lithium-ion (Li-ion).
- lithium-polymer (Li-poly).
- zinc-air.

New types of Batteries are being developed for a variety of applications, such as electric vehicles, spacecraft, utility load levelling, of course, for renewable power systems.

The average voltage during discharge depends on the electrochemistry, as listed in Table 1. The selection of the electrochemistry for a given application is a matter of performance and cost optimization. In Fig.3. Specific energy and energy density of various electro-chemistries is shown.

TABLE 1

Average Cell Voltage During Discharge in Various Rechargeable Batteries

Electrochemistry	Cell Voltage	Remark
Lead-acid	2.0	Least cost technology
Nickel-cadmium	1.2	Exhibits memory effect
Nickel-metal hydride	1.2	Temperature sensitive
Lithium-ion	3.4	Safe, contains no metallic lithium
Lithium-polymer	3.0	Contains metallic lithium
Zinc-air	1.2	Requires good air management to limit Self-discharge rate

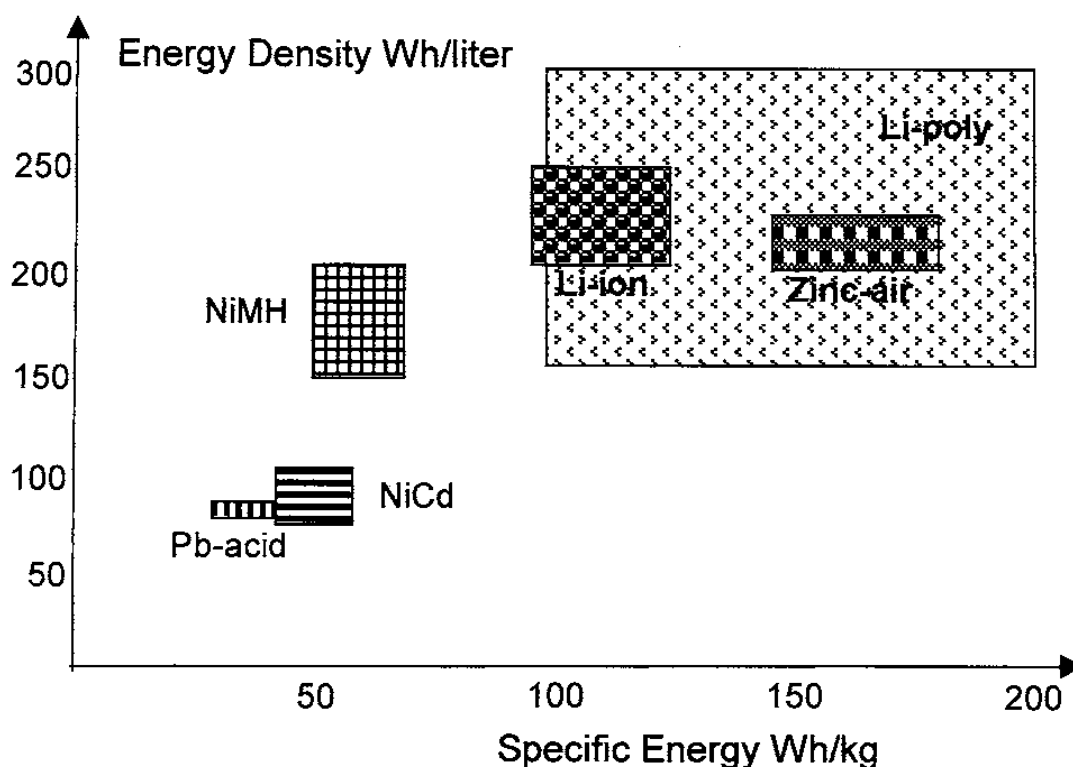


Figure.3: Specific energy and energy density of various electro-chemistries[1]

Lead-Acid:

This is the most common type of rechargeable battery used today because of its maturity and high performance over cost ratio, even though it has the least energy density by weight and volume. In the lead-acid battery under discharge, water and lead sulfate are formed, the water dilutes the sulphuric acid electrolyte, and the specific gravity of the electrolyte decreases with the

decreasing state of charge. The recharging reverses the reaction in the lead and lead dioxide is formed at the negative and positive plates, respectively, restoring the battery into its originally charged state. The lead-acid battery comes in various versions. The shallow-cycle version is used in automobiles where a short burst of energy is drawn from the battery when needed. The deep-cycle version, on the other hand, is suitable for repeated full charge and discharge cycles. Most energy storage applications require deep-cycle batteries. The lead-acid battery is also available in sealed 'gel-cell' version with additives which turns the electrolyte into a nonspillable gel. Such batteries can be mounted sideways or upside down. The high cost, however, limits its use in the military avionics.

Nickel Cadmium:

The NiCd is a matured electrochemistry. The NiCd cell has positive electrodes made of cadmium and the negative electrodes of nickel hydroxide. Two electrodes are separated by Nylon separators and potassium hydroxide electrolyte in stainless steel casing. With sealed cell and half the weight of conventional lead-acid, NiCd batteries have been used to power most rechargeable consumer applications. They have a longer deep cycle life, and are more temperature tolerant than the lead-acid batteries. However, this electrochemistry has a memory effect (explained later), which degrades the capacity if not used for a long time. Moreover, cadmium has recently come under environmental regulatory scrutiny. For these reasons, the NiCd is being replaced by NiMH and Li-ion batteries in laptop computers and other similar high-priced consumer electronics.

Nickel-Metal Hydride

The NiMH is an extension of NiCd technology, and offers an improvement in energy density over that in NiCd. The major construction difference is that the anode is made of a metal hydride. This eliminates the environmental concerns of cadmium. Another performance improvement is that it has negligible memory effect. The NiMH, however, is less capable of delivering high peak power, has high self-discharge rate, and is susceptible to damage due to overcharging. Compared to NiCd, NiMH is expensive at present, although the future price is expected to drop significantly. This expectation is based on current development programs targeted for large-scale application of this technology in electric vehicles.

Lithium-Ion

Lithium-ion technology is a new development, which offers three times the energy density over that of lead-acid. Such large improvement in the energy density comes from lithium's low atomic weight of 6.9 versus 207 for lead. Moreover, the lithium-ion has higher cell voltage of 3.5 versus 2.0 for lead acid and 1.2 for other electrochemistries. This requires fewer cells in series for a given battery voltage, thus reducing the manufacturing cost. On the negative

side, the lithium electrode reacts with any liquid electrolyte, creating a sort of passivation film. Every time when the cell is discharged and then charged, the lithium is stripped away, a free metal surface is exposed to the electrolyte and a new film is formed. To compensate, the cell uses thick electrodes, adding into the cost. Or else, the life would be shortened. For this reason, it is more expensive than NiCd. In operation, the lithium-ion electrochemistry is vulnerable to damage from overcharging or other shortcomings in the battery management. Therefore, it requires more elaborate charging circuitry with adequate protection against overcharging.

Lithium-Polymer

This is a lithium battery with solid polymer electrolytes. It is constructed with a film of metallic lithium bonded to a thin layer of solid polymer electrolyte. The solid polymer enhances the cell's specific energy by acting as both the electrolyte and the separator. Moreover, the metal in solid electrolyte reacts less than it does with liquid electrolyte.

Zinc-Air

The zinc-air battery has a zinc negative electrode, a potassium hydroxide electrolyte, and a carbon positive electrode, which is exposed to the air. During discharge, oxygen from the air is reduced at the carbon electrode (the so-called air cathode), and the zinc electrode is oxidized. During discharge, it absorbs oxygen from the air and converts into oxygen ions for transport to the zinc anode. During charge, it evolves oxygen. A good air management is essential for the performance of the zinc-air battery.

Equivalent Electrical Circuit:

For steady-state electrical performance calculations, the battery is represented by an equivalent circuit shown in Figure.4. In its simplest form, the battery works as a constant voltage source with small internal resistance. The open-circuit (or electrochemical) voltage E_i of the battery decreases linearly with the Ah of discharge Q_d , and the internal resistance R_i increases linearly with Q_d . That is, the battery open-circuit voltage is lower and the internal resistance is higher in a partially discharged state as compared to the E_o and R_o values in the fully charged state. Quantitatively,

$$\begin{aligned}E_i &= E_o - K_1 Q_d \\ R_i &= R_o + K_2 Q_d\end{aligned}$$

where K_1 and K_2 are constants to be found by curve-fitting the test data.

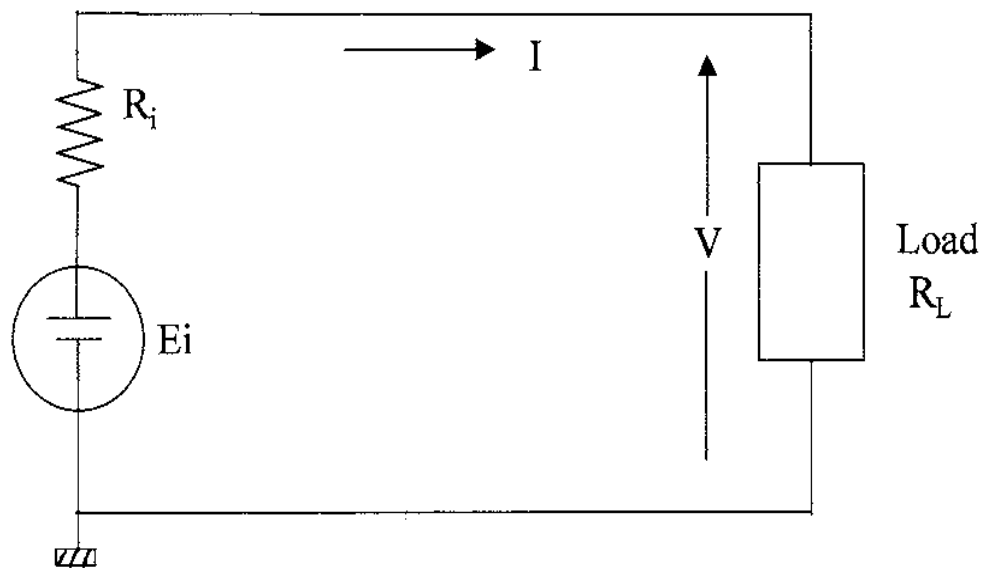


Figure.4: Equivalent electrical circuit of the battery showing internal voltage and resistance[1]

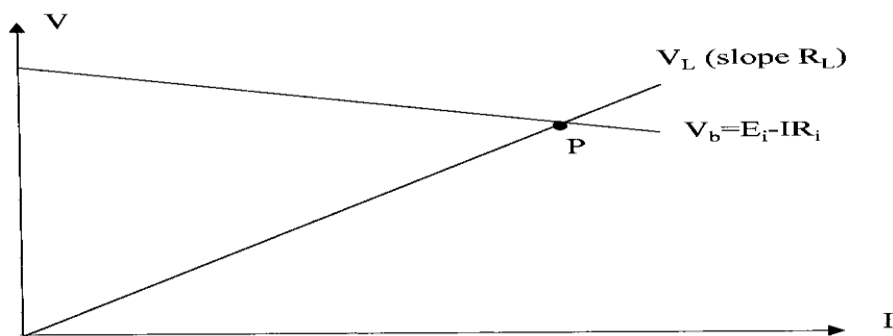


Figure.5: Battery source line intersecting with load line at the operating point[1]

The terminal voltage drops with increasing load as shown by the V_b line in Figure.5, and operating point is the intersection of the source line and the load line (point P). The power delivered to the external load resistance is $I^2 R_L$.

In fast discharge applications, such as for starting a heavily loaded motor, the battery may be required to deliver the maximum possible power for a short time. The peak power it can deliver can be derived using the maximum power transfer theorem in electrical circuits. It states that the maximum power can be transferred from the source to the load when the internal impedance of the source equals the conjugate of the load impedance. The battery can deliver maximum power to a DC load when $R_L = R_i$. This gives the following:

$$P_{\max} = E_i^2 / 4R_i$$

Since E_i and R_i vary with the state of charge, the P_{\max} also vary accordingly. The internal loss is $I^2 R_i$. The efficiency at any state of charge is therefore:

$$\eta = R_L / (R_L + R_i)$$

The efficiency decrease as the battery is discharged, thus generating more heat.

Question:

1. How does grid connected system differ from off-grid connected power systems?

- 2. Write few of the available examples of off-grid connected power systems?**
- 3. Write the working of On-grid connected power systems.**
- 4. What is organic photovoltaic solar cell? How organic photovoltaic cell works? Explain.**
- 5. What are the main challenges of an organic photovoltaic solar cell?**
- 6. Give the basic device structure and their working principle.**
- 7. What are the fabrication techniques of an organic solar cell?**
- 8. Which is the best of the three batteries: NiCd, NiMH or the Li-ion? Give reasons.**
- 9. Battery is required to store electricity from a photovoltaic generator. Which is the best device suited for storing the energy?**
- 10. What will happen if discharge in a battery is more? Will the battery be damaged? What kind of damage it will occur?**
- 11. State difference between NiCd and NiMH batteries.**

UNIT-7: POWER ELECTRONICS FOR PHOTOVOLTAIC SYSTEMS**OBJECTIVE:**

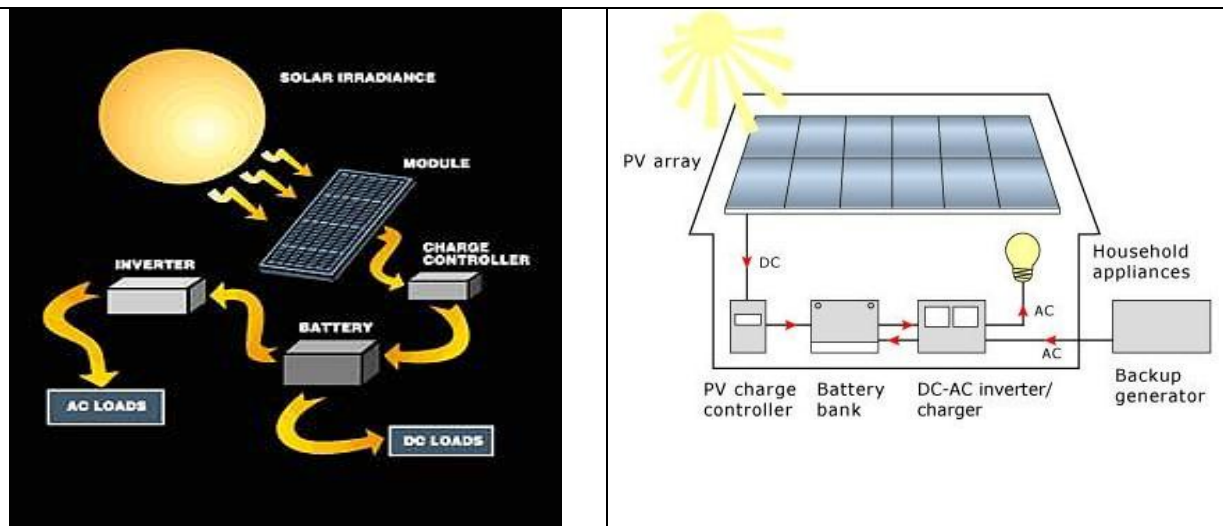
In this chapter, various components and issues related to off-grid and grid-connected Photovoltaic systems have been discussed.

INTRODUCTION:

In photovoltaic power systems, conversion of AC into DC and vice versa along with controlling of voltage and frequency is done basically with the help of power electronic circuits. Some solid state semiconductor devices capable of periodically switched on and off at desired frequency, usually performs such operations. Power electronic devices and circuits are the most common in the practice for such purpose since no applications based on other technology is able to bring significant change or improvements in power engineering till now.

7.1 OFF-GRID (STAND-ALONE) POWER CONTROL AND MANAGEMENT SYSTEMS:

Off-Grid systems are not connected to the local utility grid. These are basically stand-alone systems. The off-grid systems use the solar radiation and turn it into a useable current. These systems should produce enough energy to fulfill the energy needs of the home or the locality. Batteries are the key components of any off-grid system.



Source: <http://www.solarhaven.org>

Source: <http://www.beelandsolar.com>

Fig. 1 – Illustrations of off-grid solar photovoltaic system

7.1.1 BASIC SWITCHING DEVICES

There are various types of solid state devices which are commercially available. Some of the commonly used devices are mentioned as below.

- Bipolar junction transistor (BJT).
- Metal-oxide semiconducting field effect transistor (MOSFET).
- Insulated gate bipolar transistor (IGBT).
- Silicon controlled rectifier (SCR); they are also known as the thyristor.
- Gate turn off thyristor (GTO).

For application of these devices in a particular system, the selection of the devices is determined by the power, voltage, current, and frequency requirement in the power system. One common feature among all these devices is that all of them are having three-terminals. These devices are represented by different circuit symbols. Some of them are as shown in the figure below.

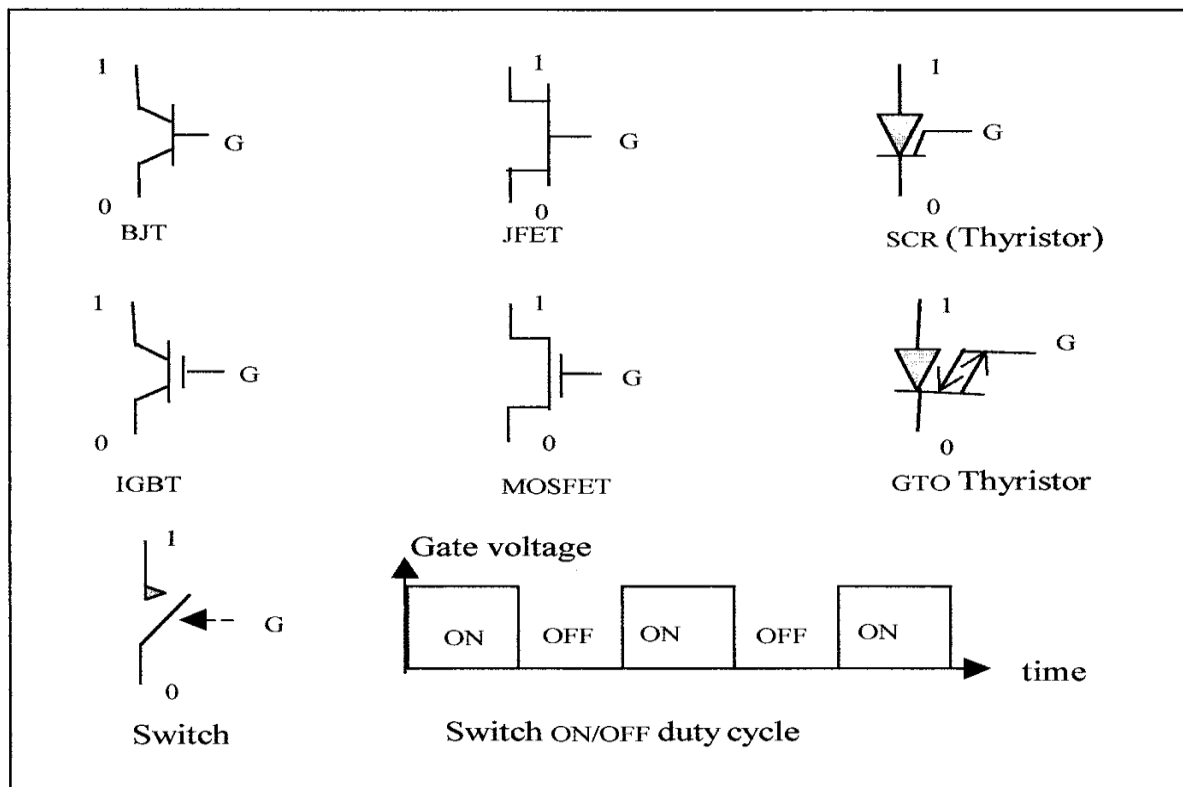


Fig. 2 - Basic semiconductor switching devices [2]

In the figures, “1” and “0” represent the two power terminals and “G” represents the control terminal. The control terminal is also known as gate terminal. The power terminals are connected to the main power circuit while the gate terminal is connected to the auxiliary control circuit. Typically, during conducting operation terminal “1” is held at higher voltage as compared to the terminal “0”.

Since the primary function of these devices is the switching of power, either on or off, their functionality can be represented by the gate controlled switch. The control signal at the gate terminal basically operates the switch. When there is no control signal applied at the gate terminal, the power terminals of the devices behave as open circuit due to the infinite resistance across them, thus performing the switching off operation. On the other hand, on

application of a control signal at the gate terminal, the resistance across the power terminals falls far below or approaches zero, thereby makes the switch on and allows current to flow freely.

The periodic on and off of the switch is usually triggered by a train of pulses of suitable frequency applied at the gate terminal. The waveform of the gate signals may be of different type, for example a rectangular waveform or other type. They may also be generated through a separate triggering circuit, often termed as firing circuit.

7.1.2 TYPICAL PV-BASED STAND-ALONE POWER SYSTEM

There are several factors which influence the design of a stand-alone PV-based power system. For example, location, climate, site characteristics, equipments to be used etc, play a major role in designing the system. The schematic of a typical PV-based stand-alone power system is shown in the figure. The selection and interconnection of the system components also requires through consideration of these factors.

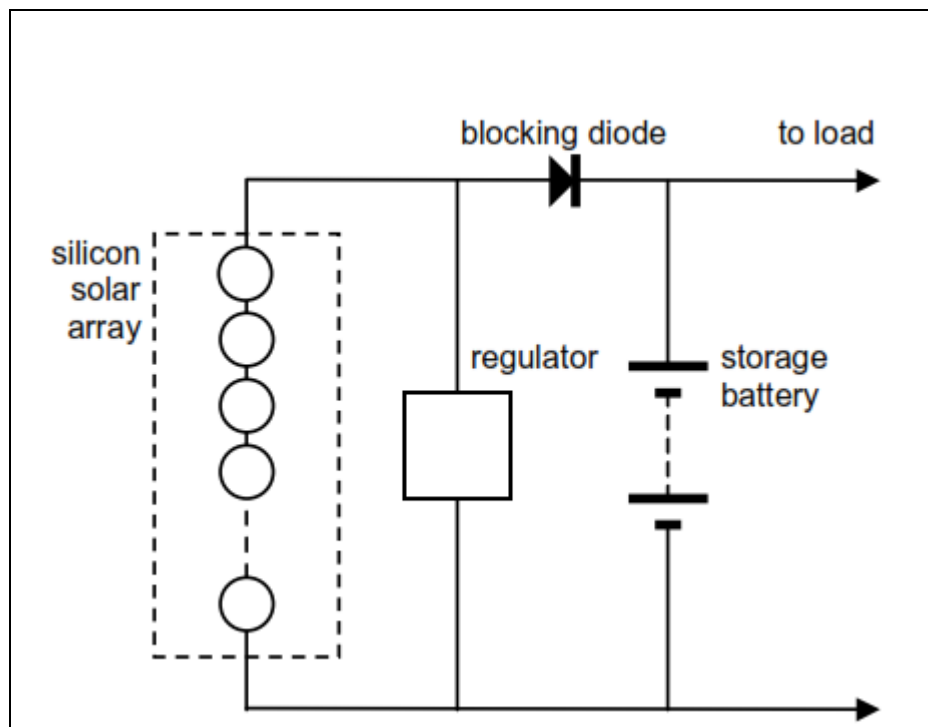


Fig. 3 - Simplified stand-alone PV power system [3]

7.1.3 SOLAR MODULES:

The main function of the solar modules in a stand-alone system is to charge a battery. A typical module, based on screen-printed or buried-contact silicon cell technology, has 36 cells connected in series and is capable of charging a 12 V battery. The un-encapsulated cells in practice normally have higher average efficiency than the cells encapsulated in modules. The main causes for this variation of efficiency are the reflection from the glass, change in

reflection from cell-encapsulate interface, mismatch losses between cells and resistive losses in interconnects.

7.1.4 BATTERIES:

Batteries are Storage devices in stand-alone power supply systems. They get charged from the solar modules and delivers power to the load as and when required. The lead-acid batteries are the most common. However there are many different types of batteries like nickel-cadmium, nickel-metal-hydride, rechargeable alkaline manganese (RAM), lithium-ion, lithium-polymer and redox batteries, which can be suitably for stand-alone PV systems applications.

The use of batteries can be made to serve the purpose of power conditioning or they can be used either as a short-term storage or long-term storage. Their applications as short term storage can facilitate the effective redistribution of load over a 24 hour period while as long term storage they can ensure the system availability throughout periods of low insolation.

7.1.5 INVERTERS:

The Inverters are required when PV-based power systems are required to drive an AC load instead of a DC load. Inverters convert direct current (DC) to alternating current (AC) with the help of switching devices. They are also used to step up the voltage level as per requirement. In most of the cases, inverters change the voltage level typically from 12, 24 or 48 V DC to 110 or 240 V AC. The output voltage may be higher than these values in case of larger systems or grid connected systems.

In standalone systems, the requirement of supplying constant voltage and frequency even under varying load conditions has to be suitably fulfilled by the inverters. Inverters are also expected to supply or absorb required reactive power in case of reactive loads existing in the system. Isolation transformers are often used in inverters for stand-alone PV systems in order to separate the DC and AC circuits. Some of the desired features of inverters for application in stand-alone PV systems are mentioned below.

- Typically, the inverters should have large input voltage range
- Their voltage waveform should be close to sinusoidal
- They should have strict control of output voltage and frequency; variation of voltage and frequency should be within around $\pm 8\%$ and $\pm 2\%$ respectively.
- High efficiency should be achievable even for low loads, for example, $>90\%$ at 10% load.
- Inverters should possess appropriate tolerance for short overloads, particularly for motor starting
- They should operate satisfactorily with reactive loads
- They should have tolerance for loads using half-wave rectification
- They should also possess tolerance for short circuits.

7.1.6 MODE CONTROLLER:

The mode controller in a standalone PV system serves as the central monitor and controller of the systems. The design of a standalone PV system must be able to incorporate other standby sources of power, for example, diesel generators, fuel cells etc. The mode controller performs the function of switching to the desired mode for power generation as per the requirements. Basically, the mode controller is used to perform the following primary functions –

- To monitor and control the health and state of the system.
- To monitor and control the battery state-of-charge.
- To switch on the standby power source, for example, the diesel generator, whenever needed, and to shut it off when not required.
- To shed the low priority loads in accordance with the preset schedule.

The mode controller typically comprises of microcomputer and software for appropriate functioning of source selection, battery management and load shedding strategy. The common disturbances like insolation changes resulting from movements of the cloud, variation in the wind speed, sudden load changes, short circuit faults etc are suitably considered in a comprehensive design.

7.1.7 BALANCE OF SYSTEM (BOS) COMPONENTS:

The cost of establishing a photovoltaic power supply system includes many other costs apart from the solar modules. The balance of system or BOS refers to the batteries, regulators, inverters and other system components in a collective manner. The other factors which are likely to add to the cost of a photovoltaic power supply system may be transportation, installation, land requirement, site preparation, drainage, electrical wiring, mounting structures and housing. These costs are likely to dominate, as the PV prices fall. Some of the commonly used BOS components are the constituents of the electrical wiring system, mounting and housing. these components should be highly reliable as well as durable in order to of provide a trouble-free operation for at least 20 years at the expense of a reasonable initial cost.

7.1.7.1 WIRING:

The cost of wire can be very high particularly in two cases –

1. For low voltage, high current applications and
2. When current needs to be conducted over a long distance.

In a PV power system, copper wire should be ideally used though it involves more cost than aluminium wire. However, aluminium wire may also be acceptable for very long runs under certain conditions. During the design of a system, the cross section of the wires

should be suitable selected so that the resistive losses between the solar photovoltaic array and the battery is limited to less than 5 % or as per the standards applicable for the purpose.

7.1.7.2 OVER-CURRENT PROTECTION:

The over-current protection devices usually include circuit breakers or fuses. The main purpose of these devices is to protect the equipment as well as personnel. The ratings of these devices should perfectly match the voltage and current requirement of the systems in which they are to be used.

7.1.7.3 SWITCHES:

Switches are basically used to isolate the system components, namely, the array, battery, controller and the load. Switches should be properly enclosed in order protect them from the environment. Usually the DC switches are more expensive as compared to the AC switches. They are also heavy duty ones. In no cases AC switches should be used in place of DC switches. Typically switches are rated for 1.2 times the array open circuit voltage. Specific recommendations must be followed in selecting the appropriate switches.

7.1.7.4 CONNECTORS:

Connectors are important components in a PV system since they can significantly affect the reliability of the system. Following recommendations related to the connectors can help minimizing the problems in a PV system.

1. Connector and wire sizes should be compatible.
2. A ring type connector should be preferred in place of a spade-type connector.
3. The wire after stripping the insulation should be properly cleaned, with solvent if necessary, and crimping tool should be used to attach the connector to the wire.
4. Connections between subsystems using terminal strips should be made in weather resistant boxes. Terminals and connectors must be of similar type of metal.
5. Proper attention should be given to those places where a bare wire might touch metal at a different potential and should be rectified.
6. Battery cable terminations should be crimped. Stainless steel bolts, nuts, washers and spring washers should be used bolted battery connections.

7.1.7.5 EARTHING (GROUNDING):

Earthing is a way of providing low resistance paths from some selected points within the PV system to the earth or ground. In some cases, earthing may not be required, for example where double insulation is used. Equipment grounding refers to ensuring all metal enclosures as well as all the parts of the array frame which may be touched by hands are well earthed. The connection of a current-carrying conductor, commonly the negative one, to the earth is referred as system earthing. Arrangement of system earthing should take into account of the manufacturer's requirements for power conditioning equipment, such as inverters etc.

7.1.7.6 METERING AND ALARMS:

Appropriate metering for battery terminal voltage, input current etc and also for generator run hours, in case backup generator is used, should be incorporated. Provision of alarms should be there to indicate the high and low battery voltage along with other desirable parameters.

7.1.7.7 BATTERY HOUSING:

Batteries must be protected from both man and environment. The housing should be able to give protection from acid and the evolved gas. The rate of self-discharge of a battery increases if it is directly placed on the concrete. The rate becomes higher especially in case of moist concrete. So placing of batteries directly on the concrete should be avoided.

7.1.7.8 MODULE MOUNTING:

The power output from a PV array is affected by the type of module mounting. The support structures vary widely and they have a significant share in the capital cost of the PV system. The mounting structures also influence the maintenance requirements. The most common type of structures is the fixed arrays. The modules are supported by the structure at a fixed angle which is determined by the requirement and the site. A minimum tilt angle of 10 degree is recommended to facilitate natural cleaning of the array by the rain. In the seasonally-adjusted tilting structure, the array angle can be manually adjusted monthly or seasonally, against the horizontal axis in order to increase the array output. In the single-axis tracking system, the array can be tilted automatically at hourly interval or more frequently, if required, along the vertical axis. This system allows the array to follow the sun from east to



Source: <http://www.solarhaven.org>

Fig. 4 – Typical Mounting of solar modules

west and thereby increase the power output significantly. Again In the two-axis tracking system, power output can be further increased by tracking the sun along both the vertical and horizontal axes, that is, along both the north-south and east-west axes.

7.2 GRID CONNECTED POWER CONTROL AND MANAGEMENT SYSTEMS

The grid connection of solar photovoltaics power system can be done in two ways. In one mode the arrays are installed at the end use site, for example, on the rooftops etc. In the second mode, they can also be connected as utility scale generating stations. With the passage of time, the photovoltaic power systems have successfully changed its phase from stand alone to large grid connected ones. In the grid connected systems, power flow occurs both way between the grid and the site. Whenever required, power is supplied from the grid to the site loads. On the other hand, the excess power from the site, whenever available, is absorbed by the grid.

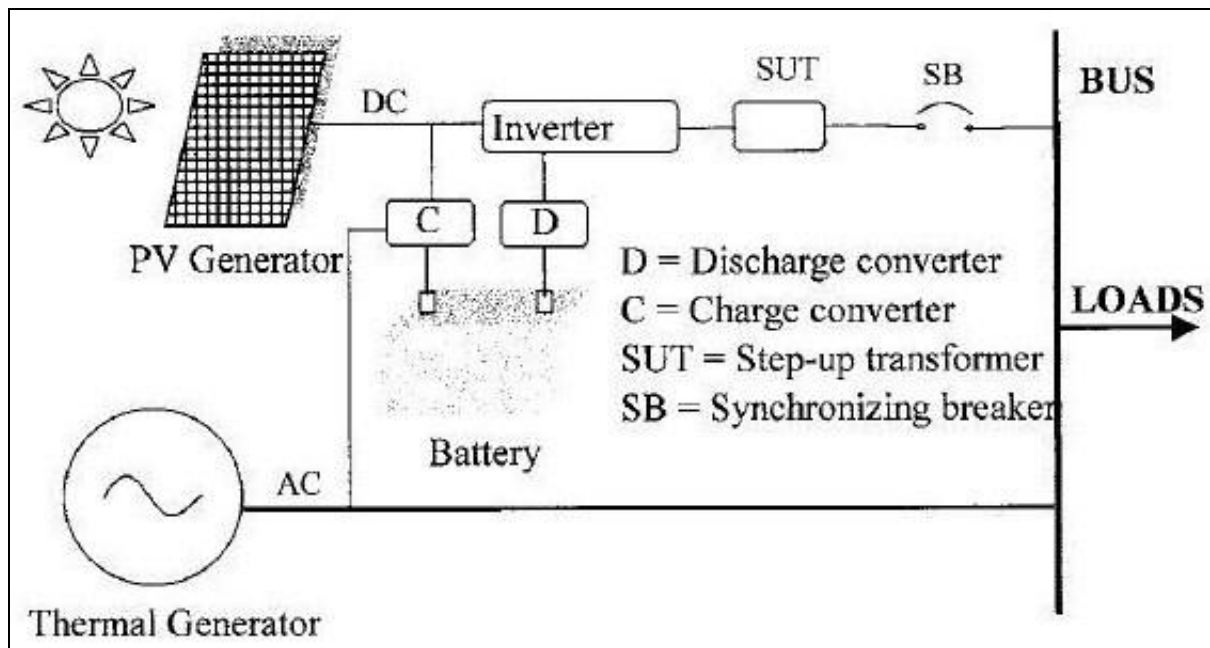


Fig. 5 – Electrical schematic of grid connected photovoltaic system [2]

7.2.1 INTERFACE REQUIREMENTS:

The interfacing of the PV systems is done through the synchronizing breaker at the output end of the inverter. The site voltage at the breaker terminals decides the direction of flow of power. Before connecting the PV systems to the grid, following points should be ensured:

- The magnitude and phase of the voltage generated must match the desired magnitude and direction of the power flow. In a closed-loop control system, by making the appropriate choice of transformer turn ratio and/or the rectifier/inverter firing angle, controlling of the voltage can be done.

- The frequency of the voltage must be same as that of the connecting grid. Setting the utility frequency as a reference for the inverter switching, the requirement for frequency matching can be effectively achieved.

7.2.2 SYNCHRONIZING WITH THE GRID:

The synchronization with the grid basically refers to the connection of the PV system to the grid at appropriate conditions for voltage, frequency and phase angle. There are sensors in the synchronizing breaker in order to monitor the voltage level and phase angle of the site as well as the grid. These sensors dictate the appropriate instant for connecting the PV system to the grid. There are also some in built automatic protection devices or circuits which prevent from closing the breaker under inappropriate conditions. There are certain conditions which must be fulfilled for effective synchronization or closure of the synchronizing breaker. These can be summarised as below.

1. The frequency of the system must be as close as possible with the grid frequency, preferably about one-third of a hertz higher.
2. The magnitude of the terminal voltage must match with that of the grid, preferably a few percent higher.
3. The phase sequence of the two three-phase voltages must be the same.
4. The phase angle between the two voltages must be within 5 degrees.

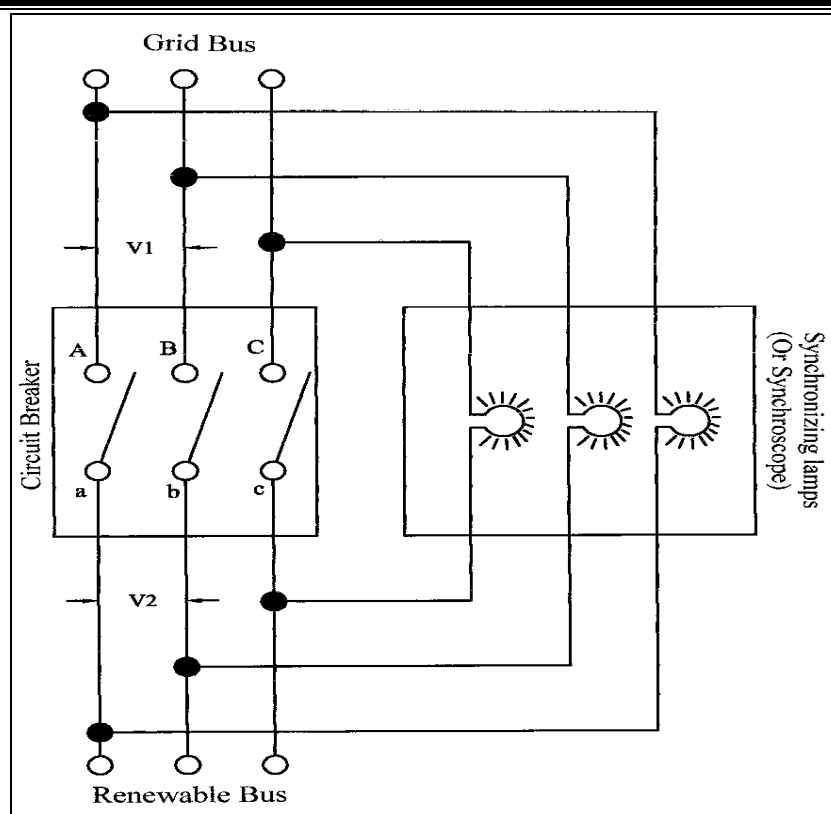


Fig. 6 - Synchronizing circuit using three synchronizing lamps or the synchroscope [2].

7.2.3 INRUSH CURRENT:

It is observed that during synchronization there exists an unavoidable difference between the voltages of the site and the grid. Even though it is small, it results in the flow of an inrush current between the site and the grid. Typically this inrush current follows an exponential behaviour decided by the internal resistance and inductance and decays to zero. The level of the difference between the voltages at the instant of closing the breaker determines the initial magnitude of this inrush current.

The magnitude of the inrush current can be found out as follows:

Let, ΔV = difference between the voltages of the site and the grid
at the closing instant due to any reason

The inrush current resulting from the sudden application of voltage to the system by closing the breaker is determined by the sub-transient reactance of the machine X_d'' .

This implies that,

$$I_{\text{inrush}} = \Delta V / X_d''$$

where, I_{inrush} = inrush current in the system

Since the inrush current is determined by the sub-transient reactance X_d'' , the inrush current is basically reactive. If the magnitude of the inrush current exceeds the permissible limit, thermal or mechanical damage may occur.

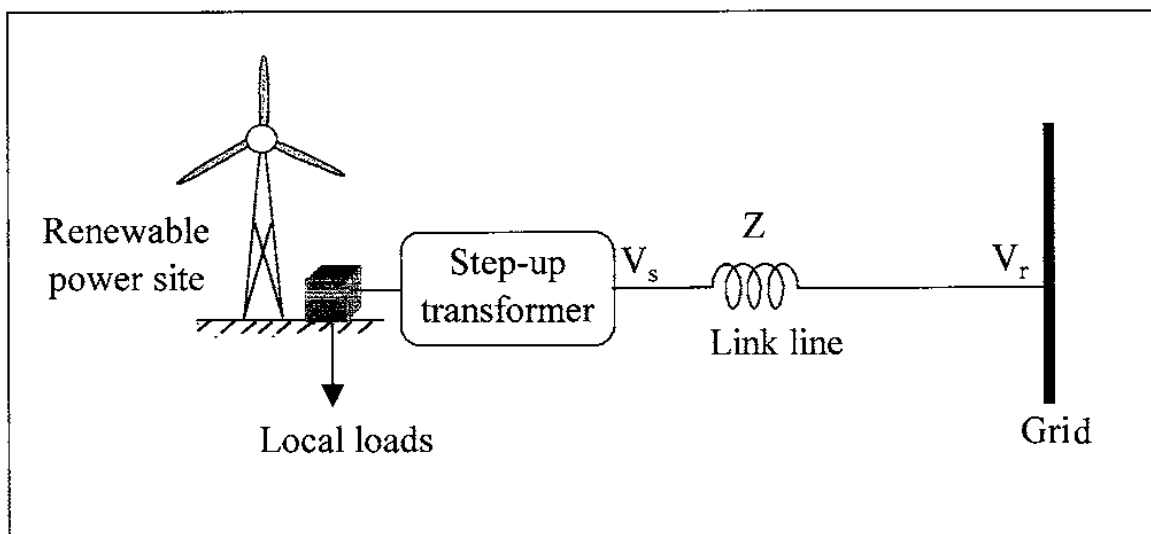
7.2.5 SAFETY:

Safety issues must be suitably addressed in case of grid- connected solar PV power systems. The systems should be able to provide protection to the human, particularly during the repair and maintenance of the utility while feeding power to the grid. Generally some internal circuits are included in the system to detect the faults which switches off the inverter. The circuit breaker interfacing the grid and site can get quickly disconnected in case of accident or emergency.

In some interconnected systems, large capacitors may be connected at the PV site for improving power factor. Here the site generators may be generating terminal voltage drawing their required excitation power from the capacitors which would have been zero otherwise. The line capacitance may also keep the generators self excited. These factors are suitably taken care of by the internal protection circuits to enable human safety.

7.2.6 OPERATING LIMIT:

The interconnection of a renewable energy power site with the utility grid sets the operating limit in two ways, namely, voltage regulation and stability limit. The link line connecting the site and the grid can often be treated as an electrically short transmission line of up to 50 miles long. In such situations ignoring the ground capacitance and ground leakage resistance which are negligible, the equivalent circuit comprises of a resistance and reactance in series. Power flows through the line from the site to the grid and vice versa as per demand requirement. The transmission line impedance affects the voltage regulation as well as the maximum power transfer capability of the link line.



[link \[2\]](#)

7.2.6.1 VOLTAGE REGULATION:

The phasor diagram of the voltage and current at the sending and receiving ends can be shown as in the figure.

Neglecting the shunt impedance,

$$I_s = I_r = I$$

Where, I_s = current at the sending end

I_r = current at the receiving end

I = current in the line

Let V_s and V_r be the sending end and receiving end voltages. Then the sending end voltage will be equal to the vector sum of the receiving end voltage and in the impedance drop in the line.

This implies,

$$V_s = V_r + I Z$$

$$\text{Or, } V_s = V_r + I (R + jX)$$

Where, R = resistance of the line

X = reactance in the line

Z = impedance of the line

$$= R + jX$$

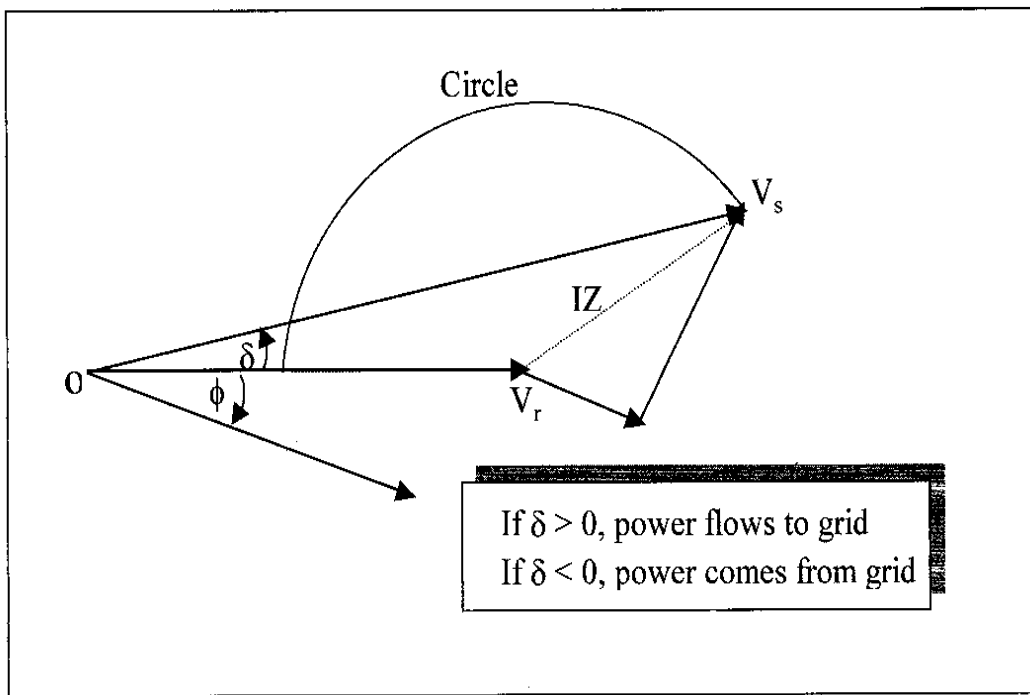


Fig. 8 - Phasor diagram of the link line carrying rated current [2]

The voltage regulation at a specified power factor indicates the rise in the receiving end voltage with respect to the full load voltage, when full load is thrown off. Voltage regulation is expressed as the percentage of the full load voltage. It can be written as,

$$\text{Voltage regulation} = [(V_{nl} - V_{fl}) / V_{fl}] \times 100 \%$$

Where, V_{nl} = magnitude of receiving end voltage at no load

$$\approx V_s$$

V_{fl} = magnitude of receiving end voltage at full load

$$\approx V_r$$

The voltage regulation is greatly influenced by the load power factor. Typically, the voltage regulation is greater when the power factor is lagging. On the other hand, voltage regulation can be the least or even negative in case of leading power factor. The circle diagram can be used for plotting the sending end voltage against to load power factor for a particular load voltage and KVA.

7.2.6.2 STABILITY LIMIT:

Stability Limit indicates the extent of maximum power that can be transferred through the line without the loss of operational stability of the system. The direction of power flow in the line can be determined from the electrical phase angle between the sending and receiving end voltages. The same stability limit can be applied in both directions of power flow in a grid connected renewable energy system. The power flowing to the grid through the transmission line can be expressed as,

$$P = V_r I \cos\phi$$

7.2.7 ENERGY STORAGE AND LOAD SCHEDULING:

In case of grid-connected large PV power plants, the provision of some local storage devices like batteries etc may be advantageous for efficient functioning of the system. For example, batteries may be used to supply the short term peak demand instead of the feeding from the grid. This helps in cutting down the payable demand charge applicable for grid. A systematic operational strategy has to be formulated for proper load scheduling as well as cost optimization. In this process, all the system constraints like battery size, the minimum on/off times, the battery charge and discharge rates, the renewable capacity limits etc, have to be suitably taken into account.



Source: <http://www.wikipedia.org>

Fig. 9 – First solar 40 MW CdTe PV array installed in Germany, consisting of 550,000 solar thin film modules from cadmium telluride which supplies about 40 000 MWh of electricity per year.

7.2.8 UTILITY INTERFACE:

The point of interconnection between the utility distribution and the grid interactive inverter is referred to as the utility interface. The various requirements of the utility like voltage, frequency, harmonics, power factor etc have to be appropriately monitored or measured at the interface. The inverter must suitably match those requirements prior to its connection to the interface. Typically, the voltage should be slightly higher than the utility in order to prevent the power flowing from the grid to inverter while the frequency must be same as that of the utility.

SUMMING UP:

The generation of power from solar energy has gained momentum throughout the world. It has been observed globally that a single or unique way of delivering electrical power is a far reaching option from both economical as well as technological point of view. Also, the electrification technologies are widely expanding in such a way that finding an optimal as well as affordable or sustainable solution for a particular electrification scheme is going to be much more complex due to the involvement of several factors. The off grid systems can efficiently operate to meet the local power requirement without depending on the grid. In case of grid connected systems, the systems must be able to take the counter measures in order to maintain the frequency and voltage stability. With the development of technologies and appropriate applications, the power generations through photovoltaic systems, whether off-grid or grid-connected, can definitely provide some relief to the present energy crisis.

PROBABLE QUESTIONS:

1. Draw a schematic of a stand-alone photovoltaic system, labelling each component, then:
 - (a) Briefly discuss the function and reliability of each component and its importance to the system.
 - (b) What are some of the more common problems that occur with each system component?
2. Give an overview of photovoltaic applications relevant to present markets, explaining why photovoltaics are both suitable and economical for each.
3. What changes are likely to take place in future PV markets and applications? What changes are needed in PV products to best access these new markets?
4. Describe the components in a grid-connected residential photovoltaic system and discuss issues relevant to the use of photovoltaics in this application.

REFERENCES:

1. Mukerjee, A.K., and Thakur, N., Photovoltaic Systems Analysis and Design, PHI Learning Private Limited, 2011.
2. Patel, M.R., Wind and Solar Power Systems, CRC Press, Boca Raton London New York Washington, D.C., 2000.
3. Wenham, S., Green, M., Watt, M., and Corkish, R., Applied photovoltaics, Second Edition, Earthscan, 2007.
4. **Error! Hyperlink reference not valid.**
5. <http://www/beelandsolar.com>

UNIT-8: SOLAR PHOTOCATALYSIS

References:

- [1]. Goswami D Y, Kreith Frank and Kreider J F, Taylor & Francis (1999) Principles of Solar Engineering, Taylor & Francis, USA
- [2]. Galvez, B. Julian., Rodriguez, M. Sixto., 2003, Solar Detoxification, United Nations Educational, Scientific and Cultural Organization (UNESCO).
- [3]. www.psa.es
- [4]. www.apra-europe.org
- [5]. Ni, Meng., Leung, M.K.H., Leung, Dennis., Sumathy, K., 2007, A review and recent development in photocatalytic water splitting using TiO_2 for hydrogen production, Renewable and sustainable energy reviews, 11, 401-425.

SOLAR PHOTOCATALYSIS

This unit describes an alternative to energy conversion and utilization that combines sunlight and chemistry to produce chemical reactions which can be used in an energy efficient manner for a variety of applications. It outlines the basic chemical and physical phenomena that are related with photonic interactions. The use of photocatalysis for degradation organic contaminants and its other useful end-use has been described. This unit also outlines the influencing parameters related to solar heterogeneous photocatalysis reactions.

INTRODUCTION:

Photo-Catalysis is defined as "acceleration by the presence of as catalyst". A catalyst does not change in itself or being consumed in the chemical reaction. This definition includes photosensitization, a process by which a photochemical alteration occurs in one molecular entity as a result of initial absorption of radiation by another molecular entity called the photosensitized. Chlorophyll of plants is a type of photocatalyst. Photocatalysis compared to photosynthesis, in which chlorophyll captures sunlight to turn water and carbon dioxide into oxygen and glucose, photocatalysis creates strong oxidation agent to breakdown any organic matter to carbon dioxide and water in the presence of photocatalyst, light and water(see Fig.1).

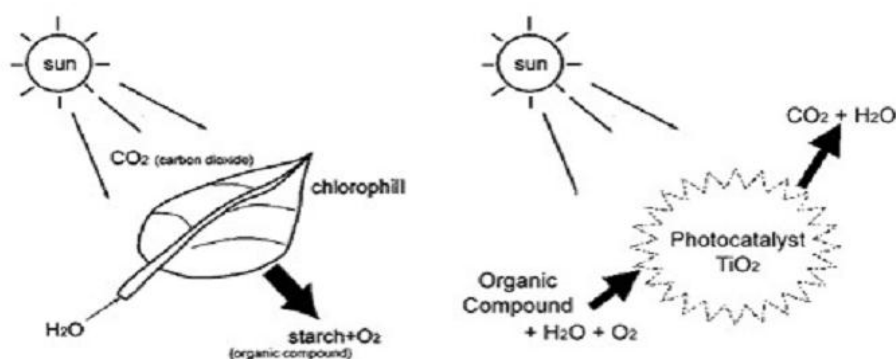


Fig.1: Similarity of function between chlorophyll and photocatalyst

Different types of semiconductor materials that are used as photocatalysts include TiO₂, CdS, ZnO, GaP, WO₃ etc. Among these TiO₂ is the most commonly used one due to its strong resistance to chemical and photocorrosion, environment friendly nature and cost effectiveness.

Mechanism of solar photocatalysis:

When a photocatalyst like titanium dioxide (TiO₂) absorbs Ultraviolet (UV) radiation from sunlight or illuminated light source (fluorescent lamps), it will produce pairs of electrons and holes. The electron of the valence band of titanium dioxide becomes excited when illuminated by light. The excess energy of this excited electron promoted the electron to the conduction band of titanium dioxide therefore creating the negative-electron (e⁻) and positive-hole (h⁺) pair. This stage is referred as the semiconductor's 'photo-excitation ' state. The energy difference between the valence band and the conduction band is known as the 'Band Gap '. Wavelength of light necessary for photoexcitation is calculated by Eq.1

$$\lambda = \frac{hc}{U} \quad (1)$$

where, h is Planck's constant (6.6× 10⁻³⁴ J-s), c is the speed of light, λ is the wavelength and U is the energy of a photon. The photon energy should be greater than the band gap energy of a particular catalyst.

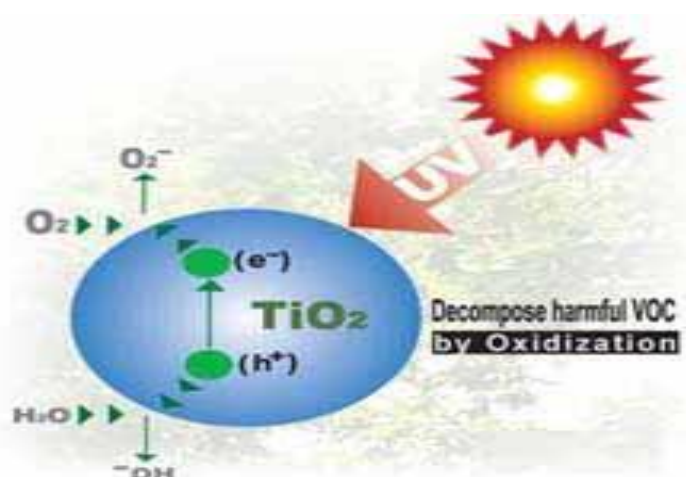


Fig2: Schematic diagram showing how TiO₂ acts as photocatalyst

The positive-hole of titanium dioxide breaks apart the water molecule to form H^+ and hydroxyl radical ($*OH$). The negative-electron reacts with oxygen molecule to form super oxide anion (O^{2-}). This cycle continues when light is available (see Fig.2). The hydroxyl radical thus generated is a powerful oxidising agent and plays a major role in various application of photocatalyst.

Solar Detoxification Pilot Plant:

The design procedure for a pilot solar detoxification system requires the selection of a reactor, catalyst operating mode (suspension or fixed matrix), reactor-field configuration (series or parallel), treatment-system mode (once-through or batch), flow rate, pressure drop, pretreatment, catalyst and oxidant loading method, pH control, etc., so a pilot plant has to be as versatile as possible to allow for these variables and, at the same time, provide sufficient confidence in the experiments carried out in it. A pilot plant must fulfil all the present and future requirements of the research to be performed in it. In Fig. 3 a detailed drawing of a plant is given. Usually, a detoxification pilot plant is constructed with several solar collectors. All the modules are connected in series, but with valves that permit to bypass any number of them (see Fig. 3, “collector by-pass”). Sampling valves are in the outlet of each of the modules. All the tubes and valves are black HDPE, material chosen because it is strongly resistant to chemicals, weather-proof and opaque, in order to avoid any photochemical effect outside of the collectors. There are storage-feeder tanks available, also made of HDPE and having different capacities, where the test mixtures are prepared. Four different operating modes are possible: recirculation, once-through, partial recirculation, and system cleaning.

When concentrating solar collectors are used, the temperature of the water, which flows through them, rises considerably. Obviously, the slower the flow rate used in once-through experiments and the longer recirculation experiments, the greater the increase of temperature is. Therefore, to avoid evaporation and damage to plastics, cooling is necessary, and a closed circuit water-cooling system has to be installed. A centrifugal pump with an electric motor (calculated to provide sufficient flow when the maximum length of the

system is used) has to be installed to move the water to be tested in the reactor. The flow rate (in batch mode) has to be such that it guarantees only a small amount of reactant is converted each time through the reactor, and the concentration throughout the system remains relatively constant (this reasoning will become clear below). Either a flow-rate control loop made up of a flow meter connected to a controller, which in turn governs an automatic electric valve, or an electric pump with a speed controller has to be installed to regulate the flow to the rate desired. The most important sensors required for the system are temperature, pressure and dissolved oxygen (at least in the reactor outlet). As oxygen is required for the oxidation of organics, an injection system at the reactor inlet allows oxygen to be added to the reactor. Atmospheric oxygen can be also stirred into the reaction medium in the reservoir tank. A UV-radiation sensor must be placed in a position where the solar UV light reaching the photoreactor can be measured, permitting the evaluation of the incident radiation as a function of hour of the day, clouds, atmospheric or other environmental variations. All these data have to be sent by an appropriate transmitter from the sensors to a computer, which stores the results for later evaluation. To clean the system, a drainage tube, with an active carbon filter to retain any organic compound not decomposed during the experiments, must be hooked up to the sewage pipelines.

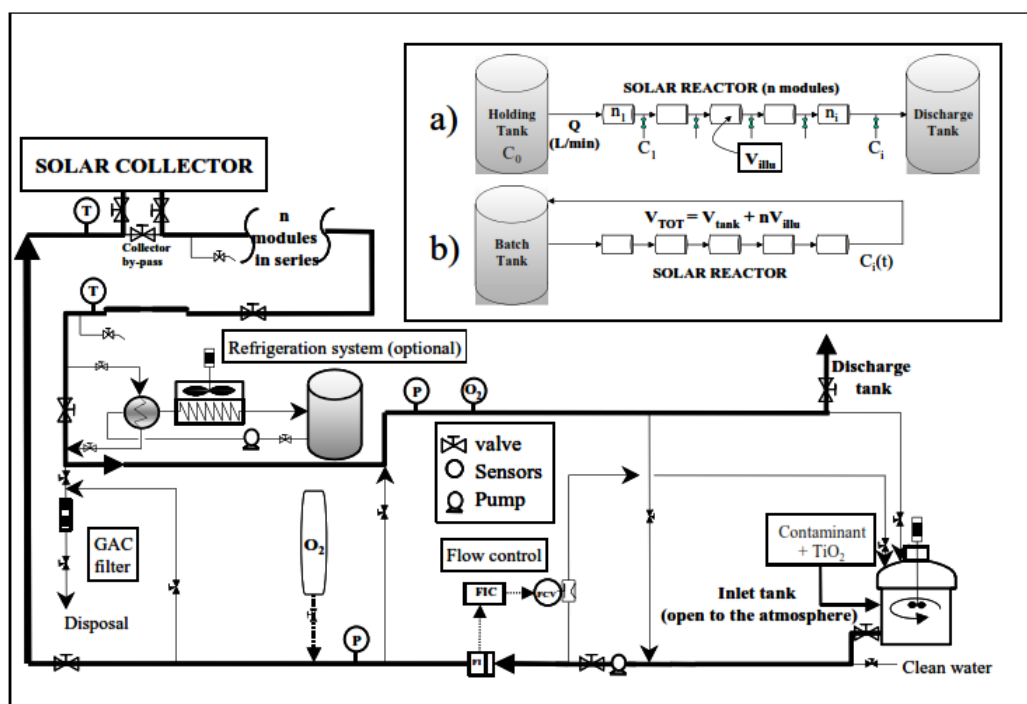


Fig 3: Photocatalytic Detoxification Pilot Plant scheme (once-through mode is shown). In the inset is shown the schematic of two pilot plant operation concepts: A (a) once-through operation and (b) a batch operation.

Operation of Pilot Plants:

In the once-through mode (shown in Fig.3) the experimental procedure begins when the pump is turned on and the system is filled with clean water. Those modules necessary are selected and the corresponding valves are set to bypass the rest. Then the water is pumped through the circuit and the modules are covered. Obviously, the maximum pump flow rate is necessary for this procedure. The amounts required for obtaining the initial concentrations of catalyst, contaminant and any other ingredient in the experiment are added to the holding tank. When the time needed for mixture to be completed has expired, this is verified by taking samples at two different points in the reactor at the same time for analysis. A few minutes later two more samples are taken and, if the four coincide, the concentration of the reactive may be considered to be the same throughout the reactor. Simultaneously, the automatic control sets the flow rate (Q), which will then be kept constant during the experiment, oxygen injection is activated and valves are adjusted so that the fluid goes to the

discharge tank. After that the modules to be used are put into operation (uncovered). This marks the beginning of the experiment.

The modules are kept illuminated a little longer (experimental time) than necessary to allow the water in the holding tank to go through the reactor and approach the discharging tank. This time (t_{exp}) is (Eq.2):

$$t_{exp} = \frac{V_{tube} + nV_{mod}}{Q} \quad (2)$$

Where, Q is the flow rate, V_{tube} is the volume in the pipes between the modules and the tank and V_{mod} is the volume in each module, with n the number of modules in series. At this time, samples are taken at all the valves in the outlets of each of the modules in the experiment. This provides “ n ” number of samples with different residence or illumination times ($t_{R,i}$) to enable determination of kinetics. Under these conditions, the reactor behaves according to the ideal plug-flow model as explained later. The residence time corresponding to each sample collected at the end of the experiment is calculated with the following equation (Eq.3):

$$t_{R,i} = \frac{n_i V_{illu}}{Q} \quad (3)$$

where i is the number of modules through which the samples have passed before being collected and V_{illu} is the volume in the illuminated section of each module. When the test is over, n samples have been obtained with a reactor residence time that is a function of the flow rate. Thus, if the procedure is repeated at a different flow rate, that group of samples has a different ($t_{R,i}$, Concentration) and the number of points necessary to evaluate any experiment can be obtained.

Solar detoxification pilot plants are frequently operated in a recirculating batch mode. In this scheme, the fluid is continuously pumped between the reactor and a tank in which no reaction occurs, until the desired degradation is achieved. The systems are operated in a discontinuous manner by recirculating the solution with an intermediate reservoir tank and centrifugal pump. This type of operation differs little from the previous one. When concentration of the

reactive is the same throughout the reactor, oxygen injection (if necessary) is activated and the position of the valves is maintained so that the fluid begins and ends up in the holding tank (now called the batch tank). The automatic control sets the maximum flow rate which has to be such that it guarantees that only a small amount of reactant is converted each time it goes through the reactor. Then the modules that are going to be used are put into operation. This begins the experiment. Recirculation is continued and the test lasts however long required, even up to several days. Samples may now be taken at any of the sampling ports, since as the system is in recirculation mode; t is the same for samples taken at any point in the system. The $(t_{R,i}, \text{Concentration})$ pairs are thus obtained (Eq.4).

$$t_{R,i} = \frac{V_{illu}}{V_{TOT}} t_{exp,i} \quad (4)$$

where, V_{TOT} is the volume of the entire pilot plant. V_{illu} and V_{TOT} are defined at the beginning of the experiment by the number of modules used and the level of water in the batch tank. The experimental time (t_{exp}) is the difference in time between the initial sample (initial concentration of the pollutant, $t_{exp}=0$) and samples collected during the experiment ($t_{exp} > 0$).

Fundamental parameters in solar photocatalysis:

Direct Photolysis:

For pollutants to be dissociated in the presence of UV light, the pollutants must absorb light with a reasonable quantum yield. Organic pollutants generally absorb light at lower wavelengths. In any case, the focus here is on fundamental photocatalytic parameters and therefore the photolytic effect will be discussed from this point of view. These tests have to be performed in order to find out the decomposition rates without the semiconductor. As TiO_2 readily sticks to the glass in the photoreactors, it is necessary to carry out these tests at the beginning, before the catalyst comes into contact with the photoreactors. In pilot-plant-scale experiments, removal of the thin coating of catalyst on the tubes after TiO_2 suspensions have circulated through them is a very hard, complex and expensive task. After these tests have been performed, the photocatalytic experiment results may be considered accurate and the kinetic

parameters can be determined properly. Any side effect of the photocatalytic reaction rate can be quantified and subtracted from the global rate, resulting in the real photocatalytic reaction rate.

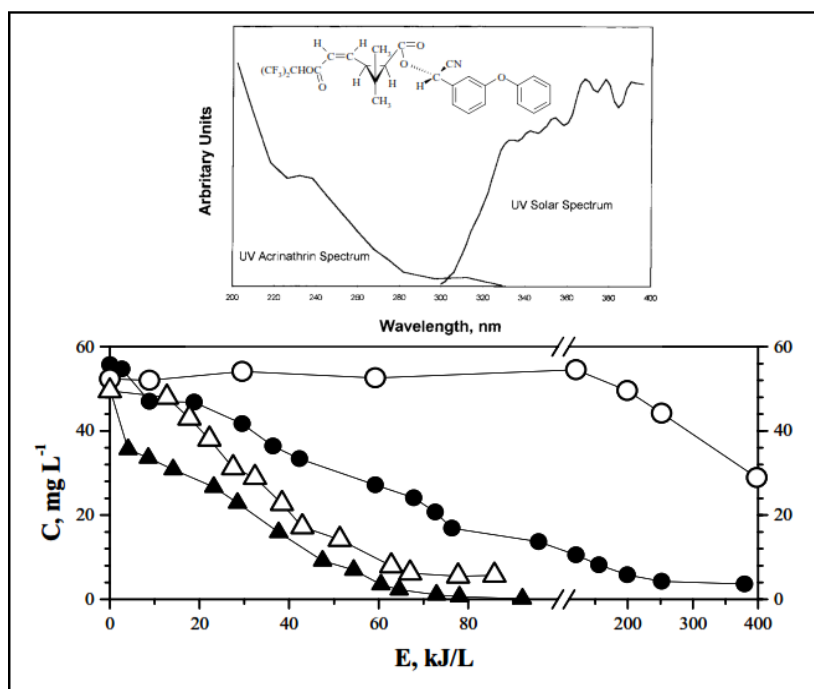


Fig 4: Disappearance of commercial acrinathrin by photolysis (●) and photocatalysis (▲) and evolution of Total Organic Carbon (open symbols). UV spectra between 200 and 400 nm of acrinathrin and sunlight is also shown.

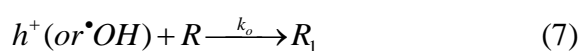
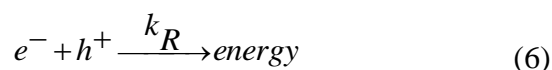
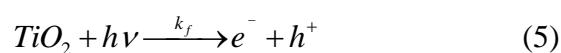
The case of acrinathrin is a good model of this effect (see Fig. 4). Its spectrum overlap slightly in the 300-330 nm region with the Solar spectrum and, therefore, solar photons can produce photoalteration processes after being exposed to the environment. But such natural photodegradation is very slow: $E = 400$ kJ/L to reach 10 % of the initial concentration under aerobic well-illuminated conditions. And the TOC content is near 50 % of the initial at this moment. This effect should be very similar when acrinathrin is present in natural waters. In surface water degradation is extremely slow and in ground water almost negligible. So disposal of acrinathrin into the environment could be very risky. When TiO_2 is used (Fig. 4), the degradation rate is increased and acrinathrin degradation is practically complete. A commercial formulation (Rufast, acrinathrin 15%) has been used and the presence of other organics in

the formulation produces TOC to be the double than the stoichiometric quantity corresponding to acrinathrin.

Radiant Flux:

Since 1990 there has been a clarification of the kind of solar technology which should be involved in detoxification. The question was if to concentrate the radiation is really necessary for the photocatalysis technology and if a non-concentrating collector can be as efficient as concentrating ones. Initially it was thought that the last ones were the ideal alternative and in fact, the first large pilot plants operate with them. However, their high cost and the fact that they can only operate with direct solar radiation (this implies their location in highly insolated areas) led to consider the alternative of static non-concentrating collectors. The reason of using one-sun systems for water treatment is firmly based on two factors, first the high percentage of UV photons in the diffuse component of solar radiation and second the low order dependence of rates on light intensity.

It has been experimentally measured that above a certain flux of UV photons, reaction rate changes from one to half-order dependence to the intensity. This modification does not seem to happen at determined radiation intensity, as different researchers obtain different results. It is presumable that the experimental conditions affect significantly. Most authors impute the transition of $r = f(I^{1.0})$ to $r = f(I^{0.5})$, to the excess of photogenerated species (e^- , h^+ and $\bullet OH$). A very simple explanation could be the following (based on the first stages of the process). The first stages considered are: (i) formation of electron/hole pairs (Eq.1), (ii) recombination of the pairs (Eq.2) and (iii) oxidation of a reactant R (Eq.3).



From these reactions, the concentration of holes is:

$$\frac{d[h]}{dt} = k_f I - k_R [e][h] - k_0 [h] R \quad (8)$$

where I is the intensity of incident radiation. If it is considered that $[e] \approx [h]$, then in stationary state:

$$\frac{d[h]}{dt} = 0 \rightarrow k_f I = k_R [h]^2 + k_0 [h] R \quad (9)$$

When I is very high, a large number of holes and electrons are generated and therefore $k_R [h]^2 \gg k_0 [h] R$:

$$k_f I \approx k_R [h]^2 \rightarrow [h] \approx K I^{0.5} \quad (10)$$

As the reaction rate depends on the amount of hydroxyl radicals present, and these are generated in the holes, then $r \propto I^{0.5}$ when I is high. Under these conditions, the quantum yield diminishes because of the high rate of recombination of e-/h+ pairs formed. In the same manner, when I is small, the inverse is true, $k_R [h]^2 \ll k_0 [h] R$:

$$k_f I \approx k_0 [h] R \rightarrow [h] \approx K' I \quad (11)$$

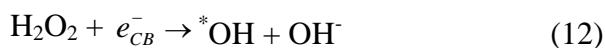
At higher radiation intensities, another transition from $r = f(I^{0.5})$ to $r = f(I^0)$ is produced. At this moment, the photocatalytic reaction leaves its dependence on the received radiation, to depend only on the mass transfer within the reaction. So, the rate is constant although the radiation increases. This effect can own to different causes, as can be the lack of electrons scavengers (i.e. O_2) or organic molecules in the proximity of TiO_2 surface and/or excess of products occupying active centres of the catalyst, etc. Really, these phenomena appear more

frequently when working with supported catalyst, and/or at low agitation level. This implies low catalyst surface in contact with the liquid and smaller turbulence. This does not favor the contact of reactants with the catalyst and the diffusion of products, from the proximity of the catalyst to the liquid.

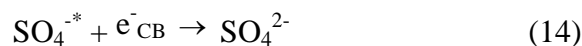
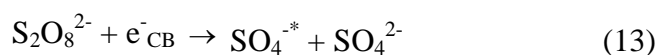
These effects may be appreciably attenuated if some product that reduces the importance of the electron/hole recombination is added. When the electrons are trapped, recombination of e^-/h^+ is impeded. Either way, addition of oxidants can improve the efficiency of the process at high illumination intensities. Moreover, this type of compounds can increase the quantum yield even at low irradiation levels due to their strong oxidizing character. The use of inorganic peroxides has been demonstrated to enhance the rate of degradation of different organic contaminants remarkably because they trap the photogenerated electrons more efficiently than O_2 . It must be mentioned here that in many highly toxic wastewaters where degradation of organic pollutants is the major concern, the addition of an inorganic anion to enhance the organic degradation rate may be justified. Another advantage related to the use of this type of oxidant comes up when solar energy is the photon source. Although scientific research on photocatalytic detoxification has been conducted for at least the last three decades, industrial/commercial applications, engineering systems and engineering design methodologies have only been developed recently. The increase of the photocatalytic reaction rate with these additives would decrease photoreactor dimensions proportionally and dramatically decrease overall costs. The oxidizing substance should not generate any toxic by-product. Hydrogen peroxide is the obvious candidate and it has been tested with a large number of compounds. Also, it is a very commonly used chemical and, so, very cheap.

Being an electron acceptor, hydrogen peroxide can be a beneficial oxidizing agent because it reacts with conduction band electrons to generate hydroxyl radicals which are required for the photomineralization of organic pollutants. The effect depends on H_2O_2 concentration, generally showing an optimum range of concentration. At higher concentration values the improvement starts to lessen. Inhibition could be explained in terms of TiO_2

surface modification by H₂O₂ adsorption, scavenging of photoproducted holes and reaction with hydroxyl radicals.



Peroxydisulphate can be also a beneficial oxidizing agent in photocatalytical detoxification because $\text{SO}_4^{\bullet-}$ is formed from the oxidant compound by reaction with the semiconductor photogenerated electrons (e_{CB}^-). The peroxydisulfate ion accepts an electron and dissociates (Eq13). The sulfate radical proceeds through the reactions shown in Eqs 14 and 15. In addition, the strongly oxidizing $\text{SO}_4^{\bullet-}$ ($E_0 = 2.6 \text{ V}$) can directly participate in the degradation processes.



The effect of both oxidants is shown in Fig.5. 25 mg/L of PCP is used as model compound in a 2-axis parabolic trough photoreactor). For comparing photoreactivity results obtained under different conditions of irradiation, the measured values of the different species concentration have been considered as a function not of the reaction time but of the cumulative photonic energy, E_{hv} , incident on the reactor.

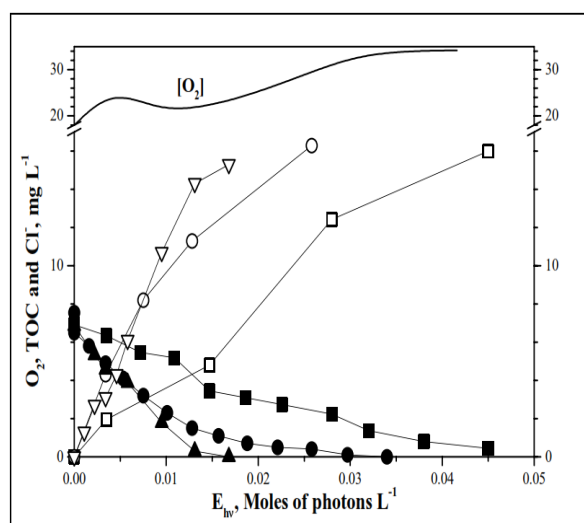


Fig. 5: Pentachlorophenol (shown as TOC) mineralization (■) with H₂O₂ 10mM (●) and with S₂O₈ 1mM (□) with a TiO₂ amount of 0.2 g L⁻¹. Chloride

production (open symbols) and O_2 evolution during H_2O_2 experiment are also shown.

The results presented in Fig.5 demonstrate that hydrogen peroxide and peroxydisulphate enhance the photocatalytic reaction rate. The first increases the reaction rate by a factor of two and the second by a factor of five, respectively. The $S_2O_8^{2-}$ effect is more noticeable in the last part of the reaction. The presence of peroxydisulphate seems to affect essentially the mineralization of the degradation intermediates. Oxygen has not been injected during the H_2O_2 experiment but it reaches a value near 4 times more than the usual dissolved oxygen in water at ambient pressure (see point 2.4.2). This demonstrates that the application of hydrogen peroxide could be very useful when it is not possible to obtain an adequate concentration of oxygen in the reactor (a difficult engineering problem when the reactor is very long and narrow very usual in solar tubular reactors).

But, other oxidants have been used in photocatalysis for reducing solar (or artificial) UV exposure time: ClO_3^- , BrO_3^- , IO_4^- , HSO_5^- . Nevertheless, these additives are very expensive compared to hydrogen peroxide and peroxydisulphate, and their application would dramatically increase treatment cost. Even more importantly, they do not dissociate into harmless products (Br^- and I^-), because hundreds of mg/L of these anions are undesirable in water.

Initial concentration of contaminant:

It is well known that in photocatalysis the degradation rate observed for an organic substrate follows saturation behaviour. After a certain concentration is achieved, the rate increments very little and in some cases a decrease is observed. The optimum contaminants concentration in water before the photocatalytic treatment must permit the maximum reaction rate. So, the initial concentration of contaminants in the wastewater can be optimized, when possible. Since hydroxyl radicals react non-selectively, numerous intermediates are formed en-route to complete mineralization at different concentrations. Because of this, all tests have to be carried out using TOC as crucial parameter,

because the photocatalytic treatment must destroy not only the initial contaminant, but any other organic compound as well. The results shown in Fig.6 are examples of the experiments carried out with mixtures of different commercial pesticides. It is possible to see that mineralization, once begun, maintains the same slope until at least 60-70% of the initial TOC has been degraded.

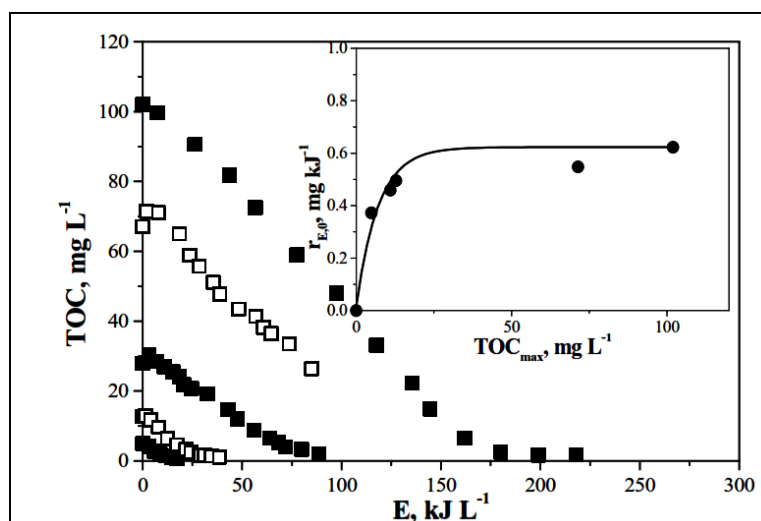


Fig. 6: Pesticides decomposition at different initial concentrations. Maximum rate” as function of TOC maximum TOC is shown in the inserted graphic.

As the reaction is not expected to follow simple models like first or zero order kinetics, overall reaction rate constants cannot be calculated. The complexity of the results, of course, is caused by the fact that the TOC is a sum parameter often including a lot of products that undergo manifold reactions. One parameter is proposed in order to obtain a practical point of comparison for various experiments: the maximum gradient of the degradation curve, which is the gradient of the tangent at the inflection point ($r_{E,O}$). It has the unit of a zero-order rate constant (mg/kJ instead of mg/min) and therefore appears to be easy to handle. Furthermore this gradient can be roughly considered as the initial rate of the mineralization reaction, because it is preceded by a period of nearly constant TOC level. This parameter $r_{E,O}$ is referred to as “maximum rate”. In the graphic insert in Fig.6, it may be observed that the initial rate is steady from 20-30 mg of

TOC per litre. At this concentration, saturation occurs and the reaction rate becomes constant.

Once the optimum initial concentration is known, a model for predicting plant behaviour is necessary. This model must allow calculation of the area of solar collectors required for treating water contaminated with different amounts of pesticides. Although different authors admit that the Langmuir-Hinshelwood (L-H) model is not a perfect explanation of the mechanism of the photocatalytic process, they do agree on its usefulness, since the behaviour of the reaction rate versus reactant concentration can very often be adjusted to a mathematical expression with it. In the present case, instead of using the L-H model [$r = kKC/(1+KC)$] directly, the use of an alternative model is preferred for fitting experimental data in large solar photocatalytic plants, by an approximate kinetic solution of the general photocatalytic kinetic system, which has the analytical form of an L-H equation. With these considerations, the rate of TOC disappearance is given by Eq.16 (analogous to L-H model but without its original significance).

$$R_{E,0} = \frac{\beta_1 [\text{TOC}]_{\max}}{\beta_2 + \beta_3 [\text{ToC}]_{\max}} \quad (16)$$

The experimental results shown in Fig.6 have been used to calculate the constants (β_i). By inversion of Eq.16 these constants can be calculated from the intercept and the slope of the line of fit (Eq.17), which is shown in the inset in Figure 7.

$$\frac{1}{r_{E,0}} = \frac{\beta_2}{\beta_1} + \frac{\beta_3}{\beta_1} \frac{1}{[\text{TOC}]_{\max}}; \quad \frac{\beta_3}{\beta_1} = 1.67 \text{ mg}^{-1}\text{kJ} \quad \frac{\beta_2}{\beta_1} = 5.07 \text{ kJ L}^{-1} \quad (17)$$

Using these values, experimental results and the corresponding lines of fit are shown in Fig.7. The lines of fit were drawn with Eq.18 using the constants reported previously.

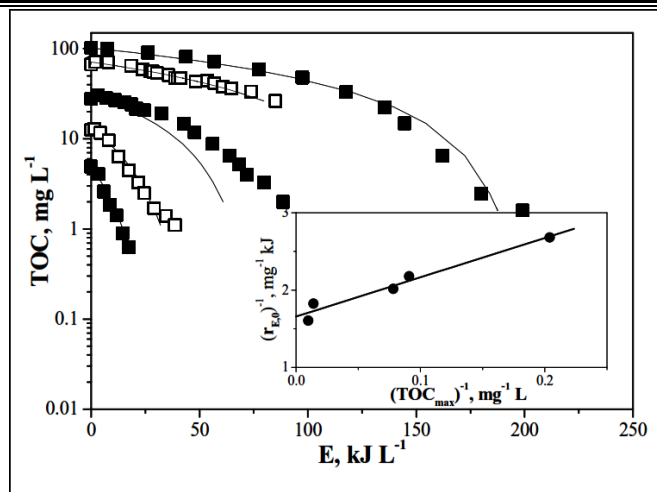


Figure7: Application of the proposed kinetic model for mineralization of a pesticide mixture. The inset shows the fit of Eq.17.

$$\frac{1}{\beta_1} \{ \beta_2 \ln (\frac{[TOC]_{max}}{[TOC]}) + \beta_3 ([TOC]_{max} - [TOC]) \} = EUV \quad (18)$$

The experimental results agree reasonably well with the model proposed and the constants calculated. This equation allows TOC degradation to be predicted as a function of initial TOC and available radiation, and the reverse, incident energy on the reactor necessary to reach a specific degree of mineralization. As seen in Fig. 7, fits are not perfect, but taking into account the experimental and accumulative errors, the adjustment may be considered acceptable. These errors could have been produced in the following measurements: (i) reactor volume and experiment time; (ii) analytical determinations; (iii) UV radiation measurement and (iv) calculation of r_{EUV} from the maximum slope of each of the experiments shown in Fig. 7 inset. Therefore, useful design equations may be obtained with a Langmuir-Hinshelwood type model, in spite of not fitting the heterogeneous photocatalytic reaction mechanism. For now these equations must be obtained at pilot plant size, however, they will be useful for larger plants if the same type of collector is used.

Factors affecting Solar Photocatalysis:

Relationship between particle size, reactor diameter and TiO₂ concentration:

Incident radiation on the reactor and length of path inside the reactor are fundamental in determining optimum catalyst concentration. This summarizes

the conclusions if the radiation comes from a source of radiation placed outside the photoreactor (as in a reactor illuminated by solar radiation):

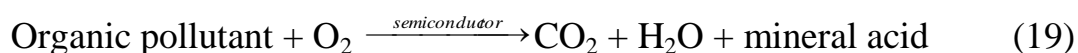
- If the path length is short (1-2 cm max.), maximum reaction rate is obtained with 1-2 g L⁻¹ of TiO₂
- If the path length is several centimetres long, the appropriate catalyst concentration is several hundred milligrams per litre.

In all the cases described above, a “screening” effect is produced when the TiO₂ concentration is very high. The reaction rate diminishes due to the excessive opacity of the solution, which prevents the catalyst farthest in from being illuminated. Approximately, 1g L⁻¹ of catalyst reduces transmissivity to zero in a 1-cm-inner-diameter cylinder. For the solar reactors, it is therefore necessary to find out the optimum catalyst concentration experimentally. That is, the minimum concentration at which the maximum reaction rate is obtained. When catalyst concentration is very high, after travelling a certain distance on an optical path length, turbidity impedes further penetration of light in the reactor. The percentage of photons absorbed by the suspension and the percentage of photons scattered by the TiO₂ particles is a very complex problem that cannot be solved experimentally, but must be experimentally estimated.

The titanium dioxide employed in the photocatalytic experiments is disposed as a colloidal suspension. The great difference between considering the TiO₂ from dry powder and TiO₂ particles suspended in an aqueous medium is the mean size of the particles. If two samples with the same catalyst concentration but dispersed with different protocols (ultrasounds and stirring) are compared, sonicated samples are found to be more efficient. Although in stirred samples there are fewer TiO₂ clusters, larger clusters screen light better than small ones. The photocatalytic experiments carried out with different particle sizes have demonstrated that efficiencies are better with small particles than with larger particles only when reactor diameter and catalyst concentration are optimized to allow UV photons to penetrate along the entire photoreactor path length. In this case, it is not possible to talk about particle radius, because TiO₂ powder is irregularly shaped, and when it is dispersed in an aqueous

medium the “particles” (300-600 nm sized) are clusters of primary particles (20-40 nm sized), not spherical or monodisperse. This leads to the conclusion that light extinction in colloidal suspensions is a determining parameter for solar photoreactor design. It should also be recalled that small particle sizes cause additional problems for catalyst separation after photocatalytic treatment. The best inner reactor diameter, for solar photocatalytic applications is in the range of a few centimetres with a few hundred mg of TiO₂ per litre. The area/volume ratio is also a crucial parameter, and if this ratio is optimized the reactor efficiency would also be increased.

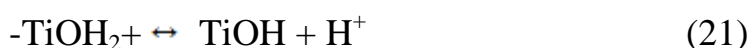
Influence of Oxygen: In semiconductor photocatalysis for water purification, the pollutants are usually organic and, therefore, the overall process can be summarized by Eq.19. Given the reaction stoichiometry of this equation, there is no photomineralization unless O₂ is present. The literature provides a consensus regarding the influence of oxygen. It is necessary for complete mineralization and does not seem to be competitive with other reactive during the adsorption on TiO₂ since the places where oxidation takes place are different from those of reduction. Therefore, injection of pure O₂ becomes necessary in once-through experiments (see Fig. 3) at low flow rates. At high flow rates or with recirculation, the addition of oxygen is not always necessary since the illumination time per pass is short. The water again recovers the oxygen consumed when it reaches the tank (open to the atmosphere and stirred).



The concentration of oxygen also affects the reaction rate but it seems that the difference between using air (p_{O2}= 0.21 atm) or pure oxygen (p_{O2}= 1 atm) is not drastic. In an industrial plant it would be purely a matter of economy of design.

pH influence:

The oxide/electrolyte interface has an electrical surface charge, which strongly depends on the pH of the medium. The electrokinetically mobilized charge is a determining parameter in the colloidal stability of the oxide particle suspensions. This involves the study of particle sizing depending on the pH; if the pH is equal to the Point of Zero Charge (PZC) the particles aggregate and ensembles are larger. The pH of the aqueous solution significantly affects TiO_2 including the charge of the particle and the size of the aggregates it forms. 300 nm sizes increase to 2-4 μm when dispersion reaches PZC. The zero surface charge yields zero electrostatic surface potentials that cannot produce the interactive rejection necessary to separate the particles within the liquid. This induces a phenomenon of aggregation and TiO_2 clusters become larger. This effect is clearly related to the capability of the suspension for transmitting and/or absorbing light. Furthermore, larger clusters sediment more quickly than small particles, thus the agitation necessary to maintain perfect homogeneity must be more vigorous. The PZC for TiO_2 is around 7. Above and below this value, the catalyst is negatively or positively charged according to:



The abundance of all the species as a function of pH: $\text{TiOH} \geq 80\%$ when $3 < \text{pH} < 10$; $\text{TiO}^- \geq 20\%$ if $\text{pH} > 10$; $\text{TiOH}_2^+ \geq 20\%$ when $\text{pH} < 3$. Under these conditions, the photocatalytic degradation of the ionisable organic compounds is affected by the pH. At first sight a very acidic solution appears to be detrimental and a very basic solution to be favorable, since the variations are modest or non-existent around neutrality. In many cases, a very important feature of photocatalysis is not taken into account when it is to be used for decontamination of water, is that during the reaction, a multitude of intermediate products are produced that may behave differently depending on the pH of the solution. To use only the rate of decomposition of the original substrate could yield an erroneous pH as the best for contaminant degradation. Therefore, a

detailed analysis of the best pH conditions should include not only the initial substrate, but also the rest of the compounds produced during the process.

Temperature influence:

Because of photonic activation, photocatalytic systems do not require heating and operate at room temperature. The true activation energy is nil, whereas the apparent activation energy is often very low (a few kJ/mol) in the medium temperature range (20°C-80°C). However, at very low temperatures (-40°C-0°C), activity decreases and activation energy becomes positive. The decrease in temperature favours reactants adsorption, which is a spontaneous exothermic phenomenon, but also favours adsorption of the final reaction products, desorption of which tends to be the rate-limiting step. By contrast, at "high" temperatures (>70-80°C) for various types of photocatalytic reactions, the activity decreases and the apparent activation energy becomes negative. When temperature increases above 80°C, nearing the boiling point of water, the exothermic adsorption of reactants is disfavoured and this tends to become the rate-limiting step.

In addition to these mechanical effects, other consequences of plant engineering must be considered. If temperature is high, the materials used for the plant should be temperature resistant and oxygen concentration in water decreases. Consequently, the optimum temperature is generally between 20 and 80°C. This absence of need for heating is attractive for photocatalytic reactions carried out in aqueous media and in particular for environmental purposes (photocatalytic water purification). There is no need to waste energy heating water that already possesses a high thermal capacity.

6. Applications of solar photocatalysis:

As stated in the mechanism of solar photocatalysis, the positive hole of TiO₂ breaks apart the water molecule to form H⁺ and hydroxyl radical (*OH). The hydroxyl radical thus formed is an extremely powerful oxidising agent. Utilizing this strong oxidation strength of hydroxyl radical, photocatalytic

oxidation can effectively disinfect, deodorize and purify air, water and different surface area.

Various applications of photocatalysis (see Fig.8) are given below:

1. As Anti-Bacterial agent: Photocatalyst does not only kill bacteria cells, but also decompose the cell itself. The TiO_2 photocatalyst has been found to be more effective than any other antibacterial agent, because the photocatalytic reaction works even when there are cells covering the surface and while the bacteria are actively propagating. The end toxin produced at the death of cell is also expected to be decomposed by photocatalytic action. TiO_2 does not deteriorate and it shows a long-term anti-bacterial effect. Generally speaking, disinfections by TiO_2 are three times stronger than chlorine, and 1.5 times stronger than ozone.
2. As Deodorizing agent: On the deodorizing application, the hydroxyl radicals accelerate the breakdown of any Volatile Organic Compounds (VOC) by destroying the molecular bonds. This will help combine the organic gases to form a single molecule that is not harmful to humans thus enhance the air cleaning efficiency. Some of the examples of odour molecules are: Tobacco odour, formaldehyde, nitrogen dioxide, urine and faecal odour, gasoline, and many other hydrocarbon molecules in the atmosphere.
3. As air-purifying agent: The photocatalytic reactivity of TiO_2 can be applied for the reduction or elimination of polluted compounds in air such as NO_x , cigarette smoke, as well as volatile compounds arising from various construction materials. Also, high photocatalytic reactivity can be applied to protect lamp-houses and walls in tunnelling, as well as to prevent white tents from becoming sooty and dark. Atmospheric constituents such as chlorofluorocarbons (CFCs) and CFC substitutes, greenhouse gases, and nitrogenous and sulphurous compounds undergo

photochemical reactions either directly or indirectly in the presence of sunlight. In a polluted area, these pollutants can eventually be removed.

4. As a water purifying agent: Photocatalyst coupled with UV lights can oxidize organic pollutants into non-toxic materials, such as CO₂ and water and can disinfect certain bacteria. This technology is very effective at removing further hazardous organic compounds (TOCs) and at killing a variety of bacteria and some viruses in the secondary wastewater treatment. Pilot projects demonstrated that photocatalytic detoxification systems could effectively kill fecal coli form bacteria in secondary wastewater treatment.

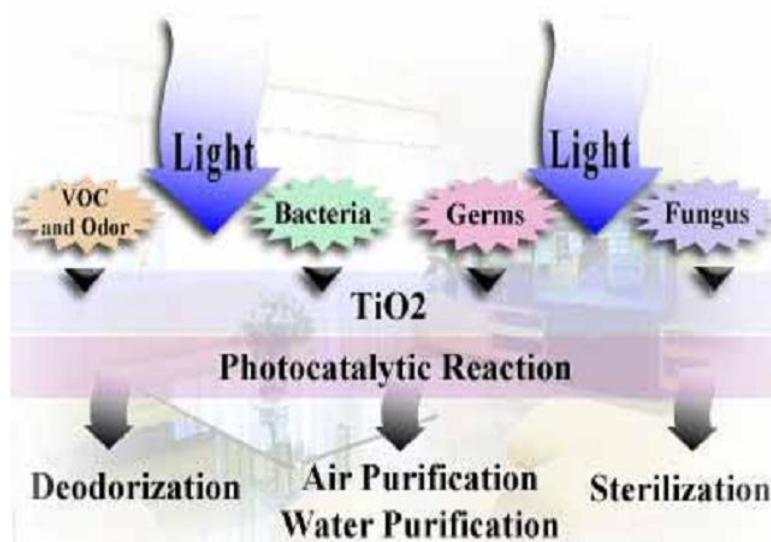


Fig8: Various application of solar photocatalysis

5. As anti fogging and self cleaning agent: Most of the exterior walls of buildings become soiled from automotive exhaust fumes, which contain oily components. When the original building materials are coated with a photocatalyst, a protective film of titanium provides the self-cleaning building by becoming antistatic, super oxidative, and hydrophilic. The hydrocarbon from automotive exhaust is oxidized and the dirt on the walls washes away with rainfall, keeping the building exterior clean at all times.

When the surface of photocatalytic film is exposed to light, the contact angle of the photocatalyst surface with water is reduced gradually.

After enough exposure to light, the surface reaches super-hydrophilic (Fig. 9) . In other words, it does not repel water at all, so water cannot exist in the shape of a drop, but spreads flatly on the surface of the substrate. And the water took the form of a highly uniform thin film, which behaves optically like a clear sheet of glass.

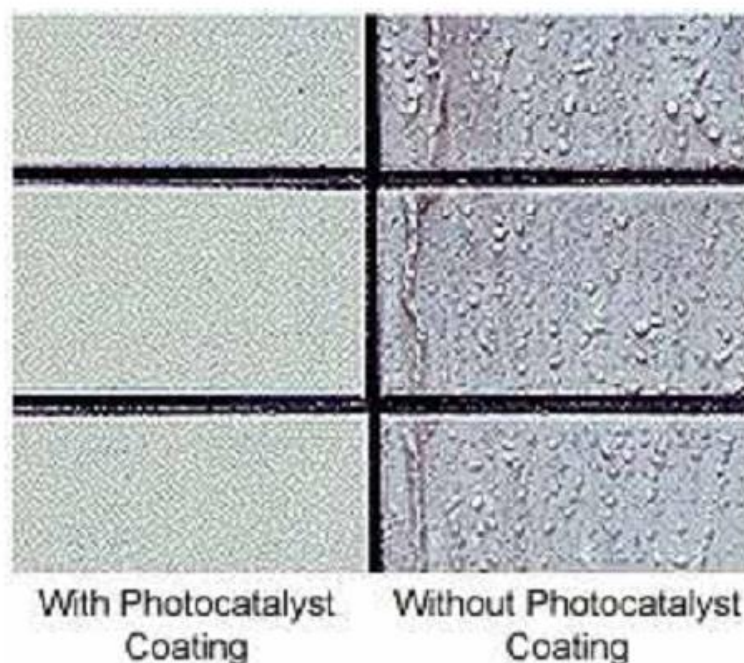


Fig9: Super hydrophilic nature of photocatalyst

6. Photocatalytic water splitting to produce Hydrogen: It is a major area of research now a day as hydrogen has higher specific energy density, no emission of green house gases during combustion and is abundance in nature in the form of water. Solar energy can be utilised in water splitting to produce hydrogen in presence of photocatalyst like TiO_2 . Like photocatalytic water/air purification, photocatalytic hydrogen production also requires photogenerated electron/hole pairs. The basic difference is that in case of air/water purification, valence band holes are the key elements that induce decomposition of contaminants. On the other hand when photocatalysis is applied to perform water splitting for hydrogen production, the reducing conduction band electrons become important as their role is to reduce protons to hydrogen molecules.

QUESTIONS:

1. What do you mean by solar photocatalysis? Write down the basic mechanism of solar photocatalysis.
2. Give a short description on solar detoxification pilot plant.
3. Write down the fundamental parameters in solar photocatalysis.
4. How solar photocatalysis can be affected by the following: (a) catalyst concentration, (b) presence of oxygen and (c) pH
5. Photocatalytic film is a self cleaning agent. Describe it.
6. What is the basic difference when photooctalyst is used for decomposition of contaminants and water splitting agent?